

**Synthesis and Properties of Polymer/Layered Silicate Clay
Nanocomposites**

A Thesis Submitted to the
University of Pune

For the degree of
DOCTOR OF PHILOSOPHY
In
CHEMISTRY

By
S. R. MALLIKARJUNA

Polymer Science and Engineering Division
National Chemical Laboratory
PUNE 411 008

January 2009

CERTIFICATE

Certified that the work incorporated in this thesis entitled "**Synthesis and properties of polymer/layered silicate clay nanocomposites**" submitted by Mr. **S. R. Mallikarjuna** was carried out by the candidate at National Chemical Laboratory, Pune-08, under my supervision. Such materials as obtained from other sources have been duly acknowledged in this thesis.

January 2009

Pune

Dr. S. Sivaram

(Research Supervisor)

DECLARATION

I hereby declare that the thesis entitled “**Synthesis and properties of polymer/layered silicate clay nanocomposites**” submitted for Ph. D. degree to the University of Pune has been carried out at National Chemical Laboratory, Pune, India under the supervision of **Dr. S. Sivaram**, Division of Polymer Science and Engineering, National Chemical Laboratory, Pune-411008. The work is original and has not been submitted in part or full by me for any degree or diploma to this or any other University.

January 2009

Pune

(S. R. Mallikarjuna)

*Dedicated to
My Family*

ACKNOWLEDGEMENT

*I take this opportunity to express my gratitude to **Dr. S. Sivaram**, my research supervisor, mentor, for his invaluable guidance, teaching, support and advice throughout the course of this investigation. His commitment, dedication and leadership qualities are the attributes that I wish to take forward with me along with the chemistry that I learnt with him. Although this eulogy is insufficient, my sincere regards and reverence are for him, forever.*

I am extremely grateful to Dr. C. Ramesh for the stimulating scientific discussions and suggestions. Whenever I approached him with some problems he was always ready to help.

I am thankful to Drs. P. P. Wadgaonkar C. V. Avadhani, , T. P. Mohandas, S. P. Vernekar, B. B. Idage, C. Bhaskar, A. K. Lele, K. Guruswamy, Deenadayalan, Raut and J. Jog on this occasion for their suggestions, advice and valuable discussions we have had in this period. I am also thankful to Mrs. D. A. Dhoble, Dr. (Mrs). S. B. Idage, Mr. S. K. Menon, Dr. Jadhav and A. N. Bote for their help during the course of this work.

I owe deeply to ever-trustful friends Bhoje, Pratheep, Smitha, Govind, Ramesh (N), Khaja and Raghunath for always being with me in the division. I sincerely thank them for all their affection and help. Specifically I thank Bhoje for the discussions and suggestions (both scientific and non-scientific) in shaping my career both professionally and personally. The friendly attitude of my colleagues in polymer chemistry division helped in maintaining a cheerful atmosphere in the laboratory. I extend my deep sense of gratitude towards them.

I express my heartfelt thanks to Raghunadh, Yanjarappa, Sandhya, Gnaneshwar, Rajesh, Dyaneshwar, Arun, Rahul, and Subramanyam for their willing help during the initial stages of my thesis work and friendly support.

I also whole-heartedly thank the Tamil Sangam, Telugu group, and Kannada friends who made my stay at NCL memorable and pleasant. The long list goes on starting right from Ramesh, Murugan, Kicha, Pasu...upto Selva, Balki, Pambu Sankar, Pratap etc. I should specially mention the comfort and the friendship, which I enjoyed with Easwar, Sankar, Subbu, Jayanthi, Mangal, Nagendra, Ramanujam and Kannan.

I thank authorities of NMR facility, CMC and PPC of NCL for their timely help. I also thank CSIR for the award of a research fellowship. I should specially thank Mr. Gholap for his help in TEM measurements at the last moment.

*I am deeply and thoroughly indebted to my family members for their sacrifices, patience, and kind support throughout my upbringing. I am deeply indebted to my **Doddappa** and Dr. Thatha for their values in life that I have had the good fortune to see, experience and learn, and wish to specifically thank them for being instrumental in shaping my career in education.*

Finally, my acknowledgement would not be complete without thanking the Almighty, for the strength and determination to put my chin up when faced with hardships in life.

(S. R. Mallikarjuna)

Contents

| | |
|------------------------|-----|
| Contents | i |
| Abstract | vii |
| Abbreviations | ix |
| List of Figures | xi |
| List of Tables | xv |

Chapter 1: Introduction

| | | |
|---------|---|----|
| 1.1 | Introduction | 1 |
| 1.2 | Structure of clay and the organoclay | 3 |
| 1.3 | Types of polymers used for nanocomposites preparation with layered silicate | 5 |
| 1.4 | Nanocomposite structure and their characterization | 5 |
| 1.5 | Methods of preparation of nanocomposites | 7 |
| 1.5.1 | Intercalation of polymers or prepolymer from solution | 7 |
| 1.5.2 | In-situ intercalative polymerization method | 8 |
| 1.5.3 | Melt intercalation method | 8 |
| 1.6 | Choice of the organoclay | 8 |
| 1.6.1 | Thermal stability of the modifiers | 10 |
| 1.6.2 | In situ polymerization and reactive modifiers for the clays | 15 |
| 1.6.2.1 | Ring opening polymerization | 16 |
| 1.6.2.2 | Radical polymerizations | 17 |
| 1.6.2.3 | Condensation polymerizations | 17 |
| 1.6.2.4 | Olefin polymerizations | 19 |
| 1.6.2.5 | Living polymerization | 20 |
| 1.6.2.6 | Thermoset polymers | 23 |
| 1.6.3 | Polymeric surfactant modifiers | 25 |
| 1.7 | Properties of nanocomposites | 25 |
| 1.7.1 | Mechanical properties | 25 |

| | | |
|-------|--|----|
| 1.7.2 | Barrier property | 29 |
| 1.7.3 | Thermal properties of nanocomposites | 30 |
| 1.7.4 | Crystallization behavior | 33 |
| 1.7.5 | Rheological behaviour | 34 |
| 1.7.6 | Other properties | 34 |
| 1.8 | Applications and Commercial developments | 35 |
| 1.9 | Conclusions | 37 |
| | References | 38 |

Chapter 2: Scope and objectives

| | | |
|--|---------------------|----|
| | Scope and objective | 45 |
|--|---------------------|----|

Chapter 3: Polyurethane/Clay Nanocomposites via in-situ Solution Polymerization

| | | |
|-------|---|----|
| 3.1 | Introduction | 47 |
| 3.2 | Experimental | 49 |
| 3.2.1 | Materials | 49 |
| 3.2.2 | Preparation of hydroxyethyl dimethyl hexadecylammonium bromide | 50 |
| 3.2.3 | Preparation bis(hydroxy ethyl) methyl hexadecylammonium bromide | 50 |
| 3.2.4 | Preparation bis(hydroxyethyl) methyl- 2-hydroxymethyloctadecyl ammonium bromide | 50 |
| | 3.2.4.1 Alkylation of dimethyl malonate with hexadecyl bromide | 51 |
| | 3.2.4.2 Reduction of hexadecylated malonate to 2-(hydroxy methyl) octadecanol | 51 |
| | 3.2.4.3 Monobromination of 2-(hydroxy methyl) octadecanol to 2-(hydroxy methyl) octadecyl bromide | 52 |

| | | |
|-----|---|----|
| | 3.2.4.4 Preparation bis(hydroxyethyl)methyl-2-hydroxymethyl octadecyl ammonium bromide | |
| | 3.2.5 Reactivity of modifier salts with phenyl isocyanate | 52 |
| | 3.2.6 Preparation of organoclays | 53 |
| | 3.2.7 Estimation of isocyanate content | 53 |
| | 3.2.8 Preparation of prepolymer terminated with isocyanate from EHG and TDI | 53 |
| | 3.2.9 Preparation PU/Cloisite 30B nanocomposites with different amounts of trifunctional monomer | 54 |
| | 3.2.10 Preparation PU/Cloisite 25A nanocomposites with different amounts of trifunctional monomer | 55 |
| | 3.2.11 Preparation of PU/clay nanocomposites with varying functionality in the organoclays | 56 |
| | 3.2.12 Preparation of Thermoplastic polyurethane | 56 |
| | 3.2.13 Preparation of Thermoplastic polyurethane/clay nanocomposites | 56 |
| | 3.2.14 Characterization | 57 |
| 3.3 | Results and discussion | 58 |
| | 3.3.1 Preparation of organomodifiers for the clay | 59 |
| | 3.3.2 Reactivity of hydroxyls in the modifier with phenyl isocyanate | 61 |
| | 3.3.3 Preparation of organoclays with various functionality in the modifier | 63 |
| | 3.3.4 Reactivity of hydroxyl of modifier in Cloisite 30B with isocyanate | 64 |
| | 3.3.5 Preparation of prepolymer terminated with isocyanate | 65 |
| | 3.3.6 Effect of branching agent | 65 |
| | 3.3.6.1 WAXD | 65 |
| | 3.3.6.2 TEM | 67 |
| | 3.3.7 Effect of functionality of the modifier in the organoclay | 73 |
| | 3.3.8 Effect of functionality of the modifier in the organoclay on thermoplastic Polyurethane | 77 |
| | 3.3.9 Dynamic mechanical analysis of thermoplastic polyurethanes | 81 |

| | | |
|-----|------------|----|
| 3.4 | Conclusion | 84 |
| | References | 84 |

Chapter 4: Polycarbonate/Clay Nanocomposites via in-situ Melt Polymerization

| | | |
|---------|---|-----|
| 4.1 | Introduction | 87 |
| 4.2 | Experimental | 88 |
| 4.2.1 | Materials and measurements | 88 |
| 4.2.2 | Synthesis of modifiers for the clay | 90 |
| 4.2.2.1 | Synthesis of 10-bromodecan-1-ol from decane-1,10-diol | 90 |
| 4.2.2.2 | Synthesis of hydroxydecylacetoacetate | 91 |
| 4.2.2.3 | Synthesis of 13-hydroxytridecan-2-one | 91 |
| 4.2.2.4 | Synthesis of 2,2-bis(4-hydroxyphenyl)tridecanol | 91 |
| 4.2.2.5 | Synthesis of 2,2-bis(4-hydroxyphenyl)tridecyl bromide | 92 |
| 4.2.2.6 | Synthesis of 2,2-bis(4-hydroxyphenyl)tridecyl-(2',3'-dimethylimidazolium) bromide | 92 |
| 4.2.2.7 | Synthesis of 2,2-bis(4-hydroxyphenyl)tridecyl triphenyl phosphonium bromide | 92 |
| 4.2.3 | Synthesis of organoclays | 93 |
| 4.2.4 | Synthesis of PC/ clay nanocomposites with various organoclays | 93 |
| 4.3 | Results and Discussion | 94 |
| 4.3.1 | Organomodifiers for the clay and its preparation | 94 |
| 4.3.2 | Organoclays and its preparation | 95 |
| 4.3.3 | Thermal analysis organoclays | 96 |
| 4.3.4 | Preparation of PC/clay nanocomposites | 97 |
| 4.3.5 | Structure of PCCN using WAXD | 99 |
| 4.3.6 | Structure of the PCCN using TEM | 101 |
| 4.3.7 | Glass transition temperatures | 107 |
| 4.3.8 | Dynamic mechanical analysis | 108 |
| 4.4 | Conclusions | 110 |

Chapter 5: Syndiotactic Polystyrene (sPS)/Clay nanocomposites via Solvent Casting

| | | |
|-------|---|-----|
| 5.1 | Introduction | 113 |
| 5.2 | Experimental | 114 |
| 5.2.1 | Materials | 114 |
| 5.2.2 | Preparation of organoclay | 114 |
| 5.2.3 | Preparation of SsPS ionomers | 115 |
| | 5.2.3.1 Preparation of acetyl sulfate | 115 |
| | 5.2.3.2 Preparation of SsPS | 115 |
| | 5.2.3.3 Preparation of SsPS ionomers | 115 |
| 5.2.4 | Preparation of SsPS ionomer /clay nanocomposites | 116 |
| 5.2.5 | Characterization | 116 |
| 5.3 | Results and Discussion | 117 |
| 5.3.1 | Preparation of sulfonated sPS and its ionomers | 117 |
| 5.3.2 | Thermal stability of the organoclay and the nanocomposites | 119 |
| 5.3.3 | Structure of sPS/organoclay nanocomposites | 120 |
| 5.3.4 | Structure of SsPS ionomer/organoclay nanocomposites | 121 |
| | 5.3.4.1 Effect of ionomer content | 121 |
| | 5.3.4.2 Effect of type of ionomer | 123 |
| 5.3.5 | Structure of SsPS ionomer/closite Na ⁺ nanocomposites | 125 |
| 5.3.6 | Crystallization behaviour of SsPS ionomer/organoclay nanocomposites | 126 |
| 5.4 | Conclusions | 127 |
| | References | 128 |

Chapter 6: Polypropylene/clay nanocomposites via melt mixing

| | | |
|----------|--|-----|
| 6.1 | Introduction | 130 |
| 6.2 | Experimental | 131 |
| 6.2.1 | Materials | 131 |
| 6.2.2 | Preparation of potassium succinate grafted polypropylene ionomer | 132 |
| 6.2.3 | Preparation of nanocomposites | 132 |
| 6.2.4 | DSM micro extruder and injection molder | 133 |
| 6.2.5 | Wide Angle X-Ray Diffraction (WAXD) | 134 |
| 6.2.6 | Transmission Electron Microscopy (TEM) | 134 |
| 6.2.7 | Thermal analysis Thermal analysis | 135 |
| 6.2.8 | Polarized Optical Microscopy | 135 |
| 6.2.9 | Universal Testing Machine (UTM) | 135 |
| 6.3 | Results and Discussion | 136 |
| 6.3.1 | Preparation of Potassium succinate grafted polypropylene | 136 |
| 6.3.2 | Structure of the nanocomposites | 137 |
| 6.3.2.1. | WAXD | 138 |
| 6.3.2.2. | TEM | 139 |
| 6.3.3 | Thermogravimetric analysis | 142 |
| 6.3.4 | Crystallization behavior | 144 |
| 6.3.4.1 | Differential Scanning Calorimetry | 144 |
| 6.3.4.2 | Polarized Optical Microscope | 145 |
| 6.3.5 | Mechanical properties (flexural modulus) | 146 |
| 6.4 | Conclusions | 147 |
| | References | 148 |

Chapter 7: Summary and conclusions

Synthesis and properties of polymer/layered silicate clay nanocomposites

Abstract

Polymer nanocomposites are a novel class of composites, that are particle-filled polymers, in which at least one dimension of the dispersed particles is in the nanometer range. Amongst all the potential nanocomposite precursors, those based on clay and layered silicates have been more widely investigated. Large improvements in properties are achieved when the clay layers are thoroughly dispersed and exfoliated in the polymer matrix. Therefore, in this thesis various strategies are explored to obtain better dispersion of clay layers in candidate polymers and to study the property enhancements of the resultant nanocomposites.

The present thesis is organized and presented in seven chapters. A brief overview of preparation, properties and application of polymer clay nanocomposites are discussed in the first chapter. The scope and objectives of the thesis are described the second chapter. In the third chapter, various factors that affect the structure and dispersion of clay in the PU were established and the dynamic mechanical properties of the thermoplastic PU were correlated with the organoclay used. The fourth chapter describes the preparation and properties of exfoliated polycarbonate/clay nanocomposites via *in-situ* polymerization using a novel modifier for the clay, which contain a reactive bisphenol group that can be incorporated in polycarbonate backbone during in-situ polymerization. In the fifth chapter, the effect of ionomer content and cation type on the intercalation/exfoliation efficiency of the sulphonated syndiotactic polystyrene ionomer/organoclay nanocomposites is described and their crystallization behavior are correlated with the dispersion of the clay. The sixth chapter describes the efficiency of a novel compatibilizer based on potassium succinate-*g*-polypropylene for the preparation of polypropylene/organoclay nanocomposites and compared with the routinely used maleic anhydride-*g*-polypropylene. The mechanical and crystallization behavior were correlated with the dispersion of organoclay in the PP matrix.

Thus, it has been demonstrated that when the interaction of the polymer chains with the layered silicate clay improved either by modifying the surface of the clay to suitably interact with polymer or modify the polymer by functionalization results in better dispersion. The properties of the nanocomposites obtained were correlated with the structure of the clay dispersion in the polymer matrix.

List of abbreviations

| | |
|-----------|---|
| APS | Aminopropyl siloxane |
| ATRP | Atom transfer radical polymerization |
| BPAIMI | 12,12-bis(4-hydroxyphenyl) tridecyl-2,3-dimethylimidazolium bromide |
| BPAIMMMT | 12,12-bis(4-hydroxyphenyl) tridecyl-2,3-dimethylimidazolium ion exchanged montmorillonite |
| BPAP | 12,12-bis(4-hydroxyphenyl) tridecyltriphenylphosphonium bromide |
| BPAPMMT | 12,12-bis(4-hydroxyphenyl) tridecyltriphenylphosphonium ion exchanged montmorillonite |
| C16IMI | Hexadecyl-2,3-dimethylimidazolium bromide |
| C16IMIMMT | Hexadecyl-2,3-dimethylimidazolium ion exchanged montmorillonite |
| C16P | Hexadecyltriphenylphosphonium bromide |
| C16P-MMT | Hexadecyltriphenylphosphonium ion exchanged montmorillonite |
| C20A | Cloisite 20A |
| CEC | Cation exchange capacity |
| DGEBA | Diglycidyl ether of bisphenol A |
| DMA | Dynamic mechanical analysis |
| DSC | Differential scanning calorimetry |
| FTIR | Fourier Transform-Infra Red spectrum |
| HDT | Heat distortion temperature |
| KPPSA | Potassium succinate-g-polypropylene ionomer |
| KSsPS | Potassium salt of sulfonated syndiotactic polystyrene |
| MMT | Montmorillonite |
| N-6 | Nylon-6 |
| NaSsPS | Sodium salt of Sulfonated syndiotactic polystyrene |
| OMLS | Organomodified layered silicate |
| PBO | Polybenzoxazole |
| PBS | Polybutylene succinate |

| | |
|--------|--|
| PC | Polycarbonate |
| PCCN | Polycarbonate/clay nanocomposites |
| PCL | Polycarolactone |
| PCN | Polymer clay nanocomposites |
| PEO | Polyethylene oxide |
| PET | Polyethylene terephthalate |
| PHA | Polyhydroxamide |
| PLA | Polylactic acid |
| PLS | Polymer layered silicate |
| PMMA | Poly(methyl methacrylate) |
| PNC | Polymer nanocomposites |
| PP | Polypropylene |
| PPMA | Maleated polypropylene |
| PS | Polystyrene |
| PtBA | Poly(t-butyl acrylate) |
| PU | Polyurethane |
| PVDF | Polyvinylidene fluoride |
| RbSsPS | Rubidium salt of sulfonated syndiotactic polystyrene |
| SEC | Size exclusion chromatography |
| sPS | Syndiotactic polystyrene |
| SsPS | Sulfonated syndiotactic polystyrene |
| TEM | Transmission electron micrograph |
| TGA | Thermogravimetric analysis |
| TPU | Thermoplastic polyurethane |
| WAXD | Wide angle X-ray diffraction |
| XRD | X-ray diffraction |

List of Figures

- 1.1 Structure of 2:1 Phyllosilicate
- 1.2 Structure of nanocomposites
- 1.3 Illustration of different states of dispersion of organoclays in polymers with corresponding WAXS and TEM results.
- 1.4 Degradation of the imidazolium quaternary salt according to S_N2 mechanism
- 1.5 Degradation of the imidazolium quaternary salt according to S_N1 mechanism
- 1.6 Degradation mechanism of phosphonium ion
- 1.7 Schematic illustration for synthesis of Nylon-6/clay nanocomposite
- 1.8 A schematic drawing of the formation process of polymer tethered APTS-kenyaite
- 1.9 Schematic representation of the modification and ion-exchange of Laponite with [Zr(q-C₅H₅)₂Me(thf)]BPb and propene polymerisation.
- 1.10 Structure of clay modifiers containing the initiator moiety
- 1.11 The schematic representation showing the exchange of cations in clay with organocations containing initiator moiety for insitu ATRP
- 1.12 Reactions of amine functionalized clay to give various other functionalities
- 1.13 Formation of tortuous path in PLS nanocomposites
- 1.14 Schematic representation of combustion mechanism and ablative reassembly of a nanocomposite during cone calorimeter experiments
- 3.1 (a) ¹H NMR spectra of phenyl carbamate of 1OH
- 3.1 (b) NMR spectra of phenyl carbamate of 2OH
- 3.1 (c) NMR Spectra of phenyl carbamate of 3OH
- 3.2 WAXD patterns for organoclays such 1OHMMT, 2OHMMT and 3OHMMT
- 3.3 IR spectra to show the reactivity of Cloisite 30B and Cloisite 25A with phenyl isocyanate
- 3.4 (a) WAXD pattern of PU/Cloisite 30B nanocomposites with varying amount of trimethylol propane
- 3.4 (b) WAXD pattern of PU/Cloisite 25A nanocomposites with varying amount of

- trimethylol propane
- 3.5 TEMs of PU/Cloisite 30B nanocomposite with 1.7 wt % branching agent
 - 3.6 TEMs of PU/Cloisite 30B nanocomposite with 3.4 wt % branching agent
 - 3.7 TEMs of PU/Cloisite 30B nanocomposite with 5.2 wt % branching agent
 - 3.8 TEMs of PU/Cloisite 30B nanocomposite with 7.0 wt % branching agent
 - 3.9 TEMs of PU/Cloisite 25A nanocomposite
 - 3.10 TEMs of PU/Cloisite 25A nanocomposite with 7.0 wt % branching agent
 - 3.11 WAXD pattern of PU/clay nanocomposites with 1OHMMT, 2OHMMT and 3OHMMT
 - 3.12 TEMs of PU/3OH-MMT nanocomposites
 - 3.13 TEMs of PU/2OH-MMT nanocomposites
 - 3.14 TEMs of PU/1OH-MMT nanocomposites
 - 3.15 WAXD pattern of PU/clay nanocomposites with 1OHMMT, 2OHMMT and 3OHMMT
 - 3.16 TEMs of TPU/3OH-MMT nanocomposites
 - 3.17 TEMs of TPU/2OH-MMT nanocomposites
 - 3.18 TEMs of TPU/1OH-MMT nanocomposites
 - 3.19 DMA Plots of G' and $\tan \delta$ versus temperature for various samples (a) pristine TPU-1OH, (b) pristine TPU-2OH, (c) pristine TPU-3OH, (d) TPU-1OHMMT, (e) TPU-2OHMMT, and (f) TPU-3OHMMT.
 - 3.20 Tensile storage modulus (G') of various samples measured by dynamic mechanical analysis (a) pristine TPU-1OH, (b) pristine TPU-2OH, (c) pristine TPU-3OH, (d) TPU-1OHMMT, (e) TPU-2OHMMT, (f) TPU-3OHMMT
 - 4.1 Thermograms of the organoclays
 - 4.2(a) WAXD pattern of BPAP-MMT, and the PC nanocomposites with BPAP-MMT at various compositions
 - 4.2(b) WAXD pattern of C16P-MMT, and the PC nanocomposites with C16P-MMT at various compositions.
 - 4.2(c) WAXD pattern of pristine C16IM-MMT, Pristine BPAIM-MMT, PC-C16IM-3.6 and PC-BPAIM-3.6
 - 4.3 TEM pictures of PCCN with BPAP-MMT 1.8 wt %. (PC-BPAP-1.8)

- 4.4 TEM pictures at of PCCN with BPAP-MMT 3.6 wt %. (PC-BPAP-3.6)
- 4.5 TEM pictures of PCCN with BPAP-MMT 5.4 wt %. (PC-BPAP-5.4)
- 4.6 TEM pictures of PCCN with C16P-MMT 3.6 wt %. (PC-C16P-3.6)
- 4.7 TEM pictures of PCCN with 3.6 wt % PC-C16IMI-MMT (PC-C16IM-3.6)
- 4.8 TEM pictures of PCCN with 3.6 wt % PC/BPAIMI-MMT (PC-BPAIM-3.6)
- 4.9 Storage modulus (E') of PCCNs (a) with BPAP-MMT and (b) with C16P-MMT obtained from DMA
- 5.1 Typical FTIR spectra of sPS and SsPS
- 5.2 Typical ^1H NMR spectra of sPS and SsPS
- 5.3 TGA thermogram of (a) organoclay, (b) RbSsPS 3.8 mole %/organoclay nanocomposite and (c) RbSsPS 3.8 mole %
- 5.4 a) WAXS pattern of cloisite Na^+ , organoclay, sPS and sPS/organoclay nanocomposite. b) TEM micrograph of sPS/organoclay nanocomposite
- 5.5 WAXD pattern of SsPS ionomer/organoclay nanocomposites with different ionomer content and cation type (a) H^+ , (b) Na^+ , (c) K^+ and (d) Rb^+
- 5.6 TEM micrographs of SsPS ionomers 3.8 mole %/organoclay nanocomposites (a) SsPS, (b) NaSsPS, (c) KSsPS and (d) RbSsPS
- 5.7 WAXD pattern of 3.8 mole % SsPS ionomers/cloisite Na^+ nanocomposites with different cations: (a) cloisite Na^+ (b) NaSsPS/cloisite Na^+ (c) KSsPS/cloisite Na^+ (d) RbSsPS/cloisite Na^+
- 6.1 DSM Microextruder and injection molder
- 6.2 The FT IR spectrum of PPMA and KPPSA
- 6.3 WAXD patterns of nanocomposites of (A) binary composites (B) 15 wt % of the compatibilizers (C) 20 wt % of the compatibilizers (D) 25 wt % of two compatibilizers; In the sample code, the number indicates wt % of the compatablizer, C indicates 5 wt % cloisite 20A, D for the samples prepared by direct mixing route and M for the samples prepared by masterbatch route
- 6.4(a) Typical TEM micrographs of PPMA25C-M
- 6.4(b) Typical TEM micrographs of KPSA25C-M
- 6.5(a) TGA Thermograms of cloisite Na, Cloisite 20A, PP, PPMA25, KPSA25,

PPMA25C-M and KPSA25C-M

- 6.5(b) TGA derivative thermograms of cloisite Na, PP, PPMA25, KPSA25, PPMA25C-M and KPSA25C-M
- 6.6 DSC thermogram curves of the matrix polymers and the nanocomposites during the cooling from melt at 10°C/min.
- 6.7 Polarized optical microscope pictures of PP, PP/Compatibilizer and PP/Compatibilizer/ Organoclay nanocomposites obtained at room temperature after cooling from melts at 10°C/min.

List of tables

- 1.1 Commercially available products based on polymer – clay nanocomposites
- 3.1 List of organoclays used and the structure of their modifiers
- 3.2 Compositions of monomers in the preparation of PU/Cloisite 30B nanocomposite
- 3.3 Compositions of monomers in the preparation of PU/Cloisite 30B nanocomposite
- 3.4 The weight loss on charring at 900 °C from TGA and d- spacing for the organoclays from WAXD for the organoclays
- 4.1 TGA and d- spacing for the organoclays
- 4.2 Data table showing the sample code, compositions, glass transition temperature of the composites and the matrix polymer, molecular weights and inherent viscosity of the matrix polymer
- 5.1 Clay gallery height from WAXD data of SsPS ionomers/clay nanocomposites
- 5.2 Crystallization temperature on cooling from the melt for various samples
- 6.1 d - spacing of nanocomposites and organoclay
- 6.2 Thermal degradation behavior of PP matrix and its nanocomposites
- 6.3 Flexural modulus of the matrix polymer and the nanocomposites

1. Introduction

1.1 Introduction

Materials and material development are fundamental to our very culture. We even ascribe major historical periods of our society to materials such as the stone age, bronze age, iron age, steel age (the industrial revolution), polymer age, silicon age, etc. This reflects how important materials are to us. As the 21st century unfolds, it is becoming more apparent that the next technological frontiers will be opened through a better understanding and optimizing material combinations and their synergistic function, hence blurring the distinction between a material and a functional device comprised of distinct materials. The nanoscale, and the associated excitement surrounding nanoscience and technology, affords unique opportunities to create these revolutionary material combinations. These new materials promise to enable the circumvention of classic material performance trade-offs by accessing new properties and exploiting unique synergisms between constituents that only occur when the length scale of the morphology and the critical length associated with the fundamental physics of a given property coincide.

Polymer nanocomposites are a new class of composites, that are particle-filled polymers for which at least one dimension of the dispersed particles is in the nanometer range. Polymer nanocomposites have been an area of intense industrial and academic research for the past 20 years. PNCs represent a radical alternative to conventional filled polymers or polymer blends— a staple of the modern plastics industry. In contrast to conventional composites, where the reinforcement is on the order of microns, PNCs are exemplified by discrete constituents on the order of a few nanometers.

One can distinguish three types of nanocomposites, depending on how many dimensions of the dispersed particles are in the nanometer range. When the three dimensions are in the order of nanometers, we are dealing with isodimensional nanoparticles, such as spherical silica nanoparticles obtained by in situ sol gel methods [1,2] or by polymerization promoted directly from their surface [3], but also can include semiconductor nanoclusters [4] and others . When two dimensions are in the nanometer

scale and the third is larger, forming an elongated structure, we speak about nanotubes or whiskers as, for example, carbon nanotubes [5] or cellulose whiskers [6,7] which are extensively studied as reinforcing nanofillers yielding materials with exceptional properties. The third type of nanocomposites is characterized by only one dimension in the nanometer range. In this case the filler is present in the form of sheets of one to a few nanometer thick to hundreds to thousands nanometers long. This family of composites can be gathered under the name of polymer-layered crystal nanocomposites.

Amongst all the potential nanocomposite precursors, those based on clay and layered silicates have been more widely investigated probably because the starting clay materials are easily available and because their intercalation chemistry has been studied for a long time [8,9]. The important characteristics pertinent to application of clay minerals in polymer nanocomposites are their richest intercalation chemistry, high strength and stiffness and high aspect ratio of individual platelets, abundance in nature and low cost. First, their unique layered structure and high intercalation capabilities allow them to be chemically modified to be compatible with polymers, which makes them particularly attractive in the development of clay-based polymer nanocomposites. In addition, their relatively low layer charge ($x = 0.2-0.6$) means a relatively weak force between adjacent layers, making the interlayer cations exchangeable. Therefore, the intercalation of inorganic and organic cations and molecules into the interlayer space are facile, which is an important aspect of their uses in polymer nanocomposite manufacturing. Among the smectite clays, MMT and hectorite are the most commonly used ones while others are sometimes useful depending on the targeted applications. Moreover, although smectite clays are naturally not nanoparticles, they can be exfoliated or delaminated into nanometer platelets with a thickness of about 1 nm and an aspect ratio of 100–1500 and surface areas of 700–800 m²/g. Each platelet has very high strength and stiffness and can be regarded as a rigid inorganic polymer whose molecular weight (ca. 1.3×10^8) is much greater than that of typical polymer. Therefore, very low loading of clays is required to achieve equivalent properties compared to the conventional composites. Finally, and importantly, they are ubiquitous in nature and therefore inexpensive. Owing to the nanometer-size particles obtained by dispersion, these nanocomposites exhibit markedly

improved mechanical, thermal, optical and physico-chemical properties when compared with the pure polymer or conventional (microscale) composites. There are several reviews and books published highlighting the major developments in this area of polymer/clay nanocomposites and discuss various preparation techniques, characterization and the properties that those materials can display; their potential and commercial applications [10-25]. Here in this chapter, a brief overview of preparation, properties and application of polymer clay nanocomposites were discussed with a special emphasis on choice of the organoclay and organo-modification for the preparation of various polymer clay nanocomposites.

1.2 Structure of clay and the organoclay:

The layered silicates commonly used in nanocomposites belong to the structural family known as the 2:1 phyllosilicates. Their crystal lattice consists of two-dimensional layers where a central octahedral sheet of alumina or magnesia is fused to two external silica tetrahedron by the tip so that the oxygen ions of the octahedral sheet do also belong to the tetrahedral sheets as shown in Figure 1.1.

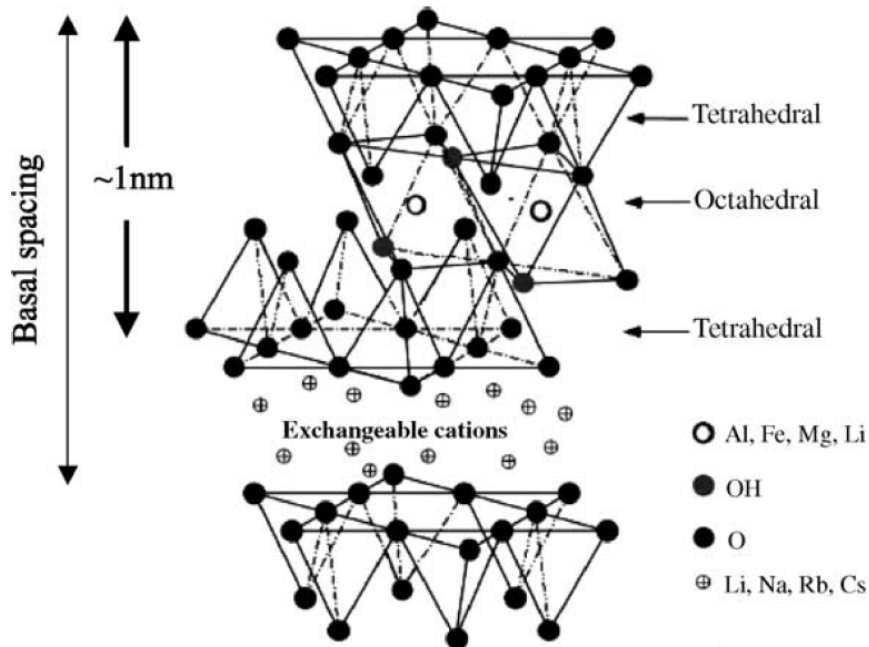


Figure 1.1: Structure of 2:1 Phyllosilicate

The layer thickness is around 1 nm and the lateral dimensions of these layers may vary from 300 Å to several microns and even larger depending on the particular silicate. These layers organize themselves to form stacks with a regular van der Waals gap in between them called the interlayer or the gallery. Isomorphic substitution within the layers (for example, Al^{3+} replaced by Mg^{2+} or by Fe^{2+} or Mg^{2+} replaced by Li.) generates negative charges that are counterbalanced by alkali or alkaline earth cations situated in the interlayer. As the forces that hold the stacks together are relatively weak, the intercalation of small molecules between the layers is easy [8].

In order to mix these hydrophilic layered silicates with polymers, it has to be modified into organophilic (organoclay) by exchanging the cations of the interlayer with cationic surfactants such as alkylammonium or alkylphosphonium (onium) salts. The maximum extent to which these cations can be exchanged is called cation exchange capacity (CEC), and generally expressed in mequiv/100 g. Montmorillonites, hectorite and saponite are the most commonly used layered silicates. The organoclays prepared were generally characterized by WAXD and TGA. Depending on the chain length of the onium cations, and the way in which it aligns in the interlayer gallery, the interlayer distance changes and can be characterized by observing the characteristic shift for the 001 peak by WAXD. The organic content in the organoclay can be obtained from thermogravimetric analysis by measuring the weight loss at 900 °C. In some of the studies, for reducing the hydrophilicity of the clays, the hydroxyl groups at the edges of the platelets were reacted with silane coupling agents.

Nowadays, several pristine and organoclays are available commercially. Commercial organoclays include Cloisite 10A, 15A, 20A and 30B produced from Southern Clay Products (U.S.A.) [26], Bentone 107, 108, 109 and 2010 from Elementis Specialties Company [27], Nanomer 1.30P, 1.31PS, 1.44P, 1.44PS, 1.44PT and 1.28E from Nanocor, Inc. (U.S.A.) [28], Nanofil 2, 5, 9, SE 3000 and SE 3010 from Sud-Chemie (Germany) [29] as well as Dellite 72T from Laviosa Chimica Mineraria (Italy). Synthetic fluoromica clays (Somasifl ME100) are supplied to Asian customers by Co-op Chemicals, Japan. Most of these commercially available organoclays were modified with ammonium cations and few of them were with silane modification. Other than these above-mentioned commercial organoclays there were several reports on the use of

custom modified organoclays depending on the method of preparation and the polymer matrix.

1.3 Types of polymers used for nanocomposites preparation with layered silicate: Although the intercalation chemistry of polymers when mixed with appropriately modified layered silicates has long been known [30, 8], the field of PLS the field of nanocomposites has gained momentum recently. Two major findings have stimulated the revival of interest in these materials: first the report from the Toyota research group of a nylon-6 (N6)/montmorillonite nanocomposite, which showed pronounce improvements in thermal and mechanical properties; and second the observation by Vaia et al that it is possible prepare naocomposite by melt mixing the polymers with layered silicates. Today efforts are being conducted globally, using almost all types of polymer matrices. The large variety of polymer systems used in nanocomposites preparation with layered silicate can be conveniently classified into vinyl polymers, condensation polymers, polyolefins, speciality polymers and biodegradable polymers and were thoroughly reviewed elsewhere.

1.4 Nanocomposite structure and their characterization. The nanocomposites can be classified into three types depending on the structure and arrangement of the clay in the polymer matrix as shown in Figure 1.2. They are (a) Intercalated nanocomposites, in which the polymer chains are inserted in the interlayer gallery and increases the interlayer distance resulting in a well ordered multilayer morphology built up with alternating polymeric and inorganic layers. (b) flocculated nanocomposites which are similar to intercalated nanocomposites where in the clay platelet sizes have been increased by flocculation due to hydroxylated edge-edge interaction. (c) exfoliated or delaminated nanocomposites, where the individual clay layers are separated and uniformly distributed in a continuous polymer matrix.

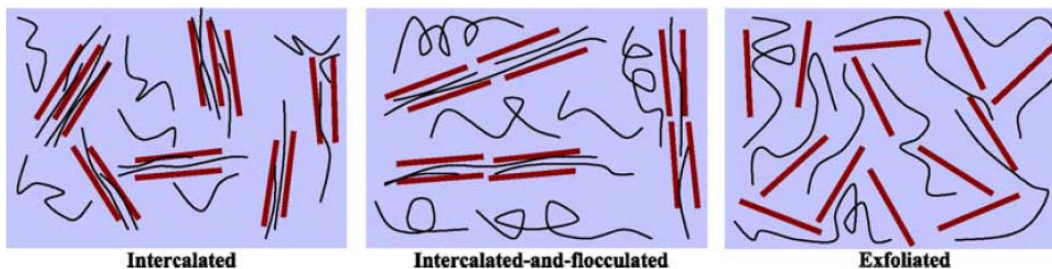


Figure 1.2: Structure of nanocomposites

X-ray diffraction (XRD) is commonly used for the characterization of the structure of nanocomposites. For an intercalated structure, the (0 0 1) characteristic peak for the organoclay tends to shift to lower angle regime due to the expansion of the basal spacing as show in fig. Although the layer spacing increases, there still exists an attractive force between the silicate layers to stack them in an ordered structure. In contrast, no peaks are observed in the XRD pattern of exfoliated polymer nanocomposites due to loss of the structural registry of the layers. The absence of Bragg diffraction peaks in the nanocomposites may indicate that the clay has been completely exfoliated or delaminated as shown in Figure 1.3 [31].

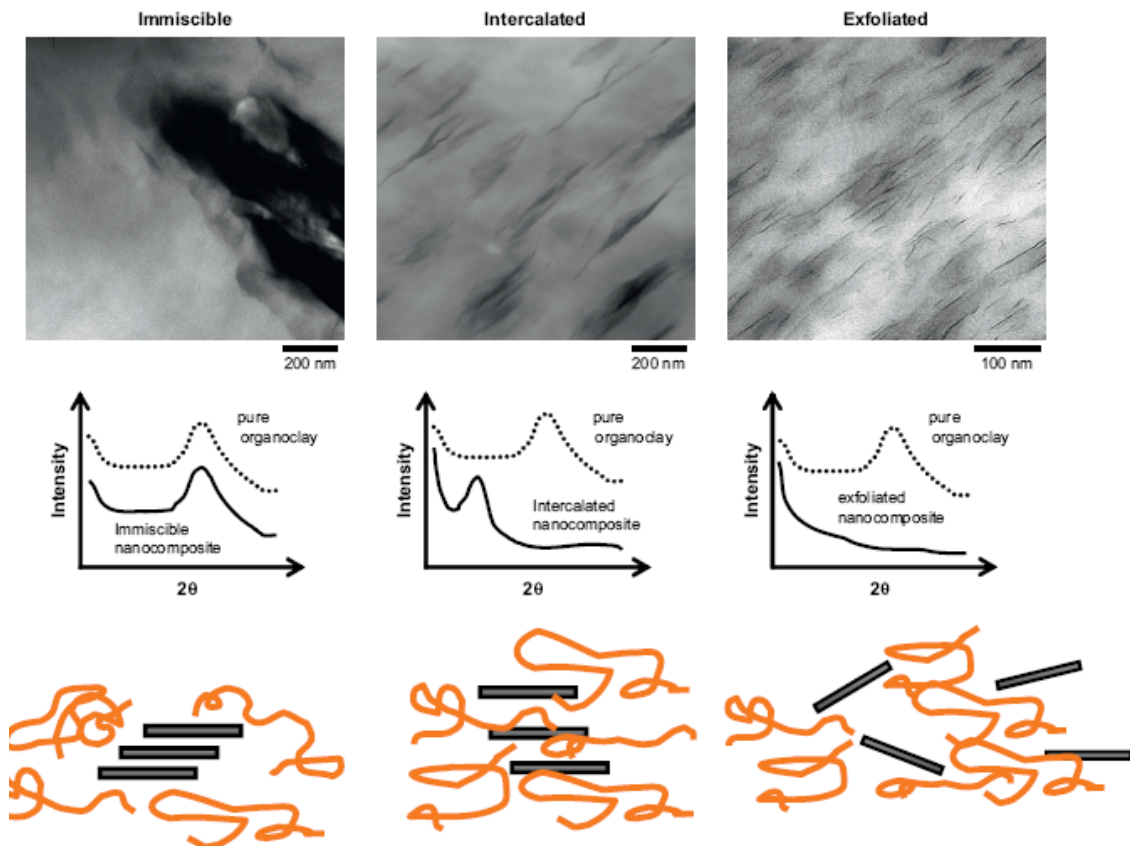


Figure 1.3: Illustration of different states of dispersion of organoclays in polymers with corresponding WAXS and TEM results.

The absence of Bragg diffraction peaks in the XRD patterns should not be used as the sole evidence for the formation of an exfoliated structure. Morgan and Gilman [32] and

Eckel et al. [33] pointed out that XRD analysis alone could lead to false interpretations of the extent of exfoliation. Several factors such as clay dilution, peak broadening and preferred orientation make XRD characterization of polymer nanocomposites susceptible to errors. Further transmission electron microscopic observation is needed to confirm formation of exfoliated nanocomposites [33]. XRD does not yield the information relating to the spatial distribution of the silicate in the polymer matrix because all its data are averaged over the whole regions of the specimen. On the other hand, transmission electron microscopy (TEM) can provide useful information in a localized area on the morphology, structure and spatial distribution of the dispersed phase of the nanocomposites. Vaia et al. indicated that the features of the local microstructures from TEM give useful detail to the overall picture that can be drawn from the XRD results [34]. Thus XRD and TEM techniques are regarded as complementary to each other for materials characterization of the clay–polymer nanocomposites. Besides these two well defined structures, other intermediate organizations can exist presenting partial intercalation and exfoliation. To confirm these structures, TEM offers a qualitative understanding of the internal structure, spatial distribution of various phases, and views of the defect structure through direct visualization.

1.5 Methods of preparation of nanocomposite: Several strategies have been considered to prepare polymer-layered silicate nanocomposites. They include

1.5.1 Intercalation of polymer or prepolymer from solution: When the polymer solution was mixed with dispersion of clay, the polymer chains intercalate and displace the solvent within the interlayer of the silicate. Upon solvent removal, the intercalated structure remains, resulting in the nanocomposite formation. The entropy gained by desorption of small molecules of solvent, which compensates for the decrease in conformational entropy of larger size of intercalated polymers acts as the driving force for the formation of nanocomposites. Requirement of large quantities of solvents and non-availability of many compatible polymer- clay solvent system limits the use of this method.

1.5.2 *In-situ intercalative polymerization method:* In this method, the layered silicate is swollen within the liquid monomer or a monomer solution so that the polymer formation can occur between the intercalated sheets. Polymerization can be initiated either by heat or radiation, by the diffusion of a suitable initiator, or by an organic initiator or catalyst fixed through cation exchange inside the interlayer before the swelling step.

1.5.3 *Melt intercalation method:* This method involves annealing, statically or under shear, a mixture of the polymer and OMLS above the softening point of the polymer. This method has great advantages over either in situ intercalative polymerization or polymer solution intercalation. First, this method is environmentally benign due to the absence of organic solvents. Second, it is compatible with current industrial process, such as extrusion and injection molding.

The enhancement of the mechanical properties depends on the interaction of the polymer chains on the clay platelet surface. This is mainly affected by amount of the clay loading and extent of dispersion so as to allow maximum platelet surface available to interact. Therefore the key issue in the design of polymer–clay nanocomposites is to monitor the dispersion of clay platelets on nanometer scale in a polymer matrix. Accordingly, it is necessary to understand the interaction between the clay surfaces and the intercalants to prepare exfoliated clay–polymer nanocomposites. In other words, understanding the structure of organoclays and the interaction of surfactant–clay is of crucial importance in design, fabrication and characterization of exfoliated nanocomposites.

1.6 Choice of the organoclay: Proper selection of organoclays depends mainly on the type of polymer matrix used. Fornes et al. investigated the effect of the structure of alkylammonium compounds on the dispersion of MMT in polyamide-6 during melt compounding [35]. They reported that the alkylammonium compound consisting of one alkyl tail is more effective than the quaternary cation having two alkyl tails in forming exfoliated nanocomposites. They explained this in terms of the competition between the effects of platelet–platelet interactions and the interaction of the polymer with the organoclay platelet. Polyamide-6 because of its polarity or strong hydrogen-bonding

characteristic has some affinity for the pristine surface of the clay. In this case, the organic modifier consisting of two alkyl tails shields more silicate surface than one alkyl tail, thereby precluding desirable interactions between the polyamide and the clay surface [35]. On the other hand, nanocomposites made from a non-polar polymer like linear low-density polyethylene (LLDPE) showed complete opposite trends. In that case, the two-tailed organoclay formed nanocomposites exhibit better exfoliation and mechanical properties than a one-tailed organoclay [36]. Manias et al. demonstrated that the polypropylene–MMT nanocomposite formation can be achieved by two ways, i.e. either by using neat polypropylene and semi-fluorinated surfactants for the silicates, or by using functionalised polypropylenes and common organo-montmorillonites [37,38]. In the first case, a semi fluorinated alkyltrichlorosilane ($\text{CF}_3\text{-(CF}_2)_5\text{-(CH}_2)_2\text{-Si-Cl}_3$) was used to modify C18-MMT, rendering it miscible with neat or unfunctionalised PP. This surfactant was tethered to the MMT surface through a reaction of the trichlorosilane groups with hydroxyls in the cleavage plane of the MMT. In the second case, several functional groups were grafted to PP in a random-copolymer fashion. The functionalized PP samples were aimed to render the polymer–MMT interactions more thermodynamically favorable than the surfactant– MMT interactions.

As mentioned above, interactions between the PA6 chains and pristine MMT via hydrogen bonding facilitate the intercalation of PA6 molecules into the galleries of MMT. In general, organic molecules can intercalate the galleries of the clays by interacting with the clay surface via ion–dipole, dipole–dipole and hydrogen bonding [39-41]. Recently, Hansen solubility parameters, $\delta_t^2 = \delta_d^2 + \delta_p^2 + \delta_h^2$ [42,43] has been adopted by the researchers to characterize the dispersion of organoclays in organic solvents [39-41]. The parameters take the dispersive (δ_d), polar (δ_p) and hydrogen-bonding (δ_h) forces acting together to disperse MMT in various solvents into account. It is noted that Hildebrand and Scott proposed the original definition of solubility parameter, $\delta = (E/V)^{1/2}$, where E is the molar cohesive energy and V is the molar volume. The cohesive energy is the energy associated with the net attractive interactions of the material. This is a well established approach for characterizing the inorganic powder (e.g. carbon black) dispersion in solvents [44]. Hansen then extended the Hildebrand

parameter to polymer–solvent systems, particularly for polar and hydrogen bonding interactions [41-43]. Ho et al. demonstrated that Cloisite 15A dispersed in chloroform was fully exfoliated, whereas it formed tactoids in benzene, toluene and p-xylene, which possess different values of solvent solubility parameter [39.] They further indicated that the polar (δ_p) and hydrogen bonding (δ_h) forces affect primarily the exfoliated structure or tactoid formation of the suspended platelets in particular solvents [40]. Similarly, Choi et al. reported that δ_h is an important factor for the dispersion state of Na-MMT in a liquid or solvent. The polar components (δ_p) and hydrogenbonding components (δ_h) of organic liquids determined the dispersion and basal spacings of Na-MMT in various solvents and monomers [41-43]. The Hansen solubility parameters are particularly useful for the preparation of polymer–clay nanocomposites via the solution intercalation route [47].

1.6.1 Thermal stability of the modifiers

The quaternary ammonium ion is nominally chosen to compatibilize the layered silicate with a given polymer resin. However, the molecular structure, such as alkyl chain length, number of alkyl chains and unsaturations, is also the determining factor of the thermal stability of the polymer/MMT nanocomposites [48]. Although these modification agents have been gaining significant success in the preparation of polymer/MMT nanocomposites, their common shortcoming is the poor thermal stability. The thermal stability of the organoclay component is of major importance, as many polymer composites are either melt-blended or intercalated at high temperatures to yield distribution of filler in the nanoscale. All the nanocomposite components may be subjected to high temperatures during preparation process, further processing and service time. If the processing temperature is higher than the thermal stability of the organoclay, then decomposition occurs, and the interface between the filler and the matrix polymer is effectively altered. There has been done a substantial work on studying the degradation process of organoclays and nanocomposites as well as significant successes were noted in the elaborating of thermally stable organic modifiers for compatibilizing the clay and polymer matrix, but still some questions remain unanswered.

To circumvent the detrimental effect of the lower thermal stability of alkyl ammonium-treated MMT, several works have been dealing with preparation of alkyl-imidazolium molten salts treated MMT clays *via* ion exchange of the Na^+ -MMT with imidazolium salts and compared them to the conventional quaternary alkyl ammonium MMT [49,50]. Ngo et al. [51] and Begg et al. [52] found out that imidazole is resistant to ring fission during thermal rearrangements of 1-alkyl- and 1-aryl-imidazoles at temperatures above 600 °C, thus indicating that the imidazolium cation was more thermally stable than the alkyl ammonium cation. Notably, earlier research indicated that the facility with which various groups are cleaved from quaternary salts involves $\text{S}_{\text{N}}1$ or $\text{S}_{\text{N}}2$ mechanisms [53]. The pyrolysis of the imidazolium quaternary salt proceeds most likely *via* $\text{S}_{\text{N}}2$ process (Figure 1.4).

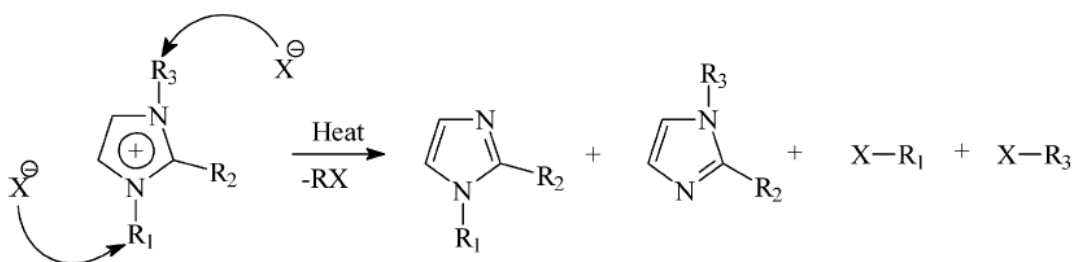


Figure 1.4: Degradation of the imidazolium quaternary salt according to $\text{S}_{\text{N}}2$ mechanism

Awad et al. [49] studied also the influence of the anion type on thermal stability of the imidazolium salts. The hexafluorophosphate, tetrafluoroborate and bis(trifluoromethylsulfonyl)imide salts showed more than 100 °C increase in the onset decomposition temperature compared to the halide salts. The thermal stability increased in the order: $\text{PF}_6 > \text{N}(\text{SO}_2\text{CF}_3)_2 > \text{BF}_4 > \text{Cl}, \text{Br}$. Additionally, the imidazolium thermal stability was affected by the type of isomeric structure of the alkyl side group. This was evidenced by the observation that both 1-butyl-2,3-dimethyl-imidazolium tetrafluoroborate and hexafluorophosphate salts had higher onset decomposition temperature than 1,2-dimethyl-3-isobutyl-imidazolium tetrafluoroborate and hexafluorophosphate salts, respectively. The degradation reaction presumably proceeds *via* $\text{S}_{\text{N}}1$ reaction since the cleavage of the tertiary carbon atom is likely to occur (Figure 1.5).

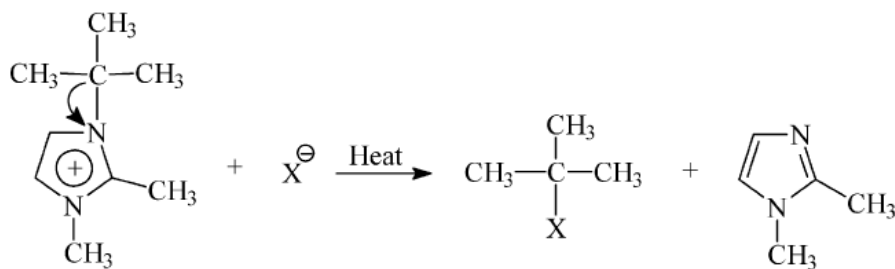


Figure 1.5: Degradation of the imidazolium quaternary salt according to SN1 mechanism

Further, methyl substitution in the 2-position (i.e. between the two N atoms) has been reported to enhance the thermal stability [55]. This is evident from the increase in the onset decomposition temperature of both 1-butyl-2,3-dimethyl-imidazolium chloride and 1,2-dimethyl-3-hexadecyl-imidazolium chloride compared to 1-butyl-3-methyl-imidazolium chloride and 1-hexadecyl-3-methyl-imidazolium chloride, respectively; this effect may be due to the high acidic character of the C2 proton. The experimental results concerning the thermal stability of imidazolium intercalated MMT showed a great increase as compared to ammonium-modified MMT. Moreover, higher thermal stability was observed for dimethyl hexadecyl-imidazolium-intercalated MMT than the dimethyl hexadecyl-imidazolium chloride and bromide salts, which was explained as due to the removal of the halide effect. However, it was observed that there was no significant improvement in the thermal stability of the intercalated tetrafluoroborate and hexafluorophosphate compounds comparing to molten salts due to the weak nucleophilicity of BF_4^- and PF_6^- anions. The results also indicated that the thermo-oxidative stability of imidazolium-treated MMT decreased as the chain length of the alkyl group attached to the nitrogen atom increased. FTIR analysis of the decomposition products showed among decomposition products water, carbon dioxide and hydrocarbons [49]

Xie and coworkers explain the degradation mechanism for the organoclay obtained by phosphonium ion modification. According to their study, due to the greater steric tolerance of the phosphorus atom and the participation of its low-lying d-orbitals in the processes of making and breaking chemical bonds, phosphonium salts are generally capable of undergoing a wider range of reactions and behave differently than their ammonium counterparts toward an external base (B). The following types of reactions

have been established for tetraalkyl phosphonium salts under appropriate conditions (1) Nucleophilic substitution reaction at the α -carbon center, $[S_N(C)]$: where the attendant nucleophilic anion (e.g., a halide) displaces a triphenylphosphine group. This is effectively the reverse of the quaternization reaction. Because there is a change in oxidation state from the reactant (P at +5 oxidation state) to the product (P at +3 oxidation state), this reaction can also be regarded as a reductive elimination process.

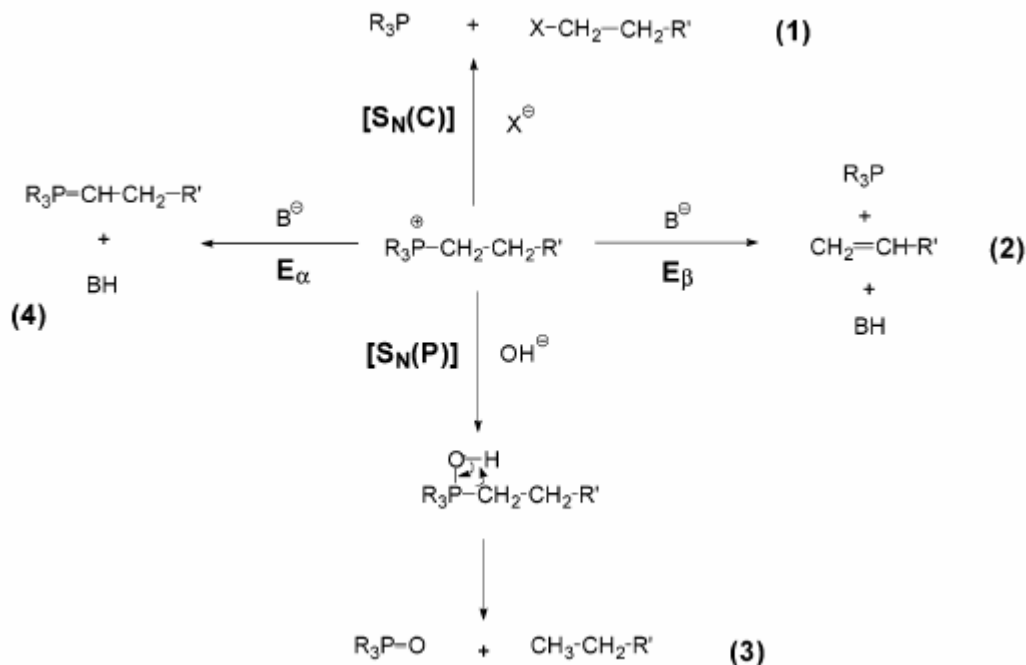


Figure 1.6: Degradation mechanism of phosphonium ion

(2) β -Elimination, E_β : where the β -proton is abstracted by a base in concert with the expulsion of triphenylphosphine from the α -carbon. (3) Substitution at phosphorus, $[S_N(P)]$: where a hydroxyl anion attacks the phosphorus center to form a five-coordinate intermediate, followed by concomitant separation of a phosphine oxide and an alkane. This reaction is primarily driven by the formation of a strong phosphoryl (P=O) bond. (4) α -Elimination, E_α : which is actually an α -proton abstraction process and the basis for the synthetically useful reaction for converting carbonyl compounds to olefins (Wittig reaction). However, this reaction typically requires a strong base such as alkyllithium or aryllithium reagents. Thus, reactions 1-3 are most likely to occur as the primary processes during the thermal decomposition of quaternary phosphonium compounds either in neat

state or intercalated within montmorillonite. Indeed, the pyrolysis/GC-MS of neat phosphonium salts indicated that both $[S_N(C)]$ and E_β elimination reactions are involved, confirmed by the presence of both alkenes and alkyl (or aryl) halides in the pyrolysis products. However, the $[S_N(C)]$ reaction is probably more favored in neat phosphonium salts at lower temperatures, considering the initial attack of the halide anion on the β -hydrogen is unfavored. Similar to the pristine salts, tertiary phosphine and long-chain olefins are observed as the decomposition products from the alkyl P-MMTs but at lower temperatures (250 vs 300 C). This indicates the occurrence of a β -elimination mechanism upon degradation of P-MMT. Additionally, phosphine oxide and octadecane are also detected from P-C18, consistent with the $[S_N(P)]$ pathway associated with hydroxyls along the sheet edge. The absence of alkyl halides indicates that the $[S_N(C)]$ reaction is suppressed by the removal of the bromide anion and replacement by the aluminosilicate sheet. The neat negative charge of the aluminosilicate is dispersed over numerous bridging oxygen, depending on the crystallographic location of the isomorphic substitution. The weak Lewis basicity of the siloxane surface is thought to be insufficient to drive the $S_N(C)$ reaction.

Thermal degradation studies of phosphonium ion modified montmorillonites were studied by TGA and pyrolysis/GC-MS. Thermal degradation on phosphonium ions such as triphenyldodecyl phosphonium(P-C12), tributyltetradecyl phosphonium(P-C14), tributylhexadecyl phosphonium(P-C16), tributyl octadecyl phosphonium(P-C18), tetraphenyl phosphonium(P-4Ph), tetraoctyl phosphonium(P-4C8) and ammonium ion such as tetraoctylammonium(N-4C8) were studied. It was shown that, the thermal decomposition process of phosphonium cations within montmorillonite follows multiple reaction pathways due to catalytic and morphological effects of the aluminosilicate matrix. In general, the nonisothermal decomposition behaviour for P-MMT and N-MMT share similar characteristics. β - elimination and nucleophilic substitution occur in both the cases. In contrast to previous studies on N-MMTs, the architecture of the phosphonium cation is reflected in the thermal stability of the P-MMTs. Comparison of P-C14, P-C16, and P-C18 indicates that the alkyl chain length does not influence the thermal stability of corresponding P-MMTs, paralleling previous observation from alkyl N-MMTs and in agreement with the anticipated decomposition reactions. However, the

stability of a longer chain, symmetric alkyl P-MMT, such as P-4C8, is ~ 30 °C greater than that of tributyl alkyl phosphonium MMTs, even though the stability of the salt is only slightly greater (0-5 °C). Similar dependence on architecture is not observed for N-MMTs. The initial decomposition temperature for tetraoctyl quaternary ammonium modified montmorillonite (N-4C8) and the corresponding salt is similar to that of other trimethyl alkylammonium MMTs and salts. The increased stability of P-4C8 probably reflects increased steric resistance around the P center inhibiting the bimolecular reactions at the P. The substantially greater stability of the tetraaryl phosphonium arises from the alternative decomposition pathways. When aryl alkyl phosphonium is present, such as triphenyl alkyl montmorillonite (P-C12), lower stability (~ 20 °C) relative to tetraaryl phosphonium is observed. Nonetheless, the stability is ~ 15 °C greater than tetraalkyl P-MMTs. The steric hindrance provided by the phenyl group is probably the major contributor to this behavior. Alternatively, the possibility of $p\pi-d\pi$ interactions between the P and phenyl groups, resulting in the delocalization of the positive charge can also diminish the susceptibility of the alkyl chain to β -elimination, increasing the thermal stability of P-C12.

1.6.2 In-situ polymerization and reactive modifiers for clay

It is strongly believed that the dispersion of the clay layers in the polymer matrix and the interaction of the clay layers with matrix affect the nanocomposite properties. The enhancements in the properties were maximum, when the clay layers are completely exfoliated and the interaction of the polymer chain with clay layers are strongest. It can be understood that when the interactions are stronger, the dispersion is also improved. Therefore to improve the interaction of the polymer chains with clay surface, the strategy used is to anchor the polymer chains on to the clay surface. This was achieved through anchoring the polymer chains with the clay modifiers, which are in turn anchored to the clay surface via ionic bonding. This can be achieved by designing suitable functional groups in the modifier of the clay which when reacted can anchor the polymer chains either during initiation of polymerization, or during the polymerization process or during the post polymerization process. To this end, there are several reports in the literature, with all types of polymers, which are prepared by various methods such as ring opening

polymerization, various radical polymerizations which include living radical polymerizations, olefin polymerizations, condensation polymerization, etc., reiterating the better dispersion of clay layers due to anchoring of the polymer chains. Some of the examples were shown in the literature, where the polymer was anchored to the clay surface through reactive modifiers during melt processing stage. In all these cases, it was shown that when the modifier does not have the reactive anchoring group, resulted in poor dispersion of clay as compared to the modifier with reactive anchoring group. Another strategy to disperse the clay is to design the locus of polymerization to be at the interlayer gallery so that the polymer chain grows inside the interlayer gallery and as the polymer chains grow pushes the clay layers apart and thus exfoliates the clay layers to give better dispersion.

1.6.2.1 Ring opening polymerization

The Toyota research group had first reported the ability of α , ω -amino acids ($\text{COOH}-(\text{CH}_2)_{n-1}-\text{NH}_2^+$, with $n=2,3,4,5,6,8,11,12,18$, modified Na^+ -MMT to be swollen by the ϵ -caprolactam monomer at 100 °C and subsequently initiate its polymerization to obtain nylon 6/MMT nanocomposites [56]. For the intercalation of ϵ -caprolactam, they chose the ammonium cation of ω -amino acids because these acids initiate the ring opening polymerization of ϵ -caprolactam and thus anchor the polymer chains on to the clay surface through the modifier by formation of amide bond. It has been shown that the chain length of the modifier amino acid plays crucial role in the swelling behavior of the organoclay with the monomer. A conceptual scheme for the synthetic method is presented in Figure 1.7.

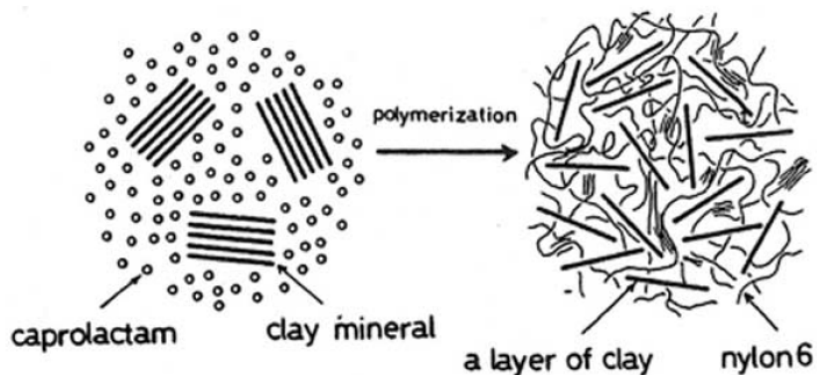


Figure 1.7: Schematic illustration for synthesis of Nylon-6/clay nanocomposite

Reichert et al also used the same method for the preparation of nylon12/MMT nanocomposite by in-situ ring opening polymerization of ω -lauryllactam. In a similar attempt to prepare polycaprolactone/clay nanocomposites, Messersmith and Giannelis [57] have used protonated ω -aminolauric acid to modify clay and prepare nanocomposite insitu ring opening polymerization of caprolactone to obtain uniformly dispersed and fully exfoliated nanocomposites.

1.6.2.2 Radical polymerizations

Akelah and Moet [58,59] used this insitu intercalative polymerization technique for the preparation of PS-based nanocomposites. They have used Na^+ MMT and Ca^+ MMT modified with vinylbenzyl trimethylammonium cation for the preparation of nanocomposites. The resulting nanocomposites were found to have intercalated structures and the extent of intercalation depends on the solvent used. Although PS anchors on to the clay surface through the copolymerization with vinyl moiety in the modifier, it did not result in exfoliation of clay may be because sufficient styrene monomer could not penetrate in to the clay gallery during polymerization, as the clay is not sufficiently organophilic. In an attempt to determine differences in thermal stability caused by organoammonium and phosphonium salt treatments of clay fillers in nanocomposites, Zhu et al [60] have studied the preparation of PS nanocomposites and found that the exfoliated nanocomposites were obtained when the modifier for the clay filler has a long alkyl chain and also a vinylbenzyl group which can copolymerize with styrene.

1.6.2.3 Condensation polymerizations.

The dispersability of the clay by using polar monomers or the precursor (prepolymers) for the polymers were exploited by dispersing the clay using the monomers or prepolymers with or without the use of suitable solvents followed by polymerization. There are several reports on the synthesis of PET/clay nanocomposites. Ke et al [61] have prepared PET/clay nanocomposite via in situ polymerization by dispersing the organoclay in water along with the monomers. Another route that developed by Nanocor, Inc. [62] is based on the novel exfoliation of clays into ethylene glycol using suitable modifier for the clay followed by insitu polymerization. Imai et al [63] reported the

preparation of high modulus PET/expandable fluorine mica nanocomposites with novel reactive compatibilizer, which can copolymerize with PET.

An insitu intercalative polymerization technique was successfully used by Hsu and Chang [64] in order to prepare polybenzoxazole (PBO)/clay nanocomposite from its polymer precursor polyhydroxyamide (PHA) and an organoclay. PHA/organoclay nanocomposite film was first prepared by solvent casting method in which dimethylacetamide was used as solvent. Finally, the exfoliated PBO/clay nanocomposite was obtained by curing the film to form benzoxazole ring.

A large number of reports discuss the preparation of various polyurethane (PU)/clay nanocomposite by in-situ polymerization. In some of the reports the PU/clay nanocomposites were prepared by dispersing the organoclay containing reactive hydroxyl groups with the polyol and followed by addition of diisocyanate monomer and the diol. In some of the reports, the nanocomposites were prepared by first mixing the organoclay containing hydroxyl group with isocyanate terminated prepolymer and allowed to react with the hydroxyls of the organoclay followed by addition of short chain diol to undergo polymerization. The presence of the reactive hydroxyl groups in the modifier for the clay showed improved properties for the nanocomposite prepared as compared to the nanocomposites prepared using organoclays containing no reactive hydroxyl groups. In another report, the organoclay/polyol nanocomposite was prepared in the first step by in-situ ring opening polymerization of caprolactone followed by chain extension with diisocyanates.

Leu et al [65] have prepared covalently bonded layered silicate/polyimide nanocomposites. Here amino functionalized –layered silicate (APTS-kenyaite) was mixed with poly(amic acid) (BTDA-ODA type) containing an anhydride end group, the amino group of APTS-kenyaite react with the anhydride end group of poly(amic acid) to form covalently bonded polymer tethered silicates. A schematic drawing of the formation process of polymer tethered APTS-kenyaite is presented in Figure 1.8.

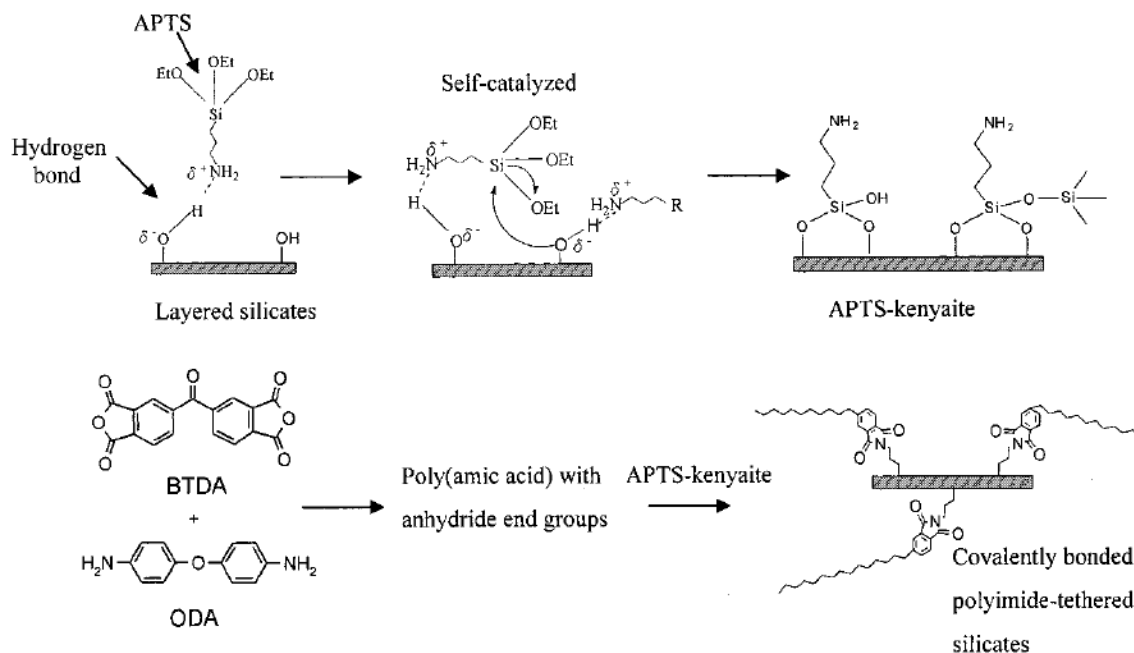


Figure 1.8: A schematic drawing of the formation process of polymer tethered APTS-kunyaite

1.6.2.4 Olefin polymerizations

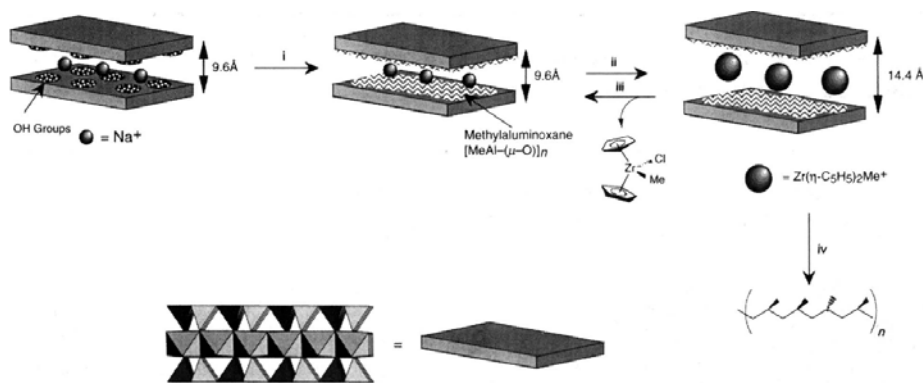


Figure 1.9: Schematic representation of the modification and ion-exchange of Laponite with $[Zr(\eta-C_5H_5)_2Me(thf)]BPb$ and propene polymerisation. *Reagents and conditions:* i, MAO, toluene, 24 h, room temp.; ii, $[Zr(\eta-C_5H_5)_2Me(thf)]BPb$, MeCN, 12 h room temp.; iii, NaCl, thf, 12 h, room temp.; iv, propylene, 5 bar, 45 °C, toluene.

For the preparation of polyolefin nanocomposites, Tudor et al [66] first used insitu polymerization method. Metallocene based catalyst, $([Zr(\eta-C_5H_5)_2Me(THF)]^+)$, for polymerization of polyolefins was intercalated into methylaluminoxane (MAO) treated layered silicate, by cation exchange reaction. When the polymerization of propylene was conducted using this intercalated catalyst, which forces the polymer to grow in the

interlayer gallery and delaminate the clay layers to give exfoliated PP/clay nanocomposites. Bergman[67] intercalated the clay with aliphatic 1-tetradecylammonium cations, to make an organically modified fluorohectorite. The exchanged fluorohectorite was mixed in toluene with a Brookhardt-type Pd catalyst [$\{2,6\text{-iPr}_2\text{C}_6\text{H}_3\text{N}=\text{C}(\text{Me})\text{C}(\text{Me})=\text{NC}_6\text{H}_3\text{iPr}_2\}\text{Pd}(\text{CH}_2)_3\text{CO}_2\text{-Me}][\text{B}(\text{C}_6\text{H}_3(\text{CF}_3)_{2-3,5})_4]$], and the white organoclay turned into an orange-brown product. Perfluoroborates were then used as an activator to initiate polymerization with ethylene at 80 psi of the monomer pressure and 22 °C. The recovered dry solid was a rubbery clay/ethylene nanocomposite. The catalyst had a turnover frequency of 162 h⁻¹. The X-ray powder diffraction of the nanocomposite showed disappearance of ordering in the clay structure during polymerization, indicating that the clay was exfoliated or became totally disordered. Using a MAO activator and quaternized clay fillers in an approach similar to Bergman's, Mulhaupt et al [68] made high-density polyethylene (PE)/montmorillonite nanocomposites with high catalyst efficiency. They showed that by decreasing the aliphatic hydrocarbon chain length in the alkylammonium cations from 18 to 4, the catalyst efficiency increases, which suggests a homogeneous polymerization process. Sun and Garces [69] reported the preparation of PP/clay nanocomposites by in situ intercalative polymerization with metallocene/clay catalyst under mild conditions. Jin et al [70] developed an in situ exfoliation method during the polymerization by fixing a Ti-based Ziegler-Natta catalyst at the inner surface of MMT. They have used organic salts with hydroxyl groups for the modification of MMT, because hydroxyl groups in intercalation agents offer facile reactive sites for anchoring catalysts in between silicate layers.

1.6.2.5 Living polymerization

Nanocomposites based on homo and copolymers of butadiene were prepared by in-situ living anionic polymerization in presence of organoclay, which are modified by exchanging with quaternary ammonium ions [71-73]. The dispersion of the organoclay improved by addition of toluene in the solvent medium or the styrene content in the copolymer was increased. The living nature of the reaction may be suspected because the molecular weights of the polymer obtained were quite broad. The molecular weight

distribution of the polymer matrix in the nanocomposites was fairly narrowed down when the edge hydroxyl groups on the clay were reacted with titanium coupling agents. [74]. Sogah et al [75] have prepared fully dispersed polystyrene clay nanocomposite by intragallery nitroxide mediated living free radical polymerization via silicate-anchored initiator. The structure of the organo-modifier used for the clay containing initiator moiety was shown in the Figure 1.10(a).

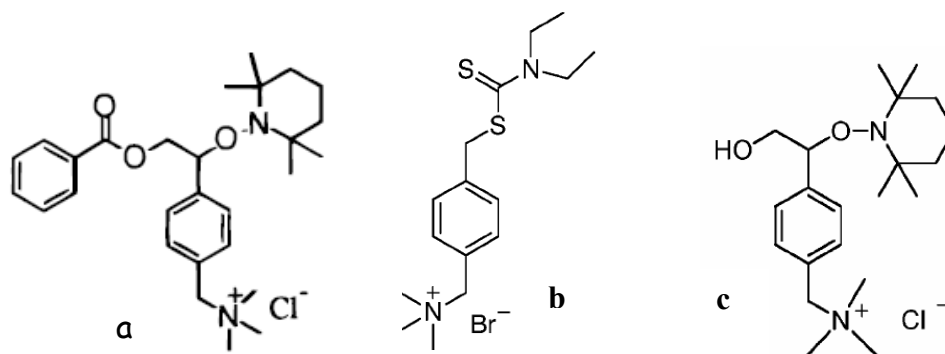


Figure 1.10: Structure of clay modifiers containing the initiator moiety

In an another effort for the direct preparation of dispersed polymer silicate nanocomposite via insitu living polymerization from silicate anchored initiators, Di and Sogah have designed and prepared a dithiocarbamate photoiniferter-modified silicate Figure 1.10(b). Subsequent living free radical polymerization of variety of monomers gave dispersed polymer silicate nanocomposites [76]. Thus PS, PMMA, PtBA/silicate nanocomposites were prepared with controlled molecular weight and PDI. They have also shown that by employing sequential monomer addition, polystyrene-b-polymethyl methacrylate /silicate nanocomposites were prepared. One principal finding is that exfoliated nanocomposite with very high silicate content (above 20 wt%) could readily be prepared which can be used as masterbatches in preparing all kinds of nanocomposite by simple blending. The same authors in an another report have shown that fully exfoliated poly(styrene-b-caprolactone)/silicate nanocomposites were prepared via one pot, one step in-situ living polymerization from silicate-anchored bifunctional initiator [77]. The structure of the initiator is shown in Figure 1.10(c). The polymer chains were attached to the surface of the silicate layers at the junction between the two blocks. The molecular weights of the polymer and the concentration of clay in nanocomposite were controlled

by diluting the initiator with non-initiating salt. Extensive study was done on atom transfer radical polymerization in the preparation of polymer nanocomposites using a copper catalyst and an initiator. Shipp et al have shown that block copolymer brushes based on poly(styrene-*b*-butyl acrylate) can be grown on the surface of exfoliated and intercalated clay layers by exchanging with organocations containing initiator moiety [78].

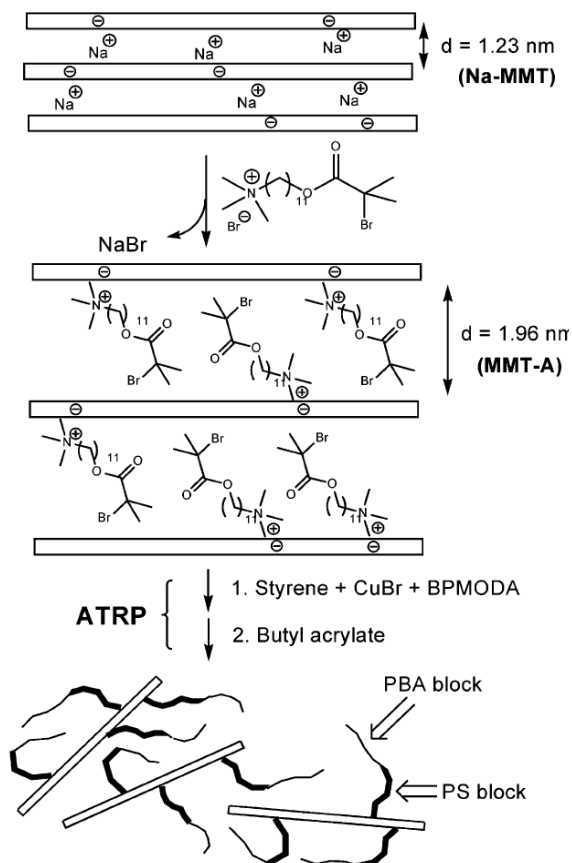


Figure 1.11: The schematic representation showing the exchange of cations in clay with organocations containing initiator moiety for insitu ATRP

The homopolymer clay nanocomposites of MMA, styrene and n-butyl acrylate were prepared by insitu atrp with predictable molecular weights and low dispersities, both characteristics of living radical polymerization. [79] Mathias et al have prepared covalently functionalized laponite clay through a condensation reaction of the clay silanol groups with mono and trifunctional alkoxy silanes [80]. The work focus on primary amine containing modification through APS treatment. Attaching primary amines to the edges

of clay opens up a wide range of possible functionalization reactions. Thus APS treated clay was reacted to give attached methacrylate, benzophenone and tertiary bromine groups capable of polymerization, photoinitiation, ATRP initiation respectively. Reaction schemes are shown in Figure 1.12.

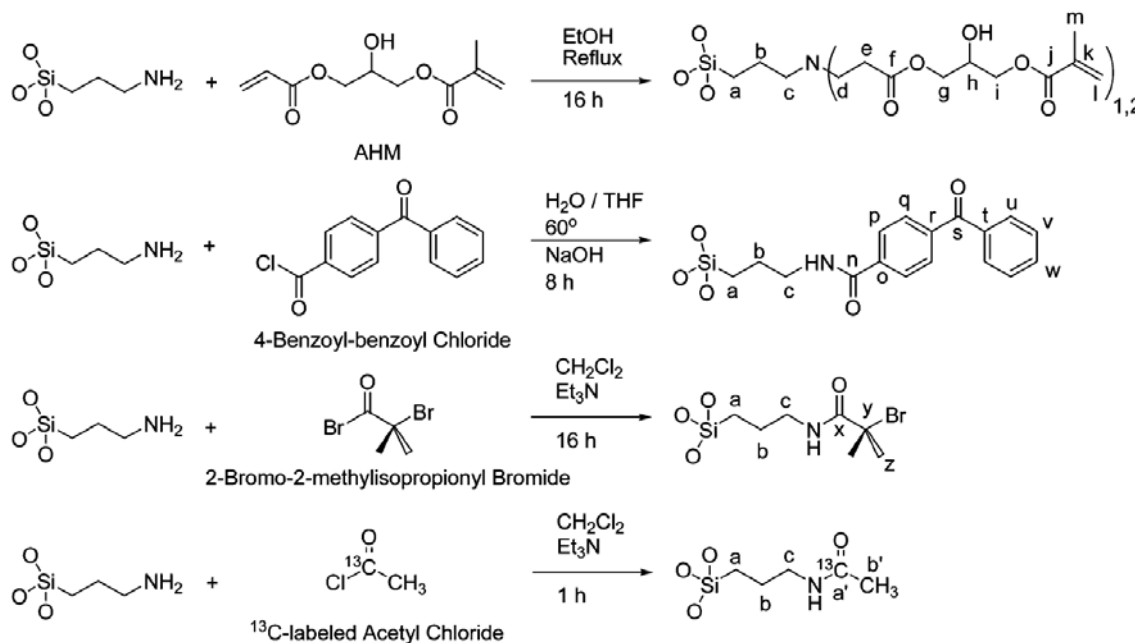


Figure 1.12: Reactions of amine functionalized clay to give various other functionalities

Covalantly bonded layered silicate/polystyrene nanocomposites were synthesized via ATRP in presence of initiator modified layered silicate based on megadite [81]. Wang et al have shown that exfoliated PS-PMMA-PS triblock copolymer/clay nanocomposites can be prepared by insitu ATRP. [82] Bhowmick et al have prepared polyethylacrylate /clay nanocomposites by insitu ATRP and shown that the rate of ATRP has improved in presence of organoclay which may be due to the interaction of carbonyl of the monomer with the clay surface.

1.6.2.6 Thermoset polymers

Messersmith and Giannelis [83] first reported the preparation of epoxy resin based nanocomposites with clay. They analyzed the effects of different curing agents and curing conditions on the formation of nanocomposites based on the diglycidyl ether of bisphenol A (DGEBA), and Cloisite

30B. Subsequently, Pinnavaiah et al, in a series of reports have studied the effect of various parameters on the preparation and properties of the clay nanocomposites based on epoxy resin DGEBA. The effect of acidity of the organoclay used for the preparation of nanocomposite based on DGEBA was studied by using modifiers for the clay with a series of acidic cations and found that with decreasing acidity of the modifier cation, the epoxy-clay delamination temperature has increased [84]. The effect of alkyl chain length of the modified MMT was studied and shown that the structures obtained such as an intercalated, partially exfoliated or fully exfoliated depends on the alkyl chain length of the modifier [85]. There are various reports to study the effect of CEC of the organoclay, type of modifiers on the preparation of nanocomposites based on DGEBA, which are cured with different amines [86-88]. Simon et al [89] have reported the morphology, thermal relaxation and mechanical properties the clay nanocomposites based on epoxies with varying epoxy functionalities. Three different types of resins were used: bifunctional DGEBA, trifunctional triglycidyl p-aminophenol (TGAP), and tetrafunctional tetraglycidyl diaminodiphenylmethane (TGDDM). All were cured with diethyltoluenediamine. MMT modified with octadecylammonium cation was used for the preparation of nanocomposites. The nanocomposites based on higher functionalities showed poor dispersion of clay as compared to the nanocomposites based on DGEBA. Chen et al have studied the exfoliation mechanism and thermal–mechanical properties of surface-initiated epoxy nanocomposites. Time-resolved high-temperature X-ray diffraction, DSC, and isothermal rheological analyses revealed that the interlayer expansion mechanism might be separated into three stages. These stages relate to the initial interlayer expansion, the steady-state interlayer expansion, and the cessation of interlayer expansion. It was found that differences in the activation energies of interlayer expansion and of curing influence the final nanostructures of the materials. This was ascribed to the evolving modulus of the extragallery polymer such that the interlayer expansion stopped when the modulus of the extragallery polymer became equal to or exceeded the modulus of the intragallery polymer. Variations in ultimate properties were attributed to the formation of an interphase layer, where the interphase is hypothesized to be the epoxy matrix plasticized by surfactant chains.

1.6.3 Polymeric surfactant modifiers

A variety of types of polymerically modified clays, including one-end terminated, α - ω two-end terminated, and multiple-cation containing polymeric “surfactants” have been synthesized and used for the modification of layered silicates and clays and was thoroughly reviewed [90]. These polymerically modified nanofillers are usually highly expanded compared to the common organo-clays based on cationic surfactants such as alkyl ammoniums. The polymerically modified clays usually show outstanding thermal stability and may be directly melt compounded with various polymers, i.e., a compatibilizer or a masterbatch is not required even for polyolefin systems. Polymerically modified clay and polymer matrices are frequently immiscible, but with proper design of the polymerically modified clay and the processing conditions, the clay clusters can be significantly reduced in size and can become well-dispersed, and thus nanocomposite formation can still be achieved. In addition, polymeric “surfactants” as organic modifications for clay offer unparalleled opportunities to incorporate additional functionalities that target specific property improvements, beyond the dispersion of the fillers in the polymer matrix. For example, incorporating phosphate moieties in polymeric “surfactants” for clays can significantly reduce the flammability of the nanocomposite.

1.7 Properties of nanocomposites

1.7.1 Mechanical properties

The polymer–clay nanocomposites exhibit extremely large interface polymers due to the confinement of polymer chains within the galleries of clay platelets of large surface area per unit volume. It is considered that the confinement of polymer–clay interactions would affect the local chain dynamics to a certain extent. Since several chemical and physical interactions are governed by surfaces, polymer–clay nanocomposites can have substantially different properties from conventional polymer microcomposites. Several micromechanical models have been developed to predict the macroscopic behavior of polymer microcomposites. These include Halpin–Tsai, Mori–Tanaka, etc. The models generally include a simple route for evaluating individual contributions of component properties such as the matrix and the filler modulus, the volume fraction, the filler aspect ratio, the filler orientation, etc.

Halpin and Tsai developed a well-known composite theory for predicting the stiffness of unidirectional composites as a function of aspect ratio [91-93]. This theory is based on the early micromechanical works of Hermans [94] and Hill [95]. Hermans generalized the form of Hill's self-consistent theory by considering a single fiber encased in a cylindrical shell of the matrix that is embedded in an infinite medium assumed to possess the average properties of the composite. Halpin and Tsai reduced Herman's results into a simpler analytical form adapted for a variety of reinforcement geometries, including discontinuous filler reinforcement. The overall composite moduli E_c can be predicated by:

$$\frac{E_c}{E_m} = \frac{1 + \zeta\eta\phi_f}{1 - \eta\phi_f}$$

where η is given by

$$\eta = \frac{E_f/E_m - 1}{E_f/E_m + \zeta},$$

where E_c , E_f , and E_m represent the overall Young's modulus of the composite, filler, and matrix, respectively, ϕ_f is the volume fraction of the filler, ζ is a shape parameter dependent upon the geometry of the filler and the loading direction, which is a function of aspect ratio L/t :

$$\zeta = f\left(\frac{L}{t}\right)$$

To calculate the aspect ratio of filler in intercalated nanocomposites, where the polymer chains have penetrated in the interlayer gallery and the particle is swollen, the whole intercalant cluster can be considered as the filler particle and the stiffness ratio is also obtained by considering the whole cluster. The theory predicts that the dependency of various parameters on the ratio of modulus of the nanocomposite to the matrix polymer. Particles with large aspect ratio L/t or high stiffness ratio E_f/E_m prove to be more efficient in enhancing stiffness of the nanocomposite. Therefore, The results show that exfoliation is favored over intercalation as far as the enhancement of the composite modulus is concerned. Of course, for all composite theories the properties of the matrix

and filler are considered to be identical to those of the pure components. Therefore, numerous complexities arise when comparing the composite theory to the experimental composite data, particularly for polymer-layered silicate nanocomposites, as the interaction of the polymer chain with filler interface is ignored.

The importance of the interfacial strength and the nanofiller structure in polymer-clay nanocomposites has been demonstrated using a designed polymer and nanocomposite synthesis. Interfacial interaction determines how the polymer chain interacts with the clay sheet, how an effective nanophase is formed, and how effective the new nanophase constrains the surrounding polymers. In the studied polymer-clay nanocomposites, the matrix chain mobility is largely decreased. The modulus enhancement strongly relates to the volume of the added clay as well as to the volume of the constrained polymer. It has been shown that the significant modulus enhancement of the polymer-clay nanocomposites follows a power law with the content of the clay and can be modeled well by modified Mooney's equation.

$$\ln \frac{E}{E_1} = \frac{K_E \phi_2}{1 - \phi_2 / \phi_m}$$

where E is the modulus of the nanocomposite, E_1 is the modulus of the matrix, K_E is the Einstein coefficient, ϕ_2 is the volume fraction of the filler, and ϕ_m is the maximum volume fraction that the filler can have. K_E is a function of the interaction between the filler and the matrix as well as the aspect ratio of the filler. The stronger the interaction and the higher the aspect ratio of the filler, the higher the K_E is. The strong interaction between the clay and the polymer ensures a non-slippage interface. Under the non-slippage condition:

$$K_E = 2.5 \cdot (L/t)^{0.645}$$

An excellent fit is achieved when this Mooney power function is used to describe the observed modulus change with the amount of added clay. The modulus enhancement is dominated by the high aspect ratio of the clay platelet and the interfacial strength, through the Einstein coefficient, K , when the modulus of the matrix phase is much lower than that of the clay, i.e., $E_f / E_m > 100$. The study also suggests that the structure of clay nanocomposites with strong interfacial interaction is analogous to that of semicrystalline

polymers. Here, in this clay nanocomposite, the intercalated clay phase serves as an unmeltable crystalline phase to result in the improvement of mechanical properties.

Thus the enhancement in mechanical properties of polymer nanocomposites can be attributed to the high rigidity and aspect ratio together with the good affinity between polymer and organoclay. For instance, stronger interface interactions significantly reduce the stress concentration point upon repeated distortion which easily occurs in conventional composites reinforced by glass fibers and thus lead to weak fatigue strength. The unprecedented mechanical properties of nylon 6-clay nanocomposite synthesized by *in-situ* polymerization were first demonstrated by researchers at the Toyota Central Research Laboratories [96]. Such nanocomposites exhibit significant improvement in strength and modulus, namely, 40% in tensile strength, 60% in flexural strength, 68% in tensile modulus, and 126% in flexural modulus. The RTP Company has reported equivalent property enhancement of nylon 6-clay nanocomposites synthesized by direct melt intercalation [97]. The increase in modulus is believed to be directly related to the high aspect ratio of clay layers as well as the ultimate nanostructure. Moreover, a dramatically increase was also observed in exfoliated nanostructures such as MMT based thermoset amine-cured epoxy nanocomposite and magadiite-based elastomeric epoxy nanocomposite [98]. Figures 4 and 5 show the effect of clay loading on tensile modulus [96,98-100] and yield strength [101] of some polymer nanocomposites. In contrast, a relatively small increase was reported for the intercalated nanocomposites such as those from clay and polymethylmethacrylate (PMMA) [102] and PS [103]. The interaction strength at the interface would greatly affect the mechanical properties of polymer nanocomposites. For example, polar PMMA and ionic nylon 6 interacts with clay layers which may explain the stress increase for intercalated PMMA nanocomposites and exfoliated nylon 6 nanocomposites, respectively. The impact properties measured for nylon 6 nanocomposites showed that it was not affected much by the exfoliation process used.¹³⁹ In the case of polypropylene (PP) nanocomposite[104], the slight enhancement in tensile stress is attributed partially to the lack of interfacial adhesion between apolar PP and polar clays, which may be improved by adding maleic anhydride modified PP to the matrix. The tensile stress is even more decreased in PS intercalated nanocomposites due

to the weak interaction at PS and clay interface [59]. In thermoset nanocomposites, the exfoliation of clay minerals can also result in substantial property improvement, including enhanced mechanical properties, dimensional stability, thermal stability, chemical stability, resistance to solvent swelling, excellent transparency, together with high barrier property and reduced flammability of polymer nanocomposites. [105-107].

1.7.2 Barrier property:

Polymer nanocomposites have excellent barrier properties against gases (e.g., oxygen, nitrogen and carbon dioxide), water and hydrocarbons. Studies have showed that such reduction in permeability strongly depends on the aspect ratio of clay platelets, with high ratios dramatically enhancing gaseous barrier properties. The water permeability of exfoliated polyimide (PI) nanocomposites as shown in Figure 6 has been reported by Yano et al.⁴⁶ through the use of organoclays with different aspect ratios. The best gas barrier properties would be obtained in polymer nanocomposites with fully exfoliated clay minerals. Moreover, the aspect ratio of clay platelets was observed to affect greatly the relative permeability coefficient for PI filled with 2% of organoclay. The permeability to water vapor of exfoliated poly(caprolactone) (PCL) nanocomposites has also been investigated which indicates a dramatic decrease in the relative permeability with the increase of nanometer clay platelets [108]. The effect of clay loading on relative permeability coefficient of some polymer nanocomposites is shown in Figure 7 [109-112]. In addition, polymer nanocomposites have also shown better barrier properties against organic solvents such as alcohol, toluene and chloroform.

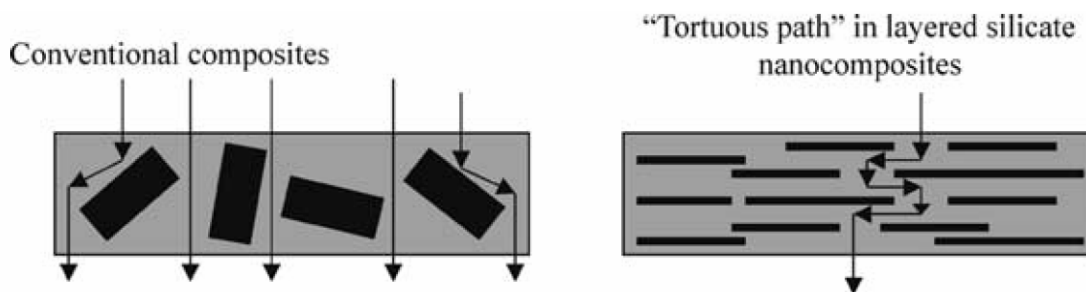


Figure 1.13: Formation of tortuous path in PLS nanocomposites

The enhanced barrier properties of polymer nanocomposites may be explained by the labyrinth or tortuous pathway model as proposed in Figure 13 [113]. When a film of polymer nanocomposites is formed, the sheet-like clay layers orient in parallel with the film surface. As a result, gas molecules have to take a long way around the impermeable clay layers in polymer nanocomposite than in pristine polymer matrix when they traverse an equivalent film thickness. It is interesting to note that the enhancement of barrier properties does not arise from the chemical interactions since it does not depend on the type of gas or liquid molecules.

1.7.3 Thermal properties of nanocomposites:

The thermal stability of polymer composites is generally estimated from the weight loss upon heating which results in the formation of volatile products. Blumstein [30] first reported the thermal stability improvement in PMMA nanocomposite, which showed that intercalated PMMA containing 10% clay degraded at about 40–50 °C higher than unfilled PMMA. Recently, there have been a great deal of reports on the improved thermal stability of nanocomposites made with various organoclays and polymer matrix.[60,114-116]. For example, the improvement in thermal stability is reported for cross-linked polydimethylsiloxane exfoliated with 10% of organomontmorillonite [117], and intercalated nanocomposites made from the polymerization of methyl methacrylate, [102] styrene [60,103,118] and epoxy precursors [119]. Due to characteristic structure of layers in polymer matrix, their shape and dimensions close to molecular level several effects have been observed that can explain the changes in thermal properties. Experimental results have shown that layers of MMT are impermeable for gases meaning that both intercalated and exfoliated structure get created in a labyrinth for gas penetrating the polymer bulk. Thus, the effect of ‘labyrinth’ limits the oxygen diffusion inside the nanocomposite sample. Similarly in the samples exposed to high temperature the MMT layers restrain the diffusion of gasses evolved during degradation. Moreover, MMT layers are thought to reduce heat conduction. In the presence of MMT layers strongly interacting with polymer matrix the motions of polymer chains are limited. This effect brings additional stabilization in the case of polymer/MMT nanocomposites. Nanocomposites exhibit more intensive char formation on the surface of sample exposed

to heat. It protects the bulk of sample from heat and decreases the rate of mass loss during thermal decomposition of polymeric nanocomposite material. More intensive formation of a char in comparison with pristine polymers can be indicative of improved flame resistance. The char formed in a case of nanocomposites performs higher mechanical resistance and therefore nanocomposites are considered as a potential ablative. The phenomena mentioned above are thought to retard the thermal decomposition processes through reducing the rate of mass loss—unfortunately, few works have been dedicated on the study of gases evolved from nanocomposites during thermal and thermo-oxidative degradation. The heat barrier effect could also provide superheated conditions inside the polymer melt leading to extensive random scission of polymer chain and evolution of numerous chemical species which, trapped between clay layers, have more opportunity to undergo secondary reactions. As a result, some degradation pathways could be promoted leading to enhanced charring. It is also suggested that the effect of more effective char production during thermal decomposition of polymer–clay nanocomposites may be derived from a chemical interaction between the polymer matrix and the clay layer surface during thermal degradation. Some authors indicated that catalytic effect of nano-dispersed clay is effective in promoting char-forming reactions. Nano-dispersed MMT layers were also found to interact with polymer chains in a way that forces the arrangement of macrochains and restricts the thermal motions of polymer domains. Generally, the thermal stability of polymeric nanocomposites containing MMT is related to the organoclay content and the dispersion. The synthesis methods influence the thermal stability of polymer/MMT nanocomposites as long as they are governing the dispersion degree of clay layers. Currently, extensive research is devoted to the synthesis of novel thermally stable modifiers (including oligomeric compounds) that can ensure good compatibility and improve the nanocomposite thermal stability due to low migration characteristics.

Another thermal behavior is the heat resistance upon external loading, which can be measured from the heat distortion temperature (HDT). The HDT of nylon 6 nanocomposites reported by Toyota researchers is increased from 65 °C of pristine nylon to 145 °C. The increase in HDT has also been observed in clay-based nanocomposites for other polymer systems such as PP [120] and poly-lactide (PLA) [121]. Such an increase

in HDT is very difficult to achieve in conventional polymer composites reinforced by micro-particles.

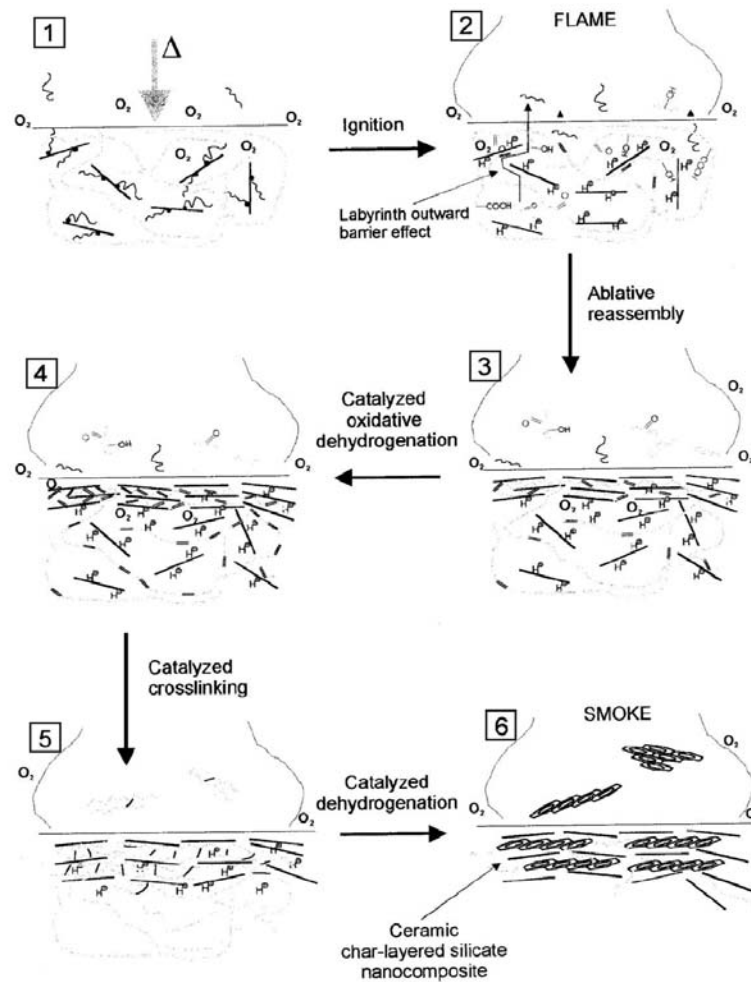


Figure 1.14: Schematic representation of combustion mechanism and ablative reassembly of a nanocomposite during cone calorimeter experiments.

Finally, flame retardancy and mechanical properties are both improved in clay-based polymer nanocomposites while the mechanical properties are always degraded in polymer composites with conventional flame-retardants. Such fire resistance of polymer nanocomposites is attributed to the carbonaceous char layers formed when burnt and the structure of clay minerals. The multi-layered clay structure acts as an excellent insulator and mass transport barrier. Char formation and clay structure impede the escape of the decomposed volatiles from the interior of a polymer matrix [122]. Gilman [115] has

recently reviewed the flame retardancy properties of nanocomposites. Flame retardancy is normally evaluated by the reduction of the peak of heat release rate (HRR).

1.7.4 Crystallization behavior

Crystallinity and crystallization behaviour of a polymer affects the structure and property of the material. In the polymer–clay nanocomposites, the dispersed clay particles in a polymer matrix always act as a heterogeneous nucleating agent for the spherulites, thereby reducing their sizes considerably. However, such nucleating effect of nanoclays is more pronounced at very low loading levels, ca. 1–5 wt.%. Above these levels, nanoclays may hinder the movement of polymers, thus retarding the crystallization of spherulites. The restricted mobility of the chains imposed by higher clay content would not allow the growth of well developed lamellar crystals [123]. The nanoclays play two roles in the crystallizations, i.e. a nucleating agent to facilitate the crystallization and a physical hindrance to retard the crystallization [124]. For the nanocomposites filled with low loading clay levels, the crystallization of polymers can be either enhanced or inhibited depending on the nature or property of polymers employed. According to the literature, enhanced crystallization of polymer due to the clay additions includes PA [125,126], PP [127,128], PE [129,130], PET [131], PBT [132,133], syndiotactic PS [134], polyvinylidene fluoride (PVDF) [134,137], etc. In some cases, the introduction of MMT filler hinders the crystallization of poly(ethylene oxide) (PEO). This is evidenced by a decrease of the spherulite growth and crystallization temperature on the basis of optical microscopy and DSC observations [138].

Apart from enhancing the crystallization rate, nanoclay platelets with large surface areas also enhance polymer–silicate interactions. In this regard, the addition of MMT fillers to polymers can stabilize a metastable phase and induce polymorphism. Typical examples are nanoclays stabilize the g-phase in polyamides [139-141] and the b-phase in PVDF [135-137]. Pure PA6 crystallize in a-phase while in presence of clay it crystallizes in otherwise a metastable g-phase at room temperature. Giannelis and coworkers have recently reported on the remarkable enhancement in the toughness of PVDF filled with organoclay (Cloisite 30B) [136]. They attributed this behavior to behavior to the structural and morphological changes induced by the organoclay particles. In general,

there are five crystalline forms or polymorphs of PVDF, i.e. a, b, g, d and e [142]. The a-phase is the dominant crystalline form over the b, and g phases in melt crystallization. It is shown from the XRD and FTIR studies, the organoMMT induces a phase transition from ordered a-crystallites to disordered, fiber-like b-phase crystallites. The formation of b-phase is also shown to be beneficial to the improvements of stiffness and toughness of PVDF. The fiber-like b-phase is considered to be much more conducive to plastic flow under applied stress. This could give rise to a more efficient energy-dissipation in the nanocomposites, thereby delaying crack formation.

1.7.5 Rheological behaviour

The linear dynamic mechanical properties of several nanocomposites have been examined at the melt state for wide range of polymer matrices including nylon 6 [143] polystyrene[144], polystyrene-polyisoprene block copolymers[145,146], PCL[147.] PP [148-150], PLA [121,151] PBS [152-154]. etc. Rheological behaviors of the nanocomposite show peculiar characteristics as compared to conventional composites. The PP/clay nanocomposites showed solid like rheological behaviour at lower frequencies which was shown to be due to frictional interactions between the silicate layers.[148] and this behavior depends on the concentration of clay in the composite. It was shown that above critical concentration of the clay, the nanocomposites form percolated structure with the clay layers and show solid like behavior. Studies on the steady shear rheological behavior of PBS/clay nanocomposites show that for very low shear rates, clay platelets take a longer time to attain planar alignment along the flow direction, and hence show a rheopexy behavior. At higher shear rates it shows time independent shear viscosity [153]

1.7.6 Other properties.

Polymer nanocomposites show significant improvement in most general polymer properties. For example they have the transparency similar to pristine polymer materials when the clay layers are completely delaminated and exfoliated in the polymer matrix because the clay platelets are about one nanometer thickness, which are of the sizes less than the wavelength of visible light and do not scatter the light. Scratch resistance,

abrasion resistance is strongly enhanced by the incorporation of layered silicates in the polymer matrix. Another interesting and exciting property is the significantly improved biodegradability of the nanocomposites made from organoclay and biodegradable polymers which is attributed to the presence of terminal hydroxylated edge groups in the clay layers and the catalytic role of the organoclay. Nanocomposites based on the intercalation of polymer electrolyte (e.g., PEO) into clay minerals are an attractive substitute of conventional polymer-salt compounds. This nanocomposite has shown to enhance the stability of the ionic conductivity at lower temperature when compared to more conventional PEO/LiBF₄ mixture. Nanocomposites with conjugated conducting polymers have also been reported including polymers such as PANI, polypyrrole, and polythiophen and have shown a significant increase in the electrical conductivity.

1.8 Applications and Commercial developments

Many companies have taken a strong interest in developing polymer nanocomposites based on clays owing to their markedly improved performance in mechanical, thermal, barrier, optical, electrical, and other physical and chemical properties. Increasing number of commercial products has become available. Some of the commercial products available in the market, their characteristics and their applications are listed in the table 1.1.

Table 1.1: Commercially available products based on polymer – clay nanocomposites.

| Polymer matrix | Property enhancement | Application | Developer / Trade name of product |
|---------------------------------|----------------------|----------------------------------|-----------------------------------|
| Polyamide 6 | Stiffness | Timing belt cover, automotive | Toyaota / Ube |
| Nylon MXD6, PP | Barrier property | Beverage containers | Imperm™; Nanocor |
| nylon 6, 66, 12 | Barrier property | Auto fuel systems | Ube |
| Thermoplastic polyolefins (TPO) | Stiffness / Strength | Exterior step assist | General Motors |
| Polyisobutylene | Permeability barrier | Tennis balls, tires soccer balls | InMat LLC |
| Nylon nanocomposite | Modulus | Medical tubing | Foster -Miller |
| Pouch with helium insert | Barrier property | Basket ball shoe pouch | Converse/Triton system |
| Nanoclay additives | Flame retardant | Flame retardant additives | Sud chemie |

The first commercial product of clay-based polymer nanocomposite is the timing belt cover made from nylon 6 nanocomposites in Toyota Motors in early 1990s [155]. These polymer nanocomposites offer high performance with significant weight reduction and affordable materials for transport industries such as automotive and aerospace. The weight advantage of the nanocomposites use in automotive industry improves the fuel efficiency and reduced carbon dioxide emissions. Polymer nanocomposites offer a promising alternative to the commonly employed flame resistant materials containing halogenous and phosphorous flame retardants. The polymer nanocomposites can be used in highly technical areas to improve the ablative properties of aeronautics. The excellent barrier properties, optical transparency of the films of clay based polymer nanocomposites offers them widely acceptable in packaging industries as wrapping films and beverage containers for processed meats, cheese, confectionary, cereals, fruit juice, dairy products, beer and carbonated drinks bottles and improves the shelf life for many types of packaged food. Nano-pigments or Planocolors, developed by TNO Materials, made from clays and organic dyes are believed as potential environment friendly substitutes for toxic cadmium and palladium pigments. The PlanoColors can be readily dispersed on a nanoscale in polymer matrix, which can be used in coatings. An improved oxygen, ultraviolet and temperature stability combined with high brilliance and color efficiency has been displayed due to the surface area of the nano-pigments. The property enhancements, especially on thermal responsivity, swelling-deswelling rate and molecular diffusion, are expected to extend clay-based nanocomposites to such applications as artificial muscles and actuators shown in table. Thermo-responsive hydrogels based on poly(N-isopropyl acrylamide)/clay nanocomposites were developed by Liag et al and Messersmith and Znidarsich. Manias and coworkers have shown that clay nanocomposites based on poly(urethane-urea) can be used biomedical applications such as blood sacs in ventricular assist devices and total artificial hearts with improved properties such as reduced gas permeability and increased mechanical properties. O'Neil et al studied the potential design of nylon 12 nanocomposites for catheter shafts which require varying mechanical properties along their length to allow for manipulation of the device. Apart from the medical device applications, polymer nanocomposites have

recently been extensively investigated for controlled drug delivery and few examples of them are summarized in the table. The remarkable electrochemical behavior of conducting polymers associated with clay minerals attracts potential applications such as modified electrodes, biosensors, solid-state batteries, smart windows and other electrochemical devices. For instance, polypyrrole nanocomposites can be developed for modified electrodes used as sensors or as devices for electrocatalysis. PEO nanocomposites could become novel electrolyte materials because of their relatively higher ambient conductivity and weak temperature dependence over conventional LiBF₄/PEO electrolyte as well as their single ionic conduction character.

1.9 Conclusions

The fact that PLS nanocomposites show concurrent improvement in various material properties at very low filler content, together with the ease of preparation through simple processes, opens a new dimension for plastics and composites. Their applications in various areas have been briefly discussed. Clay based polymer nanocomposites have been produced as energy-saving and environment-friendly automotive parts and packaging materials. Their future markets will further expand from current automotive, packaging and containers, coatings and pigments to other industries such as appliances and tools, electromaterials, building and construction. Moreover, clay-based polymer nanocomposites have shown promising applications in the biomedical and bioengineering fields. However, in spite of these efforts and some successes in commercial development of clay-based polymer nanocomposites, their design, manufacturing and applications are often empirical, and large-scale productions are still in its infancy. The reasons are mainly because of the limited theoretical knowledge on such novel nanostructure materials, such as a basic guideline for the selection of surfactants and the modification of clays for the purposes of targeted polymer matrix, the mechanisms of superior reinforcement observed as compared with their micro-counterparts, and the establishment of a simple processing-structure property relationship for such nanocomposites. Therefore, further development of polymer nanocomposite materials depends largely on our understanding of the above fundamentals in relation to their formation, processing, property prediction and design.

References:

1. J.E. Mark, *Polym. Eng. Sci.* 36 (1996) 2905;
2. E. Reynaud, C. Gauthier, J. Perez, *Rev. Metall./Cah. Inf. Tech.* 96 (1999) 169.
3. T. von Werne, T.E. Patten, *J. Am. Chem. Soc.* 121 (1999) 7409.
4. N. Herron, D.L. Thorn, *Adv. Mater.* 10 (1998), 1173.
5. P. Calvert, Potential applications of nanotubes, in: T.W. Ebbesen (Ed.), *Carbon Nanotubes*, CRC Press, Boca Raton, FL, 1997, pp. 277.
6. V. Favier, G.R. Canova, S.C. Shrivastava, J.Y. Cavaille, *Polym. Eng. Sci.* 37 (1997) 1732.
7. L. Chazeau, J.Y. Cavaille, G. Canova, R. Dendievel, B. Bouterin, *J. Appl. Polym. Sci.* 71 (1999) 1797.
8. B.K.G. Theng, *The Chemistry of Clay-Organic Reactions*, Wiley, New York, 1974;
9. M. Ogawa, K. Kuroda, *Bull. Chem. Soc. Jpn.* 70 (1997) 2593.
10. T. J. Pinnavaia, G. W. Beall, *Polymer clay nanocomposites*, John Wiley and Sons Ltd, 2000
11. J. H. Koo, *Polymer Nanocomposites: Processing, Characterization and Applications*, McGraw-Hill Publications, 2006.
12. Y-W. Mai, Z-Z. Yu, *Polymer Nanocomposites*, Woodhead publishing in materials, CRC, 2006.
13. P. C. LeBaron, Z. Wang, T. J. Pinnavaia, *Appl. Clay Science*, 15, (1999) 11.
14. M. Alexandre, P. Dubois, *Materials Science and Engg. R: Reports*, 28, (2000), 1
15. S. S. Ray, M. Okamoto, *Prog. Polym. Sci.*, (2003) 1539.
16. Viswanathan V., Laha, T.; Balani, K.; Agarwal, A.; Seal, S. *Materials Science and Engg R: Reports* 54, (2006) 121.
17. Nguyen, Q. T., Baird D. G., *Adv. Poly. Tech.* 25, (2006), 270
18. Leszynska, A., Njuguna, J., Pielichowski, K., Banerjee, J. R., *Thermochimica Acta*, 453, (2007), 75.
19. Leszynska, A., Njuguna, J., Pielichowski, K., Banerjee, J. R., *Thermochimica Acta*, 454, (2007), 1.

20. Vaia, R. A., Maguire, J. F., Chemistry of materials, 19 (2007) 2736.
21. Chen, B.; Evans, J. R. G.; Greenwell, H. C.; Boulet, P.; Coveney P. V.; Bowden, A. A.; Whiting, A.; Chem. Society Reviews, 37 (2008) 568.
22. Esfandiari, A.; Nazokdast, H.; Rashidi, A. -S.; Yazdanshenas, M.-E.; Journal of applied Sciences, 8, (2008), 545.
23. Yeh, J.-M.; Chang K.-C., J. of Ind & Eng Chem. 14, (2008), 275.
24. Ciardelli, F.; Coiai, S.; Passaglia, E.; Pucci, A.; Ruggeri, G.; Polym. International, 57, (2008), 805.
25. Paul D. R.; Robson, L. M.; Polymer 49, (2008) 3187.
26. <http://www.nanoclay.com/>
27. <http://www.rheox.com/>
28. <http://www.nanocor.com>
29. <http://www.sud-chemie.com>
30. Blumstein A. J Polym Sci A 1965;3:2665.
31. R.A. Vaia, E.P. Giannelis, Macromolecules 30 (1997) 8000.
32. A.B. Morgan, J.F. Gilman, J. Appl. Polym. Sci. 87 (2003) 1327.
33. D.F. Eckel, M.P. Balogh, P.D. Fasulo, W.R. Rodgers, J. Appl. Polym. Sci. 93 (2004) 1110.
34. R.A. Vaia, D. Klaus, E.J. Kramer, E.P. Giannelis, Chem. Mater. 8 (1996) 2628
35. T.D. Fornes, P.J. Yoon, D.R. Paul, Polymer 44 (2003) 7545
36. S. Hotta, D.R. Paul, Polymer 45 (2004) 7639
37. E. Manias, A. Touny, L. Wu, K. Strawhecker, B. Lu, T.C. Chung, Chem. Mater. 13 (2001) 3516;
38. Z.M. Wang, H. Nagajima, E. Manias, T.C. Chung, Macromolecules 36 (2003) 8919
39. D.L. Ho, R.M. Briber, C.J. Glinka, Chem. Mater. 13 (2001) 1923;
40. D.L. Ho, C.J. Glinka, Chem. Mater. 15 (2003) 1309;
41. Y.S. Choi, H.T. Ham, I.J. Chung, Chem. Mater. 16 (2004) 2522
42. C.M. Hansen, J. Paint Technol. 39 (1967) 104;
43. C.M. Hansen, J. Paint Technol. 39 (1967) 505
44. H.M. Lin, R.A. Nash, J. Pharm. Sci. 82 (1993) 1018

45. C.M. Hansen, *J. Paint Technol.* 39 (1967) 104.
46. C.M. Hansen, *J. Paint Technol.* 39 (1967) 505
47. Y. Li, H. Ishida, *Polymer* 44 (2003) 6571
48. W. Xie, Z. Gao, K. Liu, W.-P. Pan, R. Vaia, D. Hunter, A. Singh, *Thermochim. Acta* 339 (2001) 367
49. W.H.Awad, J.W. Gilman, M. Nydena, R.H. Harris Jr., T.E. Sutto, J. Callahan, P.C. Trulove, H.C. DeLongc, D.M. Fox, *Thermochim. Acta* 409 (2004) 3.
50. J.W. Gilman, W.H.Awad, R.D. Davis, J. Shields, R.H. Harris Jr., C. Davis, A.B. Morgan, T.E. Sutto, J. Callahan, P.C. Trulove, H.C. DeLong, *Chem. Mater.* 14 (2002) 3776.
51. H. Ngo, K. Le Compte, L. Hargens, A.B. Mc Ewen, *Thermochim. Acta* 97 (2000) 357.
52. C.G. Begg, M.R. Grimmett, P.D. Wethey, *Aust. J. Chem.* 26 (1973) 2435.
53. B.K.M. Chan, N.-H. Chang, M.R. Grimmett, *Aust. J. Chem.* 30 (1977) 2005.
54. A.N. Kost, I.I. Grandberg, *Adv. Heterocycl. Chem.* 6 (1966) 417.
55. R.T. Carlin, J. Fuller, in: M. Gaune-Escard (Ed.), *Molten Salts: From Fundamentals to Applications in NATO Science Series*, Kluwer, Dordrecht, 2002.
56. Usuki A, Kawasumi M, Kojima Y, Okada A, Kurauchi T, Kamigaito O. *J Mater Res* 1993;8:1174.
57. Messersmith PB, Giannelis EP. *Chem Mater* 1993;5:1064.
58. Akelah A. Polystyrene/clay nanocomposites. In: Prasad PN, Mark JE, Ting FJ, editors. *Polymers and other advanced materials. Emerging technologies and business opportunities*. New York: Plenum Press; 1995. p. 625–30.
59. Akelah A, Moet M. *J Mater Sci* 1996; 31:3589.
60. Zhu J, Morgan AB, Lamelas FJ, Wilkie CA. *Chem Mater* 2001;13:3774.
61. Ke YC, Long C, Qi Z. *J Appl Polym Sci* 1999;71:1139.
62. Tsai TY. Polyethylene terephthalate–clay nanocomposites. In: Pinnavaia TJ, Beall GW, editors. *Polymer–clay nanocomposites*. England: Wiley; 2000. p. 173–89.
63. Imai Y, Nishimura S, Abe E, Tateyama H, Abiko A, Yamaguchi A, Aoyama T, Taguchi H. *Chem Mater* 2002;14:477
64. Hsu SLC, Chang KC. *Polymer* 2002;43: 4097.

65. Leu CM, Wu ZW, Wei KH. *Chem Mater* 2002;14:3016.
66. Tudor J, Willington L, O'Hare D, Royan B. *Chem Commun* 1996;2031.
67. Bergman JS, Chen H, Giannelis EP, Thomas MG, Coates GW. *J Chem Soc Chem Commun* 1999;21:2179.
68. J. Heinemann, P. Reichert, R. Thomann, R. Mulhaupt, *Macromol. Rapid Commun.* **20**, 423–430 (1999)
69. Sun T, Garces JM. *Adv Mater* 2002;14:128.
70. Jin Y-H, Park H-J, Im S-S, Kwak S-Y, Kwak S. *Macromol Rapid Commun* 2002;23:135
71. *Polymer*, 46, 2005, 129;
72. *Macromol. Mater. Eng.* 2005, 290. 430.;
73. *J. Appl. Poly. Sci.* 102, 1167.
74. *Polymer International* 56, 399, 20070
75. Sogah et al (*J. Am. Chem. Soc.* 1999, 121, 1615
76. *Macromolecules* 2006, 39, 1020.
77. *Macromolecules* 2006, 39, 5052.
78. *Chem. Mater.* 2003, 15, 2693; *Polymer* 45 2004, 4473
79. *J. Polym. Sci. Part A. Poly. Chem.* 42, 916, 2004.
80. *Chem. Mater.* 2005, 17, 3012.
81. *J. Polym. Sci. Part A, Poly. Chem.* 43, 534, 2005.
82. *Polymer Composites*, 26, 465, 2005.
83. Messersmith P. B, Giannelis E. P. *Chem Mater* 1994; 6:1719.
84. Wang M. S, Pinnavaia T. J. *Chem Mater* 1994;6:468.
85. Lan T, Pinnavaia TJ. *Chem Mater* 1994;6:2216.
86. Lan T, Kaviratna PD, Pinnavaia TJ. *Chem Mater* 1995;7:2144.
87. Zilg C, Mulhaupt R, Finter J. *Macromol Chem Phys* 1999;200:661.
88. Kornmann X, Thomann R, Mulhaupt R, Finter J, Berglund LA. *Polym Engng Sci* 2002;42:1815
89. Becker O, Varley R, Simon G. *Polymer* 2002;43:4365
90. Jinguo Zhang, E. Manias, and Charles A. Wilkie J. *Nanosci. and Nanotechnol.* 8, 1, 2008

91. Halpin, J. C. (1969). *J. Compos. Mater.*, 3: 732.
92. Halpin, J. C. and Kardos, J. L. (1976). *Polym. Engng. Sci.*, 16(5): 344.
93. Ashton, J. E., Halpin, J. C. and Petit, P. H. (1969). *Primer on Composite Materials: Analysis*, Stamford, Conn: Technomic Pub. Co
94. Hermans, J. (1967). *Proc Kon Ned Akad v Wetensch B*, 65: 1–9
95. Hill, R. (1964). *J. Mech. Phys. Solids*, 12: 119.
96. Y.Kojima, A.Usuki, M.Kawasumi, A.Okada, Y.Fukushima, T.K urauchi, and O.Kamigaito, *J. Mater. Res.* 8, 1185 (1993)
97. L.Sherman, *Plast. Technol.* 45, 52 (1999)
98. Z.Wang and T.J.Pinna vaia, *Chem. Mater.* 10, 1820 (1998)
99. L.M.Liu, Z.N.Qi, and X.G.Zhu, *J. Appl. Polym. Sci.* 71, 1133 (1999).
100. X.H.Liu and Q.J.W u, *Polymer* 42, 10013 (2001).
101. T.D.Fornes, P.J.Y oon, H.K eskkula, and D.R.P aul, *Polymer* 42, 9929 (2001)
102. D.C.Lee and L.W .Jang, *J. Appl. Polym. Sci.* 61, 1117 (1996)
103. M.W .Noh and D.C.Lee, *Polym. Bull.* 42, 619 (1999)
104. M.J.Chung, L.W .Jang, J.H.Shim, and J.S.Yoon, *J. Appl.Polym. Sci.* 95, 307 (2005).
105. T. J. Pinnavaia and G. W. Beall, *Polymer-Clay Nanocomposites*, Wiley, London (2000).
106. R. Krishnamoorti and R. A. Vaia, *Polymer Nanocomposites: Synthesis, Characterization, and Modeling*, American Chemical Society, Washington, DC (2001).
107. S. Komarneni, *Nanophase and Nanocomposite Materials IV: Symposium held November 26–29, 2001, Boston, Massachusetts, USA*, Materials Research Society, Warrendale, Pennsylvania (2002).
108. P.B.Messersmith and E.P.Giannelis, *J. Polym. Sci., Part A: Polym.Chem.* 33, 1047 (1995)
109. J.M.Yeh, C.L.Chen, T.H.K uo, W.F .Su, H.Y .Huang, D.J. Liaw, H.Y .Lu, C.F .Liu, and Y.H.Y u, *J. Appl. Polym. Sci.* 92, 1072 (2004).
110. Y.R.Liang, Y.Q.W ang, Y.P .W u, Y.L.Lu, H.F .Zhang, and L.Q.Zhang, *Polym. Test.* 24, 12 (2005).

111. S.S.Ray , K.Y amada, M.Okamoto, and K.Ueda, *Nano Lett.* 2, 1093 (2002).
112. R.J.Xu, E.Manias, A.J.Sn yder, and J.Runt, *J. Biomed. Mater.Res., Part A* 64, 114 (2003).
113. K.Y ano, A.Usuki, and A.Okada, *J. Polym. Sci., Part A: Poly. Chem.* 35, 2289 (1997).
114. S. T. Lim, Y.H.Hyun, H.J.Choi, and M.S.Jhon, *Chem. Mater.* 14, 1839 (2002)
115. J.W .Gilman, *Appl. Clay Sci.* 15, 31 (1999).
116. M.Zanetti, G.Camino, R.Thomann, and R.Mullhaupt, *Polymer* 42, 4501
117. S.D.Burnside and E.P .Giannelis, *Chem. Mater.* 7, 1597 (1995)
118. J.G.Doh and I.Cho, *Polym. Bull.* 41, 511 (1998).
119. D.C.Lee and L.W .Jang, *J. Appl. Polym. Sci.* 68, 1997 (1998).
120. P.H.Nam, P.Maiti, M.Okamoto, M.Kotaka, M.Ohshima, N.Hasegawa, and A.Usuki, in *The First World Congress of Nanocomposites*, Chicago, USA (2001), p.281
121. S.S.Ray , K.Yamada, M.Okamoto, and K.Ueda, *Polymer* 44, 857 (2003).
122. J.W .Gilman, T.Kashiwagi, J.E.T .Bro wn, S.Lomakin, E.P .Giannelis, and E.Manias, *International SAMPE Symposium and Exhibition* 43, 1053 (1998).
123. E. Di Maio, S. Iannace, L. Sorrentino, L. Nicolais, *Polymer* 45 (2004) 8893.
124. G. Zhang, D. Yan, *J. Appl. Polym. Sci.* 88 (2003) 2181.
125. T.D. Fornes, D.R. Paul, *Polymer* 44 (2003) 3945.;
126. D.M. Lincoln, R.A. Vaia, R. Krishnamoorti, *Macromolecules* 37 (2004) 4554.
127. S. Hambir, N. Bulakh, J.P. Jog, *Polym. Eng. Sci.* 42 (2002) 1800.
128. P.H. Nam, P. Maiti, M. Okamoto, T. Kotaka, *Polym. Eng. Sci.* 42 (2002) 1864
129. S.C. Tjong, S.P. Bao, *J. Polym. Sci. Part B: Polym. Phys.* 43 (2005) 253;
130. T.G. Gopakumar, J.A. Lee, M. Kontopolou, J.S. Parent, *Polymer* 43 (2002) 5483.
131. Y. Ke, C. Long, Z. Qi, *J. Appl. Polym. Sci.* 71 (1999) 1139.
132. B.J. Chisholm, R.B. Moore, G. Barber, F. Khouri, A. Hempstead, M. Larsen, *Macromolecules* 35 (2002) 5508.
133. D.F. Wu, C.X. Zhou, F. Xie, D.L. Mao, B. Zhang, *J. Appl. Polym. Sci.* 99 (2006) 3257.
134. H.D. Wu, C.R. Tseng, F.C. Chang, *Macromolecules* 34 (2001) 2992.

135. L. Priya, J.P. Jog, J. Polym. Sci. Part B Polym. Phys. 40 (2002) 1682.;
136. D. Shah, P. Maiti, E. Gunn, D.F. Schmidt, D.D. Jiang, C.A. Batt, E.P. Giannelis, Adv. Mater. 16 (2004) 1173.;
137. D.R. Dillon, K.K. Tenneti, C.Y. Li, F.K. Ko, I. Sics, B.S. Hsiao, Polymer 47 (2006) 1678.
138. K.E. Strawhecker, E. Manias, Chem. Mater. 15 (2003) 844
139. S.C. Tjong, S.P. Bao, J. Polym. Sci. Part B: Polym. Phys. 42 (2004) 2878.
140. D.M. Lincoln, R.A. Vaia, Z. Wang, B.S. Hsiao, Polymer 42 (2001) 1621.
141. L. Incarnato, P. Scarfato, G.M. Russo, L. Di Maio, P. Iannelli, D. Arcierno, Polymer 44 (2003) 4625
142. G. Guerra, F.E. Karasz, W.J. MacKnight, Macromolecules 19 (1986) 1935.
143. Fornes TD, Yoon PJ, Keskkula H, Paul DR. Polymer 2001;42:9929.
144. Hoffman B, Dietrich C, Thomann R, Friedrich C, Mulhaupt R. Macromol Rapid Commun 2000;21: 57
145. Ren J, Silva AS, Krishnamoorti R. Macromolecules 2000;33: 3739;
146. Mitchell CA, Krishnamoorti R. J Polym Sci, Part B: Polym Phys 2002;40:1434.
147. Lepoittevin B, Devalckenaere M, Pantoustier N, Alexandre M, Kubies D, Calberg C, Jerome R, Dubois P. Polymer 2002;43:4017
148. Galgali G, Ramesh C, Lele A. Macromolecules 2001;34:852.
149. Solomon MJ, Almusallam AS, Seefeldt KF, Somwangthanaroj A, Varadan P. Macromolecules 2001;34:1864.
150. Lele A, Mackley M, Galgali G, Ramesh C. J Rheol 2002;46:1091.
151. Sinha Ray S, Maiti P, Okamoto M, Yamada K, Ueda K. Macromolecule 2002;35: 3104.
152. Sinha Ray S, Okamoto K, Maiti P, Okamoto M. J Nanosci Nanotechnol 2002;2:171;
153. Sinha Ray S, Okamoto K, Okamoto M. Macromolecules 2003;36:2355.;
154. Kornmann X, Berglund LA, Sterete J, Giannelis EP. Polym Engng Sci 1998;38:1351
155. A.Okada, K.Fukumori, A.Usuki, Y.Kojima, N.Sato, T.Kurauchi, and O.Kamigaito, *Polym. Prepr.* 32, 540 (1991)

2. Objectives of the Thesis

Polymer nanocomposites have been an area of intense industrial and academic research for the past twenty years. Amongst all the potential nanocomposite precursors, those based on clay and layered silicates have been more widely investigated probably because the starting clay materials are easily available and their intercalation chemistry has been studied for a long time. Further development of polymer nanocomposite materials depends largely on our understanding of the fundamentals in relation to their formation, processing, property prediction and design. It has been well established that when the interaction of the polymer chains with the clay surface is stronger, better is the dispersion of the clay layers in the polymer matrix. Large improvements in properties are achieved when the clay layers are thoroughly dispersed and exfoliated in the polymer matrix. The dispersion of clay depends on the method and the polymer used. Therefore, the objective of this thesis is to explore various strategies to obtain better dispersion of clay layers in candidate polymers and to study the resultant property enhancements of the nanocomposites.

In the preparation of polyurethane clay nanocomposites, in spite of several efforts, no clear understanding is evident in the literature on the structure of PU-Clay nanocomposites and its dependence on the nature of modifiers and polyols. Therefore, to understand the dispersion of clay in the polyurethane matrix, the work was focused with the objectives such as i) to study the effect of branching agents on the structure of polyurethane-clay nanocomposites and ii) to study the effect of reactive functionality of the organic modifier of the clay on the structure of the polyurethane-clay nanocomposites.

For the dispersion of clay in the polycarbonate matrix, most of the studies reported use organoclays modified with quaternary ammonium salts, which degrade at the temperatures of preparation and processing of the polymer. The objective of the present work is to prepare of polycarbonate clay nanocomposites via in situ polymerization using two novel organoclays in which the modifier is thermally stable at temperatures used for polymerization and to improve the interaction of the polymer with clay surface by designing the modifier such that it contains reactive bisphenol moiety, which can

copolymerize with the growing polymer during polymerization thereby. Further, to study the structure, molecular weights, thermal and dynamic mechanical properties of the PCCNs with above designed clay and compare them with the nanocomposites prepared with the organoclays, which are thermally stable but does not contain the reactive groups.

Studies on the synthesis of sPS/clay nanocomposites are very few mainly because of the high melting and processing temperatures and dispersion of clay in the sPS matrix was poor because of low surface energy and non-polar nature of the polymer. Therefore the objective of the present work is to improve the surface energy of the sPS by sulfonation and ionomerization and to study the effect of sulfonation content and type of ionomer (H^+ , Na^+ , K^+ and Rb^+ in the group I series of the periodic table) on intercalation/exfoliation of SsPS ionomers/organoclay nanocomposites by using WAXD and TEM. Further, to study the effect of clay dispersion on the crystallization of ionomers.

Studies on preparation and properties of Polypropylene/organoclay nanocomposites were extensively done using functionalized PP as compatibilizers as the unmodified polymer lack the intrinsic thermodynamic affinity with currently available organoclays to form well-dispersed nanocomposites. Maleic anhydride-g-polypropylene was extensively used as compatibilizer though only intercalated nanocomposites were obtained. There is a strong need to develop a new efficient compatibilizer. The main objective of the present work is to evaluate a novel metallic ionomer of PP as compatibilizer for preparing PP/organoclay nanocomposite by two different mixing routes and to study the effect of the compatibilizer, compatibilizer concentration, processing method on the dispersion of organoclay in the polymer matrix and its effect on crystallization behavior and mechanical properties. Further, to compare the properties of the obtained nanocomposites with the nanocomposites prepared using PPMA as compatibilizer.

3. Polyurethane-clay nanocomposites via *in-situ* solution polymerization

3.1 Introduction

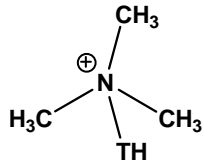
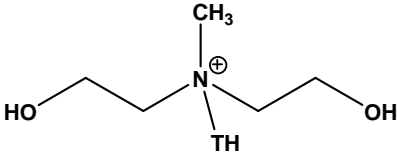
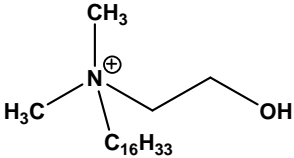
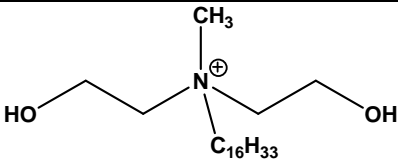
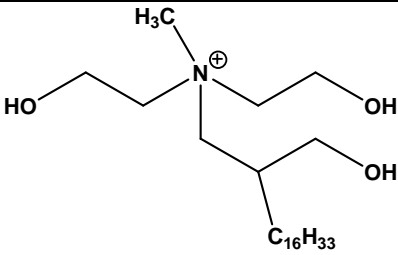
Polyurethanes (PU) are versatile polymeric materials with a wide range of physical and chemical properties with well designed combinations of monomeric materials, which can be tailored to meet the diversified demands in applications such as coatings, adhesives, and reaction injection molding plastics, fibers, foams, rubbers, thermoplastic elastomers and composites¹⁻³. However PU also have disadvantages such as low thermal stability and low mechanical strength, etc. Either chemical modification or use of inorganic filler into the polyurethane matrix may mitigate these problems. It has been found possible to improve many properties by incorporating fillers. For e.g., calcium carbonate, aluminum hydroxide, kaolin, titanium dioxide, zinc oxide, were used to improve mechanical properties⁴⁻⁹. One advantage of the use of inorganic fillers is to reduce the production cost. However, the disadvantages are that adding these inorganic fillers worsen the fatigue property and reduces elongation at break¹⁰. To overcome these disadvantages a great deal of efforts has been devoted to the development of nanostructured PU/MMT composites in recent years. Wang and Pinnavaia reported the first work on composites of PU and organically treated layered silicate clays and showed that large enhancement in tensile strength and tensile modulus for the nanocomposites as compared to the pristine polymer¹¹. This was followed by a spate of research activities on the synthesis of thermoplastic polyurethanes (TPU) via solvent mixing; melt mixing, insitu solution and bulk polymerization methods and have been shown to improve tensile strength and thermal stability without sacrificing the high elongation at break of the pristine polymer¹²⁻³⁰. In the case of *in-situ* polymerization studies, many times, clay particles were intercalated by soft polyols prior to reaction with isocyanates, drawing a parallel to the successful insitu polymerization scheme for polyamide-clay nanocomposites^{31, 32}. It is recognized that the properties of the nanocomposite are better when the interaction of the polymer chain with the surface of the clay layer is improved. This can be achieved by tethering the polymer into the surface of the clay layers, which are completely delaminated and fully exfoliated through out the polymer matrix³³. Tien and Wei¹⁸, have

shown that PU can be ionically tethered to the surface of the clay by choosing compatibilizers having reactive hydroxyl groups. They have used reactive modifiers for the clay that does not have long hydrophobic groups. It should be noted that exfoliated PU/clay nanocomposite structures were obtained whenever the functionality of the polyol used was greater than two, which induces branching and cross linking in the polyurethane architecture³⁴. This is supported by the theoretical modeling study by Balaz et al³⁵. Pattanayak and Jana have shown that partially exfoliated structures were possible to be obtained by adding the organoclay during bulk polymerization and also have shown that it depends on the type of polyol used³⁶⁻³⁹. However there is no consensus that exfoliation of nanoclay is at all possible in the linear polyurethane system. Very recently polyurethane containing cationic groups were prepared and used to obtain exfoliated clay nanocomposites by solvent casting⁴⁰.

The present work has been focused: i) to study the effect of branching agents on the structure of PU/clay nanocomposites and ii) to study the effect of reactive functionality of the organic modifier of the clay on the structure of the polyurethane-clay nanocomposites. For the first study, we prepared PU nanocomposites via *in-situ* polymerization using 2-ethyl-1, 3-hexanediol and toluenediisocyanate (TDI) as monomers and trimethylolpropane (TMP) as a branching agent. Organically modified montmorillonite clays Cloisite 30 B, (in which the modifier have a long alkyl chain and two hydroxy ethyl groups) and Cloisite 25 A (in which the modifier have only long alkyl chain and no hydroxyl groups) have been used for the same. The structure of the modifiers in Cloisite 30B and Cloisite 25A are shown in the table 1. For the second study, three different organoclays were prepared in the laboratory by exchanging the Na⁺ ions in pristine sodium montmorillonite with three different organoammonium cations such as hydroxyethyl dimethyl hexadecylammonium cation, bis(hydroxy ethyl) methyl hexadecylammonium cation and bis(hydroxyethyl) methyl- 2-hydroxymethyloctadecyl ammonium cation having hydroxyl functionality as 1, 2 and 3, respectively. The dispersion of these clays was evaluated for preparation of polyurethane-clay nanocomposites via *in-situ* solution polymerization of 2-ethyl-1, 3-hexanediol and toluenediisocyanate (TDI) monomers. In addition, the effect of these organoclays on the structure and properties of nanocomposites based on thermoplastic polyurethanes

containing polycaprolactone diol and isophorone diisocyanate with butanediol (chain extender) /clay have been evaluated.

Table 3.1: List of organoclays used and the structure of their modifiers

| Organoclay | Structure of the modifier | Name of the modifier |
|--------------|---|---|
| Cloisite 25A |  <p>Where TH = hydrogenated tallow</p> | Hydrogenated tallow trimethyl ammonium cation |
| Cloisite 30B |  <p>Where TH = hydrogenated tallow</p> | Bis(hydroxyethyl)(hydrogenated tallow) methyl ammonium cation |
| 1OHMMT |  | Hydroxyethyl dimethyl hexadecyl ammonium cation (1OH) |
| 2OHMMT |  | Bis(hydroxyethyl) methyl hexadecyl ammonium cation (2OH) |
| 3OHMMT |  | Bis(hydroxyethyl) methyl-2-(hydroxy methyl) octadecyl ammonium cation (3OH) |

3.2 Experimental

3.2.1 Materials

Cloisite 30B and Cloisite 25 A, the modified montmorillonites were obtained from Southern Clay Products, USA, was used after drying it by azeotrope distillation with toluene and stored in vacuum desiccator. 2-ethyl-1,3-hexanediol, hexadecyl bromide, bis(hydroxyethyl)methylamine, hydroxyethyl dimethylamine and isophorone diisocyanate

were obtained from Aldrich Chemical Co., USA. Trimethylol propane, 1,4- butane diol and dimethyl malonate were obtained from Sd fine chemicals, India. Toluene diisocyanate (mixture of 2,4 and 2,6 isomers in the ratio 20:80) were obtained from Narmada chemicals, India. Polycaprolactone diol (CAPA 2077A) was kindly supplied by Solavay chemicals, US.

3.2.2 Preparation of hydroxyethyl dimethyl hexadecylammonium bromide

Hydroxyethyl dimethyl amine (4.457 g, 50 mmol) was mixed with hexadecyl ammonium bromide (15.268 g, 50 mmol) in the stoichiometric ratio 1:1 and heated to 60 °C. White solid particles started forming immediately after the reaching the temperature to 60 °C and the heating was continued for another six hours to make sure that the reaction goes to completion. The reaction was found to be quantitative and hydroxyethyl dimethyl hexadecylammonium bromide (19.7 g) was obtained in pure form and used without further purification. ¹H NMR: Yield: 75%. ¹H NMR: δ 0.88 (3H, t); 1.26 (26H, m); 1.76 (2H, m); 3.38 (6H, s); 3.55 (2H, m); 3.77 (2H, b); 4.14 (2H, b); 5.03 (1H, b)

3.2.3 Preparation bis(hydroxy ethyl) methyl hexadecylammonium bromide

Bis(hydroxyethyl)methyl amine (5.958 g, 50 mmol) was mixed with hexadecyl ammonium bromide (15.268 g, 50 mmol) in the stoichiometric ratio 1:1 and heated to 60 °C. White solid particles started forming 15 minutes after the reaching the temperature to 60 °C and the heating was continued for another 8 hours to make sure that the reaction goes to completion. The reaction was found to be quantitative and bis(hydroxyethyl) methylhexadecylammonium bromide (21.2 g) was obtained in pure form and used without further purification. ¹H NMR: δ 0.88 (3H, t); 1.26 (26H, m); 1.75 (2H, m); 3.33 (3H, s); 3.54 (2H, m); 3.73 (4H, b); 4.14 (4H, b); 5.03 (2H, b)

3.2.4 Preparation bis(hydroxyethyl) methyl- 2-hydroxymethyloctadecyl ammonium bromide

The hydroxy alkyl bromide was prepared from simple starting material such as dimethyl malonate and hexadecyl bromide in three synthetic steps as follows. Further this hydroxyalkyl bromide was used for quaternization of bis(hydroxyethyl) methylamine.

3.2.4.1 Alkylation of dimethyl malonate with hexadecyl bromide

Clean dry sodium (2.0 g, 85 mmol) was placed in a three neck round bottomed flask fitted with double surface condenser, dropping funnel and septum adapter. Dry methanol (100 mL) was added on sodium slowly under cooling. Sodium methoxide was formed by evolving hydrogen gas. The cooling was removed after the evolution of hydrogen gas ceased. Dimethyl malonate (11.2 g, 85 mmol) was added under stirring and heated to gentle reflux. Then hexadecyl bromide (24.4 g, 80 mmol) was taken in dropping funnel and added slowly into the contents of the round bottomed flask over a period of 20 min. Continued reflux for 12 hours and monitored the reaction by TLC. The reaction was stopped when all the alkyl bromide was consumed. The crude reaction mixture was concentrated by evaporating methanol, diluted with ethyl acetate, washed with water several times until the washings was neutral to litmus. Pure dimethyl-2-hexadecyl malonate (18.5 g), was separated from crude by flash chromatography. Yield: 65%. ^1H NMR: δ 0.88 (3H, t); 1.26- (28H, m); 1.91 (2H, m); 3.36 (1H, t); 3.73 (6H, s)

3.2.4.2 Reduction of hexadecylated malonate to 2-(hydroxy methyl) octadecanol

Lithium aluminum hydroxide(LAH) (4.9 g, 130 mmol) was dispersed in 80 mL of dry tetrahydrofuran. Dimethyl-2-hexadecyl malonate (17.8 g, 50 mmol) was dissolved in 100 mL of dry THF and added slowly into LAH dispersion at 0 °C for 1 hour duration. After the addition was completed, the temperature of the reaction mixture was brought to room temperature on its own and then heated to mild reflux for 6 hours. The reaction was monitored by TLC analysis and stopped when there is no starting material. The excess LAH was quenched by addition of ethyl acetate. The aluminum adduct formed was cleaved by adding the reaction mixture slowly into hydrated sodium sulphate and the slurry was stirred for one hour and the filtered over celite bed. The filtrate was concentrated to get the diol. The pure 2-(hydroxy methyl) octadecanol (9.8 g) was isolated by column chromatographic separation. Yield 65%. ^1H NMR: δ 0.88 (3H, t); 1.26-1.60 (30H, m); 1.75 (1H, m); 3.61 to 3.86 (4H, 2dd).

3.2.4.3 Monobromination of 2-(hydroxy methyl) octadecanol to 2-(hydroxy methyl) octadecyl bromide

The 2-(hydroxymethyl)octadecanol (10g, 33.3 mmol) and CBr_4 (13.28g, 0.040 mol) was dissolved in dry tetrahydrofuran (100mL) and taken in three-neck round bottomed flask fitted with a dropping funnel, a condenser and a three-way stopcock. Triphenylphosphine (9.16 g, 35 mmol) was dissolved in tetrahydrofuran and added to the reaction mixture, which is kept at 0 °C slowly, drops by drop through a dropping funnel for duration of 30 minutes. The stirring was continued for another 4 hours at 0 °C. The reaction was monitored by TLC. After the reaction was over, the crude reaction mixture was concentrated by evaporating tetrahydrofuran and dissolved in ethyl acetate, washed with water. The 2-(hydroxymethyl) octadecyl bromide (9.7 g) was isolated in pure form after column chromatography. Yield: 80 %. $^1\text{H NMR}$: δ 0.88 (3H, t); 1.26 (28H, m); 1.60 (2H, m); 1.83 (1H, m); 3.47 to 3.74 (4H, 4dd).

3.2.4.4 Preparation bis(hydroxyethyl)methyl–2-hydroxymethyloctadecylammonium bromide

Bis(hydroxyethyl)methyl amine (2.98 g, 25 mmol) was mixed with hexadecyl ammonium bromide (9.1 g, 25 mmol) in the stoichiometric ratio 1:1 and heated to 60 °C in ethanol (65 mL). The reaction was monitored by TLC analysis. The reaction was continued for another 3 days and stopped by cooling it to room temperature. The reaction did not go to completion, which was evidenced by presence of the unreacted alkyl bromide and amine. A white crystalline powder of bis(hydroxyethyl)methyl–2-hydroxymethyloctadecyl ammonium bromide (6.1 g) was obtained from the pasty crude reaction mixture by repeated recrystallization in ethyl acetate. Yield: 50%. $^1\text{H NMR}$: δ 0.88 (3H, t); 1.26 to 1.44 (30H, m); 2.12 (1H, m); 3.07(1H,m); 3.33(1H,m); 3.45(1H, m); 3.28(3H, s); 3.76 (4H, b); 3.83 (1H, m); 4.12 (4H, b); 4.59 (1H, b), 4.89 (2H, b)

3.2.5 Reactivity of modifier salts with phenyl isocyanate

To demonstrate reactivity of the hydroxyl groups of the organomodifiers with isocyanates, they were mixed with calculated equivalents of phenyl isocyanate at room temperature in toluene medium in presence of the catalyst dibutyltin dilaurate and heated

at 60 °C for 2 hours. The amount of the organomodifier and the phenyl isocyanate taken were listed in the table. After the reaction, the solvent from the reaction mixture was evaporated by applying vacuum and the quantitative formation of phenyl carbamates were studied by NMR analysis

3.2.6 Preparation of organoclays

The Na montmorillonite (10 g) with CEC 92 meq/100 g, d spacing 12 Å was dispersed in water/methanol (300 mL) by stirring with an overhead stirrer at room temperature for 2 hours. The modifier (11 meq), dissolved in methanol/water mixture was poured into the dispersion of clay slowly in drops and stirred for 24 hours at 65 °C. The reaction mixture is cooled, centrifuged and washed several times with distilled water and methanol until all the bromide ions are washed off. The organoclay obtained was freeze dried under vacuum overnight. The organoclay was obtained as fine, dry powder. The interlayer d-spacing for the organomodified montmorillonite was measured from WAXD. The organic contents were measured from the thermogravimetric analysis upon heating the organoclay to 900 °C.

3.2.7 Estimation of isocyanate content

The isocyanate content is estimated by adding known excess of dibutyl amine in toluene and back titrated with HCl using bromophenol blue as the indicator. The procedure is as follows. The isocyanate solution to be estimated is taken in a conical flask and 10 mL of DBA (2N) was added and stirred for one hour. Then 25 mL isopropanol was added followed by few drops of bromothymol blue solution and then titrated with HCl. The titre value is noted and the isocyanate content were calculated

3.2.8 Preparation of prepolymer terminated with isocyanate from EHG and TDI

EHG (17.656 g) was dissolved in 180 mL of dry toluene. Then DBTDL catalyst (2.5 mL of 1 wt % solution) was added to it. Then the mixture was cooled to 0 °C. Then TDI (29.348 g) was added slowly for 40 minutes into the reaction vessel. The temperature of the reaction mixture was maintained at below 5 °C during the addition of TDI. Once the addition was over, it was allowed to come to room temperature. It came to room

temperature by 20 minutes. Then it was heated at 70 °C for one hour. The heating was stopped and cooled to room temperature. The prepolymer solution obtained was transferred to a 250 mL measuring flask fitted with a septum adapter through a cannula under positive pressure of nitrogen. The solution level was made up to 250 mL by adding dry toluene through cannula. Now the prepolymer solution was kept at room temperature under nitrogen atmosphere. This solution was used for further studies and analysis.

Isocyanate content of this prepolymer stock solution was estimated by standard titration method and was found to be 9.17 wt %.

3.2.9 Preparation PU/Cloisite 30B nanocomposites with different amounts of trifunctional monomer

Four two neck r. b. flasks fitted with condenser and septum adapter were taken and to each flask 10 mL of dry toluene was transferred under nitrogen atmosphere through a cannula. To each of them 0.130 g of Cloisite 30B was added dispersed it thoroughly by stirring it with magnetic needle. Varying amounts of trimethylolpropane (as shown in the table 3.2) were added to different r.b. flasks and accordingly EHG was added. The stirring was done for 2 hours.

Table 3.2: Compositions of monomers in the preparation of PU/Cloisite 30B nanocomposite

| Expt No. | Amt. of TMP | Amt. of EHG | Amt. of C30B | Amt. of prepolymer stock solution |
|----------|-------------|-------------|--------------|-----------------------------------|
| A | 0.1423 g | 0.0 g | 0.130 g | 10 mL |
| B | 0.1067 g | 0.0581 g | 0.130 g | 10 mL |
| C | 0.0711 g | 0.1163 g | 0.130 g | 10 mL |
| D | 0.0356 g | 0.1744 g | 0.130 g | 10 mL |

Then 10 mL of prepolymer stock solution (whose isocyanate content was estimated by standard method) was added through cannula to each flask at room temperature. Slowly the temperature was raised to 70 °C and continued stirring for four hours. The reaction was stopped by cooling it to room temperature. The solvent was

evaporated by applying vacuum. The fine powder was obtained. Analyzed by WAXD for intercalation.

3.2.10 Preparation PU/Cloisite 25A nanocomposites with different amounts of trifunctional monomer

Four two neck r. b. flasks fitted with condenser and septum adapter were taken and to each flask 10 mL of dry toluene was transferred under nitrogen atmosphere through a cannula. To each of them 0.130 g of Cloisite 25A was added dispersed it thoroughly by stirring it with magnetic needle. Varying amounts of trimethylolpropane (as shown in the table 3.3) were added to different r.b. flasks and accordingly EHG was added. The stirring was done for 2 hours.

Table 3.3: Compositions of monomers in the preparation of PU/Cloisite 30B nanocomposite

| Expt No. | Amount of TMP | Amount of EHG | Amount of C25A | Amount of prepolymer stock solution |
|----------|---------------|---------------|----------------|-------------------------------------|
| A | 0.1500 g | 0.0 g | 0.130 g | 10 mL |
| B | 0.1126 g | 0.0581 g | 0.130 g | 10 mL |
| C | 0.0711 g | 0.1163 g | 0.130 g | 10 mL |
| D | 0.0375 g | 0.1744 g | 0.130 g | 10 mL |
| E | 0 | 0.2325 g | 0.130 g | 10 mL |

Then 10 mL of prepolymer stock solution (whose isocyanate content was estimated by standard method) was added through cannula to each flask at room temperature. Slowly the temperature was raised to 70 °C and continued stirring for four hours. The reaction was stopped by cooling it to room temperature. The solvent was evaporated by applying vacuum. The fine powder was obtained. Analyzed by WAXD for intercalation.

3.2.11 Preparation of PU/clay nanocomposites with varying functionality in the organoclays

The organoclays (0.130 g each), which are modified by exchanging with various organoammonium cations having the hydroxyl functionality as 1, 2 and 3 (1OHMMT, 2OHMMT and 3OHMMT), were dispersed in toluene medium separately in round bottom flasks by stirring at 70 °C. The prepolymer stock solution (10mL) was added to the organoclay dispersion slowly at room temperature and after the addition was over the temperature was slowly raised to 70 °C for two hours to allow the isocyanate to react with the hydroxyls of the modifier in the clay. Then calculated amounts of butanediol was added to the reaction mixture and continued stirring at 70 °C for another 4 hours to get PU nanocomposites after evaporating the solvent.

3.2.12 Preparation of Thermoplastic polyurethane (TPU)

For the preparation of pristine polyurethane, a two-step procedure was used. In the first step, isocyanate terminated prepolymer was prepared by reacting polycaprolactone diol (Mn: 750) with excess of isophorone diisocyanate in the mole ratio 1: 2.1. Calculated amount of IPDI was added slowly in to the solution of polycaprolactone diol at 80 °C and stirred for 2 hours under nitrogen atmosphere in presence of dibutyltin dilaurate as catalyst. In the second step, the prepolymer was chain extended by addition of butane diol and continued stirring at 80 °C for another 4 hours to get thermoplastic polyurethane. In order to compare the properties with the nanocomposites, where the matrix polymer reacts with modifier in the clay, pristine polymers were prepared by addition of equivalent amounts of modifiers salts along with butane diol during chain extension reaction.

3.2.13 Preparation of TPU/clay nanocomposites

For the preparation of Thermoplastic Polyurethane/clay nanocomposites, the prepolymer terminated with isocyanate was prepared as described for the preparation of pristine polyurethane. Then the reaction mixture containing the prepolymer was cooled down to room temperature. A predetermined amount of the organoclay was added and stirred at room temperature for 30 minutes to disperse the clay in the reaction mixture. The

temperature was raised to 80 °C and stirred for one hour to allow the reaction of isocyanates with the hydroxyls of the modifier in the organoclay. Then butane diol was added as chain extender and continued the polymerization for another four hours. Thermoplastic polyurethane clay nanocomposites were obtained as films by pouring the reaction mixture on a glass plate and casting the film by solvent evaporation under nitrogen flow at 55 °C.

3.2.14 Characterization

Fourier-transformed infrared spectroscopy (FTIR) experiments were performed using Perkin Elmer FTIR spectrophotometer at a resolution of 4 cm⁻¹. The sample for FTIR study were prepared by taking the sample in nujol and muller. The spectrum of the muller sample was obtained after being placed between two NaCl windows.

¹H NMR spectra were recorded in CDCl₃ solution with tetramethylsilane (TMS) as an internal standard using a Bruker DSX300

The WAXD measurements were performed using Rigaku Dmax 2500 diffractometer fitted with a diffracted beam graphite monochromator. The system consists of a rotating anode generator and wide-angle power goniometer. The generator was operated at 40kV and 150 mA. The radiation was Ni-filtered Cu-K α and samples were scanned between 2 θ = 2 to 10° and the scan speed was 2°/min.

The TGA-7 unit in the Perkin-Elmer thermal analysis system was used to determine the onset of degradation and the organic content in the organoclays. The samples were heated under a flowing nitrogen atmosphere from 50 to 900 °C, at a heating rate of 10 °C/min, and the weight loss was recorded. The weight loss at 900 °C was taken as the % organic content in the organoclay.

TEM imaging was done using a TehnaiG² Transmission electron microscope operating at an accelerating voltage of 300 kV. The nanocomposite samples were sectioned into ultrathin slices (<70 nm) at room temperature using the microtome Leica Ultracut UCT equipped with a diamond knife and then mounted on 200 mesh copper grids. The density of clay particles is enough to produce contrast between polymer and clay stacks hence

staining was not required. Images were captured using charged couple detector (CCD) camera for further analysis using Gatan Digital Micrograph analysis software.

The dynamic mechanical properties of the samples were studied using Rheometrics Dynamic Mechanical Analyzer, model DMTA IIIIE that provided storage modulus, loss modulus and loss tangent ($\tan \delta$) against temperature. The T_g was measured as the temperature at which the maximum in $\tan \delta$ appeared. The scans were carried out in rectangular sample tensile testing mode at a constant heating rate of 5 °C/min and a frequency of 1 Hz from -150 °C to 80 °C. The samples were cut (with span length of 10mm and thickness X width being 0.5 mm X 7 mm) from the sheets obtained by solvent casting at 55 °C after in-situ polymerization.

3.3 Results and discussion

To study the effect of branching in PU on the structure of PU/clay nanocomposite prepared by insitu polymerization of the monomers such as 2-ethyl-1,3-hexanediol and TDI with trimethylol propane (TMP) as the branching agent. For this study, two different organoclays such Cloisite 25A and Cloisite 30B were used, Cloisite 30B was modified with a quaternary ammonium ion which contains two reactive hydroxyl groups along with a long alkyl chain while Cloisite 25A was modified contains only long alkyl chain in the modifier and do not have a reactive group. To verify the reactivity of the hydroxyl group of the modifier of the Cloisite 30B it was allowed to react with phenyl isocyanate and formation of urethane was monitored by IR analysis. Polyurethane/clay nanocomposites with varying amounts of branching agent were prepared by in situ polymerization where, the synthesized prepolymer terminated with isocyanate was added to the dispersion of organoclay, chain extender diol and the branching agent in toluene medium at 65 °C. The structure of the clay in the nanocomposite was analyzed by WAXD and TEM. The dispersability of the organoclay, Cloisite 30B in polyurethane with varying amounts of branching agent was evaluated and compared with the dispersability of the organoclay, Cloisite 25A.

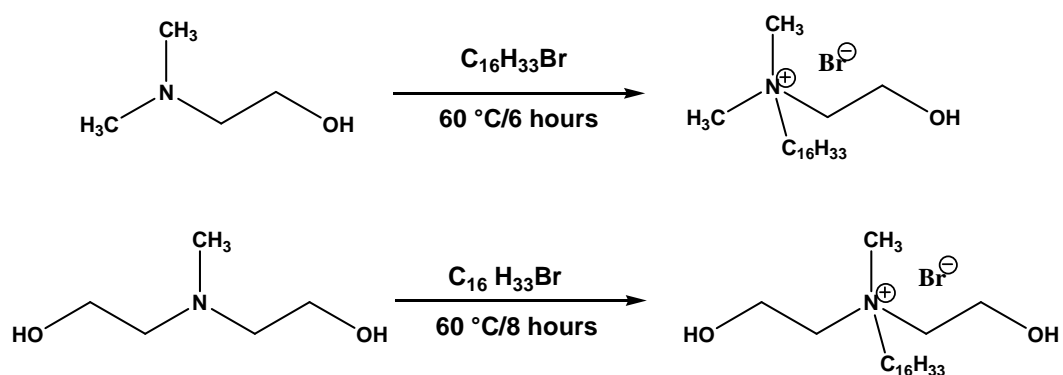
To study the effect of reactive functionality of the modifier of the organoclay on the structure of nanocomposite, organoclays modified using quaternary ammonium salts with

varying number of hydroxyl groups were prepared in the laboratory by standard ion exchange reaction with respective salts. The organoclays prepared with the varying functionality of the modifier (number of hydroxyls in the modifier) such as 1, 2 and 3 were designated as 1OHMMT, 2OHMMT and 3OHMMT respectively. To verify the reactivity of the functionality in the modifier, the quaternary ammonium salts were reacted with phenyl isocyanate in stoichiometric ratio to form urethanes and analyzed by H^1 NMR. Polyurethane/clay nanocomposites with various organoclays such as 1OHMMT, 2OHMMT and 3OHMMT were prepared by first reacting the prepolymer terminated with isocyanate with organoclays followed by chain extension with the diol. The structure of the clay in the nanocomposite was analyzed by WAXD and TEM. The enhancement in the mechanical properties of the TPU/clay nanocomposites using these organoclays, which was prepared via insitu polymerization, was evaluated. The matrix polyurethane, which is made from the monomers such as polycaprolactone diol, isophorone diisocyanate and butanediol, was chosen for this study.

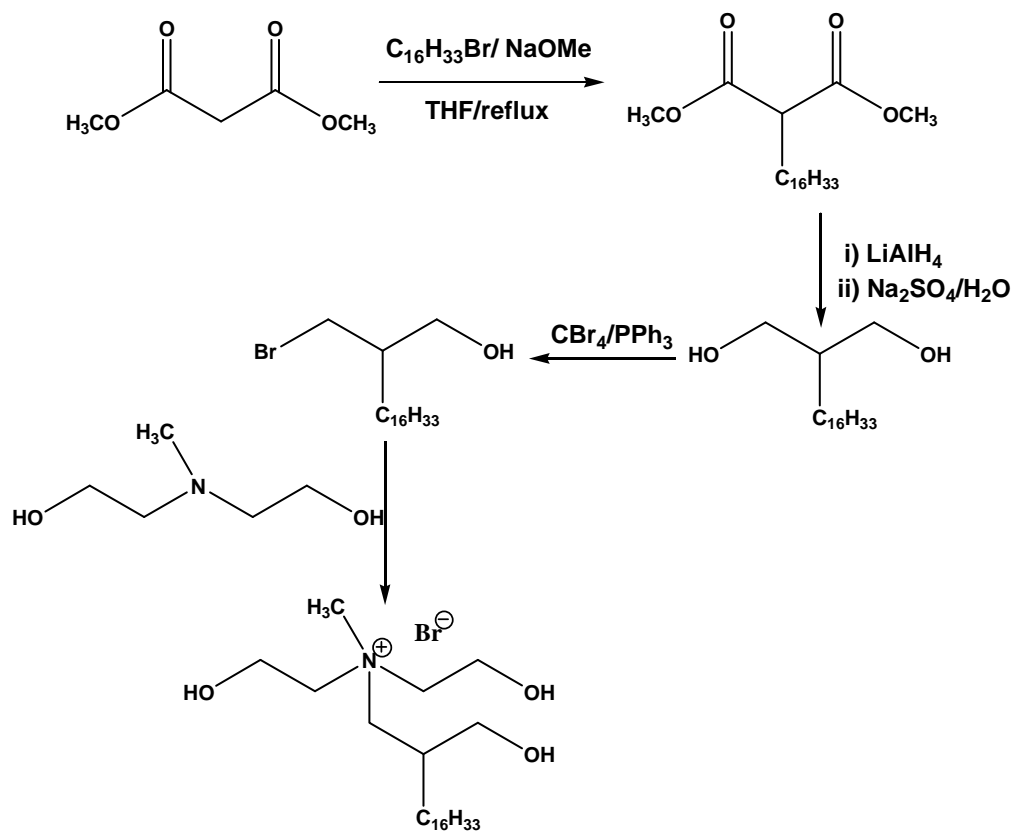
3.3.1 Preparation of organomodifiers for the clay

Hydroxyethyl dimethyl amine and bis(hydroxyethyl) methyl amine were quaternized with hexadecyl bromide to prepare quaternary ammonium salts with monohydroxy and dihydroxy functional group respectively (**Scheme 1**). To obtain a trihydroxyalkyl quaternary ammonium salt, bis(hydroxyethyl) methyl amine was quaternized with 2-(hydroxymethyl)octadecyl bromide. 2-(hydroxymethyl) octadecyl bromide was again prepared from simple starting materials as shown in the **scheme 2**. Dimethyl malonate was alkylated with hexadecyl bromide after generating nucleophilic anion using sodium methoxide which was generated insitu reaction of sodium with methanol. The hexadecylated malonate obtained was reduced to a diol, 2-(hydroxy methyl) octadecanol using lithium aluminum hydride. The diol was monobrominated by using controlled stoichiometry of the reagent such as carbontetrabromide with triphenyl phosphine to obtain 2-(hydroxymethyl) octadecyl bromide.

Scheme 1



Scheme 2



3.3.2 Reactivity of hydroxyls in the modifier with phenyl isocyanate

The reactivity of the hydroxyl groups present in the organomodifiers prepared in the laboratory was studied by reacting them with phenyl isocyanate in presence of the catalyst DBTDL. The quantitative conversion of hydroxyl groups into phenyl carbamates was studied using NMR analysis. The Figure 3.1(a), (b) and (c) show the ^1H NMR of the reacted organomodifiers containing phenyl carbamates. Phenyl Protons of the phenyl carbamate show characteristic chemical shift at δ 7.62 ppm, 7.26 and 7.02 in the ratio 2:2:1. The ratio of integrated area of one of the ^1H signals due to the phenyl protons at 7.02 ppm with respect to the terminal methyl protons of the long alkyl chain at 0.88 ppm were calculated. They showed the ratio of 1:3, 2:3 and 3:3 for the phenyl carbamates prepared with 1OH, 2OH and 3OH respectively. From this study, it can be concluded that the hydroxyl groups readily react with isocyanates to give quantitative carbamate linkages and the functionalities of the modifiers such as 1OH, 2OH and 3OH were confirmed to be 1, 2 and 3 respectively.

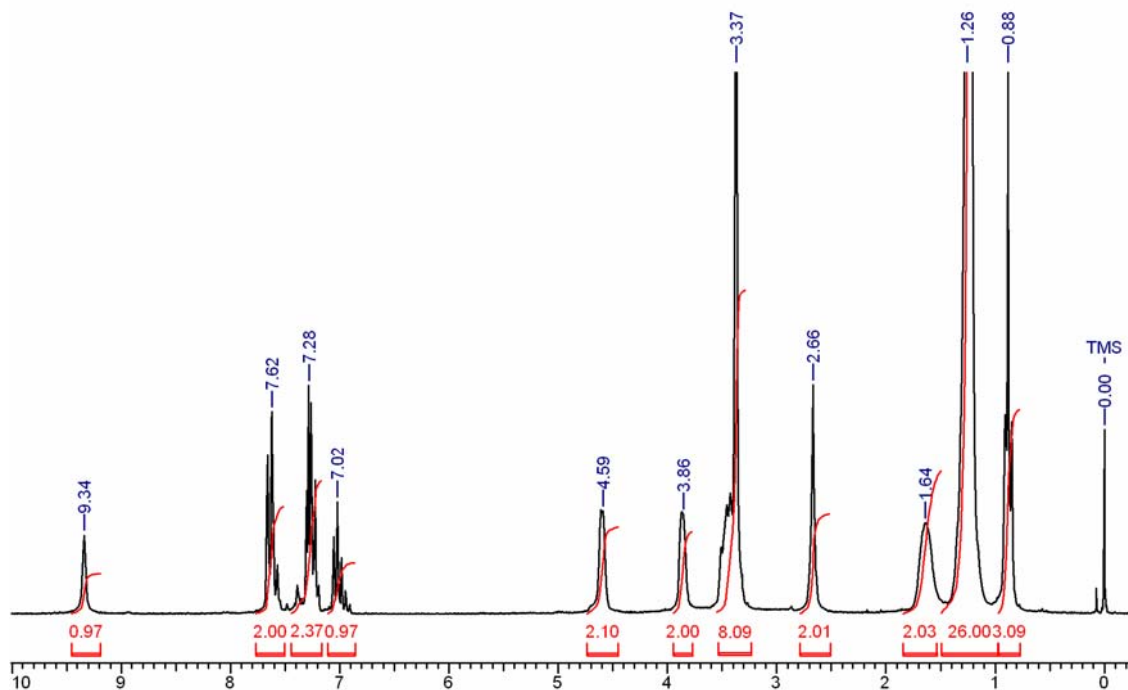


Figure 3.1 (a): ^1H NMR spectra of phenyl carbamate of 1OH

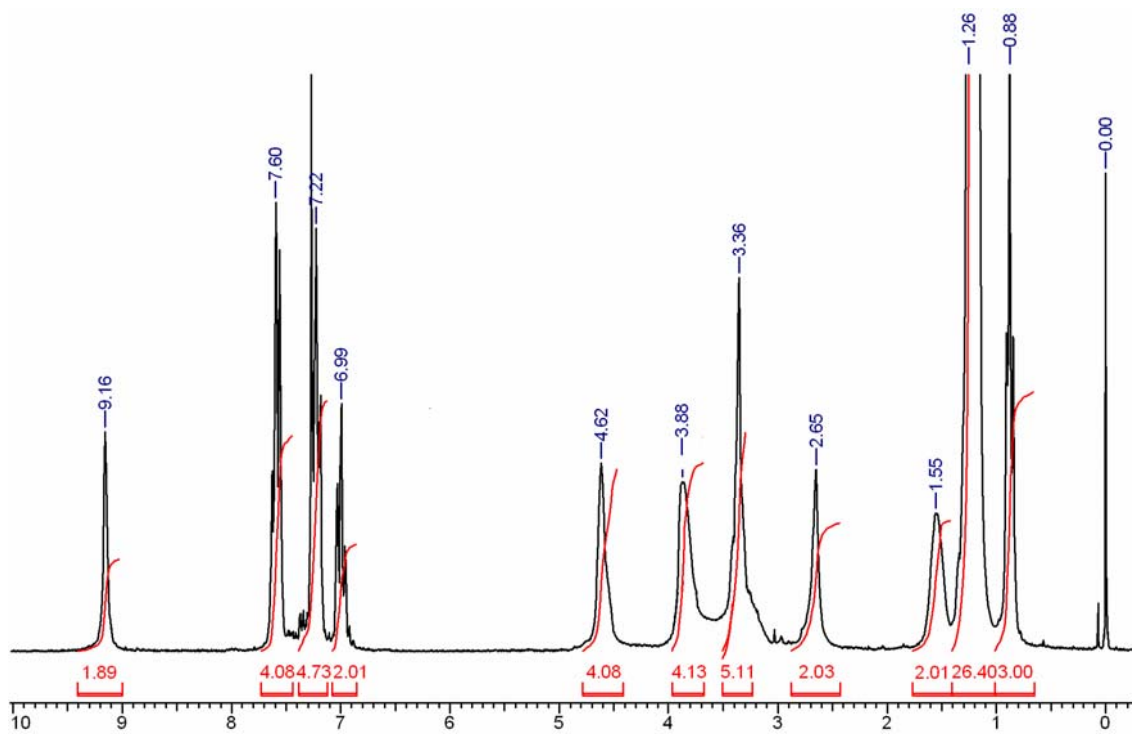


Figure 3.1 (b): NMR spectra of phenyl carbamate of 2OH

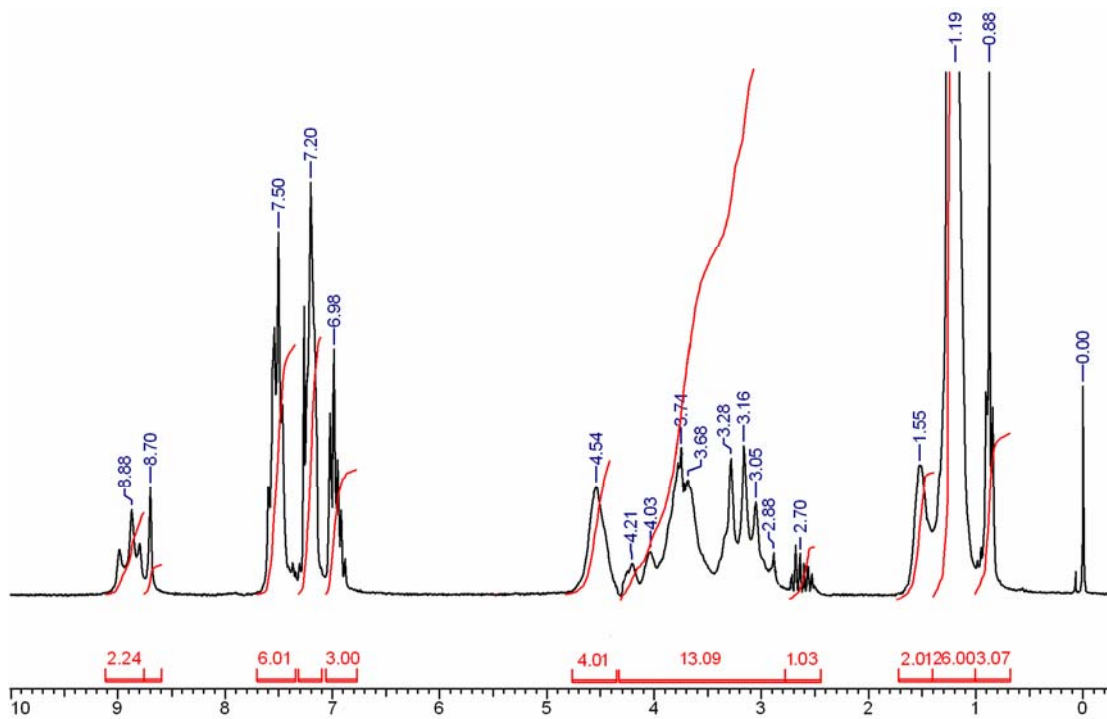


Figure 3.1 (c): NMR Spectra of phenyl carbamate of 3OH

3.3.3 Preparation of organoclays with various functionality in the modifier

The organoclays were prepared with the varying functionality of the modifier (number of hydroxyls in the modifier) such as 1, 2 and 3 and were designated as 1OHMMT, 2OHMMT and 3OHMMT respectively. They were characterized by WAXD and were shown in figure 3.2. The WAXD patterns show 001 peak, which correspond to the interlayer d-spacing of the organoclay. The Table 3.4 shows the interlayer distance of the organoclays. The interlayer distance has increased from that of Na⁺MMT due to exchange of the larger organocation with Na⁺ ion in the interlayer gallery. The larger increase in d-spacing for 3OHMMT as compared to the other two clays such as 1OHMMT and 2 OHMMT can be attributed to the presence longer alkyl chain (18 C) in the former as compared relatively smaller alkyl chain (16 C). The organic contents estimated from TGA were comparable with theoretically calculated value for the quantitatively exchanged organoclay.

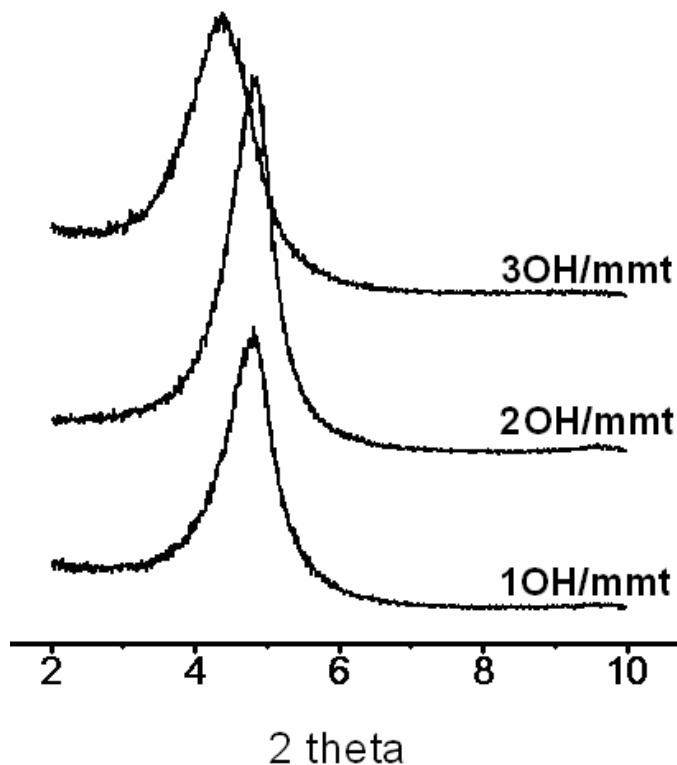


Figure 3.2: WAXD patterns for organoclays such 1OHMMT, 2OHMMT and 3OHMMT.

Table 3.4: The weight loss on charring at 900 °C from TGA and d- spacing for the organoclays from WAXD for the organoclays

| Clay | Weight loss on charring (%) | | d-spacing for clay, Å |
|--------|-----------------------------|--------------|-----------------------|
| | Theoretical | Experimental | |
| 1OHMMT | 22.7 | 22.8 | 18.5 |
| 2OHMMT | 24.5 | 24.6 | 18.5 |
| 3OHMMT | 27.5 | 27.7 | 20.2 |

3.3.4 Reactivity of hydroxyl of modifier in Cloisite 30B with isocyanate

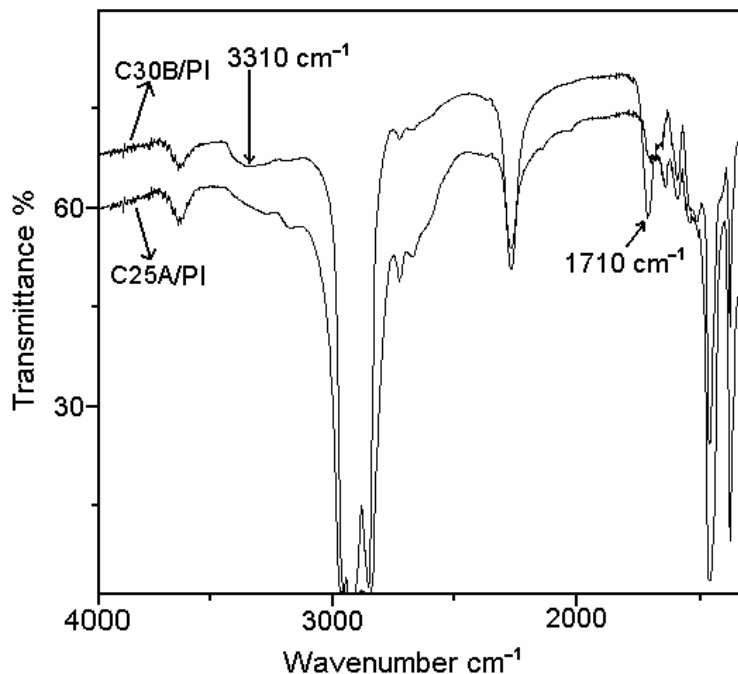


Figure 3.3: IR spectra to show the reactivity of Cloisite 30B and Cloisite 25A with phenyl isocyanate

The reactivity of hydroxyl group of the modifier in cloisite 30B with isocyanate was verified by FTIR study. Cloisite 30B was mixed with phenylisocyanate (PI) in dry toluene at 60° C for 6 hours. Then the clay was filtered and washed with solvent and then analyzed by FTIR. For comparison an organoclay without hydroxyl group (Cloisite 25A) was treated similarly and FTIR spectra was recorded. The FTIR spectra of Cloisite 30B/PI and Cloisite 25A/PI are shown in **figure 3.3**. The hydrogen bonded carbonyl and the hydrogen bonded N-H bands from the urethane groups usually appeared at 1710 and

3310 cm^{-1} , respectively, in the FTIR spectrum. There is no absorption peak observed at 1710 cm^{-1} or at 3310 cm^{-1} in the FTIR spectrum of Cloisite 25A/PI as shown in figure, indicating that there is no reaction between Cloisite 25A and PI. This implies that the polyurethane can just be absorbed on the silicate surface by the physical trap force in the untethered cloisite 25A/PU system. In the case of FTIR spectrum of Cloisite 30B/PI, distinctive absorption bands were observed at 1710 and 3310 cm^{-1} . This is a direct result of urethane group produced by reaction of hydroxyl groups in Cloisite 30B with isocyanate group of PI. Hence polyurethane chain can be tethered to Cloisite 30B through the formation of urethane bonds as confirmed by FTIR study.

3.3.5 Preparation of prepolymer terminated with isocyanate

Prepolymer terminated with isocyanate was prepared by taking toluenediisocyanate to EHG mole ratio 1: 1.4 in toluene medium. The TDI was added to the diol very slowly drop by drop using an addition funnel by cooling the reaction mixture externally using ice bath to make sure that during the polymerization, the temperature was not raised due to exotherm of the reaction. The isocyanate content was determined by standard titration method. Thus prepared prepolymer had contained 9.17 wt % isocyanate, which is close to the theoretically calculated value.

3.3.6 Effect of branching agent

3.3.6.1 WAXD

To study the effect of branching on the structure of Polyurethane/clay nanocomposites, they were prepared via insitu solution polymerization with varying amount of branching agent (trimethylol propane). The polymerization was carried out by adding the prepolymer terminated with isocyanate with an isocyanate content of 9.17 wt % was added to the dispersion of the organoclay, diol and the branching agent mixture in toluene and heated at 70 °C. For this study the organoclays such as Cloisite 30B and Cloisite 25A were used. The structures of the clay in the nanocomposite obtained were studied by WAXD and TEM. The WAXD patterns are as shown in the **figure 3.4**.

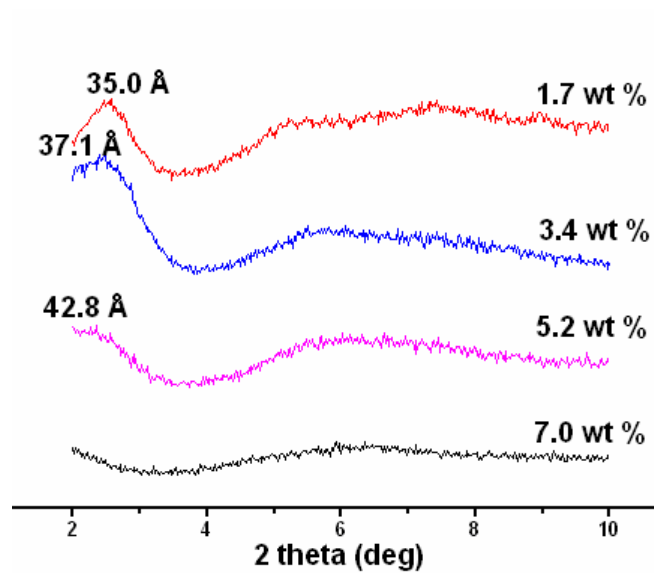


Figure 3.4 (a): WAXD pattern of PU/Cloisite 30B nanocomposites with varying amount of trimethylol propane

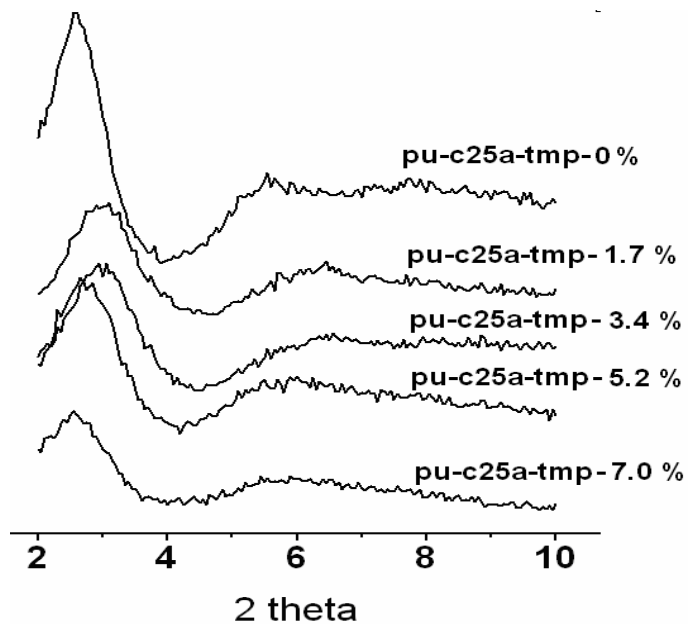


Figure 3.4 (b): WAXD pattern of PU/Cloisite 25A nanocomposites with varying amount of trimethylol propane

When Cloisite 30B was used to prepare the nanocomposite, as the amount of TMP was increased, the d-spacing increased indicating better intercalation of the polymer in the interlayer gallery with branching agent and at 7 weight % of the branching agent, the nanocomposite obtained showed disappearance of the peak for the organoclay indicating exfoliations. This result reiterates the fact that presence of branching in the architecture of the matrix polymer helps in exfoliation of organoclay as shown by the modeling studies by Balaz et al.³⁴ and are similar to the results obtained by other researchers in the synthesis of polyurethane nanocomposites³⁵.

However, when Cloisite 25A was used as the organoclay in presence of TMP, intercalated structures were obtained and with the increase in the content of TMP, there is no appreciable increase in the intercalation for the clay in the nanocomposite. This shows that presence of reactive hydroxyl groups on the modifier for the clay to anchor the polymer chains on to clay surface during polymerization was essential to obtain better dispersion of the organoclay in addition to branching of the polymer backbone.

3.3.6.2 TEM

Typical TEM pictures of the PU nanocomposites prepared using Cloisite 30B with varying amounts of branching agent such as 1.7 wt %, 3.4 wt %, 5.2 wt %, and 7 wt % were shown in figures 3.5, 3.6, 3.7, and 3.8 respectively. The figure 3.5 shows that with 1.7 wt% branching agent, intercalated structures were formed with small amounts exfoliated clay layers. As the concentration of the branching agent increases, we can observe from the figures 3.5 to 3.8, the ratio of exfoliated structures to the intercalated structures also increases and at 7 wt % of branching agent in the composition show complete exfoliation with very little intercalated structures.

TEM pictures of PU nanocomposites prepared using Cloisite 25A and with 7 wt % branching agent was shown in figure 3.9 and 3.10 respectively. It can be observed that the presence of branching agent did not show considerable effect on the intercalation and dispersion of the clay in the polymer matrix. These results further confirms that presence of reactive hydroxyl groups on the modifier for the clay to anchor the polymer chains on to clay surface during polymerization was essential to obtain better dispersion of the organoclay in addition to branching of the polymer backbone.

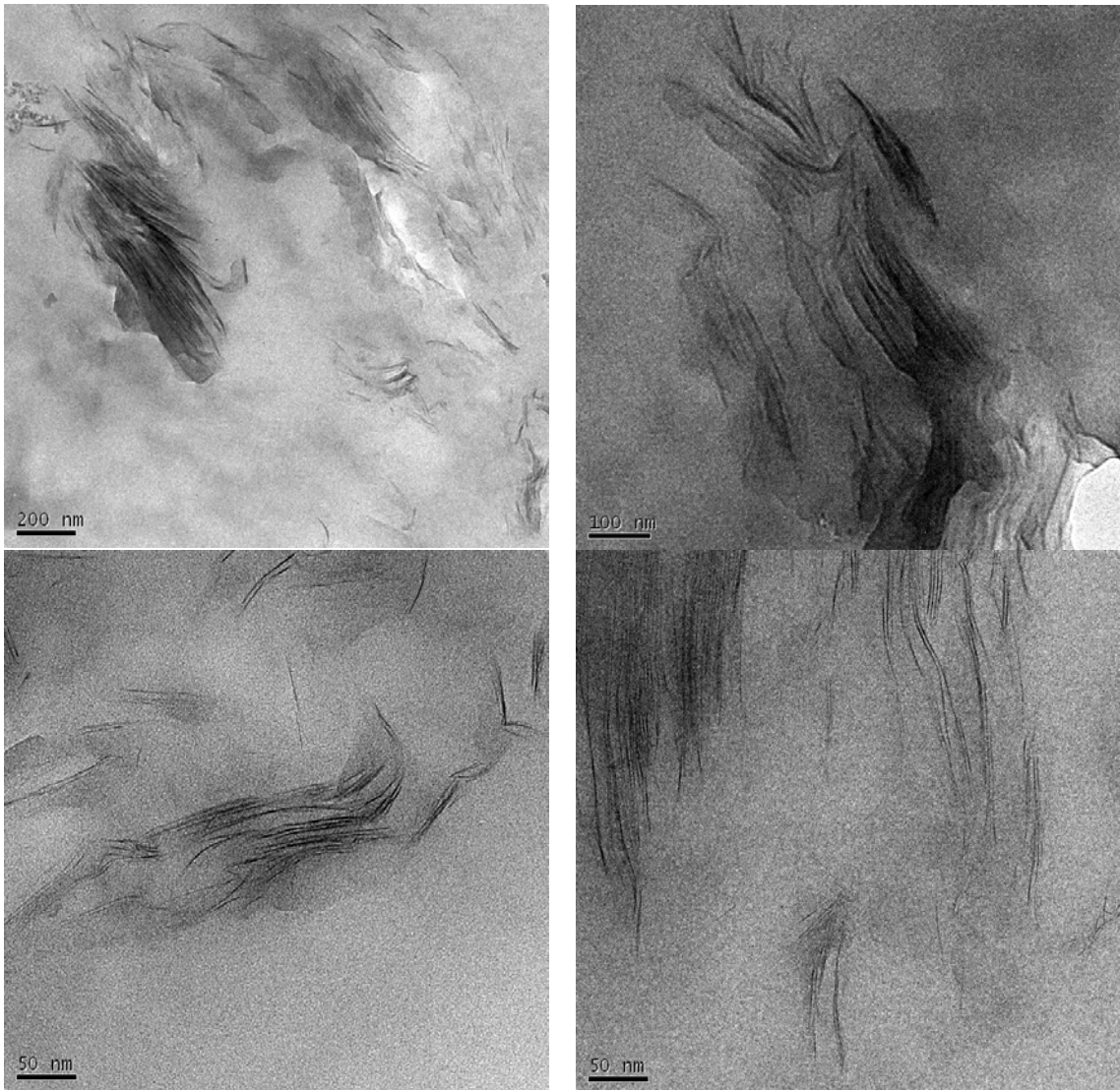


Figure 3.5: TEMs of PU/Cloisite 30B nanocomposite with 1.7 wt % branching agent

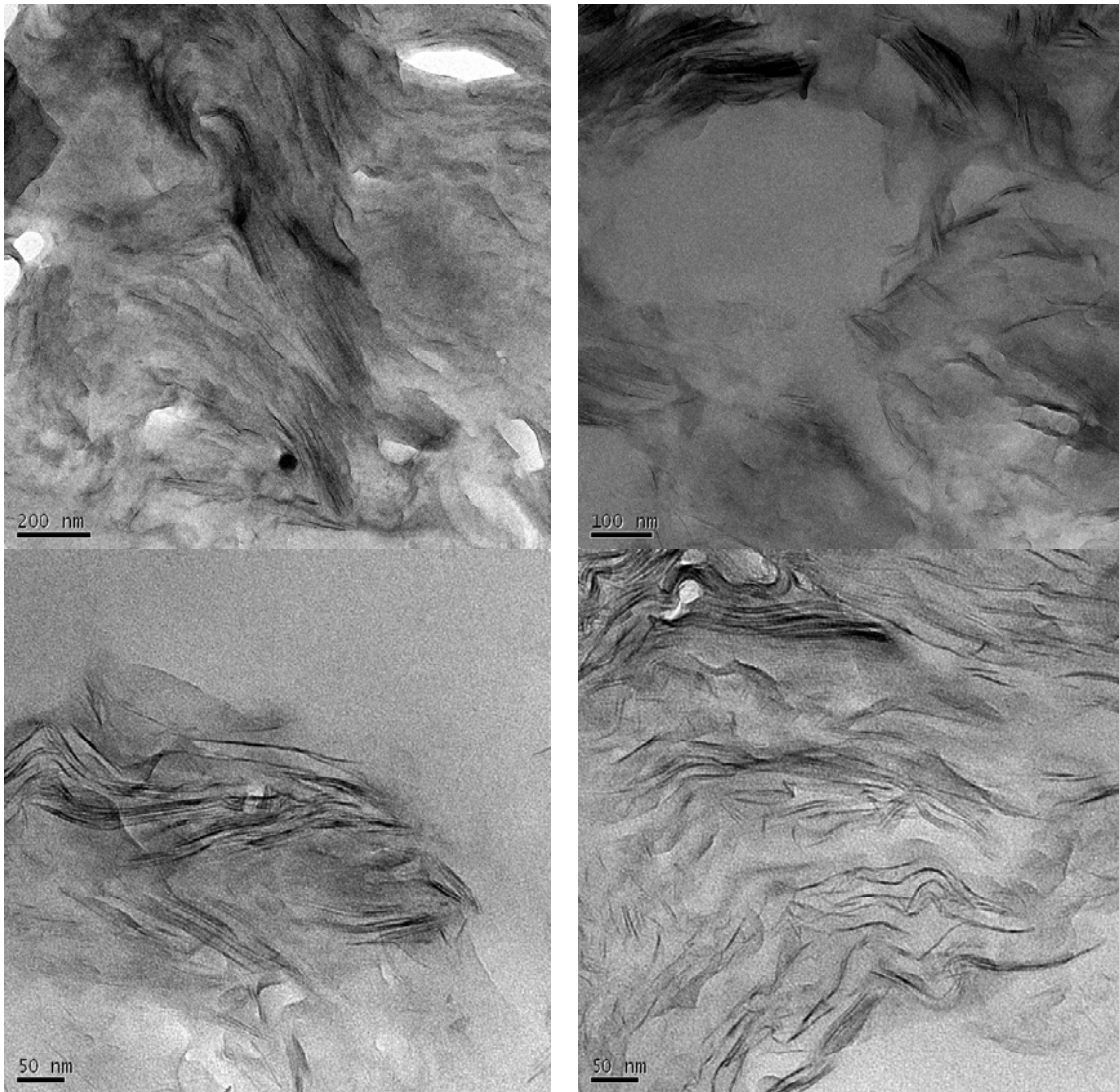


Figure 3.6: TEMs of PU/Cloisite 30B nanocomposite with 3.4 wt % branching agent

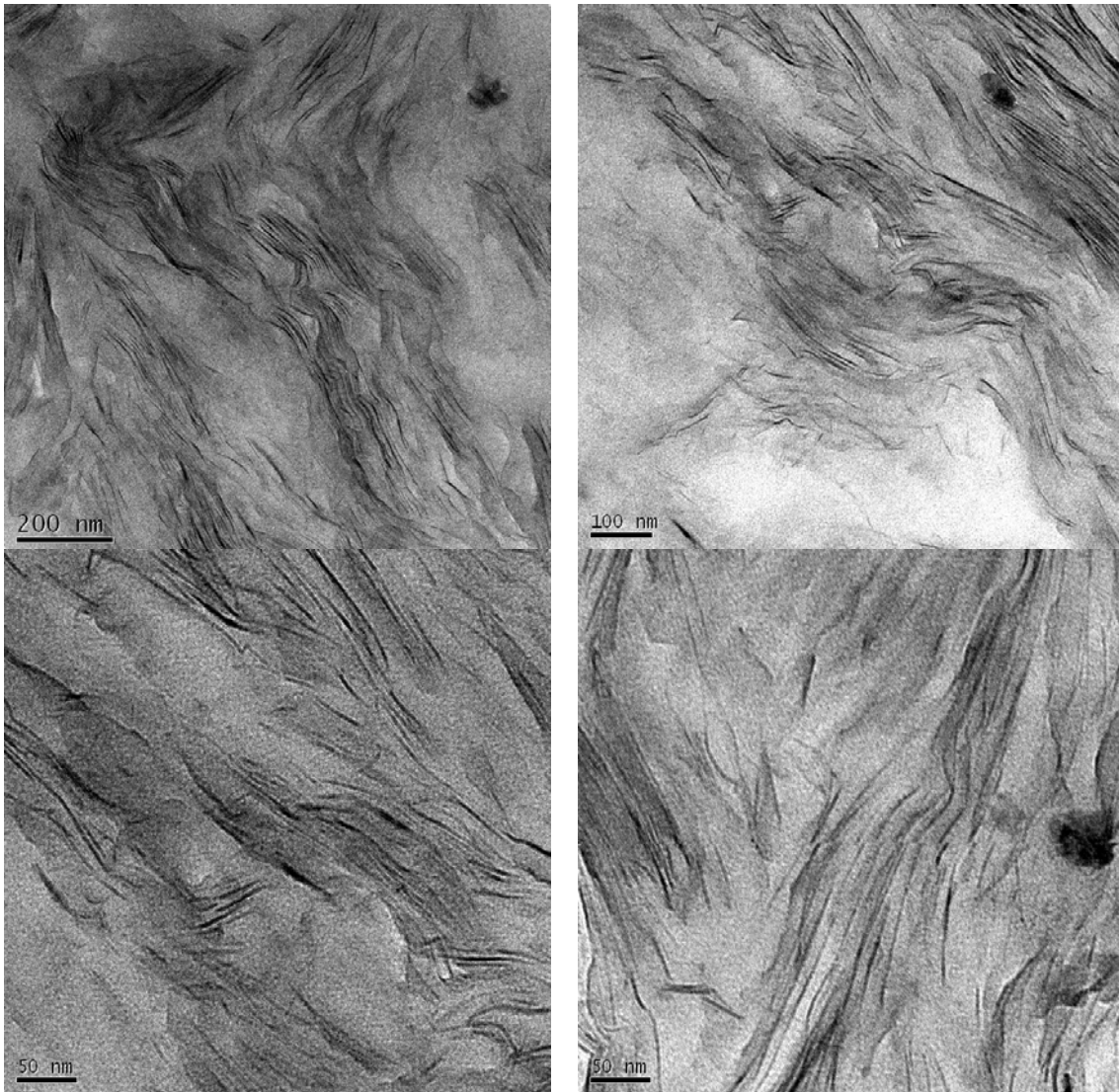


Figure 3.7: TEMs of PU/Cloisite 30B nanocomposite with 5.2 wt % branching agent

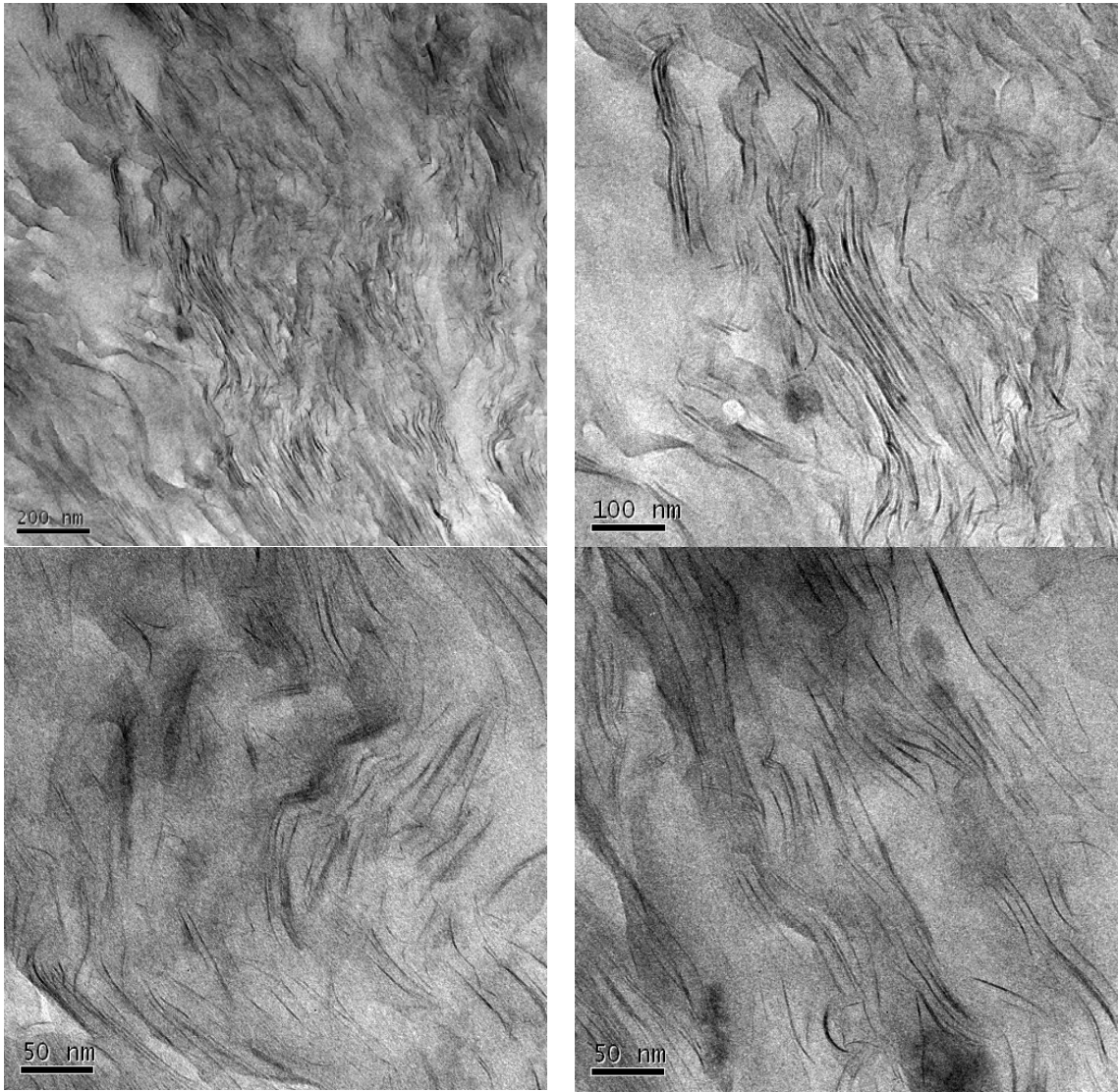


Figure 3.8: TEMs of PU/Cloisite 30B nanocomposite with 7.0 wt % branching agent

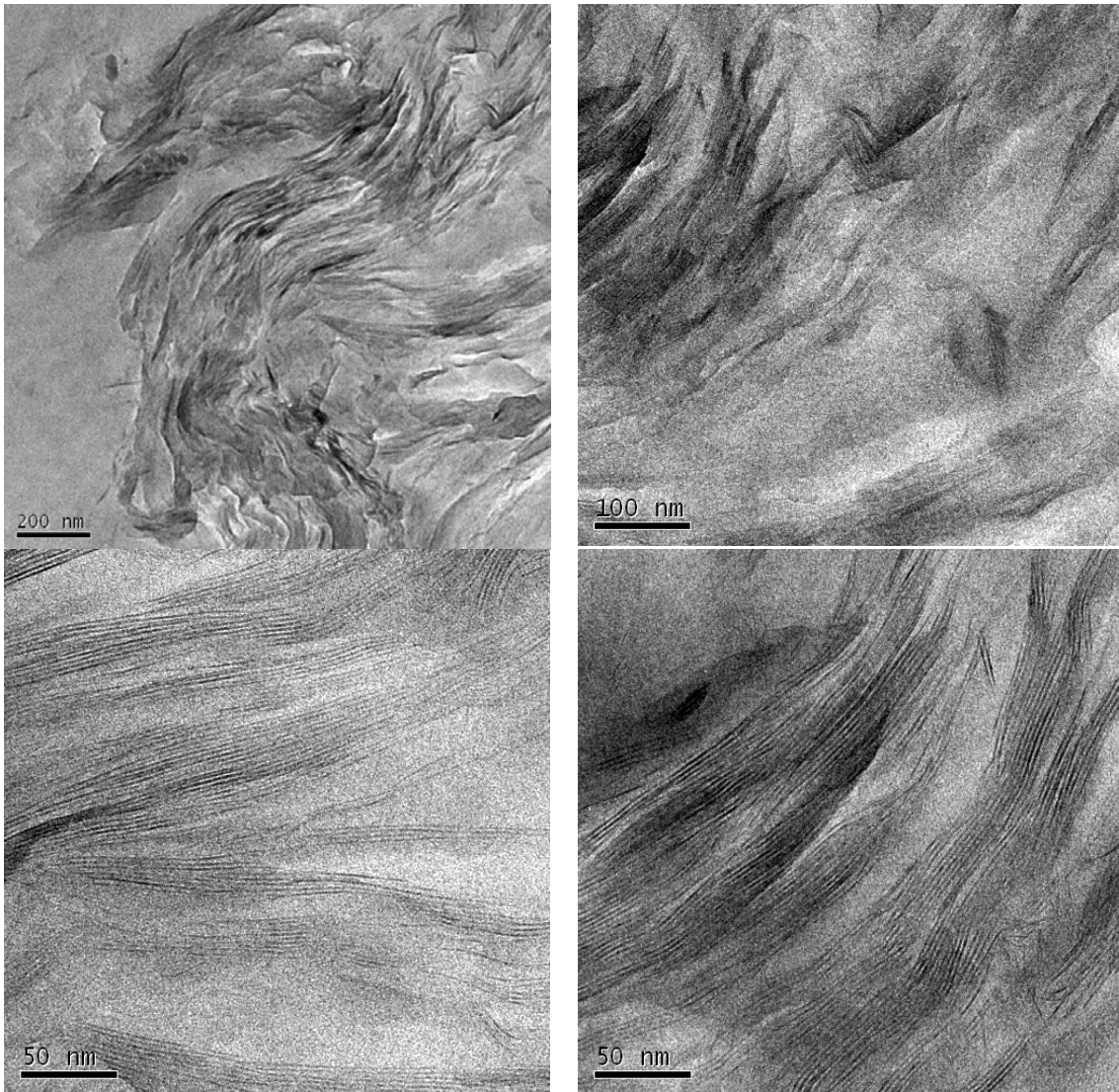


Figure 3.9: TEMs of PU/Cloisite 25A nanocomposite

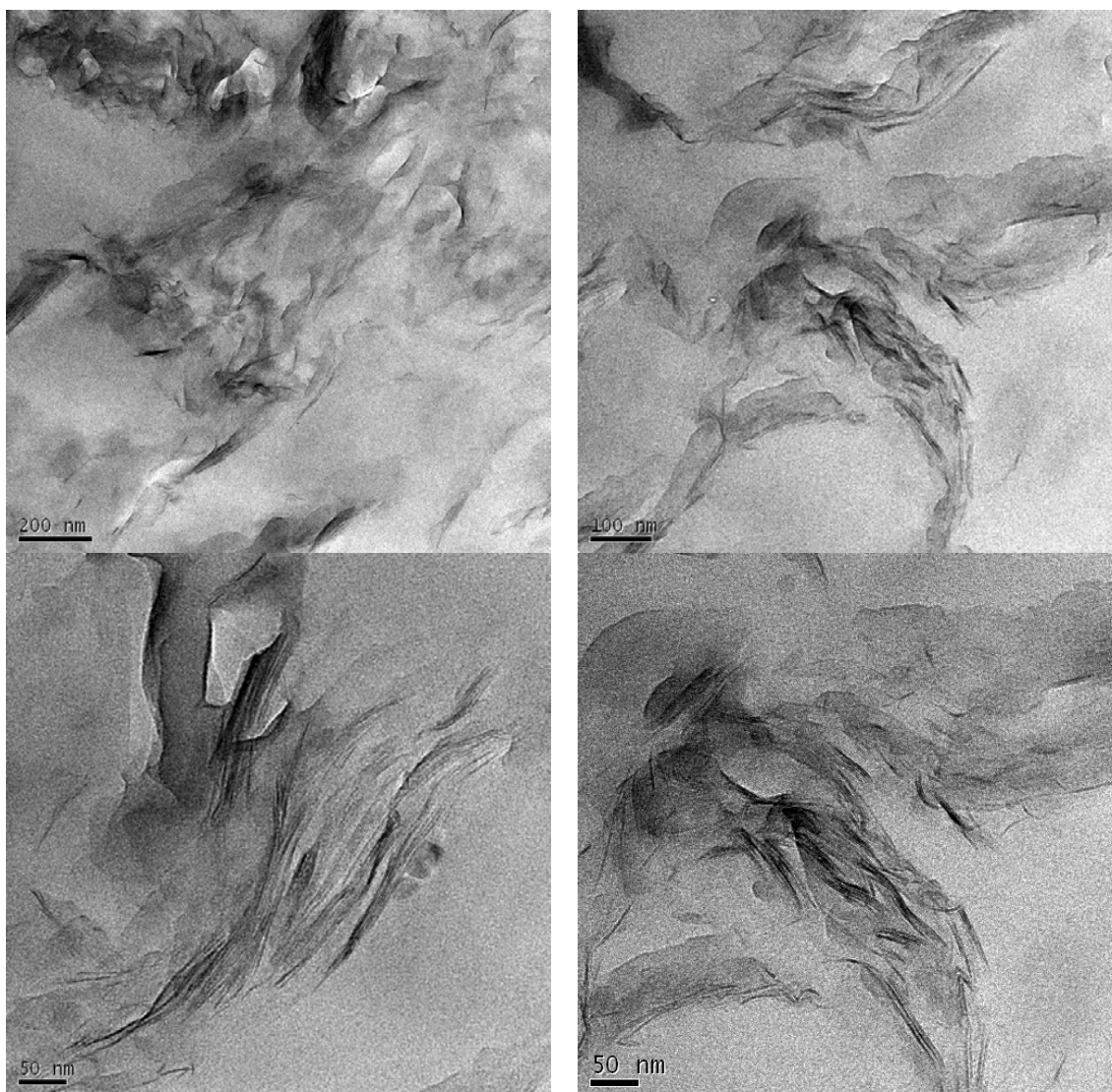


Figure 3.10: TEMs of PU/Cloisite 25A nanocomposite with 7.0 wt % branching agent

3.3.7 Effect of functionality of the modifier in the organoclay

Organoclays modified with organoammonium cations containing reactive hydroxyl groups were evaluated for the preparation of well-dispersed polyurethane/clay nanocomposites. For this study three different organoclays such as 1OHMMT, 2OHMMT and 3OHMMT were prepared in the laboratory and used. The nanocomposites were prepared via in-situ solution polymerization in a two-stage synthesis. In the first step, a prepolymer terminated with isocyanate was prepared toluene medium using toluenediisocyanate and EHG taken in the mole ratio 1: 1.4 and mixed with the dispersion of clay to allow the reaction of isocyanate in the prepolymer with hydroxyl

groups of the modifier in the organoclay. Then calculated amount of EHG was added for the chain extension reaction to obtain PU/clay nanocomposites.

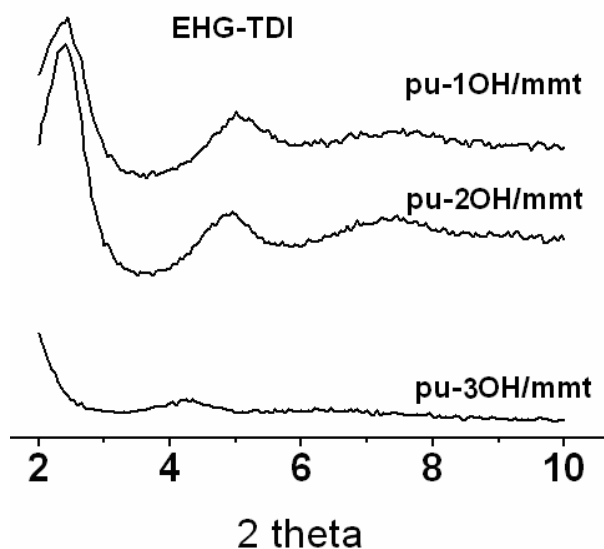


Figure 3.11 : WAXD pattern of PU/clay nanocomposites with 1OHMMT, 2OHMMT and 3OHMMT

The nanocomposites obtained was characterized by WAXD (figure 3.11) and found that when 1OHMMT and 2OHMMT were used, the d-spacing for the clay has increased from 18.5 Å for the organoclay to 34 Å in the nanocomposites indicating the formation of intercalated structures. When the organoclay used was 3OHMMT, there was no peak observed for the nanocomposite. From the pattern it can be understandable, though there was no peak observed, there may be a possibility that the peak may be shifted below 2° as one can easily see a low intensity peak corresponding 002 plane. This indicates that with 3OH-MMT, better-intercalated PU/clay nanocomposites were obtained.

TEM pictures of the PU nanocomposites prepared using the organoclays such as 3OH-MMT, 2OH-MMT and 1OH-MMT were shown in figures 3.12, 3.13 and 3.14 respectively. In all the three cases only intercalated structures were observed. The nanocomposites obtained with the organoclay 3OH-MMT show slightly higher d-spacing than the other two nanocomposites prepared using the organoclays such as 2OH-MMT and 1OH-MMT. These observations confirm the results obtained by WAXD.

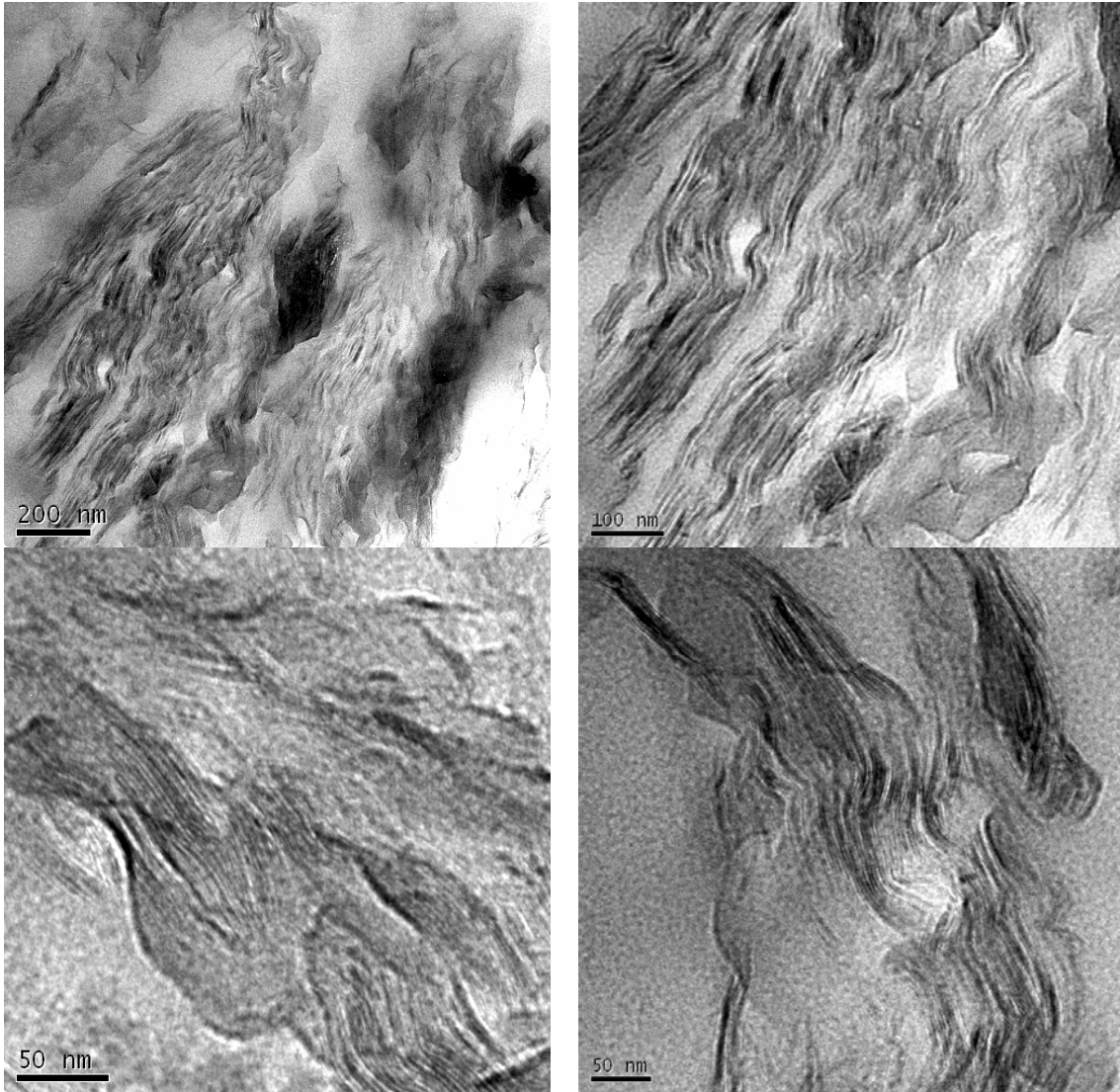


Figure 3.12: TEMs of PU/3OH-MMT nanocomposites

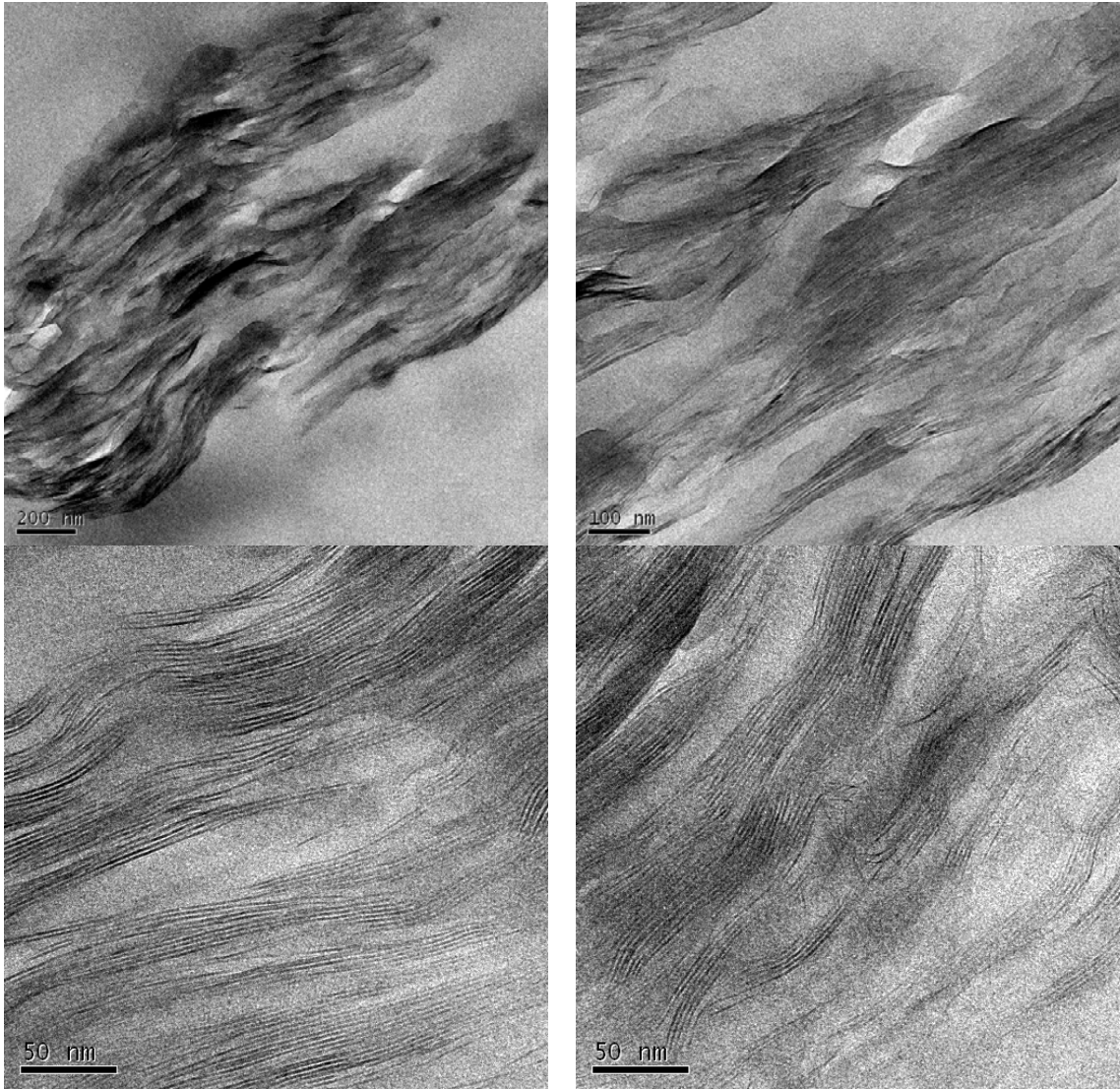


Figure 3.13: TEMs of PU/2OH-MMT nanocomposites

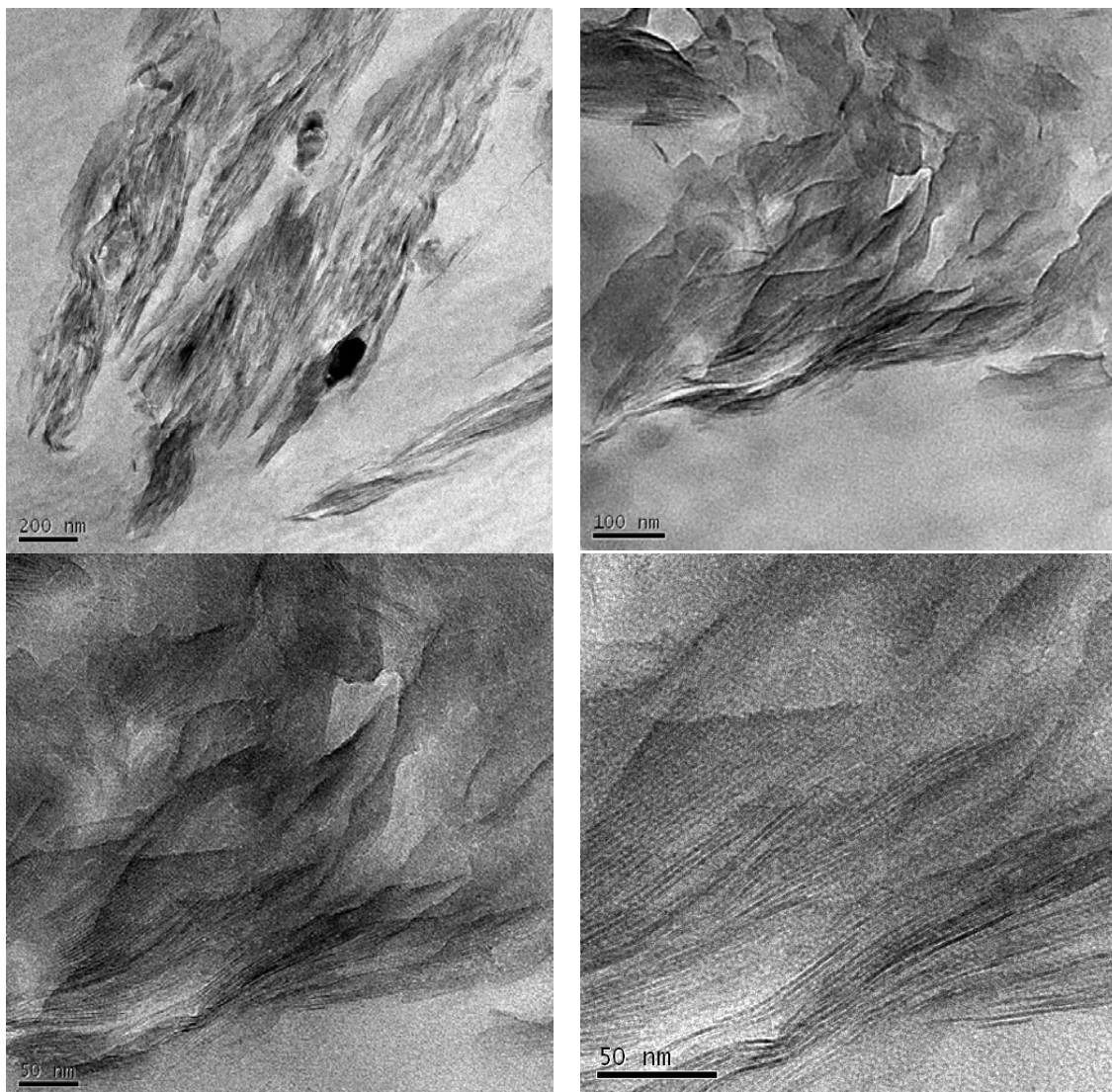


Figure 3.14: TEMs of PU/1OH-MMT nanocomposites

3.3.8 Effect of functionality of the modifier in the organoclay on thermoplastic Polyurethane

For evaluation of the use of these clays on the preparation and properties of thermoplastic polyurethanes, nanocomposites were prepared using the same method where in the prepolymer terminated with isocyanate was prepared from polycaprolactone diol and

isophorone diisocyanate in the mole ratio 1:2.1 and butane diol was used as chain extender. The structure of the nanocomposites obtained were characterized WAXD (Figure 3.15). It was found that the nanocomposites obtained using 1OHMMT and 2OHMMT show the increase in d-spacing from 18.5 Å for the organoclay to 34.0 Å for the nanocomposites. When the nanocomposites were prepared using 3OHMMT, the d-spacing has increased upto 37.1 Å. It should be noted that though the nanocomposites obtained with 3OHMMT show higher d-spacing than the nanocomposites obtained using 1OHMMT and 2OHMMT, it is not clear whether this increase is due the result better anchoring of the polymer chains with the clay surface through the hydroxyls in the modifier or is it due to higher d-spacing of the starting organoclay. It should be noted that the nanocomposites obtained in EHG and TDI system showed higher d-spacing than the TPU system when compared with the use of respective organoclays, indicate better intercalation EHG-TDI system which can be attributed to higher density of hydrogen bonding interactions with the clay surface.

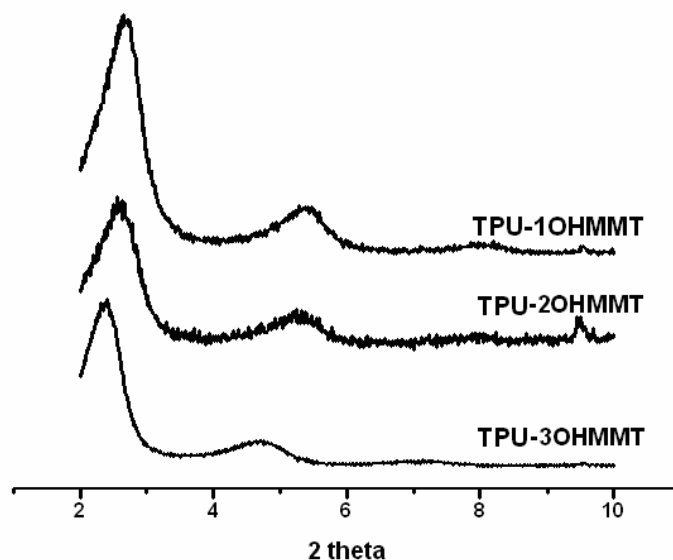


Figure 3.15: WAXD pattern of PU/clay nanocomposites with 1OHMMT, 2OHMMT and 3OHMMT

The TEM pictures of TPU nanocomposite prepared using 3OH MMT, 2OH-MMT and 1OH –MMT were shown in figure 3.16, 3.17 and 3.18. All the compositions show highly intercalated structures and the interlayer distance are comparable with WAXD data.

Again it should be noted that for a given clay (1OH-MMT, 2OH-MMT and 3OH-MMT), the extent of intercalation with the thermoplastic polyurethane system which contain polycaprolactone soft segments is poorer as compared to the extent of intercalation of the polyurethanes system that are made of only hard segments. This can be attributed to the lower polarity and the density of hydrogen bonding in the thermoplastic polyurethane system which contain polycaprolactone soft segments.

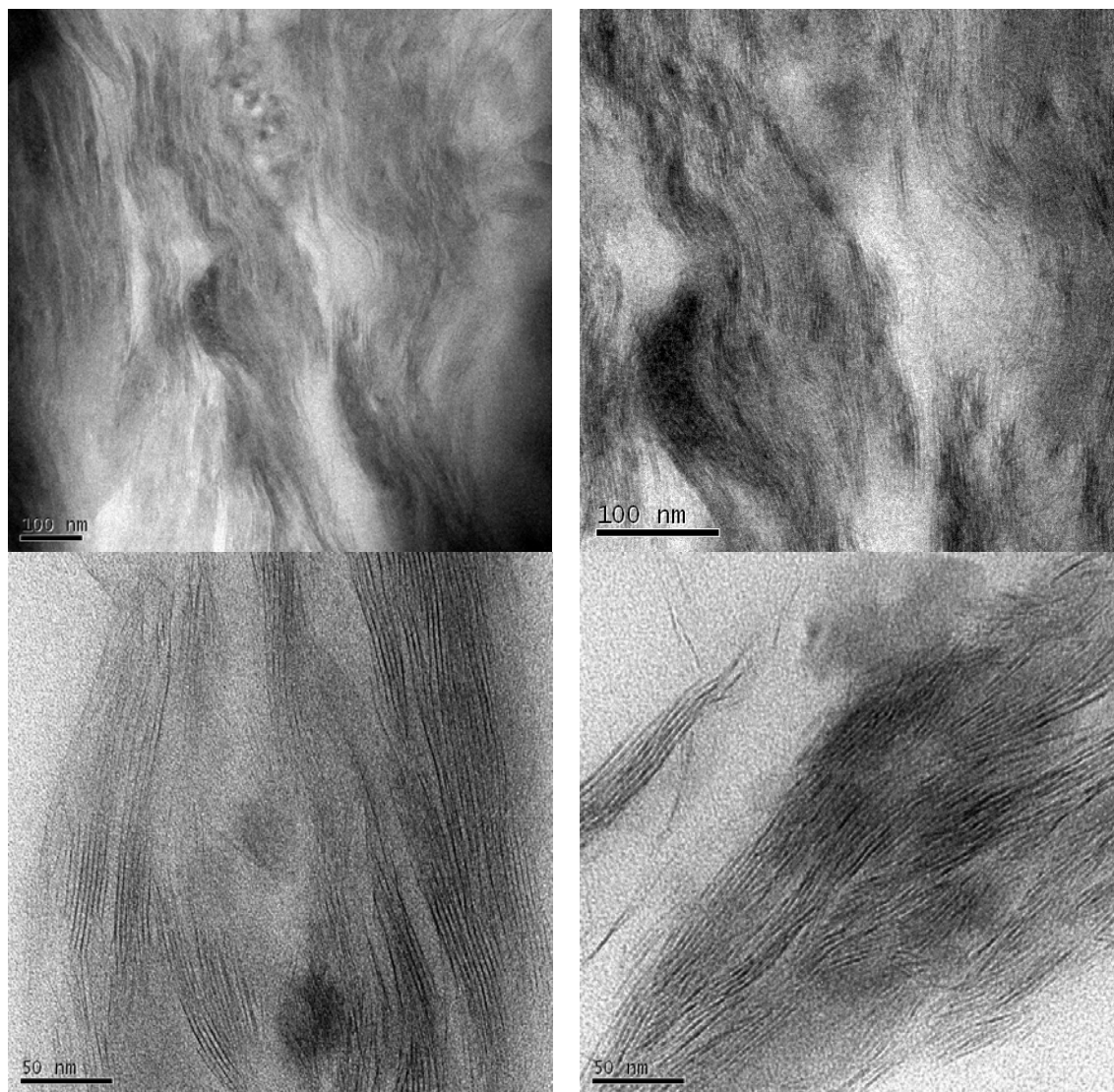


Figure 3.16: TEMs of TPU/3OH-MMT nanocomposites

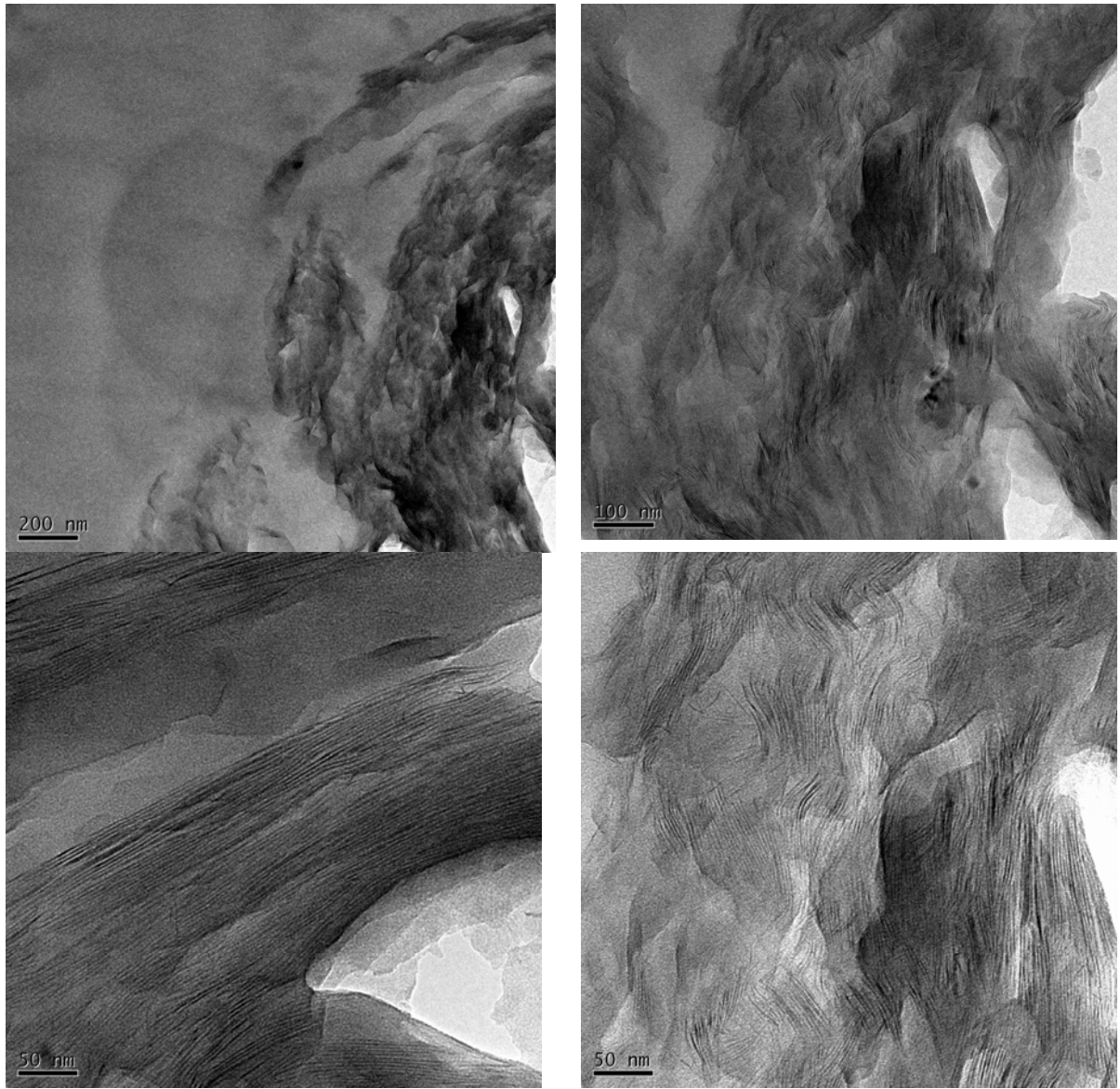


Figure 3.17: TEMs of TPU/2OH-MMT nanocomposites

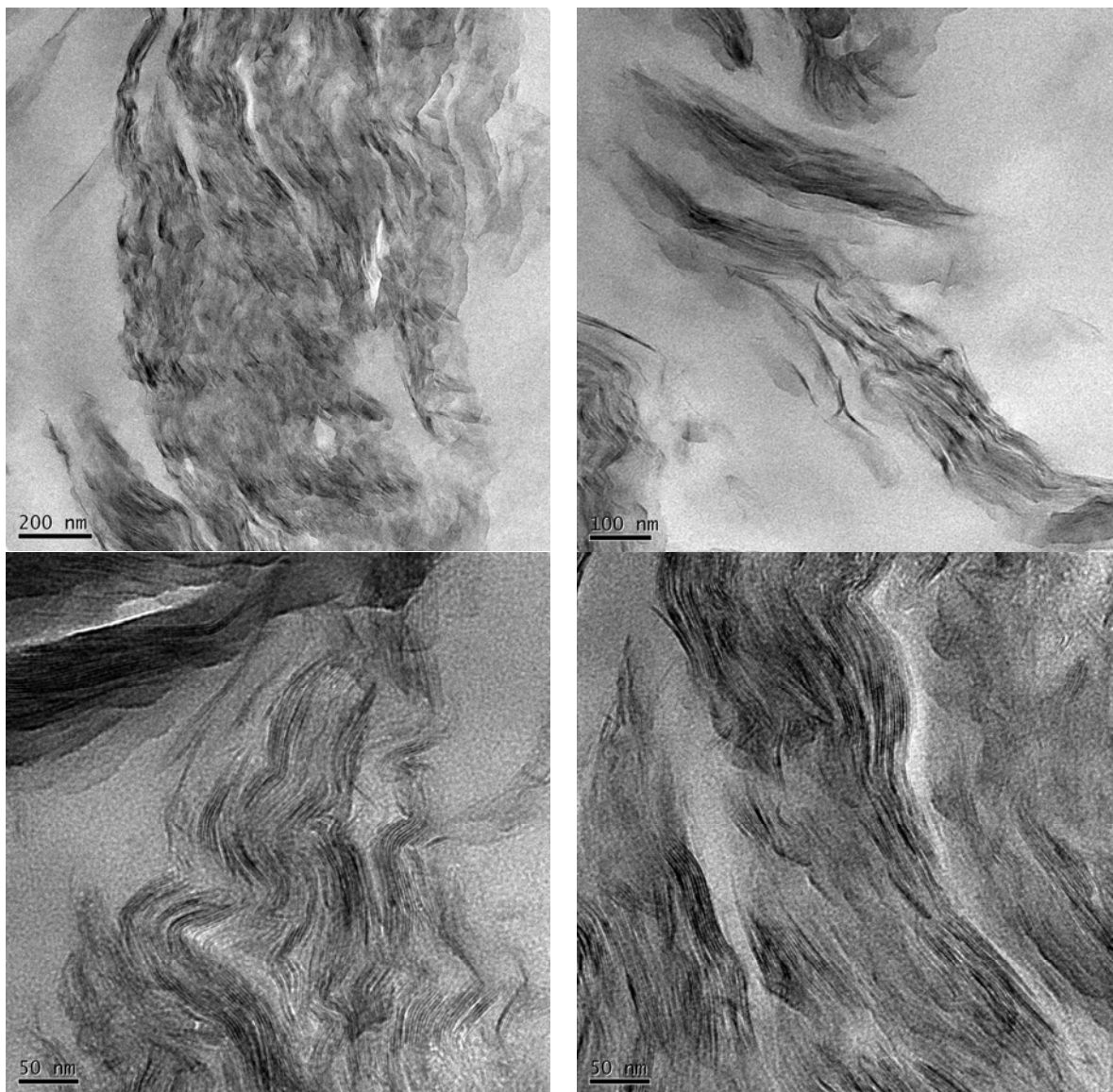


Figure 3.18: TEMs of TPU/1OH-MMT nanocomposites

3.3.9 Dynamic Mechanical analysis.

Dynamic mechanical analysis was done for the thermoplastic polyurethane nanocomposites films were studied in the tensile mode. For comparison of the properties, pristine polyurethanes were prepared with the same amount of reactive modifiers as the amount present in the organoclay, which is used in the preparation of nanocomposite. The storage moduli (G') and the $\tan \delta$ measured at the temperature range of $-150\text{ }^{\circ}\text{C}$ to $80\text{ }^{\circ}\text{C}$ were plotted and are as shown in figures 3.19 (a) to (f).

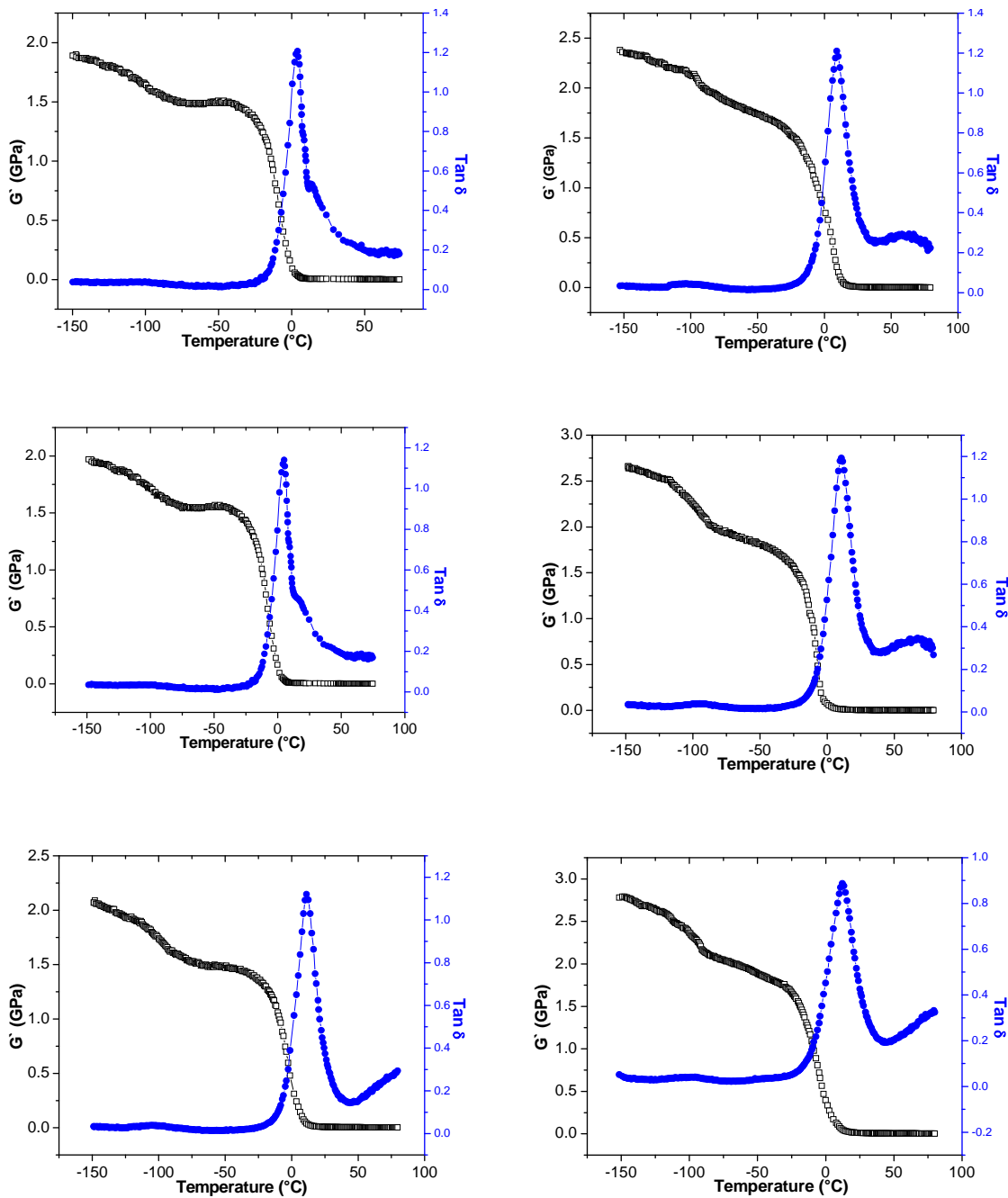


Figure 3.19: DMA Plots of G' and $\tan \delta$ versus temperature for various samples (a) pristine TPU-1OH, (b) pristine TPU-2OH, (c) pristine TPU-3OH, (d) TPU-1OHMMT, (e) TPU-2OHMMT, and (f) TPU-3OHMMT.

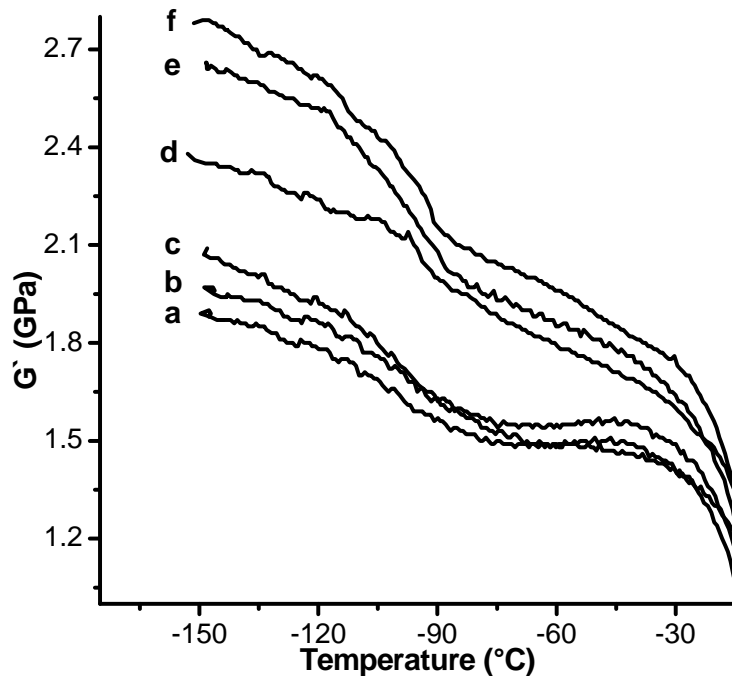


Figure 3.20: Tensile storage modulus (G') of various samples measured by dynamic mechanical analysis (a) pristine TPU-1OH, (b) pristine TPU-2OH, (c) pristine TPU-3OH, (d) TPU-1OHMMT, (e) TPU-2OHMMT, (f) TPU-3OHMMT.

Figure 3.20 shows the storage modulus (G') plotted against temperature. Two transitions were clearly observed. The first transition observed as broad peak at around $-100\text{ }^{\circ}\text{C}$ in the $\tan \delta$ plot was due to the relaxation arising from local mode motions of the methylene sequences in the polycaprolactone soft segment. The second transition was observed 5 to $10\text{ }^{\circ}\text{C}$ range, which is due to glass transition. It can be observed that for the nanocomposite samples the tensile storage moduli (G') were higher throughout the temperature below the glass transition temperature. It should also be noted that the G' of the nanocomposite samples slowly reduces as the temperature increases at the temperature range below the glass transition temperature while it is constant for the pristine thermoplastic polyurethane samples. Another important observation to be noted is that with the increase in functionality of the modifier for the clay, the nanocomposites show higher G' values throughout the temperature range below glass transition though the WAXD and TEM studies show there is no considerable difference in the variation in

the intercalation behavior. This can be attributed to the improved interaction of the polymer chain with the clay surface by anchoring through the reactive hydroxyl groups.

3.4 Conclusions

PU-clay nanocomposites prepared by in situ solution polymerization in toluene medium resulted in intercalated nanocomposites. When the organoclay modified with reactive modifier was used, it was shown that with the addition of branching agent, the extent of intercalation has improved and at higher concentrations, resulted in exfoliated structures. However when the organoclay used does not have a reactive hydroxyl groups, there was no effect on the intercalation of polymer. The nanocomposites prepared using the 3OHMMT showed better intercalations than the nanocomposites prepared organoclays modified with 1OHMMT and 2OHMMT. The structure of the nanocomposites obtained as characterized by WAXD measurements were further confirmed by TEM analysis. The dynamic mechanical analysis of the thermoplastic polyurethane clay nanocomposites show increase in storage tensile moduli at the temperatures below glass transition as compared to the pristine polymer and are effective with increase in functionality of the modifier for the clay.

References

- 1) Meckel, W.; Goyert, W.; Wieder, W. in thermoplastic Elastomers, Hanser Munich **1987**.
- 2) K. C. Frisch, Rubber Chem. Technol. **1980**, 126.
- 3) Bayer, O.; Muller, E.; Petersen, S.; Piepenbrink, H. F.; Windemuth, E. *Angew. Chem.* **1950**, 62, 57.
- 4) Goda, H.; Frank, C. W. *Chem. Mater.* **2001**; 13,2783.
- 5) Furukawa, M.; Yokoyama, T. *J. Appl. Polym. Sci.* **1994**; 53,1723.
- 6) Dolui, S. K.; *J. Appl. Polym. Sci.* **1994**, 53, 463.
- 7) Feldman, D.; Lacasse, M. A. *J. Appl. Polym. Sci.* **1994**, 51,701.
- 8) Otterstedt, E. A.; Ekdahl, J.; Backman, J. *J Appl Polym Sci* **1987**, 34, 2575.
- 9) Nunes RCR, Fonesca JLC, Pereira MR. *Polym Test* **2000**, 19, 93.

- 10) Hepburn, C. *Polyurethane elastomer*. London: Applied Science Publishers; **1982**.
- 11) Wang, Z.; Pinnavaia, T. J. *Chem. Mater.* **1998**, *10*, 3769.
- 12) Zilg, C.; Thomann, R.; Muelhaupt, R.; Finter J. *Adv Mater* **1999**, *11*, 49.
- 13) Petrovic, Z. S.; Javni, I.; Waddon, A.; Banhegyi, G. *J Appl. Polym. Sc.* **2000**; *76*, 133.
- 14) Chen, T. K.; Tien, Y. I.; Wei, K. H. *J. Polym. Sci. A: Polym. Chem.* **1999**, *37*, 2225
- 15) Chen, T. K.; Tien, Y. I.; Wei, K. H. *Polymer* **2000**, *41*, 1345.
- 16) Xu, R.; Manias, E.; Snyder, A. J.; Runt, J. *Macromolecules* **2001**; *34*, 337.
- 17) Ma, J.; Zhang, S.; Qi, Z. *J Appl Polym Sci* **2001**, *82*, 1444.
- 18) Tien, Y. I.; Wei, K. H. *Macromolecules* **2001**; *34*, 9045.
- 19) Tien, Y. I.; Wei, K. H. *Polymer* **2001**; *42*, 3213.
- 20) Hu, Y.; Song, L.; Xu, J.; Yang, L.; Chen, Z.; Fan, W. *Colloid Polym. Sci.* **2001**; *279*, 819.
- 21) Yao, K.J.; Song, M.; Hourston, D. J.; Luo, D. Z. *Polymer* **2002**, *43*, 1017.
- 22) Tien, Y. I.; Wei, K. H. *J. Appl. Polym. Sci.* **2002**, *86*, 1741.
- 23) Chang, J. H.; An, Y. U.; *J. Polym. Sci., Part B: Polym. Phys.* **2002**, *40*, 670.
- 24) Tortora, M.; Gorrasi, G.; Vittoria, V.; Galli, G.; Ritrovati, S.; Chiellini, E. *Polymer* **2002**, *43*, 6147.
- 25) Zhang, X.; Xu, R.; Wu, Z.; Zhou, C. *Polym. Int.* **2003**, *5*, 790.
- 26) Song, M.; Hourston, D. J.; Yao, K. J.; Tay J. K. H.; Ansarifard, M. A. *J. Appl. Polym. Sci.* **2003**, *90*, 3239.
- 27) Mishra, J. K.; Kim, I.; Ha, C. S. *Macromol. Rapid Commun.* **2003**, *24*, 671.
- 28) Chen, X.; Wu, L.; Zhou, S.; You, B. *Polym. Int.* **2003**; 790.
- 29) Rhoney, I.; Brown, S.; Hudson, N. E.; Pethrik, R. A. *J Appl Polym Sci* **2003**, *91*, 1335.
- 30) Osman, M. A.; Mittal, V. Morbidelli, M.; Suter, U.W. *Macromolecules* **2003**, *36*, 9851.
- 31) Kojima, Y.; Usuki, A.; Kawasumi, M.; Okada, A.; Fukushima Y.; and Kurauchi, T. *J Mater Res* **1993**, *8*, 1185.

- 32) Fukushima, Y.; Okada, A.; Kawasumi, M.; Kurauchi T.; Kamigaito, O. *Clay Miner.* **1998**, *23*, 27.
- 33) Imai, Y.; Nishimura, S.; Abe, E.; Tateyama, H.; Abiko, A.; Yamaguchi, A.; Taguchi, H. *Chem. Mater.* **2002**, *14*, 477.
- 34) Xia, H. S.; Song, M. *Polym. International*, **2006**, *55*, 229.
- 35) Singh, C.; Balazs, A. C.; *Polym. Int.* **2000**, *49*, 469.
- 36) Pattanayak, A.; Jana, S. C. *Polymer* **2005**, *46*, 3275.
- 37) Pattanayak A., Jana S. C, *Polymer* **2005**, *46*, 3394.
- 38) Pattanayak, A.; Jana, S. C. *Polymer* **2005**, *46*, 5183.
- 39) Pattanayak, A.; Jana, S. C.; *Polym. Eng. and Sci.* **2005**, *45*, 1532.
- 40) Jeong E. H., Yang J., Hong J. H., Kim T. G., Kim J. H., Youk J. H., *European Polymer Journal*, **2007**, *43*, 2286.

4. Polycarbonate-clay nanocomposites via in-situ melt polymerization

4.1 Introduction

Polycarbonate (PC) has an outstanding ballistic impact strength, good optical clarity and high heat distortion temperature. There is a continuous interest for the research on developing PC with better chemical resistance and enhanced resistance to abrasion.¹ Thus PC has been modified and tailored in many different ways, particularly by blending with other polymers for use in demanding applications. To improve the mechanical and thermal properties of the polymers, inorganic fillers have been traditionally used.² Polymer-clay nanocomposites (PCN) based on layered silicates like montmorillonite have been widely studied during the last 10 years. Because of the high aspect ratio of this dispersed layered material as fillers, dramatic improvements in the properties of the polymer can be achieved at very low filler levels.³⁻⁸ PCNs are prepared by three general methods. These are (a) intercalation of polymer or prepolymer from solution (b) in-situ intercalative polymerization and (c) melt intercalation.⁹ The resulting structure may be agglomerated microcomposite, or intercalated or exfoliated nanocomposite, which depend critically on the organoclay, polymer and method of its preparation. Of these, the *in-situ* intercalative polymerization method allows significant opportunities to alter the structure and morphology of PCN. It is recognized that the properties of the nanocomposite are enhanced when the interaction of the polymer chain with the surface of the clay layer is improved. This can be achieved by tethering the polymer onto the surface of the clay layers, which are completely delaminated and fully exfoliated throughout the polymer matrix. There are many examples where hydrophobic modifiers have functionalities capable of co-polymerization or initiating polymerization that have attracted recent attention because of their ability to produce fully exfoliated polymer-clay nanocomposites.¹⁰⁻¹⁵

Recently, to this end, there are several reports on the preparation of polycarbonate-clay nanocomposites (PCCN). For the first time Brittain et al have reported the preparation of

PCCN by ring opening polymerization of cyclic polycarbonate oligomers¹⁶. Later, many workers have prepared PCCNs by melt mixing, to study the effect of various parameters on the structure and properties of the nanocomposites¹⁷⁻²⁵. Lee et al have prepared partially exfoliated PCCN by microwave heated-solid state polymerization²⁰. Studies on the polymer blend/clay nanocomposites based on PC were explored to exploit the advantage of the combination of blend and nanotechnology²⁶⁻³¹. In most of these studies the organoclays used were modified using quaternary ammonium cations. PCCNs prepared via melt processing using organoclays modified with quaternary ammonium salts result in lowering of molecular weight and undesirable color formation^{18,19}. These quaternary ammonium cations undergo degradation at the processing temperatures via Hoffmann elimination to form amines³² and consequently induce base catalyzed chain scission reactions in the polymer³³. This problem can be mitigated by the use of more thermally stable organic cations. Organocations based on phosphonium, imidazolium, tropylium cations are stable even at 300 °C³⁴⁻³⁶. Severe et al have shown that PCCNs prepared with phosphonium ion modified montmorillonite provide better thermal stability for PC¹⁷.

In the present study, we describe the preparation of PCCNs via in situ polymerization using two novel organoclays in which the modifier is thermally stable at temperatures used for polymerization and also the modifier is designed such that it contains reactive bisphenol moiety, which can copolymerize with the growing polymer during polymerization thereby improving the interaction of the polymer with clay surface. For comparison, PCCNs were prepared under the same conditions with two organoclays, which are thermally stable but does not contain the reactive groups. The structure, molecular weights, thermal and dynamic mechanical properties of the PCCNs prepared were also described.

4.2 Experimental

4.2.1 Materials and Measurements.

Na⁺ Montmorillonite was obtained from Southern Clay products, USA. 12,12-bis(4-hydroxyphenyl)tridecyltriphenylphosphonium bromide and 12,12-bis(4-hydroxyphenyl)

tridecyl-2,3-dimethylimidazolium bromide were synthesized in the laboratory using simple starting materials such as methyl acetoacetate, decanediol and phenol as described below. ^1H NMR spectra were recorded in CDCl_3 solution with tetramethylsilane (TMS) as an internal standard using a Bruker DSX300. Organoclays were prepared from Na^+ Montmorillonite by standard exchange reaction. The organoclays were characterized by WAXD and TGA. Polycarbonate - clay nanocomposites were prepared via in-situ melt polymerization under vacuum.

Molecular weight and molecular weight distributions of polymers were determined using SEC (*Thermo separation products*) equipped with UV and RI detectors. Linear Polystyrene standards were used for calibration of the column. Chloroform filtered through 0.2 μL pore PTFE membranes was used. The sample concentration was 2 mg/mL and the injection volume was 50 μL . Inherent viscosities were determined using three- arm Schott-Gerate Ubelohde viscometer at 30 $^\circ\text{C}$ for the solutions with concentrations of 0.050 g/dL in chloroform.

The WAXD measurements were performed using Rigaku Dmax 2500 diffractometer. The system consists of a rotating anode generator and wide-angle power goniometer. The generator was operated at 40kV and 150 mA. The samples were scanned between $2\theta = 2$ to 10° and the scan speed was $2^\circ/\text{min}$.

The TGA-7 unit in the Perkin-Elmer thermal analysis system was used to determine the onset of degradation and the organic content in the organoclays. The samples were heated under a flowing nitrogen atmosphere from 50 to 900 $^\circ\text{C}$, at a heating rate of 10 $^\circ\text{C}/\text{min}$, and the weight loss was recorded. The weight loss at 900 $^\circ\text{C}$ was taken as the % organic content in the organoclay.

TEM imaging was done using a Technai G^2 F-30 model Transmission electron microscope operating at an accelerating voltage of 300 kV. The nanocomposite samples were sectioned into ultrathin slices (<100 nm) at room temperature using the microtome Leica Ultracut UCT equipped with a diamond knife and then mounted on 200 mesh

copper grids. The density of clay particles is enough to produce contrast between polymer and clay stacks hence staining was not required. Images were captured using charged couple detector (CCD) camera for further analysis using Gatan Digital Micrograph analysis software.

The thermal properties of the samples were analyzed by TA instruments Q10 differential scanning calorimeter under standard conditions. The samples were heated/cooled at the rate of 10 °C/min and the sample weight was about 5 mg and the T_g were measured from the second heating cycle.

The dynamic mechanical properties of the samples were studied using Rheometrics Dynamic Mechanical Analyzer, model DMTA IIIIE that provided storage modulus, loss modulus and loss tangent ($\tan \delta$) against temperature. The T_g was measured as the temperature at which the maximum in $\tan \delta$ appeared. The scans were carried out in single point cantilever bending mode at a constant heating rate of 2 °C/min and a frequency of 1 Hz from 35 °C to 170 °C. The samples were cut (with dimension of 25.0 X 6.0 X 1.0 mm³) from the sheets obtained by compression molding at 260 °C.

4.2.2 Synthesis of modifiers for the clay

4.2.2.1 Synthesis of 10-bromodecanol from decanediol. To a mixture of 1,10-decanediol (35.73g, 0.205 mol) and toluene (700 mL) was added concentrated HBr (29 mL of 47% aqueous solution, 0.24 mol). The heterogeneous mixture was stirred and heated at reflux for 36 hours. TLC analysis indicated substantial amounts of 1,10-decanediol still remained. Thus a further quantity of HBr (15 mL, 0.12 mol) was added and the mixture was heated at reflux for further 36 h, at which time TLC analysis showed no diol remaining. The reaction mixture was allowed to cool to room temperature and the phases were separated. The organic layer was concentrated by evaporating the toluene and diluted with ethyl acetate and washed with water, sodium bicarbonate and brine. Then the organic layer was dried over Na₂SO₄ and concentrated to yellow liquid and purification of this crude reaction mixture by column chromatography provided pure 10-

bromodecanol (43.0 g) in 90% yield. ^1H NMR: 1.2 to 1.8 (18 H, m); 3.43 (2H, t); 3.65 (2H, t).

4.2.2.2 Synthesis of methyl-(3-hydroxydecyl)acetoacetate. Clean dry sodium (9.5 g, 0.413 mol) was placed in a three neck round bottomed flask fitted with double surface condenser, dropping funnel and septum adapter. Dry methanol (200 mL) was added on sodium slowly under cooling. Methyl acetoacetate (48.3 g, 0.416 mol) was added under stirring and heated to gentle heating. Potassium Iodide (5.6 g, 0.033 mol) was added. Then 10-bromodecan-1-ol (79 g, 0.33 mol) was taken in dropping funnel and added slowly into the contents of the round bottomed flask over a period of 60 min. Continued reflux for 12 hours and monitored the reaction by TLC. The reaction was stopped when all the bromodecanol was consumed. The crude reaction mixture was concentrated by evaporating methanol, diluted with ethyl acetate, washed with water several times until the washings were neutral to litmus. Pure methyl-(3-hydroxydecyl)acetoacetate (58.3g) was separated from crude by flash chromatography. Yield: 65%. ^1H NMR: 1.26 to 1.8 (3H, s); 2.23 (3H, s); 3.43 (1H, t); 3.64 (2H, t); 3.74 (3H, s).

4.2.2.3 Synthesis of 13-hydroxytridecan-2-one from methyl-(3-hydroxydecyl)acetoacetate. Methyl-(3-hydroxydecyl)acetoacetate (54.4 g, 0.20 mol) was dissolved in dimethyl sulfoxide (150 mL) in a round bottom flask and NaCl (15 g, 0.25 mol) was added to it along with distilled water (18 g, 1.0 mol). The above mixture was heated at 150 °C for 18 hours. The reaction was continued until all the starting material was consumed which was monitored by TLC. Cooling it to room temperature stopped the reaction. Then it was poured into water and extracted with diethyl ether. The combined ether layer was washed with water, brine and then dried over sodium sulfate. Then the ether was evaporated to get 13-hydroxytridecan-2-one (32.1 g) as a white solid, which is then purified by recrystallization in hot petroleum ether. Yield: 75 %. ^1H NMR: 1.26 to 1.8 (18H m,); 2.14 (3H, s); 2.42 (2H, t); 3.64 (2H, t).

4.2.2.4 Synthesis of 2,2-bis(4-hydroxyphenyl)tridecanol from 13-hydroxytridecan-2-one. 13-hydroxytridecan-2-one (21.4 g, 0.10 mol) was mixed with phenol (56.4 g, 0.60

mol) and mercaptopropionic acid (0.106 g, 0.010 mol) was added to it. The anhydrous HCl gas was passed to the reaction mixture through a bubbler. The reaction was continued under stirring for 12 hours at 45 °C. Then the reaction mixture was dissolved in ethyl acetate and was washed with water, NaHCO₃ and then brine. The organic layer was dried over Na₂SO₄. The excess phenol in the reaction mixture was distilled out under vacuum at 60 °C. The 2,2-bis(4-hydroxyphenyl)tridecanol (25.0 g) was isolated by column chromatography. Yield: 65 %. ¹H NMR: 1.14 to 1.53 (14H, m); 1.57 (3H, s); 1.63 (2H, m); 1.77 (2H, m); 2.00 (2H, m) 4.08 (2H, t); 6.68 (4H, d); 6.93 (4H, d).

4.2.2.5 Synthesis of 2,2-bis-(4-hydroxyphenyl)tridecyl bromide from 2,2-bis(4-hydroxyphenyl)tridecanol. The 2,2-bis(4-hydroxyphenyl)tridecanol (22.37 g, 0.050 mol) and CBr₄ (19.92g, 0.060 mol) was dissolved in dry tetrahydrofuran (100mL) and taken in three-neck round bottomed flask fitted with a dropping funnel, a condenser and a three-way stopcock. Triphenylphosphine (14.41g, 0.055 mol) was dissolved in tetrahydrofuran and added to the reaction mixture, which is kept at 0 °C slowly, drops by drop through a dropping funnel for duration of 30 minutes. The stirring was continued for another 4 hours at 0 °C. The reaction was monitored by TLC. After the reaction was over, the crude reaction mixture was concentrated by evaporating tetrahydrofuran and dissolved in ethyl acetate, washed with water. The 2,2-bis(4-hydroxyphenyl)tridecyl bromide (20.1 g) was isolated in pure form after column chromatography. Yield: 90 %. ¹H NMR: 1.14 to 1.53 (16H, m); 1.55 (3H, s); 1.84 (2H, m); 1.98 (2H, m); 3.40 (2H, t); 6.68 (4H, d); 6.93 (4H, d).

4.2.2.6 Synthesis of 2,2-bis-(4-hydroxyphenyl)tridecyl-(1,2-dimethylimidazolium) bromide. Equivalent amounts of 2,2-bis-(4-hydroxyphenyl)tridecyl bromide (4.4746 g, 0.010 mol) and 1,2-dimethylimidazole (0.9613g, 0.010 mol) were mixed and heated at 100°C for 8 hours under nitrogen atmosphere. The melted mixture solidified after the reaction. 2,2-bis-(4-hydroxyphenyl)tridecyl-(1,2-dimethylimidazolium) bromide was obtained in pure form and used without further purification. ¹H NMR 1.14 to 1.48 (16H, m); 1.56 (3H, s); 1.69 (2H, m); 2.01 (2H, m) 4.03 (2H, t); 6.68 (4H, d); 6.93 (4H, d); 7.42 (2H, m)

4.2.2.7 Synthesis of 2,2-bis-(4-hydroxyphenyl)tridecyl triphenylphosphonium bromide. Equivalent amounts of 2,2-bis-(4-hydroxyphenyl)tridecyl bromide (4.4746 g, 0.010 mol) and triphenylphosphine (2.631g, 0.010 mol) were mixed and heated at 100°C for 8 hours under nitrogen atmosphere. The melted mixture solidified after the reaction. 2,2-bis-(4-hydroxyphenyl)tridecyl triphenylphosphonium bromide was obtained in pure form and used without further purification. ¹H NMR: 1.14 to 1.46 (16H, m); 1.50 (3H, s); 1.63 (2H, m); 1.93 (2H, m) 3.40 (2H, t); 6.68 (4H, d); 6.93 (4H, d); 7.72 to 7.88 (15H, multiplet).

4.2.3 Synthesis of organoclays. The Na montmorillonite (10 g) with CEC 92 meq/100 g, was dispersed in water/methanol (300 mL) by stirring with an over head stirrer at room temperature for 2 hours. The modifier (11 meq), as shown in table 1, dissolved in methanol/water mixture was poured into the dispersion of clay slowly in drops and stirred for 24 hours at 65 °C. The reaction mixture is cooled, centrifuged and washed several times with distilled water and methanol until all the bromide ions are washed off. The organoclay obtained was freeze dried under vacuum overnight. The organoclay was obtained as fine, dry powder. The interlayer d- spacing for the organomodified montmorillonite was measured from WAXD. The organic contents were measured from the thermogravimetric analysis upon heating the organoclay to 900 °C.

4.2.4 Synthesis of nanocomposites

Melt polymerization reactions were carried out in a three-neck tubular glass reactor equipped with a solid helical agitator. To remove any sodium from the surface of the glass, the reactor was soaked in 3N HCl for 24 hours followed by a soak in de-ionized water for 24 hours. The reactor was then dried in an oven overnight and stored covered until used. The temperature of the reactor was maintained using a salt bath with a PID controller and measured near the reactor and salt bath interface. The pressure over the reactor was controlled by a nitrogen bleed into the vacuum pump downstream of the distillate collection flasks and measured with a digital pirani gauge. The reactor was charged with Bisphenol-A, Diphenyl carbonate and the organoclay as per the desired

compositions prior to assembly. The reactor was then assembled, sealed and the atmosphere was exchanged with nitrogen three times. With the final nitrogen exchange the reactor was brought to near atmospheric pressure and submerged into the molten salt bath, which was at 180° C. After five minutes agitation was begun at 100 rpm. The catalyst solutions such as tetramethyl ammonium hydroxide and NaOH were added in the required amount. After 30 minutes the temperature was ramped to 210 °C. The pressure was reduced slowly to 180 mbar and phenol distillate was formed. After 30 minutes the pressure was again reduced to 100 mbar and maintained for 30 minutes. The temperature was then ramped to 240 °C and the pressure was lowered to 20 mbar. These conditions were maintained for 30 minutes. The temperature was then ramped to 260 °C and the pressure was lowered to 3.5 mbar. These conditions were maintained for 60 minutes. The temperature was then ramped to the final finishing temperature of 290 °C and the pressure was reduced to 0.030 mbar. After 4 hours the reactor was removed from the molten salt bath and cooled under vacuum. The nanocomposite was obtained after breaking the glass reactor.

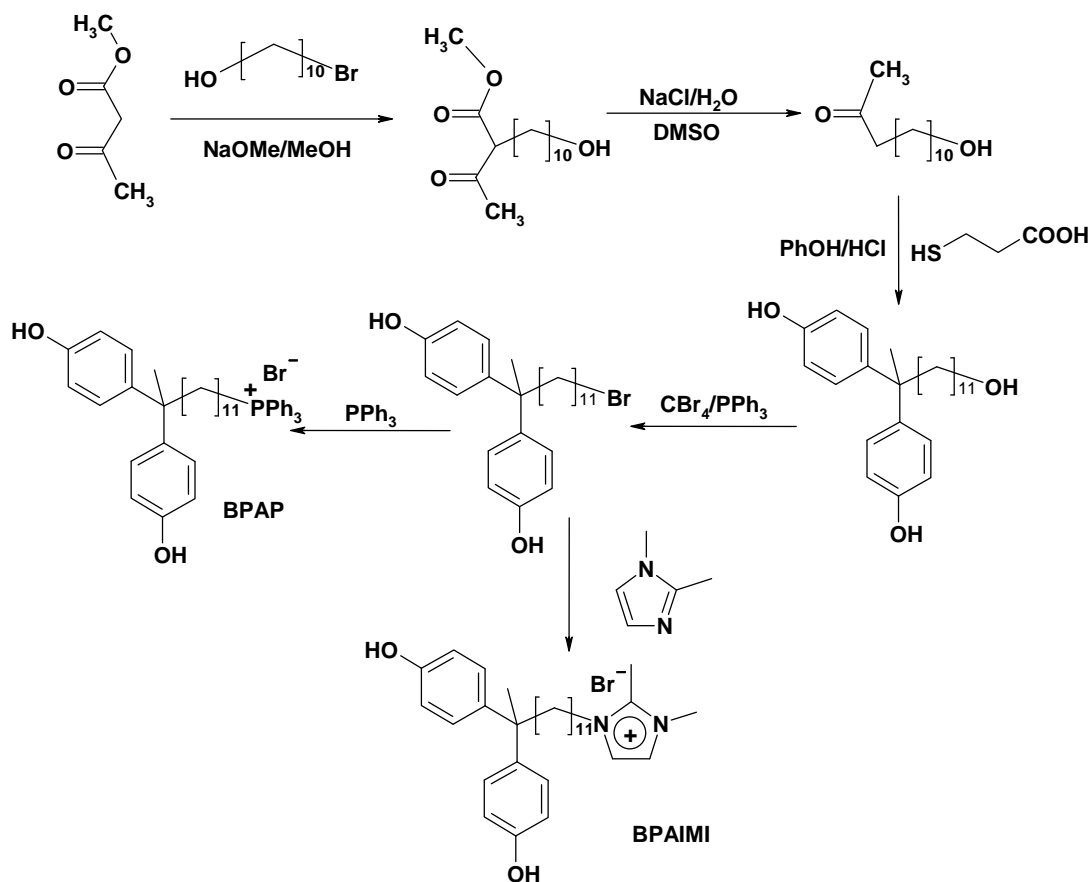
4.3 Results and discussion

4.3.1 Organomodifiers for the clay and its preparation.

In this study, we developed a novel modifier for the clay that connects PC through covalent bonds and the layered silicates through ionic bonds. To design the modifier for the clay suitable for PCCN, we set the following conditions: (1) It possesses a functionality which can copolymerize with bisphenol-A and diphenyl carbonate during in situ polymerization. (2) It possesses a cationic group that can interact with the negatively charged silicate layer. (3) It should be stable at the conditions of polymerization of PC. To satisfy condition (1) we chose the bisphenol moiety and for conditions (2) and (3) cationic moieties such as triphenylphosphonium and 1,2-dimethyl imidazolium moieties were chosen. The synthetic route for the designed reactive modifiers such as 12,12-bis(4-hydroxyphenyl) tridecyltriphenylphosphonium bromide and 12,12-bis(4-hydroxyphenyl) tridecyl-2,3-dimethylimidazolium bromide abbreviated as BPAP and BPAIMI respectively are shown in the scheme I. For comparison, modifiers for the clay were designed with conditions (2) and (3) and without the condition (1). For this purpose, the

surfactant modifiers such as hexadecyltriphenylphosphonium bromide (C16P), hexadecyl-2,3-dimethylimidazolium bromide (C16I) were prepared by quaternizing triphenylphosphine and 1,2-dimethylimidazole respectively with hexadecyl bromide.

SCHEME I



4.3.2 Organoclays and its preparation.

The four different organoclays were prepared by exchanging Na⁺ ion in montmorillonite with hexadecyltriphenylphosphonium cation, hexadecyl-2,3-dimethylimidazolium cation, 12,12-bis(4-hydroxyphenyl)tridecyltriphenylphosphonium cation and 12,12-bis(4-hydroxyphenyl)tridecyl-(2,3-dimethylimidazolium) cation which are abbreviated as C16P-MMT, C16IMI-MMT, BPAP-MMT and BPAIMI-MMT respectively by standard exchange reaction method as reported in the literature elsewhere³⁷. Typical exchange reaction involved dispersing the Na⁺ montmorillonite in a mixture of methanol/water followed by slow addition of the quaternary onium salt (in slight excess based on cation exchange capacity (CEC)) and continued stirring for 24

hours. Then it was washed thoroughly with water and methanol until there was no halide ion present and freeze dried under vacuum. The interlayer d- spacing for the organo-modified montmorillonite was measured from WAXD and is shown in table 1. The intercalation of onium ions in the interlayer gallery is evidenced by increase in d spacing observed in WAXD patterns compared to the pristine montmorillonite.

4.3.3 Thermal analysis of organoclays

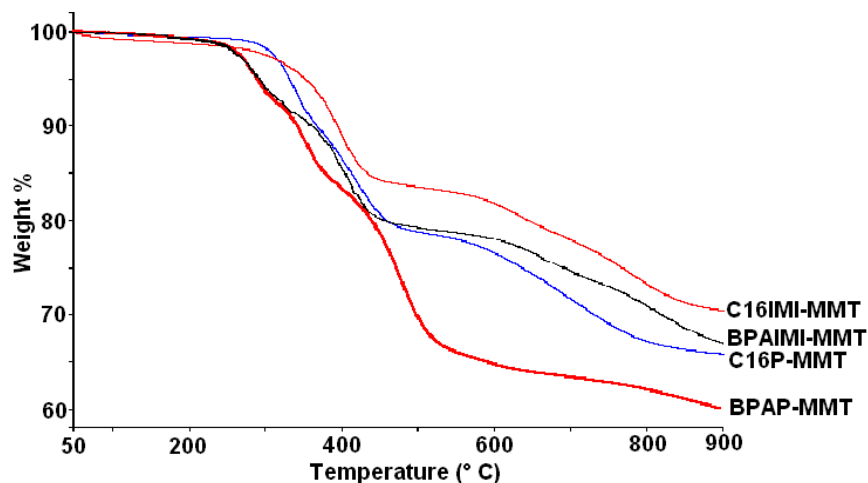
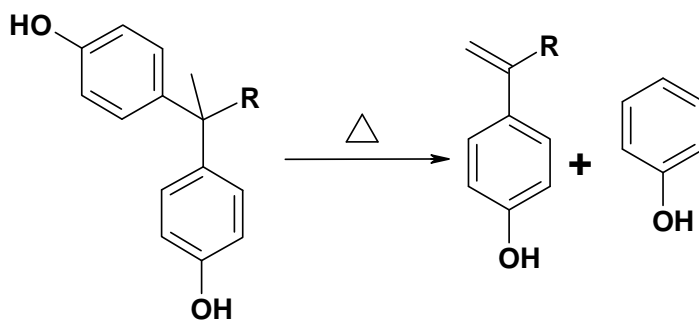


Figure 4.1: Thermograms of the organoclays

The thermal analysis of these modified clays was done using TGA. It was found that the organoclays such as C16P-MMT and C16IMI-MMT degrade only above 300 °C whereas the organoclay, BPAP-MMT and BPAIMI-MMT starts degrading at around 240 °C. The first step in degradation of BPAP-MMT and BPAIMI-MMT can be ascribed to the decomposition of the bisphenol moiety (scheme II)^{38,39}.

SCHEME II



However, such degradation is less likely once the bisphenol moiety is incorporated into a polymer structure. The organic content was obtained from percentage of degradation (obtained from TGA, figure 1) of these clays upon heating to 900°C. The values (table 4.1) of organic content indicate that all the sodium ions are completely exchanged with organocations and are comparable with the CEC.

Table 4.1: TGA and d- spacing for the organoclays

| Clay | Onset of degradation, °C | Weight loss on charring (%) | | d-spacing for clay, Å |
|------------|--------------------------|-----------------------------|--------------|-----------------------|
| | | Theoretical | Experimental | |
| C16P-MMT | 300 °C | 33 | 33 | 21.5 |
| C16IMI-MMT | 300 °C | 25 | 26 | 18.5 |
| BPAP-MMT | 248 °C | 39 | 40 | 28.7 |
| BPAIMI-MMT | 240 °C | 31 | 32 | 23.0 |

4.3.4 Preparation of PC-clay nanocomposites.

PC/clay nanocomposites were prepared via *in-situ* melt polymerization by mixing the organoclay along with bisphenol A and diphenyl carbonate in presence NaOH/tetramethylammonium hydroxide as catalyst. The nanocomposites were also prepared in the absence of catalyst. The final finishing temperature was kept at 290 °C as the modifiers start degrading after 300 °C. The compositions of the monomers, organoclay and the catalyst taken for the in-situ polymerization and the molecular weights of the polymer obtained were shown in the Table 4.2. The molecular weights of the polymer in the composites were measured after separating the polymer from the composite by selectively precipitating the clay by reverse ion exchange reaction using LiCl, a method well known in the literature⁴⁰⁻⁴². From the table it can be observed that pristine PC, which was prepared in presence of the catalyst show good molecular weights while the nanocomposites prepared under the same conditions but with addition of organoclay show lower molecular weights. When the nanocomposites were prepared in the absence of catalyst and the imidazolium cation modified organoclays were used also resulted in lower molecular weights for the polymer.

Table 4.2: Data table showing the sample code, compositions, glass transition temperature of the composites and the matrix polymer, molecular weights and inherent viscosity of the matrix polymer

| Sample | Organo-clay | Wt % of inorganic clay | Catalyst* | Tg | Matrix polymer after reverse Ion exchange | | | |
|----------------|-------------|------------------------|------------|-----|---|--------------------|------|------|
| | | | | | Tg | MnX10 ³ | PD | IV |
| PC-C16P-1.8 | C16P | 1.8 | - | 141 | 144 | 15.0 | 1.81 | 0.36 |
| PC-C16P-3.6 | C16P | 3.6 | - | 143 | 142 | 16.5 | 1.76 | 0.37 |
| PC-C16P-5.3 | C16P | 5.3 | - | 142 | 143 | 18.8 | 1.69 | 0.39 |
| PC-BPAP-1.8 | BPAP | 1.8 | - | 145 | 144 | 24.5 | 1.74 | 0.44 |
| PC-BPAP-3.6 | BPAP | 3.6 | - | 144 | 138 | 20.7 | 2.26 | 0.45 |
| PC-BPAP-5.3 | BPAP | 5.3 | - | 145 | 134 | 25.0 | 2.77 | 0.51 |
| PC-C16IM-3.6 | C16IM | 3.6 | - | 132 | 138 | 10.3 | 2.05 | 0.29 |
| PC-BPAIM-3.6 | BPAIM | 3.6 | - | 126 | 131 | 8.2 | 1.94 | 0.28 |
| PC-BPAIM-3.6-1 | BPAIM | 3.6 | TMAH/ NaOH | 128 | 132 | 8.3 | 1.91 | 0.28 |
| PC-BPAIM-3.6-2 | BPAIM | 3.6 | NaOH | 122 | 126 | 4.5 | 1.84 | 0.23 |
| PC-BPAIM-3.6-3 | BPAIM | 3.6 | TMAH | 126 | 130 | 6.8 | 1.96 | 0.26 |
| PC-BPAP-3.6-1 | BPAP | 3.6 | TMAH | 140 | 135 | 18.9 | 2.21 | 0.39 |
| PC-BPAP-1.8-2 | BPAP | 1.8 | TMAH/NaOH | 124 | 122 | 4.4 | 1.93 | 0.23 |

* Wherever mentioned, The concentration of the catalyst taken for polymerization such as TMAH was 10⁻⁴ mmol/mole of BPA and NaOH was 10⁻⁶ mmol/mole of BPA and wherever not mentioned, the catalysts were not used.

This may be due to the competitive chain scission reaction that are catalyzed by the combination of the organoclay and the catalyst system or by the imidazolium cation modified organoclay alone. The mechanism for such behaviour is not clearly known. When the nanocomposites were prepared with phosphonium ion modified organoclay, the molecular weights of the polymer in the composites were comparable to the pristine polymer obtained in presence of catalyst. The higher molecular weights obtained in these PC/phosphonium ion modified organoclay can be attributed to the catalytic potential of the phosphonium cations for the polymerization to produce PC.

4.3.5 Structure of the PCCN using WAXD

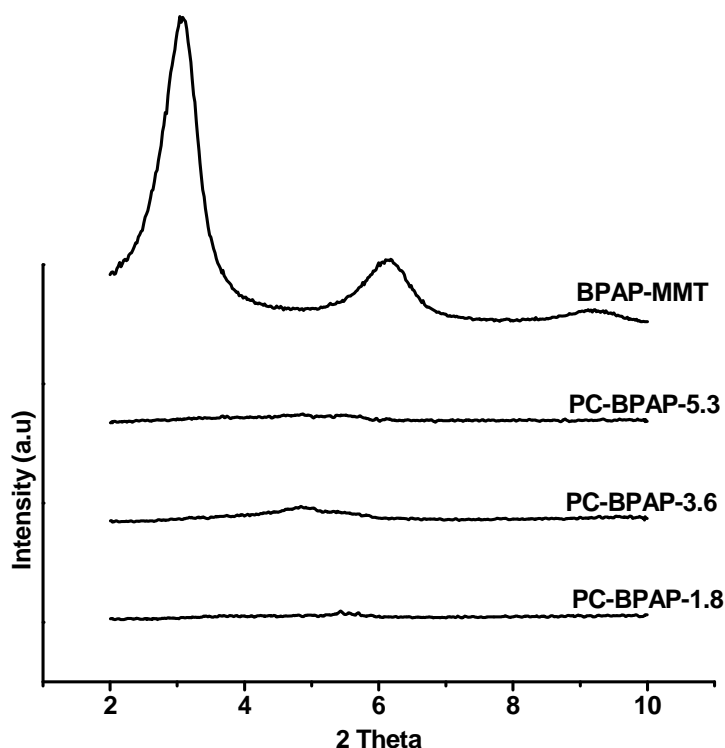


Figure 4.2(a): WAXD pattern of BPAP-MMT, and the PC nanocomposites with BPAP-MMT at various compositions

The structures of the nanocomposites obtained were characterized by WAXD and TEM. The results in the WAXD patterns of various PCCNs were figure 4.2 (a), (b) and (c). Figure 4.2(a) show that the nanocomposites prepared with BPAP-MMT at various compositions. It can be observed from the patterns that the 001 peak of the organoclay disappeared completely for the PCCNs prepared using BPAPMMT.

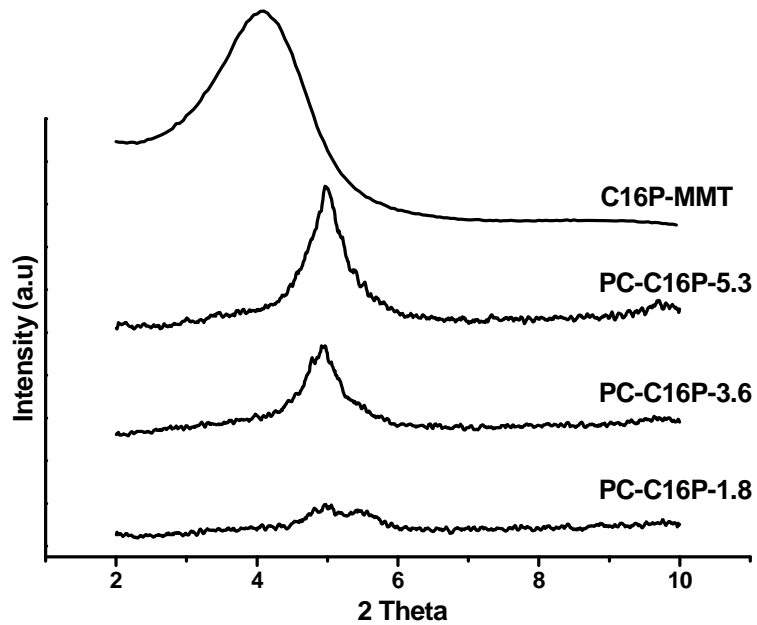


Figure 4.2(b): WAXD pattern of C16P-MMT, and the PC nanocomposites with C16P-MMT at various compositions.

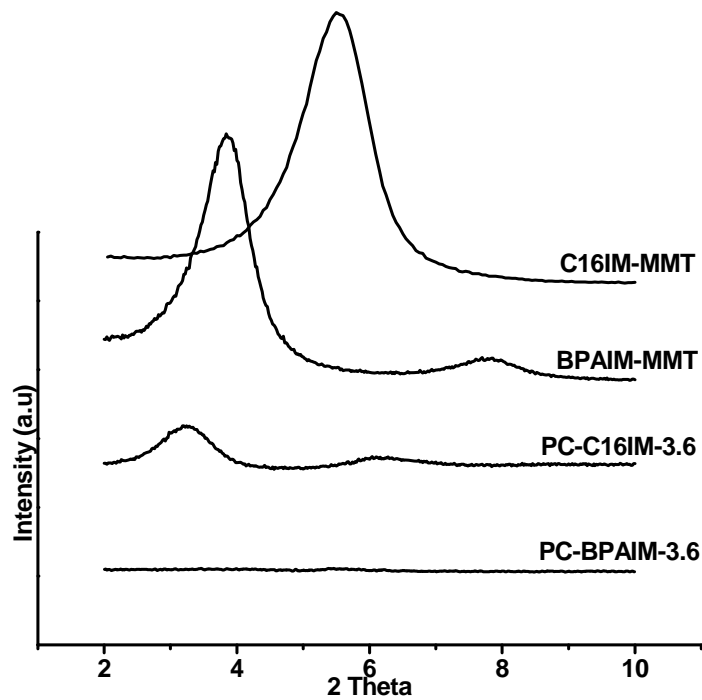


Figure 4.2(c): WAXD pattern of pristine C16IM-MMT, Pristine BPAIM-MMT, PC-C16IM-3.6 and PC-BPAIM-3.6

In the case of the PCCN prepared using C16PMMT show de-intercalation as the d-spacing decreases from 21.5 Å to 17.8 Å (Figure 4.2 (b)) where as with C16IMI-MMT, it shows good intercalation as the d-spacing increases from 18.5 Å to 27.6 Å (Figure 4.2 (c)). Also the nanocomposites prepared using BPAIMMMT also show complete disappearance of the clay peak indicating the formation of exfoliated structure (Figure 4.2 (c)).

4.3.6 Structure of the PCCN using TEM

Typical TEM pictures of the nanocomposites prepared using BPAPMMT with varying amount of clay contents such as 1.8 wt %, 3.6 wt % and 5.3 wt % were shown in figure 4.3, 4.4 and 4.5 respectively. The micrographs were shown in various magnifications. From the pictures it can be observed that for all the three compositions prepared using the organoclay, BPAPMMT, the clay layers were well dispersed and exfoliated homogeneously throughout the polymer matrix. Figure 4.6 shows typical TEM pictures of the nanocomposites prepared using C16PMMT with a clay content of 3.6 wt %. It can be observed that the clay layers are flocculated and agglomerated. From the higher magnification picture one can clearly observe that the clay layers are arranged parallel to each other very closely and the distances between the layers were comparable to the d-spacing observed from WAXD (~18 Å). Figures 4.7 and 4.8 show typical TEM pictures of the nanocomposites prepared using the organoclays such as C16IMI-MMT and BPAIMI-MMT respectively with an inorganic clay content of 3.6 wt %. From the figure 4.7, it can be confirmed that the nanocomposite obtained using C16IM-MMT form intercalated structures and the interlayer spacing, which can be measured from the picture, was comparable with d-spacing obtained from the WAXD patterns. From figure 4.8, it can be observed that, the clay layers are well dispersed and exfoliated in the polymer matrix for the PC nanocomposites prepared using BPAIM-MMT.

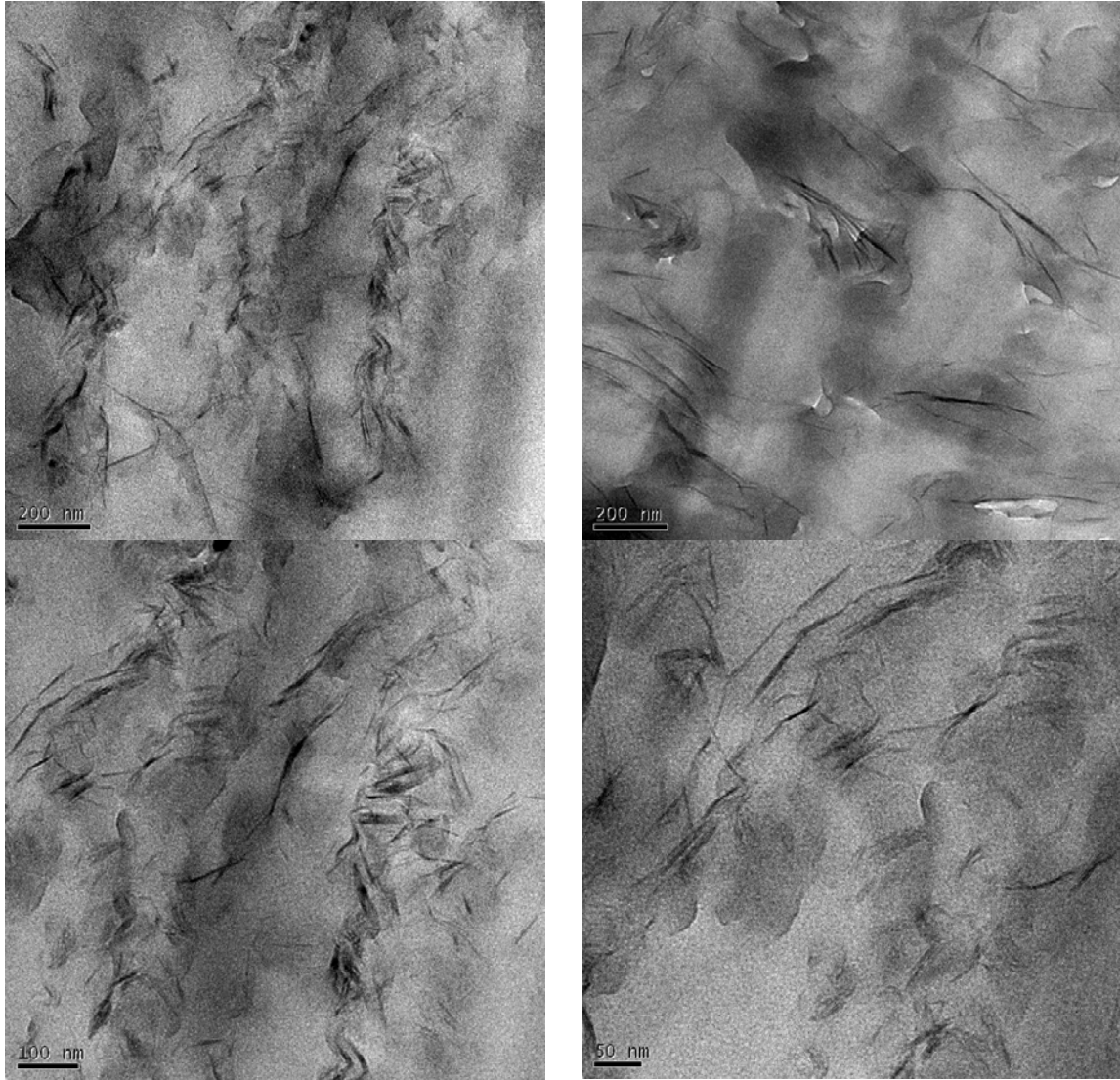


Figure 4.3: TEM pictures of PCCN with BPAP-MMT 1.8 wt %. (PC-BPAP-1.8)

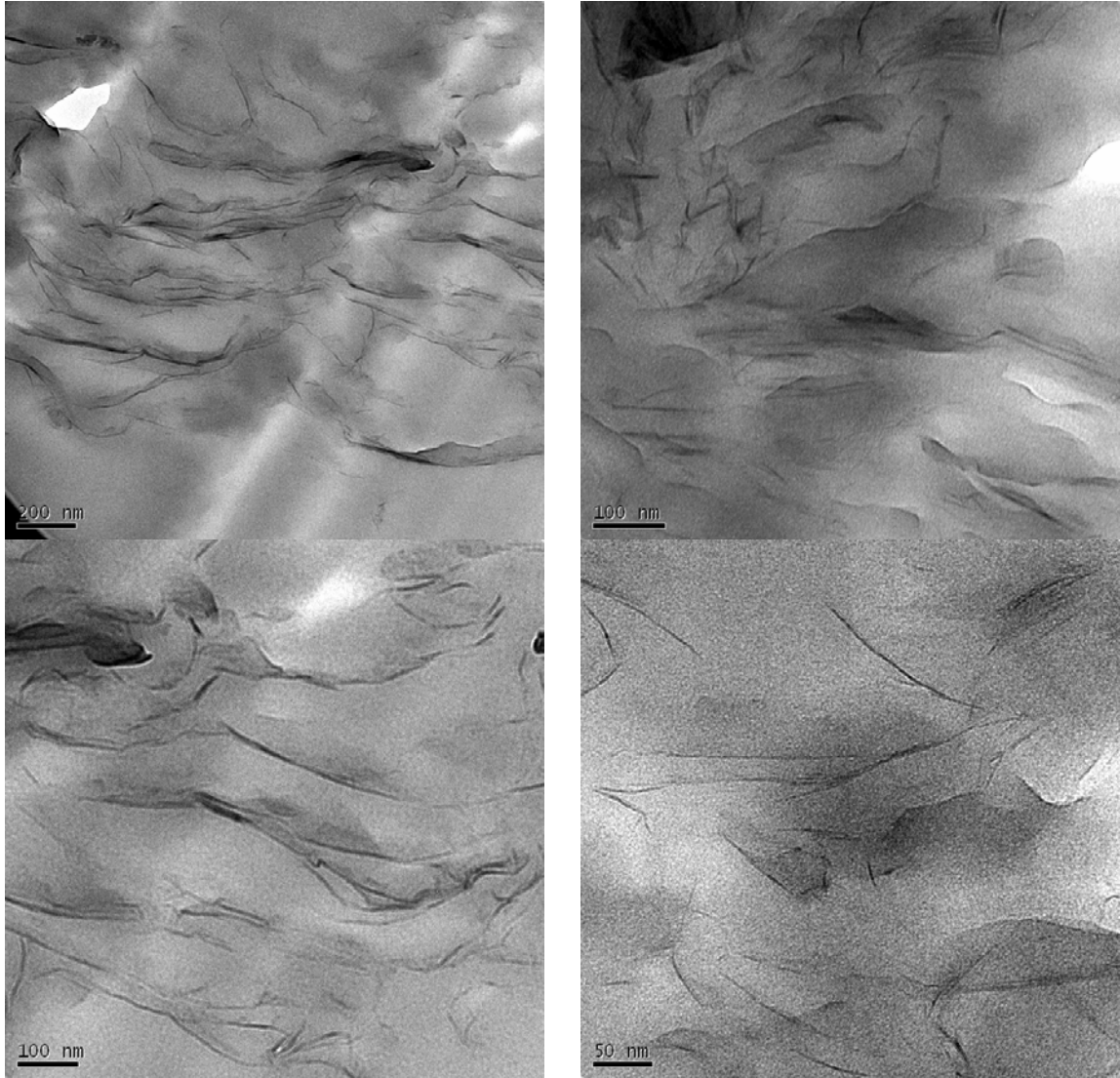


Figure 4.4: TEM pictures at of PCCN with BPAP-MMT 3.6 wt %. (PC-BPAP-3.6)

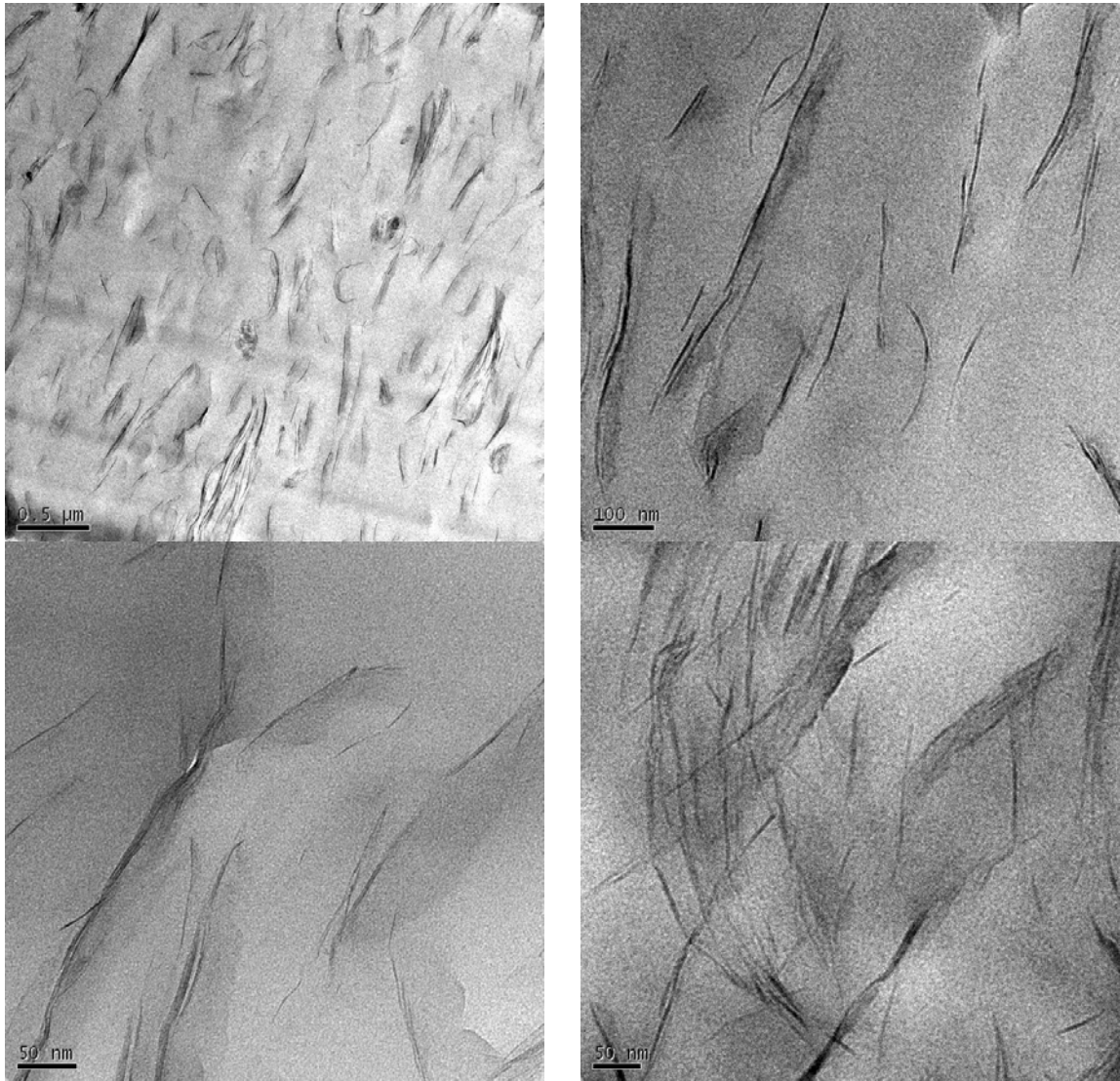


Figure 4.5: TEM pictures of PCCN with BPAP-MMT 5.4 wt %. (PC-BPAP-5.4)

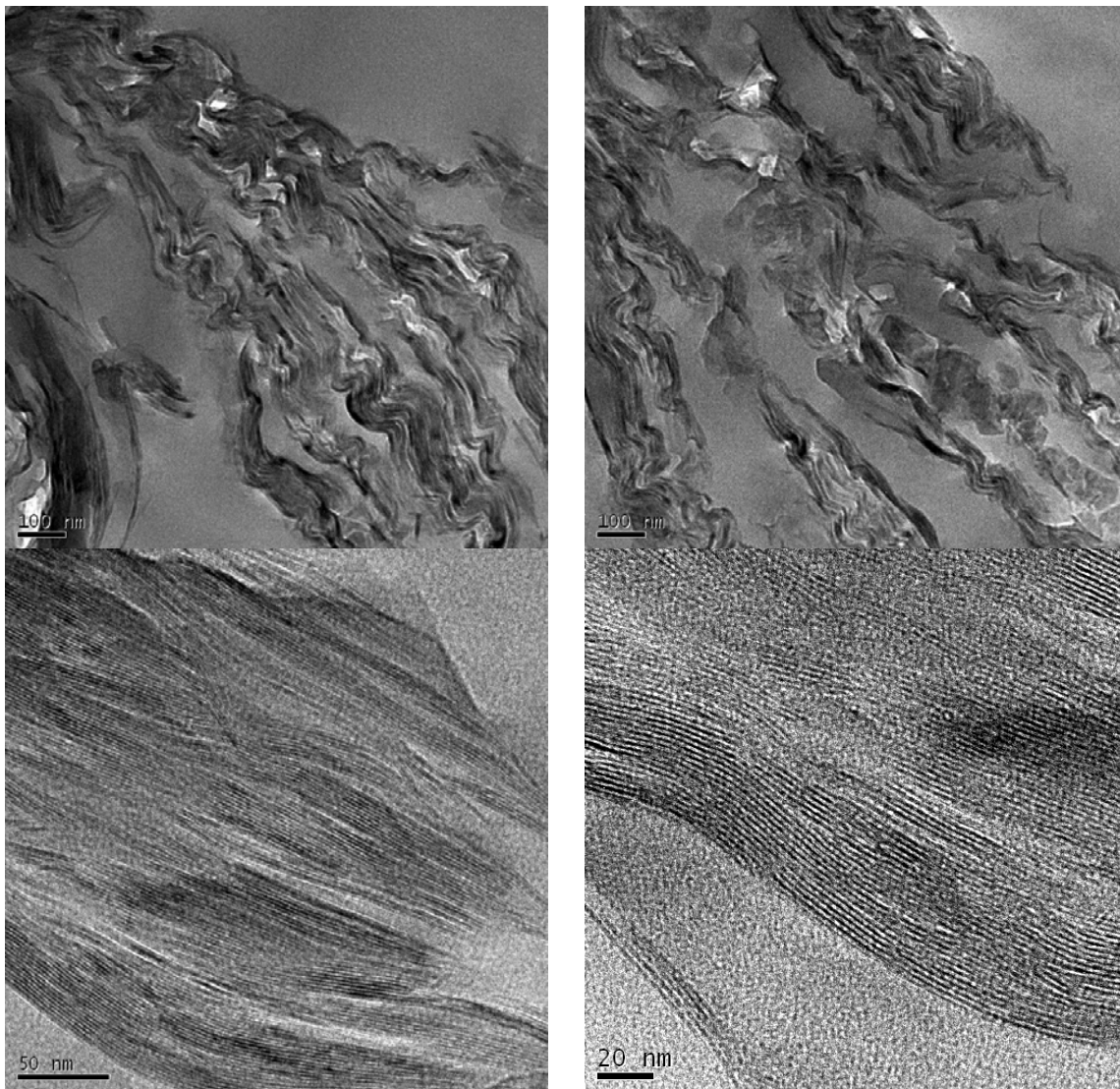


Figure 4.6. TEM pictures of PCCN with C16P-MMT 3.6 wt %. (PC-C16P-3.6)

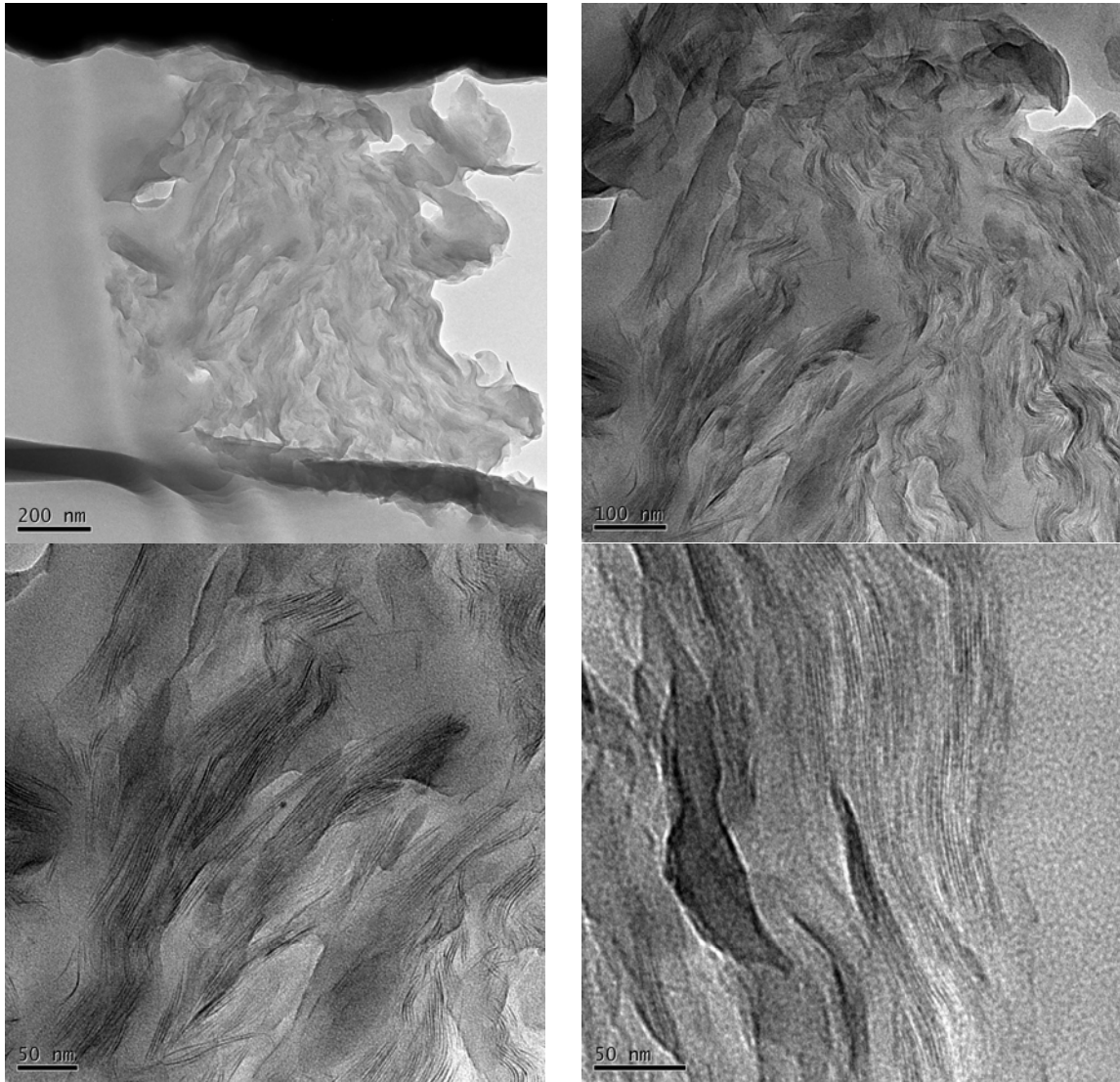


Figure 4.7: TEM pictures of PCCN with 3.6 wt % PC-C16IMI-MMT (PC-C16IM-3.6)

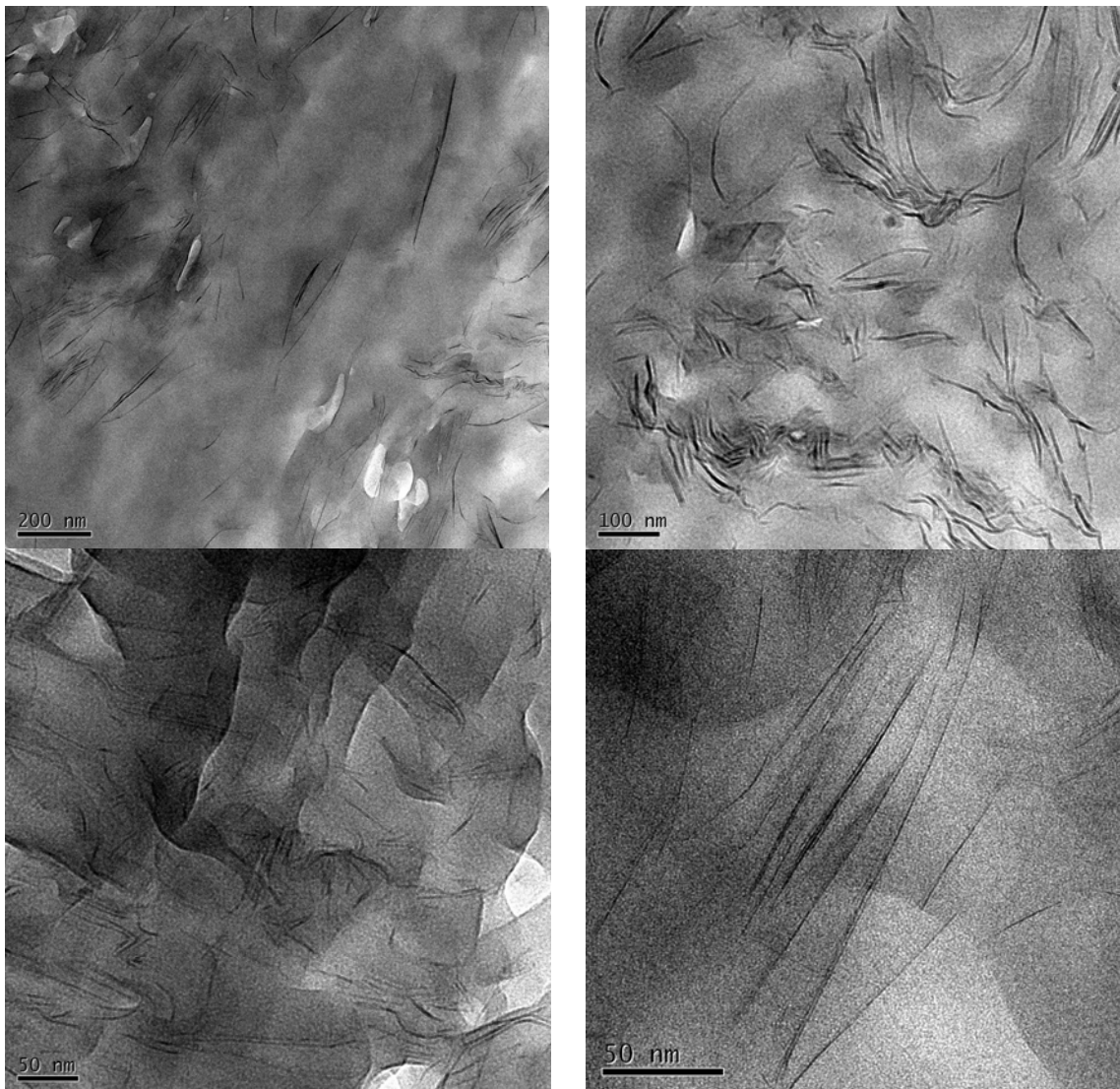


Figure 4.8: TEM pictures of PCCN with 3.6 wt % PC/BPAIMI-MMT (PC-BPAIM-3.6)

4.3.7 Glass transition Temperatures

Glass transition temperatures of the nanocomposites prepared with organoclays modified using phosphonium ions with different clay loadings were measured using DSC and were shown in the table 2. The glass transition temperatures were measured from the second heating cycle after clearing the history of the sample by heating the samples to 280 °C and cooling it to room temperature at 10 °C/min. To study the effect of nanocomposite on glass transition temperature, precipitating clay by reverse ion exchange reaction separated the matrix polymer in the nanocomposite and T_g's were measured. It can be observed

that the T_g of the matrix polymer in the exfoliated nanocomposites obtained with BPAP-MMT showed lower temperatures as compared to the nanocomposites and the difference increased with clay loading levels while there is no much effect for the agglomerated samples obtained with C16P-MMT. This behavior of lower T_g for the matrix polymer of the nanocomposites obtained from BPAP-MMT may be attributed to the presence of pendant phosphonium chloride moiety with an alkyl spacer or chain scission reaction of the matrix polymer due to presence chloride ions during the DSC measurements. In the case of the nanocomposites obtained using C16PMMT, the nanocomposites showed slightly lower glass transition temperatures compared to the recovered pristine polymer. The lowered glass transition temperature for these nanocomposites are may be due to plastisizing effect of the organomodifiers used. In the case of recovered pristine polymer the organomodifiers are washed of during precipitation process.

4.3.7 Dynamic mechanical analysis

PCCN with organoclay modified with phosphonium cations, with varying loading levels, were prepared to study the dynamic mechanical property. Lower molecular weights obtained for the polymers in the nanocomposites produced using imidazolium-modified organoclays were not useful for mechanical testing. Figure 4.9 shows the storage modulus (E') plotted against temperature. It can be observed that the at 35 °C, the nanocomposites show an increment in the storage modulus as compared to the pristine polymer and the increments are much higher in the case of exfoliated nanocomposite samples obtained using BPAP-MMT than the agglomerated composites samples obtained using C16P-MMT as compared to their respective inorganic clay loading levels.

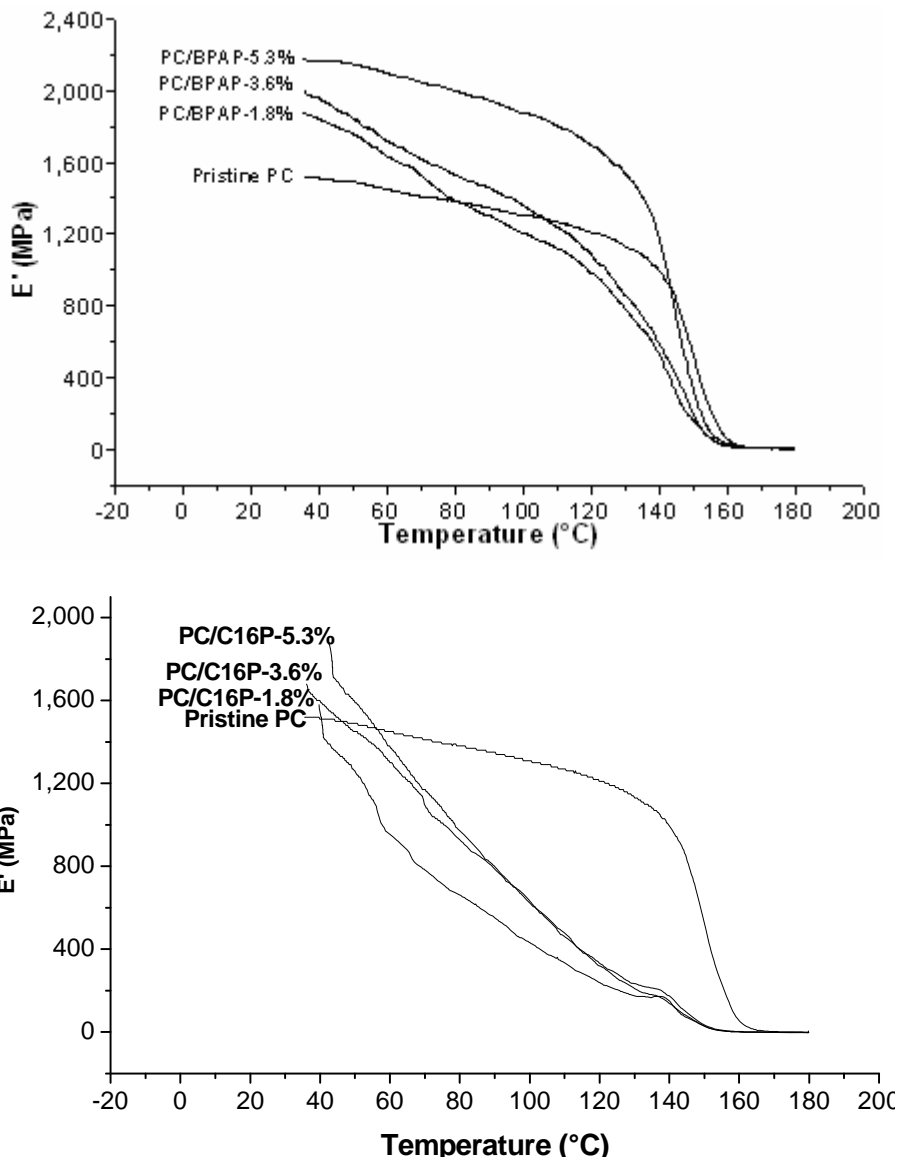


Figure 4.9: storage modulus (E') of PCCNs (a) with BPAP-MMT and (b) with C16P-MMT obtained from DMA

It can also be observed that for the exfoliated samples, the increase in storage modulus is maintained up to glass transition temperatures and suddenly drops to zero while for the agglomerated nanocomposite samples, the storage modulus keeps on decreasing rapidly with temperature. The steep decrease in the storage modulus with increase in temperature for the agglomerated composites can be attributed to the poor interaction of the polymer with the clay surface and the low aspect ratio of the dispersed clay or may be due to lower molecular weights.

4.4 Conclusion.

The organoclays, modified with thermally stable modifiers were prepared for the synthesis of polycarbonate/layered silicate nanocomposites via in-situ intercalative polymerization. We have demonstrated for the first time that polycarbonate/exfoliated layered silicate nanocomposites can be successfully prepared using a class of novel organoclays that are modified using thermally stable modifiers containing reactive functionalities while only intercalated or agglomerated structures are obtained when the organoclays used does not have a reactive functionality. The molecular weights of the polymer in the composites prepared using phosphonium cation modified organoclay were better than the imidazolium cation modified organoclay. The dynamic mechanical analysis of the exfoliated nanocomposites show better enhancement in storage modulus through out the temperature range from room temperature to below glass transition temperature as compared to the agglomerated composites. The glass transition temperatures obtained from DMA were comparable to that obtained from DSC.

References

- (1) LeGrand, D. G.; Bendler, J. T., In "Handbook of Polycarbonate Science and Technology" New York **2000**. P-107.
- (2) Friessell, W. J. In *Encyclopedia of Polymer Science and Technology*, Bikales, N. M., Ed.; John Wiley and Sons Inc: New York, 1967; Vol. 6, p 740.
- (3) Usuki, A.; Kojima, Y.; Kawasumi, M.; Okada, A.; Fukushima, Y.; Kurauchi, T.; Kamigaito, O. *J. Mater. Res.* **1993**, 8, 1179-1184.
- (4) Kojima, Y.; Usuki, A.; Kawasumi, M.; Okada, A.; Fukushima, Y.; Kurauchi, T.; Kamigaito, O. *J. Mater. Res.* **1993**, 8, 1185-1189.
- (5) *Polymer-Clay Nanocomposites*; Pinnavaia, T. J.; Beall, G. W.; Eds.; Wiley Series in Polymer Science; John Wiley & Sons Ltd: Chichester, England, **2000**.
- (6) Giannelis, E. P. *Adv. Mater.* **1996**, 8, 29-35.
- (7) Carrado, K. A. *Appl. Clay Sci.* **2000**, 17, 1-23.
- (8) Porter, D.; Metcalfe, E.; Thomas, M. J. K. *Fire Mater.* **2000**, 24, 45-52.
- (9) Ray, S. S.; Okamoto, M. *Progress in Polymer Sci.*, **2003**, 28, 1539-1641.

- (10) Imai, Y.; Nishimura, S.; Abe, E.; Tateyama, H.; Abiko, A.; Yamaguchi, A.; Taguchi, H. *Chem. Mater.*, **2002**, *14*, 477-479.
- (11) Messersmith, P. B.; Giannelis, E. P.; *Chem. Mater.*, **1993**, *5*, 1064-1066.
- (12) Weimer, M. W.; Chen, H.; Giannelis EP, Sugah DY, *J. Am. Chem. Soc.*, **1999**, *121*, 1615-1616.
- (13) Tyan, H. -L.; Liu, Y. -C.; Wei K. -H. *Chem. Mater.*, **1999**, *11*, 1942-1947.
- (14) Leu, C. -M.; Wu, Z.-W.; Wei K. -H. *Chem. Mater.*, **2002**, *14*, 3016-3021.
- (15) Zeng, C.; Lee, L. J. *Macromolecules*, **2001**, *34*, 4098-4103.
- (16) Huang, X.; Lewis, S.; Brittain, W. J.; Vaia, R. A. *Macromolecules*, **2000**, *33* 2000-2004.
- (17) Severe, G.; Hsieh, A. J.; Koene, B. E.; *ANTEC 2000*, **2000**, *2*, 1523-1526.
- (18) Yoon, P. J.; Hunter, D. L.; Paul, D. R. *Polymer*, **2003**, *44*, 5323-5339.
- (19) Yoon, P. J.; Hunter, D. L.; Paul, D. R. *Polymer*, **2003**, *44*, 5341-5354.
- (20) Yoo, Y.; Choi, K.-Y.; Lee, J. H. *Macromol. Chem. Phys.* **2004**, *205*, 1863-1868.
- (21) Mitsunaga, M.; Ito, Y.; Ray, S. S.; Okamoto, M.; Hironaka, K. *Macromol. Mater. Eng.* **2003**, *288*, **543**
- (22) Ito, Y.; Yamashita, M; Okamoto, M.; *Macromol. Mater. Eng.* **2006**, *291*, 773
- (23) Hu, X.; Lesser, A. J. *Polymer*, **2004**, *45*, 2333.
- (24) Lee, K. M.; Han, C. D. *Polymer*, **2003**, *44*, 4573.
- (25) Carrion, F-J.; Arribas, A.; Bermudez, M-D.; Guillamon, A. *European Polymer J.* **2008**, *44*, 968.
- (26) Gonzalez, I.; Eguiazabal, J. I.; Nazabal, J., *Polym. Eng. Sci.* **2006**, *46*, 864.
- (27) Zong, R.; Hu, Y.; Liu, N.; Wang, S.; Liao, G., *Polym. Adv. Technol.* **2005**, *16*, 725.
- (28) Wang, S.; Hu, Y.; Wang, Z.; Yong, T.; Chen, Z.; Fan, W. *Polym. Degrad. Stab.* **2003**, *80*, 157.
- (29) Zong, R.; Hu, Y.; Wang, S.; Song, L. *Polym. Degrad. Stab.* **2004**, *83*, 423.
- (30) Ray, S. S.; Bousmina, M.; Maazaouz, A., *Polym. Eng. Sci.* **2006**, *46*, 1121.
- (31) Wang, S.; Hu, Y.; Song, L.; Liu, J.; Chen, Z.; Fan, W. *J. Appl. Poly. Sci.* **2004**, *91*, 1457.
- (32) Xie, W.; Pan W. -P.; Hunter, D.; Vaia, R. *Chem. Mater.*, **2001**, *13*, 2979.

- (33) Foldi, V. S.; Campbell, T. W.; *J. Polym. Sci.* **1962**, *56*, 1.
- (34) Xie, W.; Xie, R.C; Pan, W.P.; Hunter, D.; Koene B.; Tan L.S.; Vaia, R. *Chem. Mater.* **2002**, *14*, 4837.
- (35) Gilman, J. W.; Awad, W. H.; Davis, R. D.; Shields, J. Harris Jr., R. H.; Davis, C.; Morgan, A. B; Sutto, T. E.; Callahan, J.; Trulove, P. C.; DeLongr H. C. *Chem. Mater.* **2002**, *14*, 3776.
- (36) Awad, W. H; Gilman, J. W.; Nyden, M.; Harris Jr., R. H.; Sutto, T. E.; Callahan, J.; Trulove, P. C.; DeLongr H. C.; Fox, D. M. *Thermochimica Acta* **2004**, *40*, 3.
- (37) Vaia, R. A.; Teukolsky, R. K.; Giannelis, E.P. *Chem. Mater.* **1994**, *6*, 1017.
- (38) Schnell, H.; Krimm, H. *Angew. Chem. Int. Ed. Engl.* **1963**, *2*, 373.
- (39) Dai, S. H.; Lin, C. Y.; Rao, D. V.; Stuber, F. A.; Carleton, P. S.; Ulrich, H. *J. Org. Chem.* **1985**, *50*, 1722-1725.
- (40) Messersmith, P. B.; Giannelis, E. P. *J Polym Sci Part A: Polym Chem* **1995**, *33*, 1047.
- (41) Lepoittevin, B.; Pantoustier, N.; Devalckenaere, M.; Alexandre, M.; Kubies, D.; Calberg, C.; Jerome,R.; Dubois, P. *Macromolecules* **2002**, *35*, 8385.
- (42) Kubies, D.; Pantoustier, N.; Dubois, P.; Rulmont,A.; Jerome, R. *Macromolecules* **2002**, *35*, 3318.

5. Syndiotactic Polystyrene/clay nanocomposites via solvent casting

5.1 Introduction

In recent years polymer/layered silicate nanocomposites have attracted great interest, both in academia and industry because they often exhibit remarkable enhancement in material properties when compared with virgin polymers at very low filler loadings¹⁻³. The enhancement in the properties of these materials are due to the interactions of the polymer chains with the surface of the clay layers and were maximum when the clay layers are completely delaminated or exfoliated in the polymer matrix.

When the surface energy of the polymer is too low, the interaction between the polymer and clay surfaces becomes difficult even if the clay surface was made organophilic. Introducing polar groups on sPS backbone can enhance surface energy of the polymers. Syndiotactic polystyrene (sPS) is an engineering semicrystalline thermoplastic material showing high melting point (about 270 °C), heat and chemical resistance, rapid crystallization and good mechanical properties.⁴⁻⁷ Reports on the synthesis of sPS/clay nanocomposites are very few mainly because of the high melting and processing temperatures. Furthermore, the low surface energy, because of the absence of polar groups, restricts sPS's interactions with polar polymers⁸ or with organoclay. The conventional quaternary ammonium modified clays decompose at the processing temperatures.⁹⁻¹² To solve this problem Park et al.^{13, 14} have utilized stepwise mixing procedure by mixing the organoclay with functionalized amorphous styrenic polymer followed by blending with sPS. Thermally stable modifiers based on phosphonium and imidazolium cations have been reported in the literature.¹⁵⁻¹⁷ Tseng et al.¹⁸ have used thermally stable modifiers based on cetylpyridinium ion for the preparation of sPS nanocomposites.

Recently, to improve the surface energy of semicrystalline polymers in the preparation of nanocomposites, many researchers introduced ionic groups on to the polymer chains. Moore et al. have introduced sodium sulfonate groups on poly(ethylene terephthalate)¹⁹ and poly(butylene terephthalate)²⁰ back bone to get exfoliated

organoclay. Nanocomposites prepared from ionomers of polypropylene,²¹ polyethylene²²,²³ and a variety of other nonpolar thermoplastics polymers²⁴⁻²⁶ also reveal good levels of organoclay exfoliation.

In this chapter we describe the preparation and characterization of nanocomposites of SsPS ionomers with organoclay. For the first time we examined the effect of sulfonation content (sulfonation level ranging from 0.5 to 3.8 mole %) and type of ionomer (H^+ , Na^+ , K^+ and Rb^+ in the group I series of the periodic table) on intercalation/exfoliation of SsPS ionomers/organoclay nanocomposites by using WAXD and TEM. We have also studied the effect of clay layers on the crystallization of ionomers.

5.2 Experimental

5.2.1 Materials:

Syndiotactic polystyrene was kindly supplied by the Dow Chemical Company, USA. The weight average molecular weight was 275000 and the melt index was 4.3. 1,1,2-Trichloroethane (TCE) and Rubidium hydroxide were obtained from Aldrich, USA. Potassium hydroxide, Sodium hydroxide and Chloroform were purchased from Merck, India. The clay, Cloisite Na^+ was from Southern Clay Products, USA. The reagents were of analytical reagent grade and were used as received. 1-hexadecyl-2,3-dimethylimidazolium bromide was prepared in the laboratory by quaternizing 1,2-dimethylimidazole with hexadecyl bromide.

5.2.2 Preparation of organoclay:

Organoclay was prepared as per the standard exchange reaction.²⁷ The Na montmorillonite (10.0 g) with CEC 92 meq/100 g, d-spacing 1.2 nm was dispersed in water / methanol (60/40, v/v, 300 mL) by stirring with an overhead stirrer at room temperature for 2 hours. 1-Hexadecyl-2,3-dimethylimidazolium bromide (4.4 g, 11.0 mmol) in water / methanol mixture was poured in to the dispersion of clay in drops and stirred for 24 hours at 65 °C. Then the reaction mixture was cooled, centrifuged and washed several times with distilled water and methanol until all the bromide ions were washed off which was confirmed by testing the washings with $AgNO_3$. The organoclay

obtained was freeze-dried under vacuum overnight. The organoclay was obtained as a fine, dry powder. The organic content in the organoclay was determined from TGA analysis and found to be 25 wt %. The interlayer d-spacing for the organo modified montmorillonite was measured from WAXD and found to be 1.85 nm.

5.2.3 Preparation of SsPS ionomers:

5.2.3.1 Preparation of acetyl sulfate

Acetic anhydride (0.210 mol) was added to 50 mL of TCE/chloroform (60/40, v/v) mixed solvent. Then the solution was cooled to below 10 °C using ice-cold water bath. Concentrated sulfuric acid (0.70 mol) was slowly added under vigorous stirring. After completing the mixing, the reaction mixture was diluted with the mixed solvent to 100 mL in a volumetric flask at room temperature. It was assumed that the reaction yield was quantitative, i.e., 70 mmol of acetyl sulfate.

5.2.3.2 Preparation of SsPS

SsPS was prepared as per the procedure reported elsewhere.²⁸⁻³⁰ In a 1 L round bottom flask syndiotactic polystyrene (6.5 g) and TCE/chloroform (60/40, v/v) mixture (500 mL) were stirred at reflux temperature (ca. 115 °C) until all the sPS was dissolved. Then the solution was cooled to 70 °C and freshly prepared acetyl sulfate solution was added under vigorous stirring, which continued for 3 h. The amount of acetyl sulfate required was determined by the desired degree of sulfonation. Ethanol (10 mL) was added to arrest the reaction and the polymer was precipitated by pouring the solution in to diethyl ether (2 L) and filtered. It was washed with hot distilled water and then dried in a vacuum oven at 70 °C for 24 h. The polymer was redissolved in TCE and precipitated in excess of diethyl ether, filtered and dried in a vacuum oven at 70 °C for 24 h. The degree of sulfonation was determined by nonaqueous titration. The efficiency of sulfonation was around 40 to 50 %.

5.2.3.3 Preparation of SsPS ionomers

The SsPS ionomers were prepared by fully neutralizing with addition of 20 % excess methanolic alkali hydroxides (NaOH, KOH and RbOH). The neutralized polymer

solution was precipitated in diethyl ether, washed with hot methanol and dried in vacuum at 70 °C for 24 hrs.

5.2.4 Preparation of SsPS ionomers / clay nanocomposites:

SsPS ionomers/organoclay nanocomposites were prepared by solution technique. Pre-weighed SsPS ionomers were dissolved in TCE at 120 °C and then organoclay (8 wt %) was added and the solution kept at 90 °C for 10 hrs under constant agitation. The solvent was evaporated to obtain a translucent film. The sample was dried under vacuum at room temperature.

5.2.5 Characterization:

The thermal properties of the samples were analyzed by TA instruments Q10 differential scanning calorimeter under standard conditions. The samples were heated under flowing nitrogen atmosphere from 0 °C to 300 °C at the rate of 10 °C/min and held for 1 minute at the maximum temperature. At the end of holding period the sample was cooled at the rate of 10 °C/min. to record the crystallization exotherm. The calorimeter was calibrated using standard protocols. The sample weight was about 5 mg in all the experiments. TGA-7 unit in the Perkin-Elmer thermal analysis system was used to determine the thermal stability of the samples as well as the amount of clay present in the nanocomposites. The samples were heated under flowing nitrogen atmosphere from 50 to 900 °C, at a heating rate of 10 °C/min. and the weight loss was recorded. The weight of the residue remaining at 900 °C was taken as the % clay content in the nanocomposite and found to be 6 wt% for all the samples.

The WAXD experiments were performed using a Rigaku Dmax 2500 diffractometer equipped with a copper target and a diffracted beam monochromator. (Cu K α radiation with $\lambda = 1.5406 \text{ \AA}$) with 2θ scan range of 2 – 10° at room temperature. The specimen of nanocomposites for WAXD was thin film samples melt pressed on a copper block sample holder at 280 °C for a period of 15 seconds. Samples for TEM were sectioned using a Lieca Ultracut UCT microtome with thicknesses of 50-60 nm using a diamond knife at room temperature. Before sectioning for TEM, the samples were heated to 280 °C for a period of 10 to 15 seconds and sized the sample so that it could be

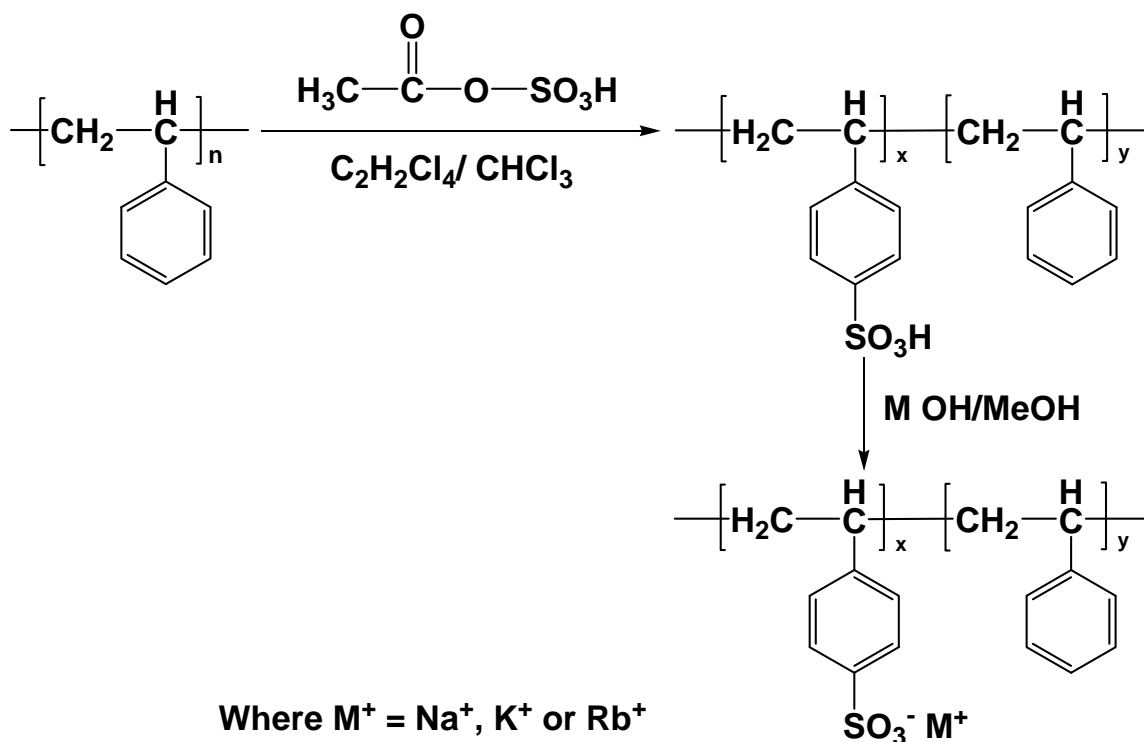
conveniently hold on the sample holder of the microtome for sectioning. The sections were collected from water on 300 mesh carbon coated copper grids. TEM imaging was done using a JEOL 1200EX electron microscope operating at an accelerating voltage of 80 kV. The density of clay particles is enough to produce contrast between polymer and clay stacks hence staining was not required. Images were captured using charged couple detector (CCD) camera for further analysis using Gatan Digital Micrograph analysis software.

5.3 Results and discussion

5.3.1 Preparation of sulfonated sPS and its ionomers

Syndiotactic polystyrene was sulfonated to different levels (0.5, 2.0, 3.2 and 3.8 mol %) The sulfonation procedure followed in the present work is according to the procedure by Li *et al* and is a modified procedure of Moore *et al* (scheme 1)^{29,30}. Alkali salts of sPS (i.e., NaSsPS, KSsPS, and RbSsPS) have also been prepared by fully neutralizing the sulfonic acid groups with respective hydroxides. The degree of sulfonation was determined by nonaqueous titrations.

Scheme 1



The FTIR spectra of sPS and SsPS samples containing 3.8 mol % sulfonic acid group are shown in Figure 5.1. The bands at 1097 cm^{-1} and 1175 cm^{-1} are observed only for sulfonated samples and sPS sample does not show these bands. The band at about 1097 cm^{-1} is attributed to the in plane skeletal vibrations of the disubstituted benzene rings. The band at 1174 cm^{-1} is assigned to symmetric stretching vibration of sulfonic acid group in polystyrene. The presence of these bands in the sulfonated sample provides evidence of sulfonation.

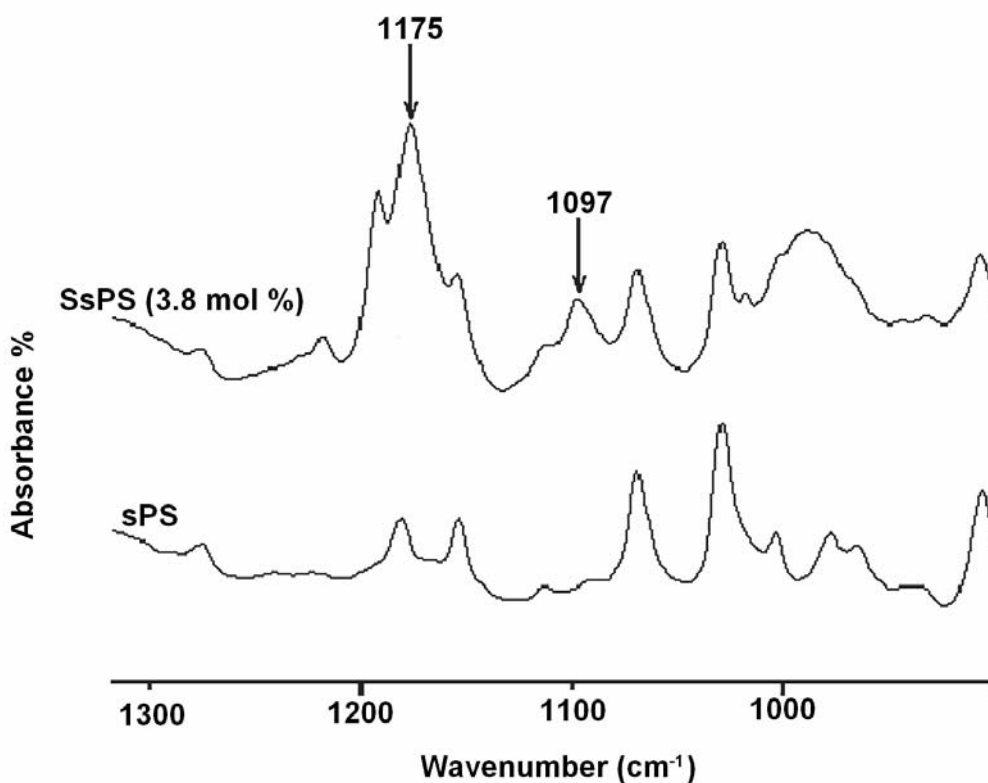


Figure 5.1: Typical FTIR spectra of sPS and SsPS.

Figure 5.2 compares the $^1\text{H-NMR}$ spectra of sulfonated sPS (3.8 mole %) with that of neat sPS. The spectra exhibit peaks at about 1.3 ppm for CH_2 (a) and 1.8 ppm for CH (b) protons. The ortho-protons (c) appear at 6.5 ppm. The meta and para-protons (d) of the unsubstituted aromatic ring appear at about 7.0 ppm. The meta-protons (e) of the substituted aromatic ring appear at about 7.5 ppm for the sulfonated sample but is absent in the sPS spectrum.

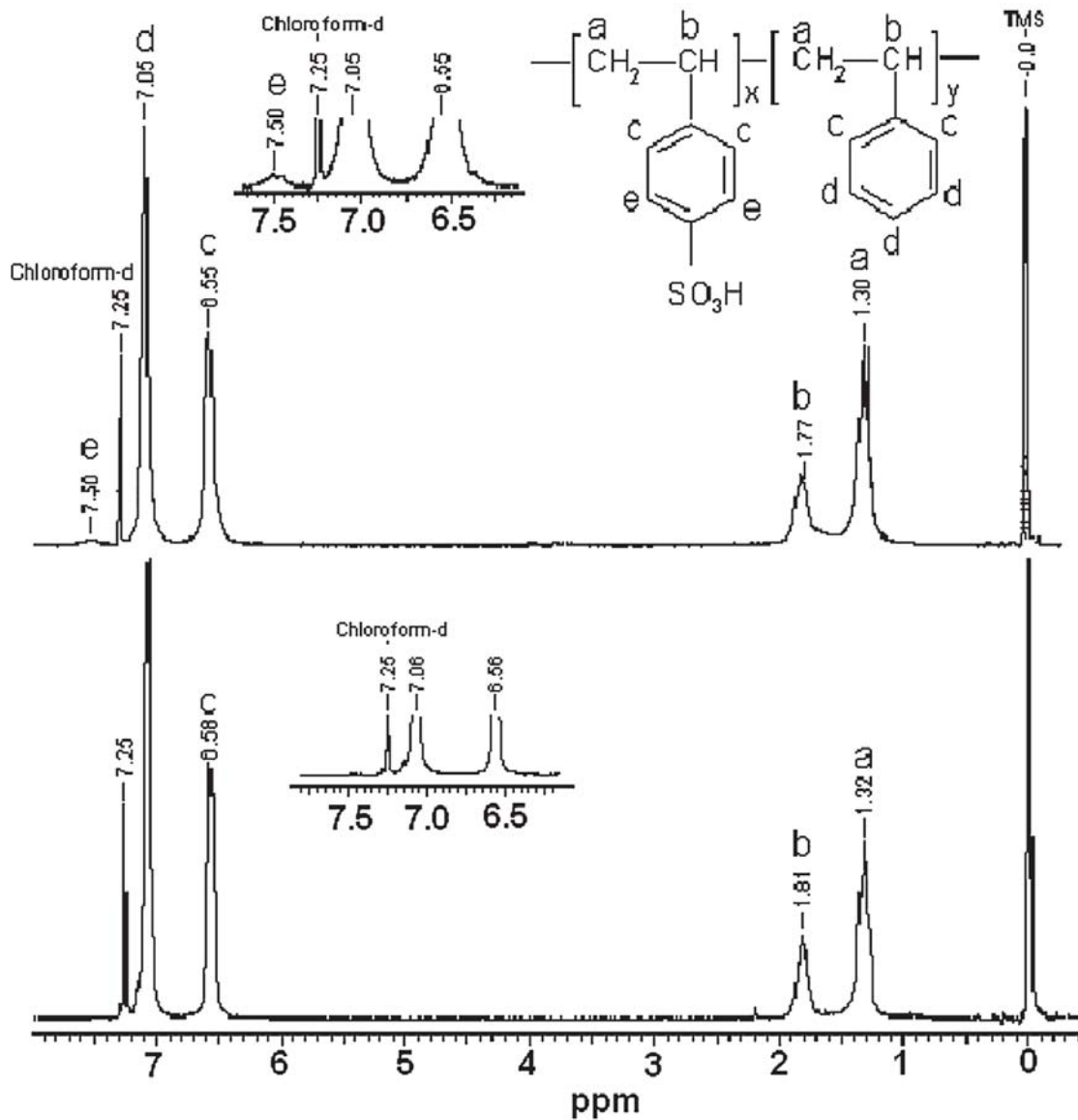


Figure 5.2: Typical ¹H NMR spectra of sPS and SsPS.

5.3.2 Thermal stability of the organoclay and the nanocomposites

The organoclay used in the present study is obtained by modification of pristine Na⁺ montmorillonite with 1-hexadecyl-2,3-dimethylimidazolium cation. Figure 5.3 shows the TGA thermograms of the organoclay (a), RbSsPS 3.8 mole %/organoclay nanocomposites (b) and RbSsPS 3.8 mole % (c). The organic content in the organoclay was found to be 25 wt % which is obtained as the weight loss at 900 °C; which matches

with the calculated 100 % cation exchange capacity. The onset of degradation of the modifier in the organoclay (295 °C, 2 % weight loss) is higher than the melting temperature of sPS, which is around 270 °C. As expected from the improved stability of the modifier, the nanocomposite also exhibits thermal stability up to 300 °C and the degradation sets in above 300°C.

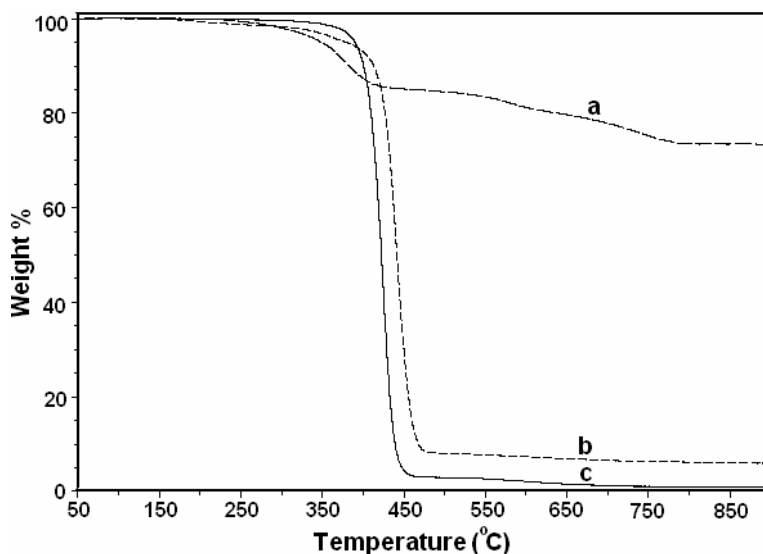


Figure 5.3: TGA thermogram of (a) organoclay, (b) RbSsPS 3.8 mole %/organoclay nanocomposite and (c) RbSsPS 3.8 mole %.

5.3.3 Structure of sPS/organoclay nanocomposites

Figure 5.4a shows the WAXS pattern for the unmodified clay, modified clay, sPS and the sPS/organoclay nanocomposite. The unmodified clay has a gallery height of 1.24 nm and upon modification it increases to 1.90 nm. The sPS/clay nanocomposite shows two peaks due to clay at $2\theta = 4.20^\circ$ and at 4.65° and the d-spacings are 2.10 and 1.90 nm respectively. This indicates that in the nanocomposite, the sPS penetrate into a fraction of the clay galleries and the gallery expands to 2.10 nm. The presence of peak at 4.65° indicates that some amount of organoclay remains without intercalation. The peak at around $2\theta = 6.8^\circ$ in the sPS and sPS/organoclay nanocomposite is due to the 110 reflection of the α crystalline form. The nanocomposites as prepared by the solution technique exhibit δ form but on heating above 200 °C all the samples exhibit only the α form and such behavior is similar to the well-established behavior of sPS.³¹ TEM micrograph in Figure 5.4b shows agglomerated structures, which further implies that the

organoclay tactoids remain intact and is consistent with XRD data. This type of behavior exhibited by sPS/organoclay nanocomposites may be due to the limited interaction of sPS with the organoclay layers as the surface energy of the sPS is low. It has been shown that intercalation/exfoliation can be obtained with suitable organoclay.^{18, 32, 33} However with the present organoclay only the agglomerated structures are obtained and this may be due to the choice of the modifier.³⁴

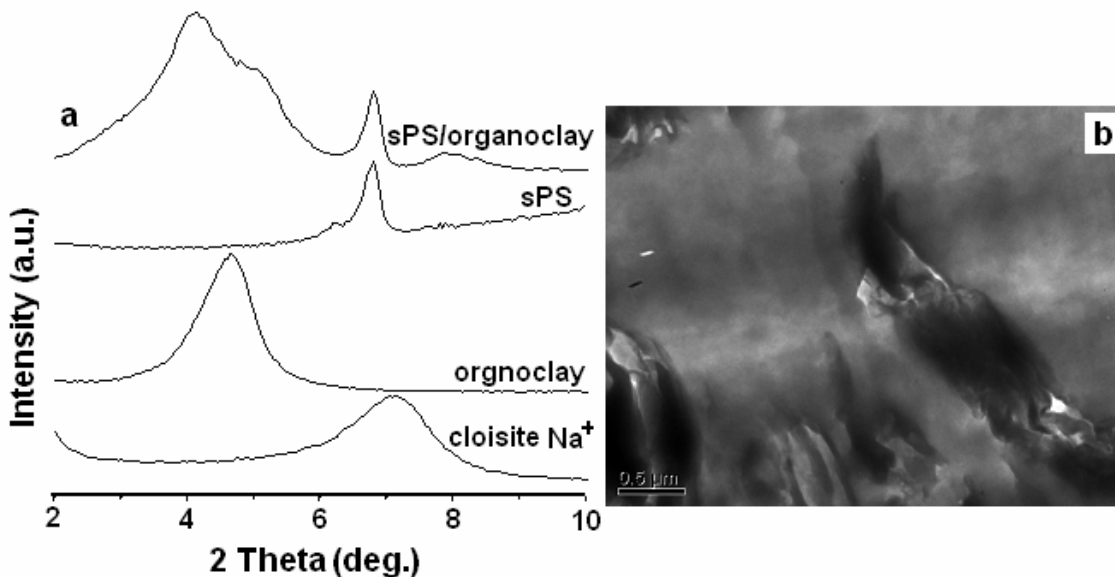


Figure 5.4: a) WAXS pattern of cloisite Na⁺, organoclay, sPS and sPS/organoclay nanocomposite. b) TEM micrograph of sPS/organoclay nanocomposite.

5.3.4 Structure of SsPS ionomer/organoclay nanocomposites

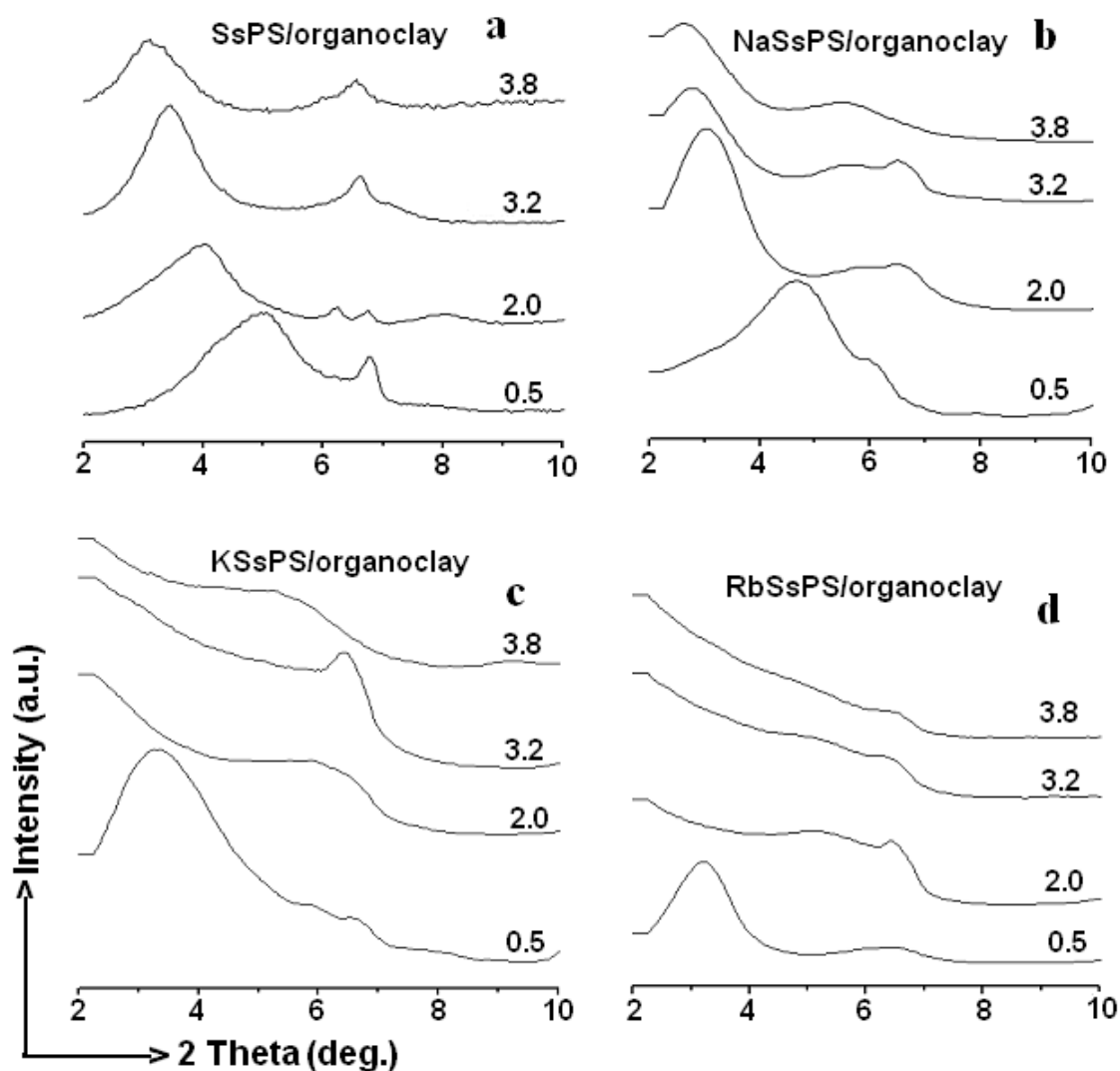
5.3.4.1 Effect of ionomer content

Table 5.1: Clay gallery height from WAXD data of SsPS ionomers/clay nanocomposites

| Sulfonation level (%) | Clay gallery height (nm) | | | |
|-----------------------|--------------------------|-----------------|----------------|-----------------|
| | H ⁺ | Na ⁺ | K ⁺ | Rb ⁺ |
| 0.5 | 1.84 | 1.90 | 2.63 | 2.72 |
| 2.0 | 2.20 | 2.94 | * | * |
| 3.2 | 2.60 | 3.15 | * | * |
| 3.8 | 2.90 | 3.40 | * | * |

* Exfoliated

Converting the sPS into sPS ionomers improves the interaction of the sPS with organoclay and Figure 5.5 shows the X-ray diffraction pattern of SsPS ionomer/organoclay nanocomposites with various degrees sulfonation and different ion types (H^+ , Na^+ , K^+ and Rb^+). The **Table 5.1** shows the gallery height of the clays for various ionomer/organoclay nanocomposites. The WAXD patterns in Figure 5.5a show that as the extent of sulfonic acid groups in sPS increases from 0.5 to 3.8 mole %, the interlayer d-spacing of the organoclay increases gradually from 1.9 to 2.9 nm, demonstrating that higher the sulfonation levels lead to better intercalation in the



nanocomposites.

Figure 5.5: WAXD pattern of SsPS ionomer/organoclay nanocomposites with different ionomer content and cation type (a) H^+ , (b) Na^+ , (c) K^+ and (d) Rb^+ .

Similarly Figure 5.5b shows that for the sodium salt of SsPS ionomer (NaSsPS)/organoclay nanocomposites, 0.5 mole % ionomer content shows little intercalation, while the extent of intercalation gradually increased up to 3.4 nm with the increase in the ionomer content to 3.8 mole %. In Figure 5.5(c) and 5.5(d), SsPS/organoclay nanocomposites prepared with K^+ and Rb^+ ionomers, show intercalation of polymer chains in to the organoclay gallery at lower levels of ionomeric content such as 0.5 mole %, while higher levels of ionomeric content show disappearance of the peaks due to clay indicating completely delaminated and disordered structure for the organoclay in the nanocomposites.

Overall it can be clearly understood from the above trends that irrespective of the ionomer cation type, the extent of dispersion of the organoclay in the polymer matrix has improved with the increase in ionomer content. This type of behavior is obvious from the fact that as the ionomer content increases, the surface energy of the polymer increases, which in turn increases the interaction of the polymer with the organoclay.

5.3.4.2 Effect of type of ionomer

It is interesting to note that the extent of interaction of the SsPS ionomer with organoclay depends on the type of cation in the SsPS ionomers. Even for low level of sulfonation i.e. with 0.5 mole % ionomer content of SsPS, with the change of cations from H^+ to Rb^+ in the SsPS ionomer/organoclay nanocomposites, the WAXD patterns show systematic changes in the gallery height. The gallery height increases marginally from 1.8 to 1.9 nm when the H^+ is changed to Na^+ . However, when the cation is changed to K^+ and Rb^+ the gallery height increases to 2.6 and 2.7 nm respectively, indicating high level of intercalation. Similarly, when the ionomer content was higher (2 to 3.8 mole %), for H^+ and Na^+ cations in the SsPS ionomer/organoclay nanocomposites, the WAXD pattern shows increase in the organoclay d-spacing indicating that the polymer chains have penetrated into the organoclay interlayer gallery. On the other hand for K^+ and Rb^+ cations in the SsPS ionomer/organoclay nanocomposites, the WAXD patterns show disappearance of the peak due to the organoclay, indicating exfoliation of organoclay in the polymer matrix. Here also it can be noted that the extent of intercalation increased

with the change in the cation type from H^+ to Na^+ and lead to exfoliations in the case of K^+ and Rb^+ .

The structure of the nanocomposites with various cations was further confirmed by TEM analysis. The typical TEM micrographs of SsPS ionomer/organoclay nanocomposites with an ionomer content of 3.8 mole % with various cations are shown in the Figure 5.6.

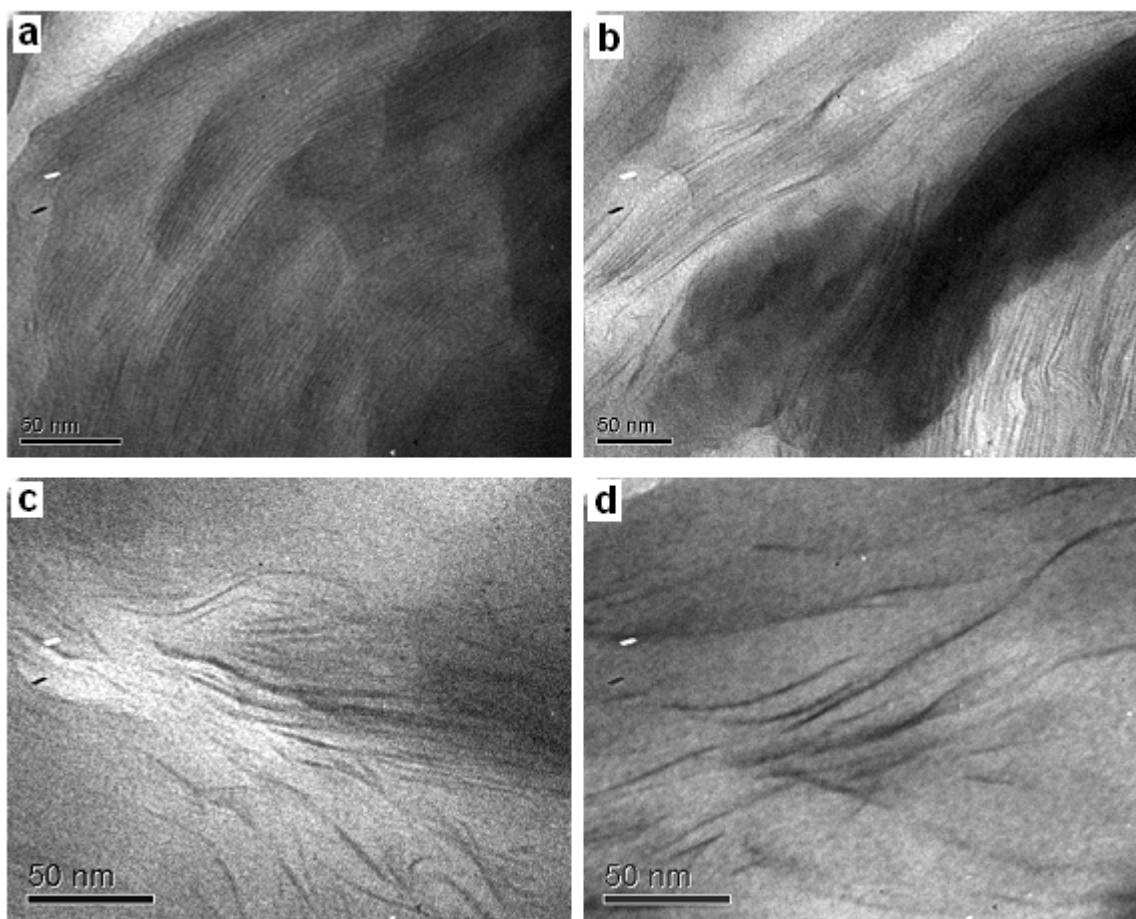


Figure 5.6: TEM micrographs of SsPS ionomers 3.8 mole %/organoclay nanocomposites (a) SsPS, (b) NaSsPS, (c) KSsPS and (d) RbSsPS

The parallel lines observed in the micrograph in Figure 5.6a and 5.6b indicate that intercalated nanocomposites were obtained with H^+ and Na^+ SsPS/organoclay nanocomposites and the distance between the parallel lines measured from the micrographs are comparable with the d-spacing obtained from WAXD. Figure 5.6c and 5.6d shows the TEM micrograph of SsPS ionomers/organoclay nanocomposite with K^+

and Rb^+ cations revealing that the clay layers are completely delaminated and exfoliated in the polymer matrix.

The extent of intercalation/exfoliation of the polymer with the organoclay depends on the extent of interaction of the polymer with the organoclay surface. Higher the polarity of the polymer, better the interaction with the organoclay, which has higher polarity and surface energy. In the above results it was observed that as the cation of the SsPS ionomer in the nanocomposites changed from H^+ to Rb^+ , the interlayer distance (d-spacing) increase and even leads to exfoliation in the case of K^+ and Rb^+ cation. This behavior of better interaction with change in cations from H^+ to Rb^+ may be attributed to the increase in polarity of the ionomeric salt. It is known that as we move down the group in the periodic table, with the increase in the size of the cation, the polarizability of the cation increases as indicated by absolute hardness parameters for the cations.³⁵ As the polarizability of the cations in SsPS ionomers increases from H^+ to Rb^+ , the interaction with the organoclay increases and resulted in exfoliation.

5.3.5 Structure of SsPS ionomer/Cloisite Na^+ nanocomposites

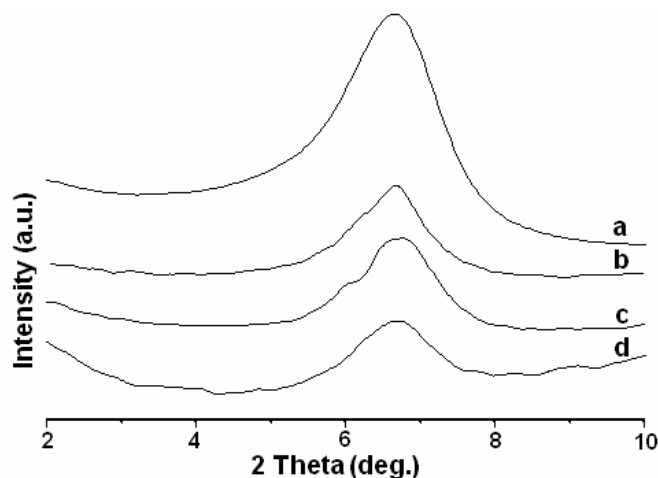


Figure 5.7: WAXD pattern of 3.8 mole % SsPS ionomers/cloisite Na^+ nanocomposites with different cations: (a) cloisite Na^+ (b) NaSsPS/cloisite Na^+ (c) KSsPS/cloisite Na^+ (d) RbSsPS/cloisite Na^+

It is also of interest to see whether the increased surface energy of the polymer is sufficient to intercalate/exfoliate the unmodified clay. To that end nanocomposites of various ionomers with highest ionomer content of 3.8 mole % were prepared with unmodified clay and the X-ray diffraction pattern is shown in Figure 5.7. In all the samples the clay peak shows no significant shift indicating the absence of intercalation of the polymer in to the gallery. These results indicate that the increased level of surface energy of the polymer achieved in the present work is not sufficient to interact with unmodified clay and necessitates the need for the clay modification for interacting with polymer. Furthermore, it shows that the nature of surface treatment will have significant effect on the interaction between the clay and the polymer.³⁴

5.3.6 Crystallization behavior of SsPS ionomer organoclay nanocomposites

The interaction of the polymer with clay layers has profound influence on the melt crystallization of the sPS ionomer. The crystallization peak temperature (T_{CC}) on cooling from melt has been taken as a measure of crystallization rate.³⁶ High T_{CC} during cooling in non-isothermal experiments indicates higher crystallization rate. **Table 5.2** gives the T_{CC} on cooling from the melt for various samples. The T_{CC} decreases with increasing sulfonation level indicating inhibition in crystallization. The crystallization is further inhibited when the H^+ ion is replaced by different cations like Na^+ , K^+ and Rb^+ . At higher sulfonation levels, ca 3.8 % most of the samples do not crystallize on cooling from the melt. The NaSsPS samples are the most affected, while RbSsPS samples showed relatively better crystallization rate under comparable cooling rate. The reduction in the crystallization rate of these samples is attributed to the ionic aggregation arising due to the coulombic interactions between the ion pairs which impedes the chain mobility.³⁷ The coulombic interactions between the ion pair become weaker with increasing size of the alkali ions.^{38, 39} The RbSsPS samples have lesser coulombic interactions and fewer aggregations of ions compared to NaSsPS samples. Hence RbSsPS samples have better crystallization rate compared NaSsPS, while the KSsPS samples takes the middle position.

Table 5.2: Crystallization temperature on cooling from the melt for various samples

| Sulfonation level (%) | Crystallization temperature (°C) | | | | | | | |
|-----------------------|----------------------------------|-----------------|----------------|-----------------|----------------|-----------------|----------------|-----------------|
| | Without clay | | | | Nanocomposite | | | |
| | H ⁺ | Na ⁺ | K ⁺ | Rb ⁺ | H ⁺ | Na ⁺ | K ⁺ | Rb ⁺ |
| 0.5 | 234 | 233 | 233 | 232 | 234 | 236 | 236 | 236 |
| 2.0 | 225 | 199 | 189 | 193 | 228 | 209 | 218 | 223 |
| 3.2 | 222 | 183 | 183 | 194 | 222 | 205 | 215 | 222 |
| 3.8 | 212 | * | * | * | 212 | 163 | 184 | 198 |

* Do not crystallize on cooling from the melt

The clay layers apparently do not influence the crystallization of the sulfonated samples as evident from the crystallization temperatures of the SsPS nanocomposites shown in **Table 5.2**. On the other hand, clay layers enhance the crystallization rate of the samples having alkali metal ions. As an example, it is clearly seen in the case of the sample sulfonated to 3.8 % and neutralized with K⁺ does not crystallize on cooling and remains amorphous. But in the nanocomposite it crystallizes at 184 °C indicating that the crystallization rate has improved. In the case of samples sulfonated to lower levels, the crystallization peaks appear at higher temperatures than the samples without clay, indicating faster crystallization rates in the case of nanocomposites. These indicate that the clay layers modified with 1-hexadecyl-2,3-dimethylimidazolium cation prevents the aggregation of ions and the crystallization rate increases. It is clear from the **Table 2** that the exfoliated nanocomposites showed better crystallization rate than the intercalated ones because of the uniformly dispersed clay layers in the polymer matrix.

5.4. Conclusions:

The interaction of sPS with organoclay was improved by increasing the surface energy of the polymer by introducing the polar ionic functional groups such as ionomers of sulfonic acids with H⁺, Na⁺, K⁺ and Rb⁺ cations. It was demonstrated that higher ionomer content leads to better interaction with the polar silicate surface of the organoclay resulting in better intercalation/exfoliation. For the first time we have shown

that by increasing the size and polarizability of the cation from H⁺ to Rb⁺, resulted in improved intercalation/exfoliation behavior even with low levels of ionomer content. The SsPS ionomers show lower crystallization rates compared to sPS due to ionic aggregation. However, in the case of SsPS ionomer nanocomposites, the interaction of the modified clay layers with the ionomer leads to less aggregation and partially restores the crystallization rates.

References:

1. LeBaron, P. C.; Wang, Z.; Pinnavaia, T. J. *Appl. Clay Sci.* **1999**, *15*, 11.
2. Alexander, M.; Dubois, P. *Mater. Sci. Eng.* **2000**, *28*, 1.
3. Ray, S. S.; Okamoto, M. *Prog. Polym. Sci.* **2003**, *28*, 1539.
4. Woo, E. M.; Sun, Y. S.; Lee, M. L., *Polymer* **1999**, *40*, 4425.
5. Vittoria, V.; Filho A. R; De Candia, F. J. *Macromol. Sci. – Phys.* **1990**, *B29*, 411.
6. Cimmino, S.; Pace, E. Di; Martuscelli, E; Silvestre, C. *Polymer* **1991**, *32*, 1080.
7. De Rosa, C.; Rapacciuolo, M; Guerra, G.; Petraccone, V. *Polymer* **1992**, *33*,1423.
8. Molner, A.; Eisenberg, A. *Polym Eng and Sci.* **1992**, *32*, 1665.
9. Xie, W.; Gao, Z.; Pan, W.-P.; Vaia, R.; Hunter, D.; Singh, A. *Polym. Mater. Sci. Eng.* **2000**, *83*, 284.
10. Xie, W.; Goa, Z.; Lui, K.; Pan, W.P.; Vaia, R.; Hunter, D.; Singh, A. *Thermochim. Acta.* **2001**, *367*, 339.
11. Jones, M.; *Jr. Organic Chemistry*, 2nd ed.; W. W. Norton & Co. Inc.: New York, **2000**; p 258.
12. Wright, A. C.; Granquist, W. T.; Kennedy, J. V. *J. Catal.* **1972**, *25*, 65.
13. Park, C. I.; Park, O. O.; Lim, J. G.; Kim, H. J. *Polymer* **2001**, *42*, 7465.
14. Park, C. I.; Choi, W. M.; Kim, M. H.; Park, O. O. *J Polym. Sci. Polym. Phys.* **2004**, *42*, 1685.
15. Zhu, J.; Morgan, A. B.; Lamelas, F. J.; Walkie, C. A. *Chem. Mater.* **2001**, *13*, 3774.
16. Gilman, J. W.; Awad, W. H.; Davis, R. D.; Shields, J.; Harris Jr. R. H.; Davis, C.; Morgan A. B.; Sutto, T. E.; Callahan, J.; Trulove, P. C.; DeLong, H. C.; *Chem. Mater.* **2002**, *14*, 3776

17. Xie, W.; Xie, R.; Pan, W.; Hunter, D.; Koene, B.; Tan, L.; Vaia, R. *Chem. Mater.* **2002**, *14*, 4837.
18. Tseng, C. R.; Wu, J. Y.; Lee, H. Y.; Chang, F. C. *Polymer* **2001**, *42*, 10063.
19. Barber, G. D.; Calhoun, B. H.; Moore, R. B. *Polymer* **2005**, *46*, 6706.
20. Chisholm, B. J.; Moore, R. B.; Barber, G.; Khouri, F.; Hempstead, A.; Larsen, M.; Olson, E.; Kelley, J.; Balch, G.; and Caraher, J. *Macromolecules* **2002**, *35*, 5508.
21. Wang, Z. M.; Nakajima, H.; Manias, E.; Chung, T. C. *Macromolecules* **2003**, *36*, 8919.
22. Shah, R. K.; Paul, D. R. *Macromolecules* **2006**, *39*, 3327.
23. Lee, J. A.; Kontopoulou, M.; Parent, J. S. *Polymer* **2005**, *46*, 5040.
24. Start, P. R.; Mauritz, K. A. *J. Polym. Sci. Polym. Phys.* **2003**, *41*, 1563.
25. Kovarova, L.; Kalendova, A.; Malac, J.; Vaculik, J.; Malac, Z.; Simonic, J. *Annu. Tech. Conf. Soc. Plast. Eng.* **2002**, *60th*, 2291.
26. Barber, G. D.; Carter, C. M.; Moore, R. B. *Annu. Tech. Conf. Soc. Plast. Eng.* **2000**, *58th*, 3763.
27. Vaia, R. A.; Teukolsky, R. K.; Giannelis, E. P. *Chem. Mater.* **1994**, *6*, 1017.
28. Govindaiah, P.; Avadhani, C. V.; Ramesh, C. *Macromol. Symp.* **2006**, *241*, 88.
29. Orler, E. B.; Yontz, D. J.; Moore, R. B. *Macromolecules* **1993**, *26*, 5157.
30. Li, H. M.; Liu, J. C.; Zhu, F. M.; Lin, S. A. *Polym. Int.* **2001**, *50*, 421.
31. Gowd, E. B.; Nair, S. S.; Ramesh, C., *Macromolecules* **2002**, *35*, 8509.
32. Ghosh, A. R.; Woo, E. M. *Polymer* **2004**, *45*, 4749.
33. Tseng C. R.; Lee, H. Y.; Chang, F. C. *J. Polym. Sci.:Part B* **2001**, *39*, 2097.
34. Shah, R. K.; Hunter, D. L.; Paul, D. R. *Polymer* **2005**, *46*, 2646.
35. Pearson, R. G. *Inorg. Chem.* **1988**, *27*, 734.
36. Pilati, F.; Toselli, M.; Messori, M.; Manzoni, C.; Turturro, A.; Gattiglia, E. G. *Polymer* **1997**, *38*, 4469.
37. Orler, E. B.; Moore, R. B. *Macromolecules* **1994**, *27*, 4774.
38. Lu, X.; Steckle, W. P.; Weiss, R. A. *Macromolecules* **1993**, *26*, 5876.
39. Hird, B.; Eisenberg, A. *Macromolecules* **1992**, *25*, 6466.

6. Polypropylene/clay nanocomposites via melt mixing

6.1 Introduction

Polypropylene (PP) is a fast growing thermoplastic and dominating the industrial applications due to its attractive combination of properties such as low density, high thermal stability, resistance to corrosion etc. and low cost. There is a strong need to improve their mechanical properties for its applications in automotive industry¹. In the recent years, polymer/layered silicate (PLS) nanocomposites have attracted great interest, both in industry and in academia, because they often exhibit remarkable improvement in materials properties when compared with virgin polymer or conventional composites at very low filler loadings²⁻⁴. These improvements can include high moduli⁵⁻¹¹ increased strength and heat resistance¹² decreased gas permeability¹³⁻¹⁷ and flammability¹⁸⁻²¹. The enhancement in the properties of these materials are due to the interactions of the polymer chains with the surface of the clay layers and were maximum when the clay layers are completely delaminated or exfoliated and well dispersed in the polymer matrix. Researchers in the recent decade have shown that reinforcement with dispersed clay in the polymer matrix enhances the mechanical properties without much affecting the density of the polymer²². Therefore, various research efforts were made to disperse clay in the PP matrix. However it was very difficult to disperse clay in the PP matrix, as the polymer was highly non polar and there are no polar groups available to interact with the clay surface. The usual organo-modification of clay did not sufficiently lower the surface energy of the clay to interact with PP chains. Unmodified polyolefins lack the intrinsic thermodynamic affinity with currently available organoclays to form well dispersed nanocomposites²³. It could be possible to improve the surface energy of PP chains. In one such successful effort, it was found that PP could be intercalated into clay gallery by using a PP oligomer containing hydroxyl groups²⁴. Later, studies on preparation and properties of PP/organoclay nanocomposites were extensively done using functionalized PP as compatibilizers²⁵⁻²⁸. Liu et. al. and Zhang et al. et. al. have prepared PP/organoclay nanocomposites by using a new kind of co-intercalation organophilic clay which could tether on the PP backbone by virtue of grafting^{29, 30}. Tudor et al and Sun and coworkers

have reported the preparation of PP/organoclay nanocomposites by insitu intercalation polymerization^{31, 32}.

To improve the surface energy of semi crystalline polymers in the preparation of nanocomposites, many researchers introduced ionic groups on to the polymer chains. Moore et al. have introduced sodium sulfonate groups on poly (ethylene terephthalate)³³ and poly (butyleneterephthalate)³⁴ backbone to get exfoliated organoclay. Nanocomposites prepared from ionomers of polypropylene³⁵ polyethylene^{36, 37} and a variety of other nonpolar thermoplastic polymers³⁸⁻⁴⁰ also reveal good levels of organoclay exfoliation. In a previous work by our group we have shown that the fully exfoliated sPS/Clay nanocomposites can be prepared by introducing metallic sulfonate groups on the polymer backbone⁴¹. Polyethylene-co-methacrylic acid ionomer containing metallic ions could disperse the clay resulting in successful exfoliated structures³⁶. However compatibilizers such as amine and ammonium functionalized PP had failed to enhance the dispersion of clay in the PP matrix as compared to maleic anhydride grafted polypropylene via melt mixing⁴².

Therefore in the present work, we have evaluated a novel metallic ionomer of PP as compatibilizer for preparing PP/organoclay nanocomposite by two different mixing routes. The effect of the compatibilizer, compatibilizer concentration, processing method on the dispersion of organoclay in the polymer matrix and its effect on crystallization behavior and mechanical properties were studied. The properties of the obtained nanocomposites were compared with the nanocomposites, which are prepared using PPMA as compatibilizer.

6.2 Experimental

6.2.1 Materials

The materials used in this study are polypropylene REPOL H034SG obtained from Riliance Industries (Pvt.) Ltd., maleated polypropylene (PPMA) selected for this work was FUSABOND M613-05, which contains 0.65 weght % maleic anhydride group. The organoclay, Cloisite20A, which was modified by dimethyl dihydrogenated tallow

quaternary ammonium, $M_2(HT)_2$ were provided by Southern Clay Products Inc. The Cation Exchange Capacity (CEC) of the clay is 95 meq per 100 grams of dry clay and the percentage of weight loss on ignition (LOI) is 38 weight %. The solvent used 1,2 - dichlorobenzene is obtained from LOBA Chemie Pvt Ltd.

6.2.2 Preparation of potassium succinate grafted polypropylene ionomer

Maleated polypropylene (PPMA) was dissolved in 1, 2- Dichlorobenzene at 120 °C. One drop of phenolphthalein indicator was added into the solution. 0.2 N base (KOH) prepared in methanol was added drop by drop to the solution until the color of the solution changes to light pink. This is then heated for another half an hour to ensure the persistence of pink color and then precipitated in excess of methanol and washed with hot methanol, filtered and dried. Then the mixture was filtered and dried in vacuum oven at 65 °C to get a pure ionomer in white color.

6.2.3 Preparation of nanocomposites

All the nanocomposites were prepared by a melt mixing technique using a twin-screw extruder, DSM Micro 5 having a net barrel capacity of 5 CC with a screw speed of 100 rpm, the barrel temperature of 190 °C and a residence time of 10 min. Nanocomposites were prepared with different concentrations of compatibilizer keeping the organoclay concentration at 5 weight %. For comparison matrix polymer compositions without clay were also prepared. Nanocomposites were prepared in two different methods. In the first method, the PP, compatibilizer and the Cloisite 20A were all melt mixed directly in a single step. In the second method, the compatibilizer was mixed with the organoclay to form a masterbatch in the first step, which was then mixed with the PP in the second step. Various compositions prepared were coded in such a way that the number in the code after the compatibilizer name indicates the percentage of the respective compatibilizer, C for 5% organoclay, and the method of preparation indicated in the sample code by D for direct mixing and M for masterbatch route.

6.2.4 DSM Micro Extruder & Injection Molder

Various compositions of nanocomposites and the matrix polymer were prepared using the DSM microcompounder. A brief overview of the different parts and processing were described using figure 6.1.



Figure 1: DSM Micro Extruder & Injection Molder

The system is comprised of four primary components: the micro-extruder (1); the feeder (2); mini-injection molder (3) and the transfer cylinder (4). Materials to be processed are weighed and placed in the feeder hopper (5). The plunger (8) transfers the materials through the tube (7) into the extruder barrel (6). Inside the barrel, the two co-rotating

screws mix, melt and force the material downward. When the material reaches the bottom of the barrel the melt is directed into the recirculation canal (11) where it travels upward and enters the main barrel cavity. This process can be repeated as long as the operator desires, typical mixing and recirculation times are 2-10 minutes. At the conclusion of the mixing and recirculation process, gate (10) is closed and the melt stream is directed out through the die orifice (9) where it immediately enters the heated transfer cylinder (13). As the melt fills the cylinder, the plunger (14) is pushed out of the cylinder. Gate (10) is closed, and the cylinder is placed in the molder cradle (16) of the injection-molding unit. A pneumatic ram (15) pushes the plunger forward, which forces the melt into the mold (17) where it is cooled and solidified. Opened split molds for stiffness beams and disks are shown in (18). This system allows the processing of small amounts of polymers and composites, into coupons suitable for physical, mechanical testing at short samples preparation and processing times.

6.2.5 Wide Angle X-Ray Diffraction (WAXD)

The WAXD experiments were performed using a Rigaku Dmax 2500 diffractometer equipped with a copper target and a diffracted beam monochromator. (Cu K α radiation with $\lambda = 1.5406\text{\AA}$) with 2θ scan range of 2-10° at room temperature. The specimens of nanocomposites for WAXD were a thin film samples melt pressed on a copper block sample holder.

6.2.6 Transmission Electron Microscopy (TEM)

Samples for TEM were sectioned using a Lieca Ultra cut UCT microtome with thickness of 50-60 nm using a diamond knife. The sections were collected from water on 300 mesh carbon coated copper grids. TEM imaging was done using a TechnaiG² Transmission electron microscope operating at an accelerating voltage of 300 KV. The density of clay particles is enough to produce contrast between polymer and clay stacks hence staining was not required. Images were captured using Charged Couple Detector (CCD) camera for further analysis using Gatan Digital Micro graph analysis software.

6.2.7 Thermal analysis

Differential Scanning Calorimetry (DSC) was studied using TA instruments DSC-Q100 differential scanning calorimeter under standard conditions. The samples were heated/cooled at the rate of 10 °C/min from 0 °C to 200 °C under flowing nitrogen atmosphere, the sample weight was about 5 mg. The crystallization temperatures T_c were recorded from the endothermic peak obtained during cooling from melt in the DSC. Thermogravimetric analysis (TGA) was done using TA instruments TGA-Q5000. The thermal stability and amount of clay present in the nanocomposites were determined from TGA. The samples were heated under flowing nitrogen atmosphere from 50 to 900 °C, at a heating rate of 10 °C/min. and the weight loss was recorded.

6.2.8 Polarized Optical Microscopy

Spherulitic morphology of the samples prepared were studied by OLYMPUS polarized optical microscope (POM) attached with a Mettler Toledo FP82HT hot stage under crossed polarizer. Thin slices were cut from the injection molded samples, inserted between two microscope cover glasses, melted at 200 °C. The slides were then transferred to the hot stage and melted at 200 °C then slides were held for one minute to ensure uniform melting. In subsequence, samples were cooled to room temperature at a constant rate of 10 °C/min. After cooling to room temperature, the photomicrographs of the sample were recorded using Olympus digital camera.

6.2.9 Universal Testing Machine (UTM)

The flexural modulus of nanocomposites was tested with Instron 4204 model universal testing machine. The test specimen bars were obtained using DSM micro-injection molding machine with a barrel temperature set at 210 °C and mold temperature at 35 °C. The injection molding pressure and holding pressure were both set at 30 bar. The dimensions of the flexural specimens were 3.20 × 12.15 × 71.0 mm. The test was conducted with a load of 1 KN at cross head speed of 2.8 mm/min and the span length was kept at 40 mm.

6.3 Results and Discussion

6.3.1 Preparation of Potassium succinate grafted polypropylene

SCHEME 1

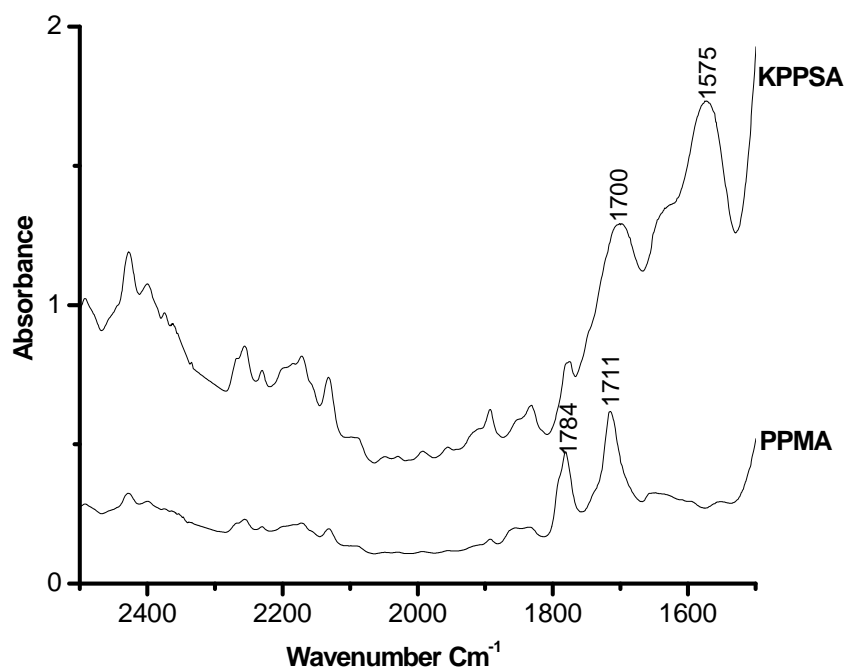
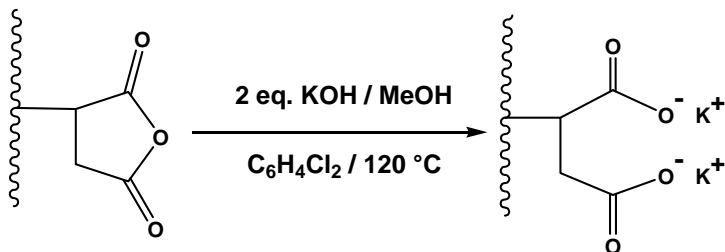


Figure 6.2: The FT IR spectrum of PPMA and KPPSA

Potassium succinate grafted polypropylene (KPPSA) was prepared in the laboratory to use as a compatibilizer in the synthesis of PP/organoclay nanocomposites by simultaneous hydrolysis and neutralization of solution of PPMA in dichlorobenzene at $120\text{ }^\circ\text{C}$ with methanolic KOH in a single step in presence of phenolphthalein as indicator as showed in scheme 1. The product was obtained by precipitating the neutralized

solution in methanol, filtered and washed with excess hot methanol to ensure phenolphthalein was thoroughly removed. Formation of potassium salt of succinate-grafted polypropylene from PPMA was confirmed by FT-IR analysis. The FTIR spectrum of PPMA and KPPSA were shown in Figure 6.2. The strong absorbance peaks at 1784 cm^{-1} and 1711 cm^{-1} observed for carbonyl group of the anhydride in PPMA disappeared and new peaks appeared at 1700 cm^{-1} and 1570 cm^{-1} corresponding to symmetric and asymmetric stretching carbonyl of carboxylate anion shows the formation of potassium succinate functionality.

6.3.2 Structure of the nanocomposites

6.3.2.1 WAXD

Cloisite 20A was chosen as the organoclay to be dispersed in the polymer matrix. Prior to evaluation of the new compatibilizer for dispersability of the organoclay in polypropylene, binary composites containing 95% compatibilizer and 5% C20A was prepared by melt mixing using DSM micro compounder at 190°C for 10 minutes with a screw speed of 100 rpm and characterized them with WAXD. The WAXD pattern (figure 6.3a) of KPPSA/C20A showed no peak for the organoclay indicating that the organoclay was completely delaminated and exfoliated in the KPPSA matrix while PPMA/C20A showed a broad low intensity peak at a d-spacing of 38 \AA indicating the presence of intercalated tactoids. The above result clearly indicates that the new compatibilizer, KPPSA containing more polar ionic functional group have better interaction with the organoclay than PPMA.

The nanocomposites were prepared by varying the concentration of the compatibilizer keeping the concentration of the organoclay, C20A, at a constant 5-wt %. Two different mixing routes were used to prepare the nanocomposites. In the first route the organoclay, compatibilizer and the matrix polymer were mixed together directly in a single step. In the second route, the organoclay was mixed with the compatibilizer in the first step to form a masterbatch followed by mixing it with the matrix PP in the second step. The properties of the nanocomposites obtained were compared with the nanocomposites prepared using PPMA as compatibilizer under identical conditions. The WAXD patterns

for the nanocomposites prepared were shown in figure 6.3b-d and their d-spacings corresponding to the clay interlayer distance were tabulated (Table 6.1).

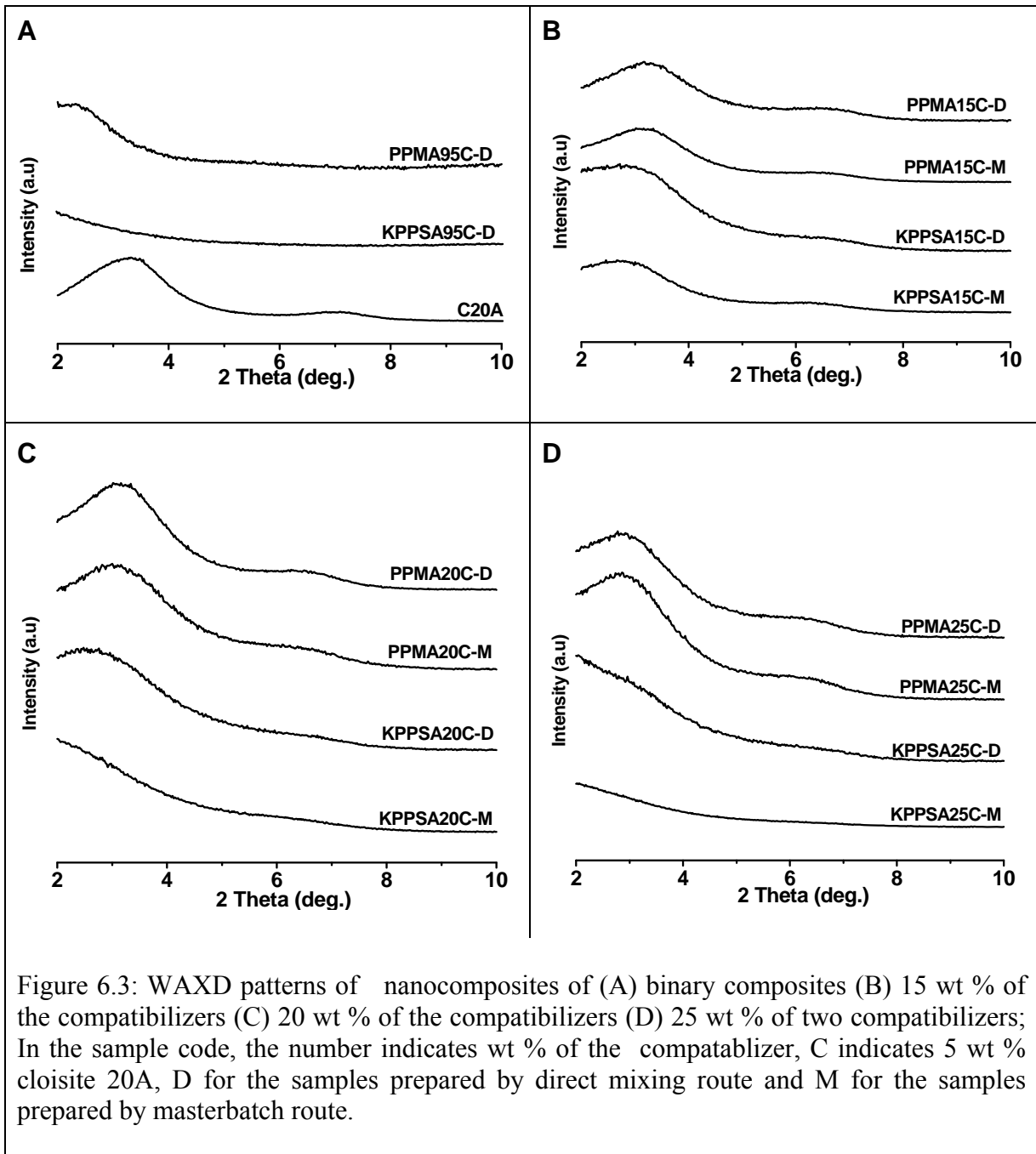


Table 6.1: d - spacing of nanocomposites and organoclay

| Sample | d-spacing (Å) | | | |
|-----------|-----------------------------------|-----------------------------------|-----------------------------------|-----------------------------------|
| | 15 weight % of the compatibilizer | 20 weight % of the compatibilizer | 25 weight % of the compatibilizer | 95 weight % of the compatibilizer |
| PPMA-C-D | 27.7 | 28.8 | 31.0 | 38.0 |
| PPMA-C-M | 28.8 | 29.4 | 31.3 | - |
| KPPMA-C-D | 30.4 | 33.7 | a | a |
| KPPMA-M | 32.2 | a | a | - |
| C20A | 24.2 Å | | | |

a – no peaks observed for the clay (exfoliated)

It can be observed that irrespective of the method of preparation, either by direct mixing or through masterbatch mixing as the concentration PPMA increases, the peak position shifts towards lower angles indicating improvement in the amount of intercalation of polymer in to the organoclay gallery, but did not lead to complete exfoliation. When the nanocomposites were prepared by direct mixing route, and KPPSA was used as compatibilizer, the WAXD patterns show higher d-spacing for the clay as compared to their PPMA counterparts. When the nanocomposites were prepared by masterbatch route with KPPSA as compatibilizer, at 15% concentration showed higher d-spacing as compared to their PPMA counterpart and at higher concentrations complete exfoliation of the clay layers was observed as compared to intercalated structures observed for their PPMA counterparts.

6.3.2.2 TEM

Typical TEM micrographs of the nanocomposites prepared by masterbatch route with 25% compatibilizer were shown in [figure 6.4\(a\) and \(b\)](#). It is clearly evident from the TEM pictures that the nanocomposites prepared with 25 wt % KPPSA as compatibilizer show completely exfoliated structures where the clay layers are completely delaminated and dispersed homogeneously in the polymer matrix while the nanocomposites prepared with 25% PPMA as compatibilizer showed intercalant clusters of clay layers suggesting intercalated structures.

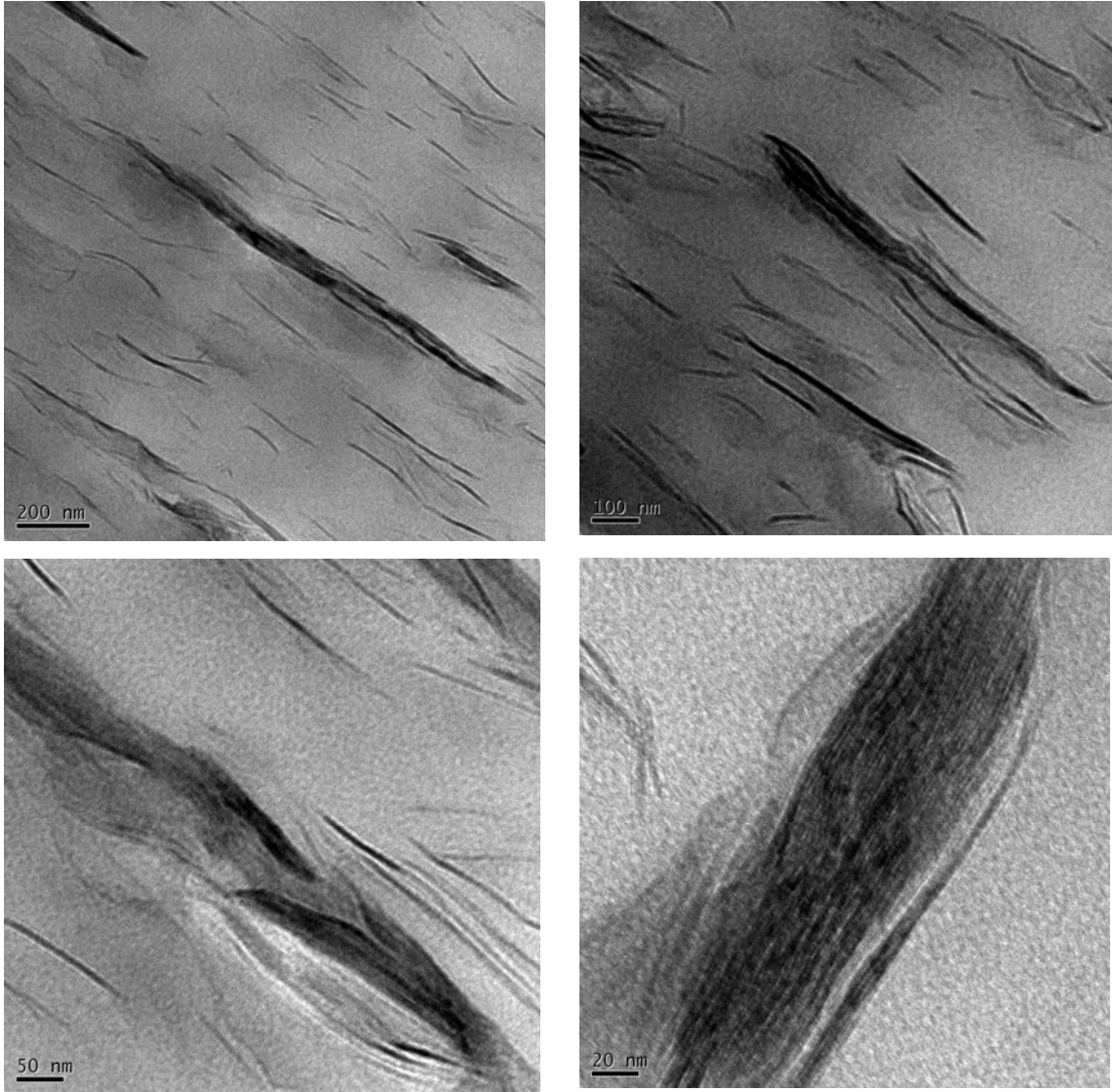


Figure 6.4(a): Typical TEM micrographs of PPMA25C-M

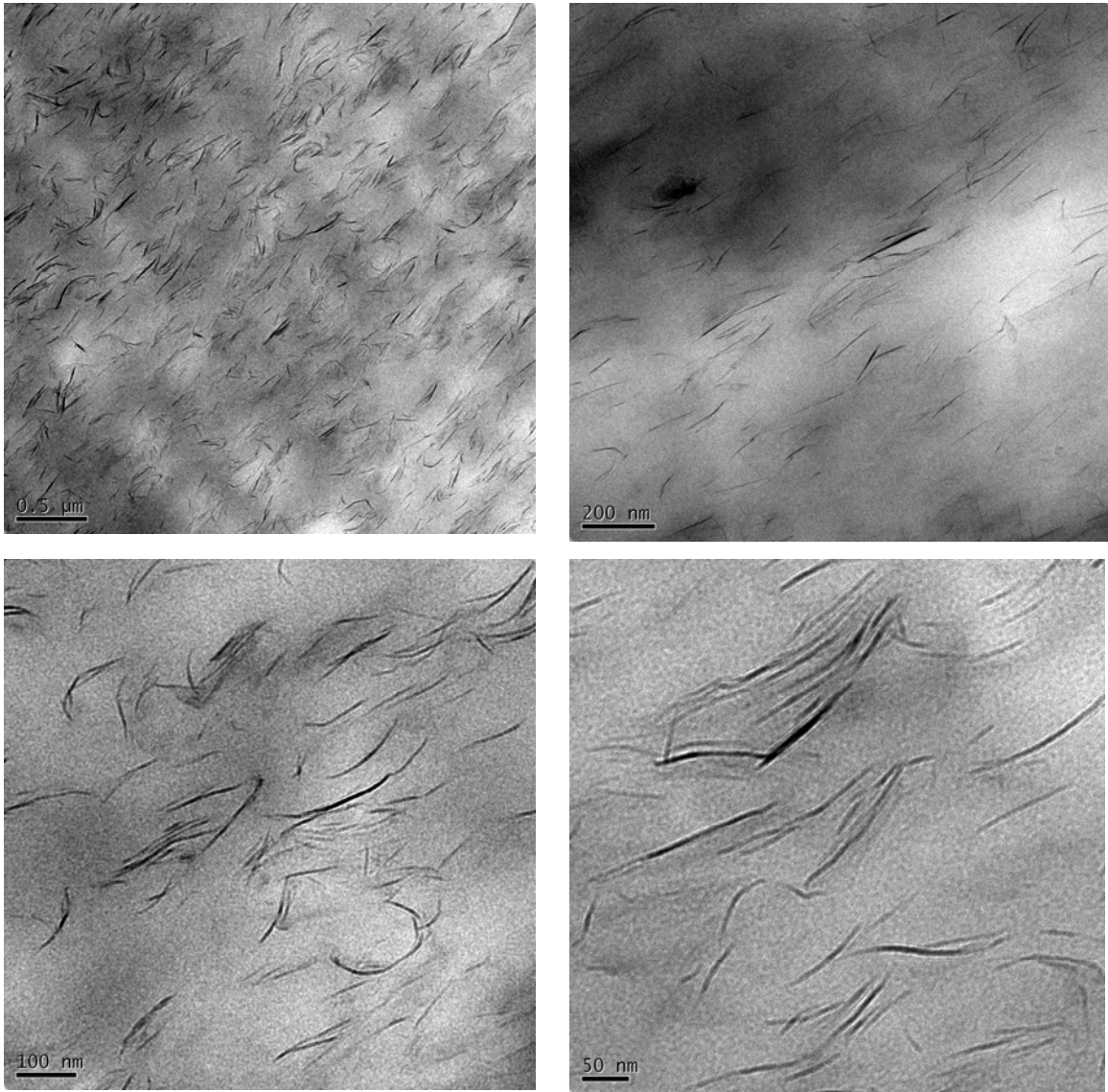


Figure 6.4(b): Typical TEM micrographs of KPSA25C-M

6.3.3 Thermogravimetric analysis

Thermogravimetric analysis (TGA) was done using TA instruments TGA-Q5000. The amount of clay present in the nanocomposites and the thermal stability were determined from TGA. The samples were heated under flowing nitrogen atmosphere from 50 to 900 °C, at a heating rate of 10 °C/min. and the weight loss was recorded. The MMT silicate content in the nanocomposites was obtained from thermogravimetric analysis as reported by Paul et. al. using the formula ^{43, 44}.

$$\text{Percentage MMT content} = \frac{\text{MMT}_{\text{char}} \text{ of nanocomposite}}{0.935}$$

The percentage of organoclay present in the nanocomposites was calculated using a simplified formula shown below.

$$\text{Percentage organoclay content} = \frac{\% \text{ MMT}_{\text{char}} \text{ of nanocomposite}}{\% \text{ MMT}_{\text{char}} \text{ of organoclay}} \times 100$$

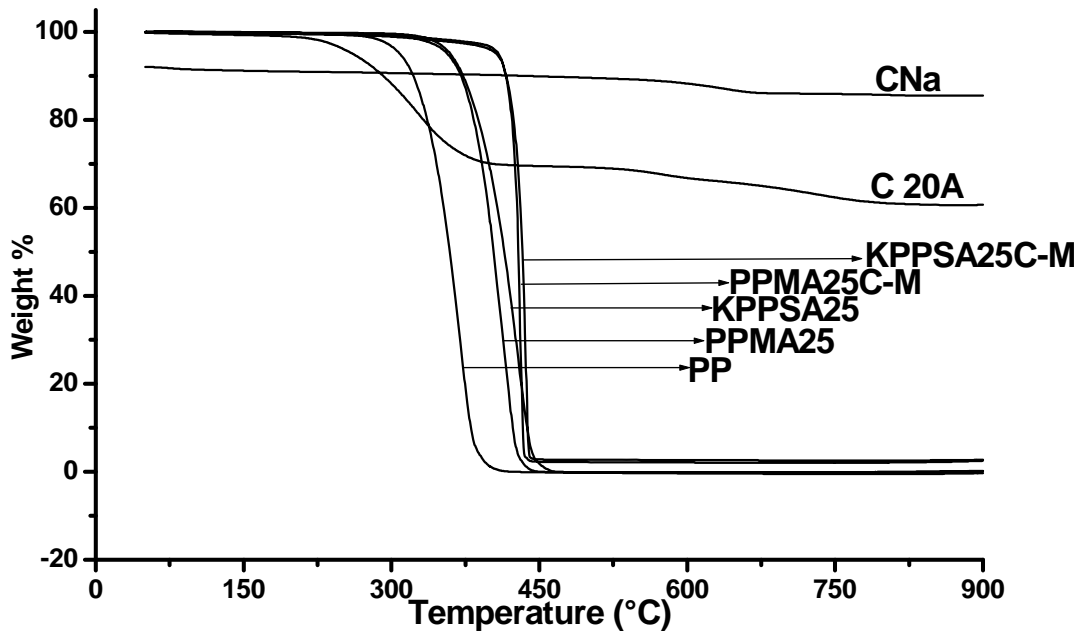


Figure 5(a): TGA Thermograms of cloisite Na, Cloisite 20A, PP, PPMA25, KPPSA25, PPMA25C-M and KPPSA25C-M

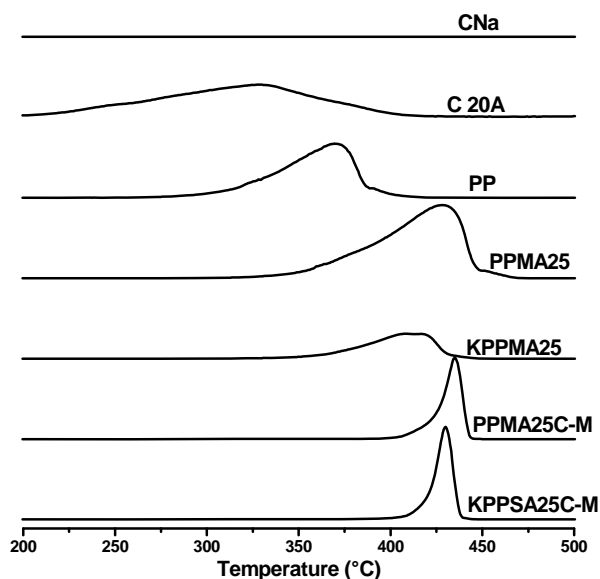


Figure 6.5(b): TGA Derivative thermograms of cloisite Na, Cloisite 20A, PP, PPMA25, KPPSA25, PPMA25C-M and KPPSA25C-M

Table 6.2: Thermal degradation behavior of PP matrix and its nanocomposites

| Sample | Onset degradation Temperature °C (T_{onset}) | Maximum degradation temperature °C (T_{max}) |
|------------|---|---|
| PP | 282 | 370 |
| PPMA25 | 329 | 428 |
| KPPSA25 | 349 | 412 |
| PPMA25C-M | 398 | 435 |
| KPPSA25C-M | 398 | 429 |

All the nanocomposites were prepared with 5 weight % organoclay in the feed. The typical thermograms and their derivative thermograms were shown in the [Figure 6.5\(a\)](#) and [6.5\(b\)](#). The onset of degradation and the maximum degradation temperature of the selected samples were listed in the [Table 6.2](#). The TGA results of the nanocomposites showed MMT_{char} contents of 3.0 weight % at 900°C which corresponds to 3.2 % of MMT content and are equivalent to the organoclay content taken in the feed. The onset of degradation has improved by about 50°C when the PPMA or KPPSA was mixed with PP and is further improved by another 50°C in the nanocomposites.

6.3.4 Crystallization behavior

6.3.4.1 Differential scanning calorimetry

Crystallization behaviors of various nanocomposites obtained were studied using DSC and POM. Typical DSC thermogram curves obtained for various nanocomposites, the matrix polymers and the pristine polypropylene during cooling from melt at 10 °C/min were shown in figure 6.5.

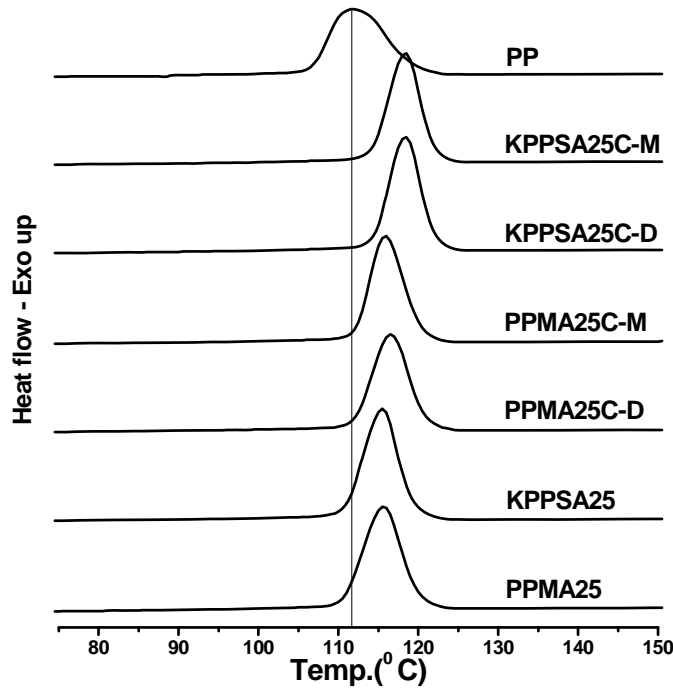


Figure 6: DSC thermogram curves of the matrix polymers and the nanocomposites during the cooling from melt at 10°C/min.

The crystallization peak temperature (T_{cc}) on cooling from melt has been taken as a measure of crystallization rate⁴⁵. High T_{cc} during cooling in non-isothermal experiments indicates higher crystallization rate. Nanocomposites show higher crystallization rate than the matrix polymers due to nucleation by clay layers as reported in the literature⁴⁶⁻⁵⁰. Exfoliated clay nanocomposites obtained with 25 wt % KPPSA showed enhanced crystallization rates as compared to intercalated nanocomposites obtained with 25 wt % PPMA, which were evidenced with higher T_{cc} . In the exfoliated nanocomposite the clay layers are completely delaminated providing large surface for nucleation than the intercalated ones resulting in higher T_{cc} .

6.3.4.2 Polarized optical microscopy

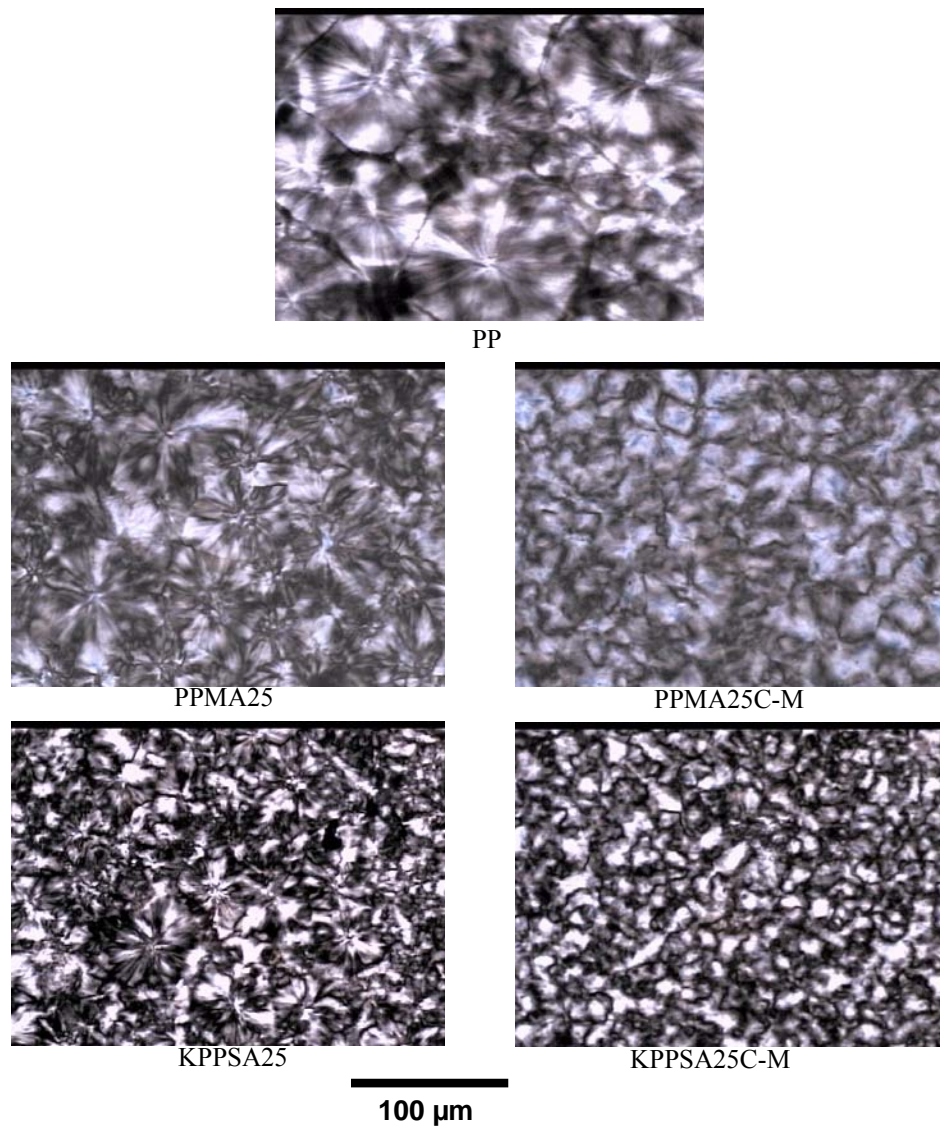


Figure 6.7: Polarized optical microscope pictures of PP, PP/Compatibilizer and PP/Compatibilizer/ Organoclay nanocomposites obtained at room temperature after cooling from melts at 10°C/min

Spherulite sizes of the nanocomposites and the matrix polymers at room temperature were determined from polarized optical microscopy (POM) after cooling the samples from melt at 10 °C/min. The POM pictures (figure 6.7) show smaller crystallite sizes of less than 35 μm for the exfoliated nanocomposites obtained with 25% KPPSA as compared to 40 to 60 μm for the intercalated nanocomposites obtained with 25% PPMA which are due to the exfoliated structures providing larger number of nucleation centers

than the intercalated ones while the matrix polymer without clay show spherulite sizes in the range 50 to 70 μm and pristine PP show a spherulite size of 75 to 100 μm .

6.3.5 Mechanical properties

Table 6.3: Flexural modulus of the matrix polymer and the nanocomposites

| Sample | Flexural modulus (MPa) with compatibilizer composition of | | |
|-------------|---|---------|---------|
| | 15 wt % | 20 wt % | 25 wt % |
| PPMA | 747 | 710 | 691 |
| KPPSA | 738 | 759 | 788 |
| PPMA-C-D | 842 | 840 | 834 |
| KPPSA-C-D | 840 | 852 | 863 |
| PPMA-C-M | 862 | 852 | 845 |
| KPPSA-C-M | 888 | 895 | 937 |
| Pristine PP | 804 | | |

The flexural modulus of nanocomposites was tested with Instron 4204 model universal testing machine. The test specimen bars were obtained using DSM micro-injection molding machine with a barrel temperature set at 210 °C and mold temperature at 35 °C. The injection molding pressure and holding pressure were both set at 30 bar. The dimensions of the flexural specimens were 3.20 × 12.15 × 71.0 mm. The test was conducted with a load of 1 KN at cross head speed of 2.8 mm/min and the span length was kept at 40 mm. Flexural moduli of the nanocomposites were measured were shown in [Table 6.3](#). To show the effect of compatibilizer in PP without clay, binary blends of Compatibilizer/PP with the respective compositions were prepared and their properties were properties were also listed. It was observed from the [Table 6.3](#) that there was small decrease in the absolute flexural moduli when compatibilizer PPMA was mixed with PP as compared to pure PP and further decreases with increase in the concentration of PPMA. When the compatibilizer KPPSA was blended with pure PP, it lowered the flexural modulus, however increased slightly with increase in concentration from 15% to 25%. The flexural moduli of all the nanocomposites prepared showed improvements as

compared to pristine PP. The improvements were highest in the case of KPPSA25C-M which contains 25% KPPSA, and was prepared by masterbatch. For a given concentration of compatibilizer irrespective of compatibilizer type, the improvements in flexural moduli were better for the samples prepared by masterbatch route than the samples show any subtle change in the flexural moduli with the change in concentration for the given method of preparation. Nanocomposites prepared using KPPSA as compatibilizer showed slight increase in flexural moduli with the increase in concentration of compatibilizer from 15% to 25% when prepared by direct mixing while the increase was significant for the samples prepared through masterbatch route.

6.4 Conclusions

Potassium succinate grafted polypropylene (KPPSA) was prepared from maleic anhydride grafted polypropylene (PPMA) and its utility as compatibilizer for the dispersion of organoclay in the PP matrix has been evaluated. The nanocomposites were prepared by melt mixing of the organoclay with PP in presence of the compatibilizer in two different routes such as by single step direct mixing method and by two step method through masterbatch route. The dispersion of clay was found to be dependent on the method of preparation, type of compatibilizer used and the amount of compatibilizer used. The dispersion of the organoclay was better with KPPSA than PPMA and the dispersion was better when the nanocomposites were prepared by two step masterbatch route than the single step direct mixing method. The dispersion of the organoclay improved with increase in the amount of compatibilizer. The nanocomposites prepared using the KPPSA as compatibilizer at above critical concentrations resulted in exfoliated nanocomposites while only intercalated structures were obtained with PPMA as compatibilizer. The exfoliated nanocomposites obtained with KPPSA show smaller spherulite sizes than the intercalated nanocomposites obtained with PPMA as the dispersed clay platelets in the PP matrix act as nucleation centers. This is further evidenced by higher crystallization rates for the exfoliated nanocomposites obtained with KPPSA than the intercalated nanocomposites obtained with PPMA as compatibilizer. The nanocomposites prepared showed improvements in the onset of degradation temperature. The flexural modulus of the exfoliated nanocomposites prepared using

novel metallic ionomer as compatibilizer showed improvements better than the intercalated nanocomposites prepared using conventional PPMA as compatibilizer. Thus we have shown that metallic ionomer such as KPPSA can act as better compatibilizer for the preparation of well-dispersed PP/organoclay nanocomposites.

References

1. Usuki, A.; Hasegawa, N.; Koto, M. *Adv. Polym. Sci.* **2005**, *179*, 135.
2. LeBaron, P. C.; Wang, Z.; Pinnavaia, T. J. *Appl. Clay Sci.* **1999**, *15*, 11.
3. Alexander, M.; Dubois, P. *Mater. Sci. Eng.* **2000**, *28*, 1.
4. Ray, S. S.; Okamoto, M. *Prog. Polym. Sci.* **2003**, *28*, 1539.
5. Ogawa, M.; Kuroda, K. *Bull. Chem. Soc. Jpn* **1997**, *70*, 2593.
6. Okada, A.; Kawasumi, M.; Usuki, A.; Kojima, Y.; Kurauchi, T.; Kamigaito, O.; In: Schaefer, D. W.; Mark, J. E. editors. *Polymer based molecular composites*, MRS Symposium Proceedings, Pittsburgh, **1990**, *171*, 45.
7. Giannelis, E. P.; *Adv Mater* **1996**, *8*, 29.
8. Giannelis, E. P.; Krishnamoorti, R.; Manias, E. *Adv Polym Sci* **1999**, *138*, 107.
9. LeBaron, P. C.; Wang, Z.; Pinnavaia, T. J. *Appl Clay Sci* **1999**, *15*, 11.
10. Vaia, R. A.; Price, G.; Ruth, P. N.; Nguyen, H. T.; Lichtenhan, J. *Appl Clay Sci* **1999**, *15*, 67.
11. Biswas, M.; Sinha Ray, S. *Adv Polym Sci* **2001**, *155*, 167.
12. Giannelis, E. P. *Appl Organomet Chem* **1998**, *12*, 675.
13. Xu, R.; Manias, E.; Snyder, A. J.; Runt, J. *Macromolecules* **2001**, *34*, 337.
14. Bharadwaj, R. K. *Macromolecules* **2001**, *34*, 1989.
15. Messersmith, P. B.; Giannelis, E. P. *J Polym Sci, Part A: Polym Chem* **1995**, *33*, 1047.
16. Yano, K.; Usuki, A.; Okada, A.; Kurauchi, T.; Kamigaito, O. *J Polym Sci, Part A: Polym Chem* **1993**, *31*, 2493.
17. Kojima, Y.; Usuki, A.; Kawasumi, M.; Fukushima, Y.; Okada, A.; Kurauchi, T.; Kamigaito, O. *J Mater Res* **1993**, *8*, 1179.
18. Gilman, J. W. *Appl Clay. Sci* **1999**, *15*, 31.

19. Dabrowski, F.; Bras, M. L.; Bourbigot, S.; Gilman, J. W.; Kashiwagi, T. in intumescent fire retarded EVA. Proceedings of the Eurofillers'99, Lyon-Villeurbanne, France; 6–9 September **1999**.
20. Bourbigot, S.; LeBras, M.; Dabrowski, F.; Gilman, J. W.; Kashiwagi, T. *Fire Mater* **2000**, *24*, 201.
21. Gilman, J. W.; Jackson, C. L.; Morgan, A. B.; Harris, Jr. R.; Manias, E.; Giannelis, E. P.; Wuthenow, M.; Hilton, D.; Phillips, S. H. *Chem Mater* **2000**, *12*, 1866.
22. Pinnavaia, T. J.; Beall, G. W. *Polymer-Clay Nanocomposites*, Wiley series in polymer science, **1997**.
23. Manias, E.; Touny, A.; Wu, I.; Strawhecker, K.; Lu, B.; Chung, T. C. *Chem. Mater.* **2001**, *13*, 3516.
24. Kato, M.; Usuki, A.; Okada, A. *J. Appl. Polym. Sci.* **1997**, *66*, 1781.
25. Kawasumi, M.; Hasegawa, N.; Kato, M.; Usuki, A.; Okada, A. *Macromolecules* **1997**, *30*, 6333.
26. Hasegawa, N.; Kawasumi, M.; Kato, M.; Usuki, A.; Okada, A. *J. Appl. Polym. Sci.* **1998**, *67*, 87.
27. Reichert, P.; Nitz, H.; Klinke, S.; Brandsch, R.; Thomann, R.; Mulhaupt, R. *Macromol. Mater. Engg.* **2000**, *275*, 8.
28. Ishida, H.; Campbell, S.; Blackwell, J. *Chem. Mater.* **2000**, *12*, 1260.
29. Liu, X.; Wu, Q. *Polymer* **2001**, *42*, 10013.
30. Zhang Y-Q, Lee J-H, Rhee J. M., Rhee K. Y. *Composites Science and Technology* **2004**, *64*, 1383.
31. Tudor, J.; Willington, L.; O'Hare, D.; Royan, B. *Chem Commun* **1996**, 2031.
32. Sun, T.; Garces, J. M. *Adv Mater* **2002**, *14*, 128.
33. Barber, G. D.; Calhoun, B. H.; Moore, R. B. *Polymer* **2005**, *46*, 6706.
34. Chisholm, B. J.; Moore, R. B.; Barber, G. D.; Khouri, F.; Hempstead, A.; Larsen, M.; Olson, E.; Kelley, J.; Balch, G.; Caraher, J. *Macromolecules* **2002**, *35*, 5508.
35. Wang, Z. M.; Nakajima, H.; Manias, E.; Chung, T. C. *Macromolecules* **2003**, *36*, 8919.
36. Shah, R. K.; Paul, D. R. *Macromolecules* **2006**, *39*, 3327.
37. Lee, J. A.; Kontopoulou, M.; Parent, J. S. *Polymer* **2005**, *46*, 5040.

38. Start, P. R.; Mauritz, K. A. *J. Polym. Sci., Polym. Phys.* **2003**, *41*,1563.
39. Kovarova, L.; Kalendova, A.; Malac, J.; Vaculik, J.; Malac, Z.; Simonic, J. *Annu. Tech. Conf. Soc. Plast. Eng.* **2002**, *60*, 2291.
40. Barber, G. D.; Carter, C. M.; Moore, R. B. *Annu. Technol. Conf. Soc. Plast. Eng.* **2000**, *58*, 3763.
41. Govindaiah, P.; Mallikarjuna, S. R.; and Ramesh, C. *Macromolecules* **2006**, *39*, 7199.
42. Lili C.; Paul, D. R. *Polymer* **2007**, *48*, 1632.
43. Fornes, T. D.; Yoon, P. J.; Keskkula H.; Paul, D. R. *Polymer* **2001**, *42*, 9929.
44. Fornes, T. D.; Yoon, P. J.; Keskkula, H.; Paul, D. R. *Polymer* **2002**, *43*, 2121.
45. Pilati, F.; Toselli, M.; Messori, M.; Manzoni, C.; Turturro, A.; Gattiglia, E. G. *Polymer* **1997**, *38*, 4469
46. Hambir, S.; Bulakh, N.; Kodgire, P.; Kalgaokar, R.; Jog, J. P. *J. Polym. Sci., Polym. Phys.* **2001**, *39*,446
47. Kodgire, P.; Kalgaokar, R.; Hambir, S.; Bulakh, N.; Jog, J. P. *J. Appl. Polym. Sci.* **2001**, *81*, 1786.
48. Maiti, P.; Nam, P. H.; Okomoto, M.; Hasegawa, N.; and Usuki, A. *Macromolecules*, **2002**, *35*, 2042.
49. Maiti, P.; Nam, P. H.; Okomoto, M.; Kotaka, T.; Hasegawa, N.; Usuki, A. *Polym. Eng. Sci.* **2002**, *42*, 9.
50. Nam, P. H.; Maiti, P.; Okomoto, M.; Kotaka, T.; Hasegawa, N.; Usuki, A. *Polymer* **2001**, *42*, 9633.

7. Conclusions

In the present thesis, various strategies were explored to obtain better dispersion of clay layers in candidate polymers such as polyurethanes, polycarbonates, syndiotactic polystyrene and polypropylene and the resultant property enhancements of the nanocomposites were correlated with structure of the nanocomposites. The salient conclusions are summarized as below.

PU-clay nanocomposites prepared by in-situ solution polymerization in toluene medium resulted in intercalated nanocomposites. When the organoclay modified with reactive modifier was used, it was shown that with the addition of branching agent, the extent of intercalation has improved and at higher concentrations, resulted in exfoliated structures. However when the organoclay used does not have a reactive hydroxyl groups, there was no effect on the intercalation of polymer. The nanocomposites prepared using the organoclay containing trifunctional modifier, 3OHMMT, showed better intercalations than the nanocomposites prepared organoclays containing mono and di-functional modifier such as 1OHMMT and 2OHMMT. The structure of the nanocomposites obtained as characterized by WAXD measurements were further confirmed by TEM analysis. The dynamic mechanical analysis of the thermoplastic polyurethane clay nanocomposites show increase in storage tensile moduli at the temperatures below glass transition as compared to the pristine polymer and are effective with increase in functionality of the modifier for the clay.

The organoclays, modified with thermally stable modifiers were prepared for the synthesis of polycarbonate/layered silicate nanocomposites via *in-situ* intercalative polymerization. We have demonstrated for the first time that polycarbonate/exfoliated layered silicate nanocomposites can be successfully prepared using a class of novel organoclays that are modified using thermally stable modifiers containing reactive functionalities while only intercalated or agglomerated structures are obtained when the organoclays used does not have a reactive functionality. The molecular weights of the polymer in the composites prepared using phosphonium cation modified organoclay were

better than the imidazolium cation modified organoclay. The dynamic mechanical analysis of the exfoliated nanocomposites show better enhancement in storage modulus through out the temperature range from room temperature to below glass transition temperature as compared to the agglomerated composites. The glass transition temperatures obtained from DMA were comparable to that obtained from DSC.

The interaction of sPS with organoclay was improved by increasing the surface energy of the polymer by introducing the polar ionic functional groups such as ionomers of sulfonic acids with H^+ , Na^+ , K^+ and Rb^+ cations. It was demonstrated that higher ionomer content leads to better interaction with the polar silicate surface of the organoclay resulting in better intercalation/exfoliation. For the first time we have shown that by increasing the size and polarizability of the cation from H^+ to Rb^+ , resulted in improved intercalation/exfoliation behavior even with low levels of ionomer content. The SsPS ionomers show lower crystallization rates compared to sPS due to ionic aggregation. However, in the case of SsPS ionomer nanocomposites, the interaction of the modified clay layers with the ionomer leads to less aggregation and partially restores the crystallization rates.

Potassium succinate grafted polypropylene (KPPSA) was prepared from maleic anhydride grafted polypropylene (PPMA) and its utility as compatibilizer for the dispersion of organoclay in the PP matrix has been evaluated. The nanocomposites were prepared by melt mixing of the organoclay with PP in presence of the compatibilizer in two different routes such as by single step direct mixing method and by two step method through masterbatch route. The dispersion of clay was found to be dependent on the method of preparation, type of compatibilizer used and the amount of compatibilizer used. The dispersion of the organoclay was better with KPPSA than PPMA and the dispersion was better when the nanocomposites were prepared by two step masterbatch route than the single step direct mixing method. The dispersion of the organoclay improved with increase in the amount of compatibilizer. The nanocomposites prepared using the KPPSA as compatibilizer at above critical concentrations resulted in exfoliated nanocomposites while only intercalated structures were obtained with PPMA as

compatibilizer. The exfoliated nanocomposites obtained with KPPSA show smaller spherulite sizes than the intercalated nanocomposites obtained with PPMA as the dispersed clay platelets in the PP matrix act as nucleation centers. This is further evidenced by higher crystallization rates for the exfoliated nanocomposites obtained with KPPSA than the intercalated nanocomposites obtained with PPMA as compatibilizer. The flexural modulus of the exfoliated nanocomposites prepared using novel metallic ionomer as compatibilizer showed improvements better than the intercalated nanocomposites prepared using conventional PPMA as compatibilizer. Thus we have shown that metallic ionomer such as KPPSA can act as better compatibilizer for the preparation of well-dispersed PP/organoclay nanocomposites.

Thus overall, it has been demonstrated that when the interaction of the polymer chains with the layered silicate clay improved either by modifying the surface of the clay to suitably interact with polymer or modify the polymer by functionalization results in better dispersion. The improved intercalation and exfoliation behavior is observed, when the polymer chains are anchored on the surface of the clay through the modifier or the polymer chains are sufficiently functionalized with polar groups such as ionomers. The properties of the nanocomposites obtained show good correlation with the structure of the clay dispersion in the polymer matrix.